Identification of novel therapeutics for the treatment of MMR deficient tumours using high-throughput screens

Delphine GUILLOTIN

Submitted in partial fulfilment of the requirements of the Degree of Doctor of Philosophy

May 2015

Centre for Molecular Oncology
Barts Cancer Institute
Barts and The London School of Medicine and Dentistry
Queen Mary University of London
Charterhouse Square
London
United Kingdom

Declaration

The material presented in this thesis is the result of original work carried out by the author, Delphine Guillotin, at the Centre for Molecular Oncology, Barts Cancer Institute, Barts and The London School of Medicine and Dentistry, Queen Mary, University of London. All external sources have been properly acknowledged.

Acknowledgements

First of all, I would like to thank Queen Mary University of London for funding my PhD and my supervisor Dr. Sarah Martin who gave me the opportunity to undertake this PhD project. I would specially like to express my gratitude to Dr. Sarah Martin for her trust, patience, understanding and encouragements over the years. They were definitely essential for the completion of my PhD.

I would like to thank all the members of my team for their support and feedback. I am also really grateful to Julie, Hagen and Tracy who helped me with the animal experiments.

I would like to say a massive thank you to my friends and colleagues Constantia Pantelidou and Margueritte El Khouri who both gave me unconditional support and friendship. They made the weekend in the lab enjoyable.

I would like to thank all the PhD students who shared the PhD office with me, for all the constructive discussion we had about our PhD experience, for the troubleshooting and help. I would like to thank all the people from TC2 for all the great chats and laughs, especially Wasfi, Katy and Rumena.

And I would like to thank others from Barts Cancer Institute who where next to me during this experience, especially Annie Backer and Delphine Lees; and all my friends from outside the lab, especially Marie LP, who were supportive and understanding.

I would like to thank Vipul and Phodis for their management and giving us the best working conditions possible.

At last, I would like to deeply thank my family who supported me from the first day even if it was difficult for them to let me move aboard to accomplish a PhD.

Abstract

The DNA Mismatch repair (MMR) pathway is responsible for the repair of base-base mismatches and insertion/deletion loops, formed during DNA replication. Mutations in MMR genes significantly increase the predisposition to cancer with MMR deficiency estimated to be present in 15-17 % of all colorectal cancers. 5-fluorouracil is the main treatment for advanced colorectal cancer however the majority of studies suggest that MMR deficient tumours are more resistant to 5-fluorouracil than MMR proficient tumours. Therefore, there is a critical clinical need to identify novel therapeutics to treat these tumours.

To this end, we have performed a high-throughput compound screen, to identify compounds that cause selective lethality in MMR deficient cell lines. We identified the potassium-sparing diuretic drug, Triamterene, as selectively lethal *in vitro* and *in vivo* in MMR deficient cell lines. Our data suggest that this selectivity is through its antifolate activity, leading to the accumulation of reactive oxygen species and DNA double strand breaks in MMR deficient cells. Interestingly, we identified a requirement, for thymidylate synthase expression, the only *de novo* enzyme for dTTP synthesis for the Triamterene cytotoxicity. NRF2 and NRF2-induced antioxidants were regulated upon Triamterene treatment and thymidylate synthase silencing, therefore suggesting a role for the antioxidant response in Triamterene toxicity. Taken together, our results suggest Triamterene as a promising novel therapeutic for the treatment of MMR deficient cancers.

In order to identify novel therapeutics to treat MMR deficient tumours, we have also performed a high-throughput siRNA screen, to identify genes that cause selective lethality in MMR deficient cell lines. We identified AURKA gene as synthetically lethal in MSH6 deficient cell lines which suggests AURKA as a promising novel therapeutic target for the treatment of MMR deficient cancers.

Taken together, in this PhD thesis we have identified two novel therapeutic strategies for the treatment of MMR deficient cancers.

Abbreviations

µM: micro molar

•O_2^-: superoxide anions

•O_2^{2-}: peroxide

•OH: hydroxyl radicals

53BP1: p53 binding protein 1

5-FU: 5-fluorouracil

8-oxodG: 8-Oxo-2'-deoxyguanosine

ADG: 3-methyladenine-DNA-glycosylases

ADP: adenosine diphosphate

AID: activation-induced deaminase

ANOVA: analysis of variance

AP: apurinic/apyrimidinic

APC: adenomatous polyposis coli

APE1: AP endonuclease 1

ARE: antioxidant response element

ATM: ataxia telangiectasia mutated

ATP: adenosine triphosphate

ATR: ataxia telangiectasia and Rad3-related protein

ATRIP: ATR Interacting Protein

AURKA: aurora kinase A

BAX: BCL2-associated X protein

Bcl2: B-cell lymphoma 2

BER: base excision repair

BRCA1: Breast Cancer type 1 susceptibility protein

BRCA2: Breast Cancer type 2 susceptibility protein

BSA: bovine serum albumin

CAF1: chaperone chromatin assembly factor 1

CDK: Cyclin-dependent kinase

cDNA: complementary DNA

Chk1: checkpoint kinase 1

Chk2: checkpoint kinase 2

Chr: chromosome

CIMP: CpG island methylator phenotype

CIN: chromosome instability

CMV: cytomegalovirus

CRC: colorectal cancer

Dam: deoxyadenine methylase

DCF: 2',7'-dichlorofluorescein

DCFDA: 2',7'-dichlorofluorescein diacetate

DDR: DNA damage response

DHF: dihydrofolate

DHFR: dihydrofolate reductase

DHFU: dihydrofluorouracil

DMEM: Dulbecco's modified Eagle's medium

DMSO: Dimethyl sulfoxide

DNA: Deoxyribonucleic acid

DNA-PKcs: DNA-dependent protein kinase catalytic subunit

DNA pol: DNA polymerase

dNTP: deoxyribonucleotide

DSB: double strand break

DTT: dithiothreitol

E. coli: *Escherichia coli*

EDTA: Ethylenediaminetetraacetic acid

EGFR: epidermal growth factor receptor

ENaC: epithelium sodium channel

ERCC1: excision repair cross-complementing protein 1

ES: Embryonic stem

Exo1: exonuclease 1

FA: folic acid

FAR: Fanconi anemia repair

FBS: fetal bovine serum

FDA: food and drug administration

FdUMP: FdUrd-5'monophosphate

FdUTP: FdUrd-5'-triphosphate

FEN1: Flap endonuclease 1

FSP: frameshift peptides

FUTP: FUrd-5'-triphosphate

G1-phase: gap 1 phase

G2-phase: gap 2 phase

GG-NER: global genome NER

GT25: 25 mg/kg Triamterene by gavage

GT50: 50 mg/kg Triamterene by gavage

H_2O_2: hydrogen peroxide

HLTF: helicase-like transcription factor

HNPCC: hereditary nonpolyposis colon cancer

HO-1: Heme oxygenase 1

HR: homologous recombination

hr: hour

ICL: inter-cross links

ICR: Institute of Cancer Research

IDL: insertion/ deletion loop

IGF-IIR: insulin-like growth factor 2 receptor

IHC: immunohistochemistry

InsP6: inositol-1,2,3,4,5,6-hexakisphosphate

IP: intraperitoneal

IPPK: 1,3,4,5,6-pentakisphosphate 2-kinase

IPT25: 25 mg/kg Triamterene by IP

IPT50: 50 mg/kg Triamterene by IP

IPV: Vehicle by IP

IR: ionizing radiation

JAK2: Janus kinase 2

Keap1: kelch-like ECH-associated protein 1

LB: Lysogeny broth

LS: Lynch syndrome

LV: Leucovorin

MAD: median absolute deviation

MBD4: methyl-CpG-binding domain protein 4

MEF: mouse embryo fibroblasts

MGMT: O^6-methylguanine DNA methyltransferase

Min: minute

mm: millimeter

mM: milli molar

MMR: DNA mismatch repair

MNNG: N-methyl-N'-nitro-N-nitrosoguanidine

M-phase: mitosis phase

MRN: MRE11-RAD50-NBS1

MSI: microsatellite instability

MSI-H: high microsatellite instability

MSI-L: low microsatellite instability

MSS: microsatellite stable

MT1: metallothionein-1

MT2: metallothionein-2

MTHFR: methylene tetrahydrofolate reductase

MTR: 5-methyltetrahydrofolate-homocysteine methyltransferase

MUTYH: mutY Homolog (*E. coli*)

N^3meA: N^3-methyladenine

N^7meG: N^7-methylguanine

NAC: N-acetylcysteine

NADPH: nicotinamide adenine dinucleotide phosphate

NER: nucleotide excision repair

NHEJ: non-homologous end joining

NIEHS: National Institute of Environmental Health Sciences

NLS: nuclear localization sequences

nM: nano molar

NOD-SCID: non-obese diabetic - severe combined immunodeficiency

NQO1: NADPH:quinone oxidoreductase 1

NRF1: nuclear factor 1

NRF2: nuclear factor erythroid 2-related factor 2

NS: non-significant

O_2: oxygen

O^6meG: O^6-methylguanine

OD: Optical density

OGG1: 8-Oxoguanine glycosylase

$ONOO^-$: peroxynitrite

p: p-value

PALB2: partner and localizer of BRCA2

PARP1: poly(ADP-ribose) polymerase 1

PBS: phosphate buffered saline

PCNA: Proliferating cell nuclear antigen

PI3K: phosphoinositide 3 kinase

PIKK: phosphatidylinositol 3-kinaserelated kinase

PINK1: PTEN-induced putative kinase 1

PLK1: polo-like kinase 1

PTEN: phosphatase and tensin homolog

RFC: replication factor C

RNA: ribonucleic acid

ROS: Reactive oxygen species

RPA: replication protein A

RPMI: Roswell Park Memorial Institute medium

RQ: Relative quantity

S. cerevisiae: *Saccharomyces cerevisiae*

S-phase: synthesis phase

SAM: S-adenosylmethionine

Sec: second

SEM: standard error of mean

SETD2: SET domain containing 2

SHMT: serine hydroxymethyltransferase

siCtrl: non-targeting control siRNA

siRNA: small interfering RNA

SMUG1: single-strand selective monofunctional uracil DNA glycosylase

SOD: superoxide dismutase

SRB: Sulforhodamine B

SSB: single strand break

STR: short tandem repeat

TC-NER: transcription-coupled NER

TDG: thymidine-DNA glycosylase

TGFβR2: Transforming Growth Factor-β type II Receptor

Th1: T helper type 1

THF: 5,10-methylene tetrahydrofolate

TLS: translesion synthesis

TMZ: temozolomide

TR: Transfection reagent

Triam: Triamterene

TS: thymidylate synthase

UDG: uracil-DNA glycosylase

UV: ultraviolet

XLF: XRCC4-like factor

XPC: Xeroderma pigmentosum group C

XRCC1: X-ray repair cross-complementing protein 1

XRCC4: X-ray repair cross-complementing protein 4

γH2AX: gamma-H2A histone family, member X

Contents

List of figures

List of tables

Introduction

1 DNA damage response

Cancer causes around 8.2 million deaths per year, which represent 14.6 % of all human deaths worldwide. The most common types of cancer are lung, prostate, colorectal (CRC) and breast cancer [1]. One of the major driving causes for tumorigenesis is genomic instability, which is associated with all cancer types [2-4]. Genomic instability can be due to an increase in basal DNA mutation rate, for example microsatellite instability (MSI) [5, 6]. Genomic instability can also be due to a vast hypermethylation of promoter CpG island sites resulting in the epigenetic silencing of tumour suppressor genes known as CpG island methylator phenotype (CIMP) [7-9]. The other cause for genomic instability is an increase in numerical and/or structural chromosome aberrations rate also called chromosome instability (CIN) [10, 11]. Genomic instability is prevented in normal cells by the DNA damage response (DDR). DDR comprises of both DNA damage signalling and DNA damage repair. DNA repair is composed of a group of pathways including direct repair, base excision repair (BER), nucleotide excision repair (NER), DNA mismatch repair (MMR), fanconi anemia repair (FAR), non-homologous end joining (NHEJ) and homologous recombination (HR) [12]. Deregulation of the DDR, by activation or inactivation, leading to genomic instability, has been found in various cancers [13, 14]. Therefore, DDR is a strategic target for cancer therapy. Most cancer radiotherapy and chemotherapy are designed to trigger DNA damage, which predominantly impact cancer cells due to their deregulated DDR and to their rapid proliferation rates relative to normal, non-cancerous cells [15-17].

1.1 DNA damage

DNA damage is widely present in cancer cells. It is estimated that up to one million DNA lesions occur in each mammalian cancer cell per day [18]. There is a wide range of DNA damage that can occur such as nucleotide, oxidative and alkylating damage, mismatches, insertion deletions loops (IDLs), apurinic/apyrimidinic (AP) sites, intra-cross links and inter-cross links (ICLs), single strand breaks (SSBs) and double strand breaks (DSBs) (Figure 1). The type of damage formed will determine which DNA damage pathway will be recruited.

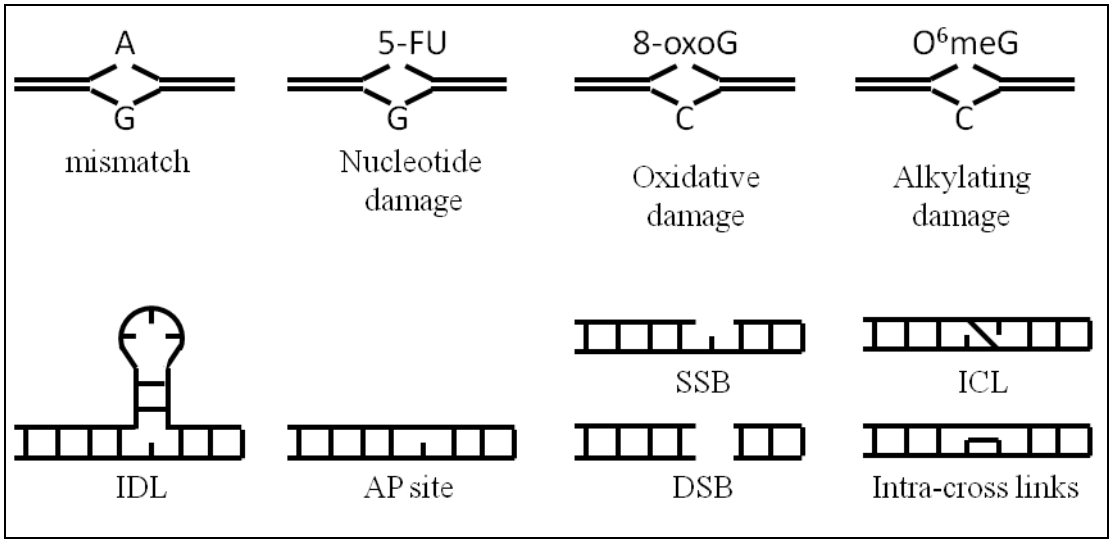

Figure 1: Types of DNA damage that can occur in mammalian cells
The different types of DNA damage are DNA mismatch, IDL, nucleotide, oxidative and alkylating damage, intra-cross link, ICL, AP site, SSB and DSB. Nucleotide, oxidative and alkylating damage can also be associated with a mismatch.

1.1.1 Oxidative stress

1.1.1.1 Reactive oxygen species

The main cause of endogenous DNA damage is reactive oxygen species (ROS) [19, 20]. They include superoxide anions ($\bullet O_2^-$), peroxide ($\bullet O_2^{2-}$), hydroxyl radicals ($\bullet OH$), oxygen (O_2), peroxynitrite ($ONOO^-$) and hydrogen peroxide (H_2O_2). A basal level of ROS is necessary for cellular homeostasis. Mitochondria are considered as the major source of ROS with 2 % of the oxygen consumed by mitochondria reduced to superoxide [21]. However, an imbalance between ROS production and degradation via the antioxidant response can lead to oxidative stress and ultimately to oxidative DNA damage. ROS is naturally increased in cancers to promote tumour progression and development [22, 23]. ROS levels can also be increased exogenously by ultraviolet (UV), ionizing radiation (IR), pollutants, tobacco and drugs.

1.1.1.2 Antioxidant response

Oxidative stress can be induced by an increase in ROS levels but also by a decrease in the antioxidant response. The antioxidant response can be non-enzymatic. Glutathione, vitamins C and E are important non-enzymatic antioxidants.

Glutathione serves as an electron donor to reduce disulfide bonds in protein cysteines [24]. Antioxidant response can also be enzymatic. For example the superoxide dismutases SOD1 and SOD2 catalyze $\bullet O_2^-$ into H_2O_2 and O_2 and the catalase peroxidase catalyzes H_2O_2 into H_2O. The antioxidant response is mainly regulated by nuclear factor erythroid 2-related factor 2 (NRF2), a member of the Cap'n'Collar family of basic region-leucine zipper transcription factors [25]. In the absence of oxidative stress, NRF2 is constitutively inactivated and degraded by forming a complex with the kelch-like ECH-associated protein 1 (Keap1). In the presence of oxidative stress, Keap1 cysteine residues are oxidized which allows Keap1 to uncouple from NRF2 [26]. Similarly, oxidative stress mediated phosphorylation of NRF2 by protein kinase C can lead to NRF2 dissociation from Keap1 [27, 28]. Disruption of the NRF2/Keap1 interaction leads to subsequent activation and translocation of NRF2 to the nucleus. In the nucleus, NRF2 binds to the antioxidant response elements (AREs) sequence (core sequence: TGAG/CNNNGC) present in the promoter region of many antioxidant genes and initiates their transcription [29-32]. Through ARE binding, NRF2 regulates itself and a number of antioxidant genes including the ones described previously, SOD1, SOD2 and catalase peroxide, in addition to genes maintaining homeostasis such as NADPH:quinone oxidoreductase 1 (NQO1) or heme oxygenase 1 (HO-1) and glutathione reductase and glutathione oxidase (Table 1) [33-38]. The nuclear factor 1 (NRF1), is another member of the Cap'n'Collar family of basic region-leucine zipper transcription factors able to bind AREs [39]. The understanding of the role of NRF1 in the antioxidant stress response is not as extended as for NRF2. However, it has been shown that NRF1 and NRF2 have compensatory but also distinct roles in the activation of antioxidant genes [39]. Knockout NRF1/NRF2 mice have elevated ROS levels, but it is not the case for NRF1 or NRF2 single knockout mice. Therefore, the role for NRF1 and NRF2 in the basal expression of antioxidant genes is thought to overlap [40]. Studies have shown that silencing NRF1 induced an increased expression of NRF2 leading to an increased antioxidant response [39, 41, 42]. Therefore, NRF1 might be a regulator of the NRF2 antioxidant response. Hence, the expression of inducible antioxidant response is thought to be largely dependent on NRF2 [41, 42].

General biochemical function	Symbol	Name
Detoxication: Phase I drug oxidation, reduction and hydrolysis	CBR1	Carbonyl reductase 1
	NQO1	NAD(P)H:quinone oxidoreductase 1
Detoxication: Phase II drug conjugation	SULT1A1	Sulfotransferase family, cytosolic, 1A, member 1
	UGT1A1	UDP glucuronosyltransferase 1 family, polypeptide A1
Detoxication: Phase III drug transport	ABCB6	ATP-binding cassette, subfamily B (MDR/TAP), member 6
Antioxidant: GSH-based system	GSR1	Glutathione reductase
	GLS	Glutaminase
	PRDX1	Peroxiredoxin 1
	TXN1	Thioredoxin
	SOD1/2	Superoxide dismutase 1/2
Carbohydrate metabolism and NADPH regeneration	G6PD	Glucose-6-phosphate 1-dehydrogenase
	UGDH	UDP-glucose dehydrogenase
Heme and iron metabolism	FTH1	Ferritin, heavy polypeptide 1
	HO-1	Heme oxygenase 1
Transcription factors and associated proteins	NRF2	Nuclear factor-erythroid 2-like 2
	PPARPG	Peroxisome proliferator-activated receptor gamma
Ubiquitin ligase substrate adaptor	Keap1	Kelch-like ECH-associated protein 1

Table 1: Genes positively regulated by Nrf2

1.1.1.3 Oxidative DNA damage

Oxidative stress leads to an interaction between ROS and cellular biomolecules such as DNA which causes oxidative DNA damage. ROS can cause more than 20 different DNA base lesions (Table 2). Guanine is the most susceptible DNA base to oxidation due to its lower electron potential. Therefore, 8-Oxo-2'-deoxyguanosine (8-oxodG) is one of the most abundant and best investigated oxidative DNA damage and is considered as the reference in oxidative DNA damage studies. Oxidative DNA damage, is recognized by different DNA repair proteins depending on the DNA base pair oxidized and, if unrepaired, leads ultimately to an accumulation of DSBs [43, 44].

Base oxidized	Oxidized product	DNA repair pathway	Proteins
Guanine	8-Oxo-2'-deoxyguanosine (8-oxodG)	BER	OGG1; MUTYH
		MMR	MSH2, MSH6; MLH1
		NER	
		dNTP pool sanitisation	MTH1, MMR
	2,6-diamino-4-hydroxy-5-formamidopyrimidine	BER	OGG1; NEIL1; NEIL3
	spiroiminodihydantoin	BER	NEIL1; NEIL3
	guanidinohydantioin	BER	NEIL1; NEIL3
Cysteine	hydroxycytosine	BER	NEIL2; NEIL3; NTH1
	5,6-dihydroxycytosine	BER	NEIL1
	5-hydroxyuracil	BER	NEIL2; NEIL3; NTH1
	5,6-dihydrouracil	BER	NEIL2
Adenine	8-hydroxyadenine	dNTP pool sanitisation	MTH1
	4,6-diamino-5-formamidopyrimidine	BER	NEIL1; NEIL3
	2-hydroxyadenine	BER	MUTYH
		MMR	MSH2, MSH6
		dNTP pool sanitisation	MTH1
Thymine	5-hydroxy-6-hydrothymine	BER	NTH1
	thymine glycol	BER	NEIL1; NEIL3; NTH1
		MMR	MSH2
		NER	
	5-hydroxy-5-methylhydantoin	BER	NEIL2; NEIL3

Table 2: DNA repair pathway responsible for oxidative DNA lesions removal

They are four pathways able to repair oxidative DNA damage: dNTP pool sanitisation which repairs the oxidized nucleotide prior its incorporation into DNA; BER, NER and MMR which repair the oxidative nucleotide incorporated into DNA.

1.1.2 Other causes of DNA damage

1.1.2.1 Endogenous DNA damage

Endogenous DNA damage is mainly caused by oxidative stress but also by a range of other endogenous modifications. DNA alkylation, usually DNA methylation, is another cause of DNA damage. An increase in S-adenosylmethionine (SAM), a reactive methyl group donor contributes to DNA methylation. The most frequent lesions due to DNA methylation are N^7-methylguanine (N^7meG) and O^6-methylguanine (O^6meG). Guanine is the most susceptible DNA base to methylation and O^6meG is thought to be the most mutagenic lesion due to nucleotide methylation [45]. N^7meG does not possess cytotoxic properties. The N^3-methyladenine (N^3meA) is the second most abundant alkylation lesion and also the most cytotoxic [45, 46]. N^7meG lesions can cause spontaneous depurination; which is another known cause of endogenous DNA damage and leads to AP sites. AP sites correspond to the cleavage of the glycosidic bond in DNA. Other sorts of DNA damage can also occur endogenously. During DNA replication, DNA mismatches and IDLs can occur. Helix-distorting damage caused by DNA supercoiling (over and under-winding) and ICLs which are the reaction of endogenous and exogenous agents to two different positions in the DNA can occur. The other types of DNA damage are AP sites, SSBs and DSBs which are intermediates in DDR pathways and therefore have various causes [47].

1.1.2.2 Exogenous DNA damage

DNA damage can also be generated exogenously. Most cancer therapies (chemotherapies and radiotherapies) are designed to trigger DNA damage. For example, alkylating agents, such as Temozolomide (TMZ) and N-methyl-N'-nitro-N-nitrosoguanidine (MNNG), cause methylation DNA damage including, N^3meG, N^7meG and O^6meG adducts; platinum compounds, such as Cisplatin, cause ICLs damage; topoisomerase inhibitors, such as Irinotecan, inhibit DNA unwinding and induce persistent SSBs or ICLs; and fluoropyrimidine agents, such as the pyrimidine analogue 5-fluorouracil (5-FU), are misincorporated into DNA and induce an accumulation of nucleotides lesions leading ultimately to DSBs. Radiotherapy leads to a range of DNA damage: mainly DSBs, but also SSBs, ICLs and oxidative DNA damage.

1.2 Mechanism of DNA repair

As discussed above, there is a wide variety of DNA damage that can occur and it is widely present in our cells [18]. The type of DNA damage that occurs will determine which DNA repair pathway is recruited to prevent genomic instability. DNA damage can be categorized in two groups: single stranded DNA damage, including SSBs and nucleotides damage (methylation, oxidation, mismatch, AP sites, intra-cross links, ICLs); and DSBs (Figure 2).

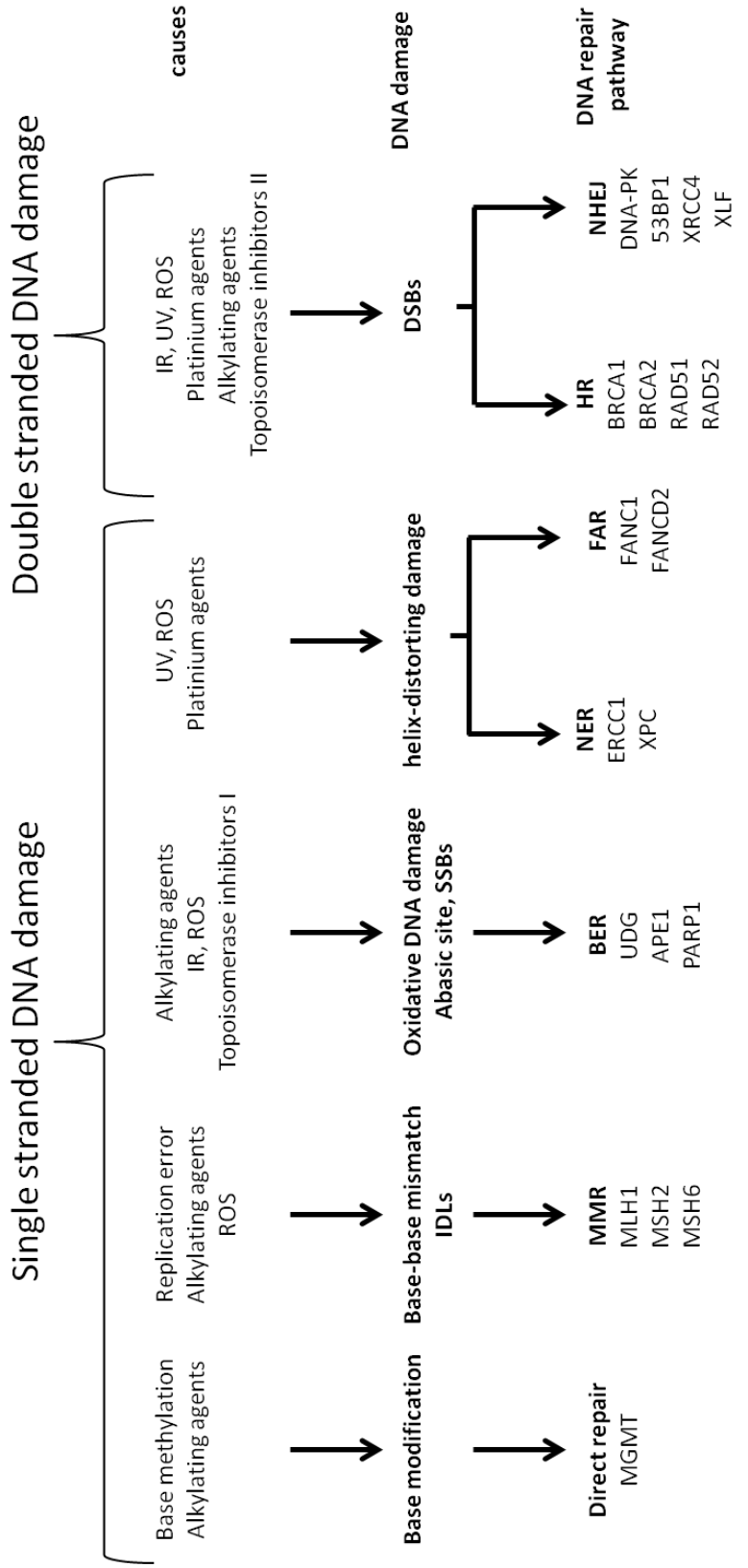

Figure 2: DDR pathways recruited for the repair of a range of DNA damage
They are two main families of DNA damage: single stranded DNA damage and double stranded DNA damage. They can be both induced endogenously or exogenously and be repaired by a range of DNA damage repair pathways.

1.2.1 Single stranded DNA damage

There is a range of DNA damage repair pathways able to repair single stranded damage. The recruitment of a specific DNA repair pathway will depend on the DNA adduct itself. All the DNA repair pathways, except direct repair, can process and repair single stranded damage in 4 steps: recognition, excision, resynthesis and ligation.

1.2.1.1 Direct repair

Direct repair is the simplest DNA repair pathway by directly reversing the lesion. It is the only pathway that does not need excision, resynthesis and ligation of DNA. The O^6meG lesions are removed by O^6meG DNA methyltransferase (MGMT) through the irreversibly transfer of the alkyl groups to nucleophilic cysteine residues in repair proteins. If not repaired, O^6meG lesions could trigger O^6meG:C to A:T transitions [45, 46, 48].

1.2.1.2 Mismatch repair (MMR)

MMR is the primary pathway responsible for the repair of base-base mismatches and IDLs that occur during DNA replication. This is the only DNA repair pathway able to recognize the lagging strand from the leading strand and therefore recognize the erroneous nucleotide in a mismatch [49]. The mechanism of MMR will be discussed in greater detail in section 2.1.

1.2.1.3 Base excision repair (BER)

BER is responsible for the repair of uracil misincorporation, oxidized base (Table 2), alkylated bases, deaminated bases, AP sites and SSBs. N^7meG is the most abundant product of alkylation damage. It is relatively innocuous; however, it is prone to spontaneous depurination leading to AP sites repaired by BER.

The damaged bases are recognized and removed by BER glycosylases to form AP sites [50]. There is a wide variety of DNA glycosylases involved in BER (Table 3) [51]. Two enzymes are responsible for the repair of 8-oxodG lesions: 8-oxodG glycosylase (OGG1) and mutY Homolog (*E. coli*) (MUTYH) [52, 53]. OGG1 is responsible for the repair of 8-oxodG:C to G:C; however, MUTYH is responsible for the repair of 8-oxodG:A mismatch to 8-oxodG:C. Therefore, MUTYH can prevent

the mutagenic transition of 8-oxodG:C to A:T by repairing the mismatch and giving time for OGG1 to repair the oxidized nucleotide. Other enzymes such as uracil-DNA glycosylase (UDG) [54], thymidine-DNA glycolase (TDG) [55], single-strand selective monofunctional uracil DNA glycosylase (SMUG1) [56] and methyl-CpG-binding domain protein 4 (MBD4) recognize and cleave a number of specific DNA lesions [57]. Redundancy amongst the BER glycosylases has been shown by knocking out the different enzymes *in vivo*. Only double or triple knockout mice displayed severe phenotypes [58-61]. For example MUTYH/OGG1 knockout mice have a shortened life span and are more prone to develop cancer in comparison with single knockout mice [62].

Symbol	BER glycosylase	Substrates
OGG1	8-oxoguanine glycosylase	8-oxodG:C; 7meG:C
MUTYH	mutY Homolog (*E. coli*)	8-oxodG:A
UNG	uracil-DNA glycosylase	U:G
TDG	thymidine-DNA glycolase	T:G; thymine glycol:G; U:G
SMUG1	single-strand selective monofunctional uracil DNA glycosylase	U; 5-hydroxyuracil; 5-formyluracil; 5-hydroxymethyluracil
MBD4	methyl-CpG-binding domain protein 4	T:G; T:T; T:C; U:G
NTH1	ntu endonuclease III-like 1	Tg; 5-oxodC; 5-oxodU
NEIL1	nei endonuclease VIII-like 1	FapyA; FapyG; Tg; 5-oxodU; 5-oxodC
NEIL2	nei endonuclease VIII-like 2	5-hydroxy-5-methylhydantoin
NEIL3	nei endonuclease VIII-like 3	FapyA; FapyG; Tg
MPG	methyl adenine glycosylase	3-meA

Table 3: BER glycosylases recognize different substrates
BER is implicated in the repair of a range of DNA damage and in red are represented the DNA base recognized by the different BER glycosylases.

After the damaged base is recognized and removed by BER glycosylases, the formed AP sites are recognized by AP endonuclease 1 (APE1) which generates SSBs [63]. SSBs are then repaired by the short-patch BER (one nucleotide replacement) or the long-patch BER (2-13 nucleotides replacement) [64]. The first step for both patches consists of DNA resynthesis by DNA polymerases (DNA pol). DNA pol β is implicated in the short-patch BER and DNA pol δ and ε are mediators for the resynthesis during long-patch BER [65]. The resynthesis step is followed by DNA ligation mediated by DNA ligase III for the short-patch and DNA ligase I for the

long-patch BER [66]. Poly(ADP-ribose) polymerase 1 (PARP1) has a major role in BER mediated SSB repair by facilitating the recruitment of repair enzymes such as the X-ray repair cross-complementing protein 1 (XRCC1) to form a PARP1-XRCC1-DNA pol β-DNA ligase III complex required for the short-patch BER [67]; and Flap endonuclease 1 (FEN1) for the long-patch BER [68]. Oxidative DNA damage is described as the main cause of endogenous DNA damage; therefore, BER is thought to be a critical pathway of DDR [69].

1.2.1.4 Nucleotide excision repair (NER)

NER removes helix-distorting damage such as intra-cross links caused by UV; but also plays a role in the repair of ROS-induced damage (Table 2) [70]. There are two types of NER pathways: the global genome NER (GG-NER) and the transcription-coupled NER (TC-NER). They only differ in the damage recognition step [70]. The GG- NER consists of a scan of the entire genome by xeroderma pigmentosum group C (XPC) to recognize helix distortion [71]. The TC-NER is recruited when the RNA polymerase II is stalled by a lesion during transcription [72]. After recognition of a helix distortion, the DNA up-stream and down-stream of the damage is removed by the excision repair cross-complementing protein 1 (ERCC1) leading to SSBs (around 30 nucleotides long), that are repaired by DNA pol δ and ε and DNA ligase I or III [70, 71, 73]. The role for NER in ROS-induced damage repair is controversial. It is unclear whether RNA polymerase II is stalled at oxidative DNA lesions [74]. However, only cells deficient in TC-NER (and not cells deficient in GG-NER) are sensitive to oxidative DNA damage [70].

1.2.1.5 Fanconi anemia repair (FAR)

FAR is not an independent DNA damage repair pathway but it is involved in ICLs repair and in NER and HR pathways [75]. This is the least understood pathway of the DDR. A core complex comprising 8 proteins (FANCA/B/D/E/F/G/L/M) is activated by ICLs and monoubiquitinates FANCD2 and FANC1. They play a platform role for the recruitment of endonucleases. Unhooking of the ICL by dual incision of the DNA strand is followed by the recruitment of translesion synthesis (TLS), NER and HR pathway proteins [76, 77].

1.2.2 Double strand breaks repair (DSBs)

DSBs can be directly induced by IR, or indirectly by accumulation of DNA lesions or collision of replication forks with SSBs. Single stranded DNA damage can be repaired with the help of the opposite strand as a template, which is not possible in case of DSBs making them the most deleterious DNA damage. There are two mechanisms for DSB repair: NHEJ and HR. NHEJ is active throughout the cell cycle, however, HR activity is restricted to S-phase [78, 79].

1.2.2.1 Non-homologous end joining (NHEJ)

NHEJ is the predominant pathway for the repair of DSBs, considered to account for more than 80 % of IR-induced DSBs repair [80, 81]. NHEJ is active throughout the cell cycle. It is an error-prone pathway as it drives direct joining of the two broken ends. DSBs are recognized by the proteins Ku70 and Ku80. They recruit DNA-dependent protein kinase catalytic subunit (DNA-PKcs) which is part of the phosphatidylinositol 3-kinaserelated kinase (PIKK) family. Ku70, Ku80 and DNA-PKcs form the DNA-PK complex for DBS stability, followed by the recruitment of p53 binding protein 1 (53BP1) for DBS resection prevention. Subsequently, DNA ligase IV, X-ray repair cross-complementing protein 4 (XRCC4) and XRCC4-like factor (XLF) ligate the broken ends to complete repair [82]. This pathway is essential in DSBs that do not occur during the S-phase of the cell cycle but it is also important in the process of the immune response for the development of a wide range of antibodies [83].

1.2.2.2 Homologous recombination (HR)

HR is the preferred pathway during S-phase since it is an error-free pathway. It takes place in 3 steps: end resection, strand invasion (DNA end-pairing or single-strand annealing) and resynthesis. The first step of the pathway is the resection of the DSB, which corresponds to the excision of the 5’ ends of the break, for accurate resynthesis of the damaged DNA using the non-damaged sister chromatid to serve as a template for repair. This step involves the MRE11-RAD50-NBS1 (MRN) complex which initiates the repair; and the BRCA1-BRCA2-PALB2 complex, composed of BRCA1, BRAC2, and partner and localizer of BRCA2 (PALB2) [84]. This complex is essential for RAD51 recruitment which is involved in the second step of the

pathway, the DNA end-pairing. Thereby, RAD51 mediates the search for homologous sequence on the sister chromatid to initiate the DNA resynthesis step [85]. An alternative model, called the single-strand annealing, does not use a sister chromatid, is RAD51 independent but depends on RAD52 for DNA ends annealing using sequence homologies of the complementary strand for DNA resynthesis [86].

1.2.3 Translesion synthesis (TLS)

TLS is a DNA damage tolerance process able to bypass damaged bases that stall replication forks. Under certain circumstances, it is favourable for the cell to bypass the damage and to repair it at a later time point in order to prevent the damaged bases to become DSBs. At an unrepaired DNA lesion site, TLS switches the regular DNA polymerase with a TLS polymerase. The main TLS polymerases are η, κ and Rev1. They are characterized by a larger active site to facilitate DNA synthesis over a damaged nucleotide. TLS polymerases have a poor processivity and low fidelity and are only used to bypass DNA damage [87]. Cells switch polymerases through proliferating cell nuclear antigen (PCNA). The ubiquitin conjugase Rad6 and the ubiquitin ligase Rad18 are recruited to stalled replication forks where they catalyze monoubiquitylation of PCNA at Lys164. TLS polymerases have increased affinity for monoubiquitylated PCNA, which facilitates their recruitment and the completion of TLS. The E3 ubiquitin-protein ligase SHPRH and the helicase-like transcription factor (HLTF) are thought to be involved in the switch back to error-free polymerases by restoring PCNA ubiquitylation status, which blocks TLS polymerases and activates error-free polymerases [88-90].

1.3 DNA damage signalling and cell cycle arrest

The DNA damage signalling pathways will recognize the DNA damage and recruit the appropriate DNA damage repair pathway and the cyclin-dependent kinases (CDKs) required for cell cycle arrest to allow time for repair.

1.3.1 Cell cycle

The cell cycle is the process of cell division and replication to obtain two identical daughter cells. It is divided in 4 phases, gap 1 (G1), synthesis (S), gap 2 (G2) and mitosis (M). S-phase is the replication phase (DNA synthesis), and M-phase is the

physical cell division phase. G1 and G2-phases are two important phases to monitor and ensure that the cells are ready to enter S and M-phase respectively. In the case where cells are not in a favourable condition for cell division, there is a cell cycle arrest [91-93]. As soon as the cell is ready and damage has been repaired, the cell cycle is resumed but, if the damage persists, the cells will undergo apoptosis through the activation of p53 [94].

1.3.2 DNA damage signalling

One of the main causes of cell cycle arrest is the presence of DNA damage [78]. DDR requires regulation of cell cycle checkpoints to allow time for repair. Ataxia telangiectasia mutated (ATM) and ATM and Rad3-related protein (ATR) are part of the PIKK family. They are two crucial proteins for the recruitment of DNA damage repair pathways (Figure 3) [95]. ATM is activated by the MRN complex, itself activated by binding DSBs [96]. ATM phosphorylates the histone H2A.X (γH2AX) which localize to the DSB, this is a crucial step for the recruitment of other DDR proteins [97]. ATM also phosphorylates the checkpoint kinase 2 (Chk2), which then either activates CDKs responsible for an S-phase arrest of the cell cycle, leading to HR repair. ATM can also recruit 53BP1 and cyclins responsible for a G1-phase arrest in the cell cycle leading to a NHEJ repair. ATR, the other kinase required for DNA damage signalling, is activated by ATR Interacting Protein (ATRIP), itself activated by SSBs or DNA replication fork collapse. It phosphorylates checkpoint kinase 1 (Chk1) leading to an S and G2/M-phase arrest of the cell cycle which gives time to the cell to repair the damage. It also recruits FAR for ICLs repair and BRCA1, RAD51 for HR repair [78, 98]. If the damage is repaired, the cells can resume their cell cycle. If the damage is too extreme for repair and therefore persists, the cells can undergo apoptosis through the activation of p53 [94]. ATM and ATR recruit Chk1 and Chk2 respectively, but the two pathways are not mutually exclusive and might be compensatory to ensure DNA damage repair [99].

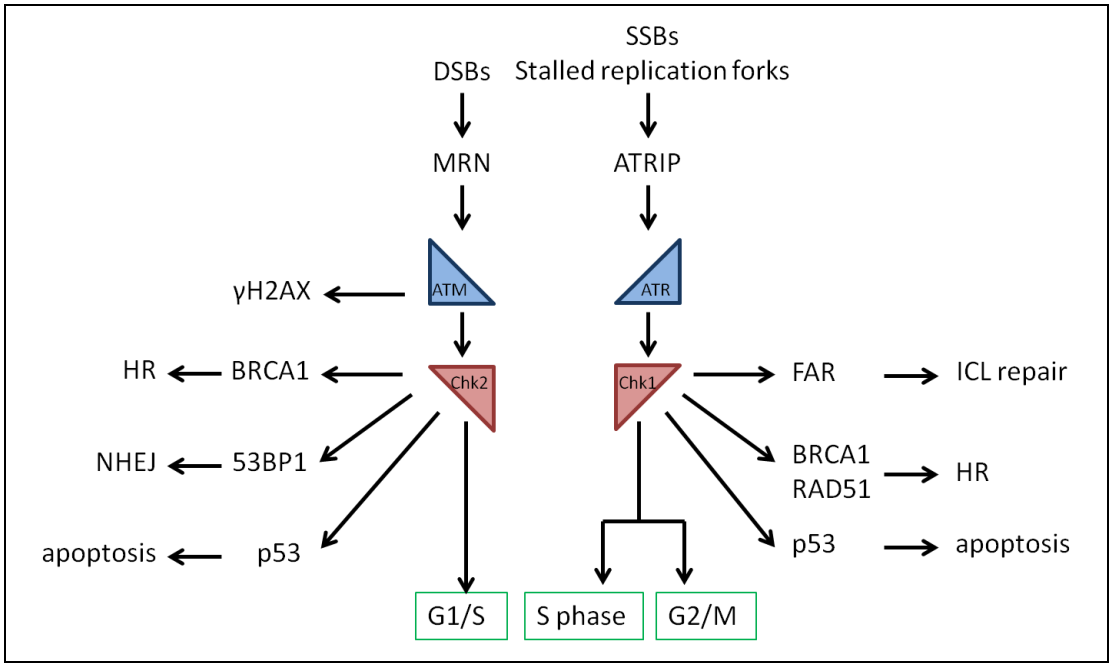

Figure 3: DNA damage signalling pathway

ATM is the enzyme responsible for DSBs signalling and ATR is the enzyme responsible for SSBs signalling. Their activation leads to the recruitment and activation of Chk2 and Chk1 responsible for the recruitment of proteins for cell cycle arrest and DNA damage repair.

1.4 Oxidative stress in cancer therapy

Oxidative DNA damage is a cause major of DNA damage and can be caused by an increase in ROS levels and/or a decrease in antioxidant response [19, 20]. ROS is naturally increased in cancers to promote tumour progression and development. An increase in ROS levels can act to induce tumour development by promoting cell cycle progression, proliferation, cell survival and energy metabolism [22, 23]. For example, ROS have been shown to up-regulate the transcription of cyclins to facilitate G1/S transition of the cell cycle [100]. However, an excessive increase in intracellular ROS levels (by chemotherapeutic treatment for example) can act as a tumour suppressor [22, 23]. Conversely, antioxidants inhibit tumour progression and excessive antioxidant response promotes tumour growth [101, 102]. For example, over-activation of NRF2 directly increases B-cell lymphoma 2 (Bcl2) protein expression, causing apoptosis inhibition; but also drug resistance and cell proliferation (Table 1) [101, 102]. As NRF2 is highly expressed in cancer cells, it represents an interesting chemotherapeutic target [25].

The role of oxidative stress in cancer has been exploited in the development of new chemotherapeutic strategies. Oxidative stress can be caused directly or indirectly [21]. For example, buthionine sulfoximine is a direct inhibitor of glutamate-cysteine ligase leading to an inhibition of glutathione synthesis [103]. Buthionine sulfoximine has been tested in phase I clinical trial for the treatment of children with neuroblastoma (NCT00002730). Phenylethyl isothiocyanate also depletes glutathione levels and has been used in phase I clinical trial as a preventive treatment of lung cancer in smokers (NCT00005883) [104]. Other drugs can cause oxidative stress indirectly. For example, one of the strategies to treat pancreatic tumours is a combination of drugs, including Gemcitabine, that all indirectly induce intracellular ROS levels to trigger apoptosis [23]. Sulindac, a FDA-approved non-steroidal anti-inflammatory drug, enhances intracellular ROS levels and has been used in phase II clinical trial for the treatment of healthy participants with increased risk of developing melanoma (NCT00841204) [105]. Other treatment such as 5-FU and IR can also induce oxidative stress indirectly [21].

NRF2 is the main mediator of the antioxidant response. Its role in cancer development and progression has been exploited in the clinic by two different strategies: NRF2 activation to prevent tumour development and NRF2 inhibition to prevent chemo-resistance and tumour progression. For example, the synthetic NRF2 inhibitor IM3829 has been shown to increase IR response in the treatment of lung tumours *in vitro* and *in vivo* [106]. Taken together, oxidative stress, a major cause of endogenous DNA damage, has a critical role in cancer development and progression; therefore, modulation of the cellular oxidative stress represents an interesting therapeutic strategy.

1.5 DNA damage response in cancer therapy

A large proportion of current cancer therapies have been designed to induce DNA damage. Deregulation of DDR, by activation or inactivation, has been found in various cancers [13, 14] and can often confer higher sensitivity to chemotherapy. Therefore, therapeutic strategies targeting the different proteins involved in DDR have been developed and translated into clinic in order to enhance therapy response (Table 4) [15, 17]. The over-expression of MGMT has been identified as the main mechanism of resistance in TMZ treatment [107]. O^6-benzylguanine is one of the

most potent MGMT inhibitors available. However, inhibition of MGMT is toxic in non-cancer cells by leading to myelosuppression [108]. Novel approaches have been developed to counteract MGMT inhibition induced side effect such as coupling MGMT inhibitors to D-glucose to specifically target cancer cells that are known to have higher glucose consumption [109]. Mutations in BER pathway, for example in DNA pol β, have been associated with a range of cancers [110, 111]. The most advanced therapeutic strategies targeting BER are APE1 inhibitors and PARP1 inhibitors. These two enzymes are generally highly expressed in tumours. The inhibition of APE1 or PARP1 increases IR and alkylating agent sensitivity [112-115]. Defects in NER, also called xeroderma pigmentosum, causes skin cancer development, and leads to UV and platinum agent sensitivity [116-118]. Fanconi anemia (FAR deficiency) is a disorder leading predominantly to acute myeloid leukemia [119]. It has been shown that the loss of at least one of the FAR genes triggers increased sensitivity to ICLs damage [76]. Defects in NHEJ have also been associated with cancer [120-122]. The inhibition of DNA-PKcs has shown to induce IR sensitivity [123]. HR is essential for genomic stability. HR defects are associated with IR and crosslinking agent sensitivity [124].

DNA damage signalling has also been associated with cancer. Increased expression and activation of the ATR/ATM dependent pathways are reported to be associated with cancer [15, 97]. The development of MRN, ATM, ATR, Chk1 and Chk2 inhibitors have been under investigations [15, 99, 125]. It is difficult to develop an inhibitor that targets specifically Chk1 and/or Chk2 with not multiple kinase targets [125]. Chk1/Chk2 double knockout mice are tumour prone, therefore it is arguable to use inhibitors of Chk1/Chk2 as chemotherapy [126]. However, recent studies have shown promising preliminary results in the development of Chk1 or Chk2 inhibitors; with, for example, the development of CCT244747, an orally bioavailable Chk1 inhibitor which showed promising response as a single agent or in combination with Gemcitabine and Irinotecan *in vivo* [127]. TP53, the gene coding for p53 protein, is considered to be mutated or inactivated in all cancer tumours [128]. TP53 inactivation confers radiotherapy and chemotherapy resistance [129]. Molecules, such as APR-246, targeting p53 mutations able to re-express its function have been developed and tested in phase I/II clinical trial with promising results [130].

Inhibition of direct repair, BER, NER, FAR, NHEJ, HR and ATM/ATR pathways have been associated with increased sensitivity to therapeutic treatments. However, this is not the case for MMR pathway. Defect in MMR pathway has been observed in a wide range of cancers and results in a mutator phenotype leading to cancer development [49, 131]. Numerous studies agree that MMR deficient tumours are resistant to a wide range of chemotherapeutic agents. These include methylating agents, platinum compounds and fluoropyrimidine agents [132-134]. Therefore, targeting this pathway would be a striking novel therapeutic strategy in cancer treatment [135, 136].

Pathway	Protein target	Inhibitors	Combinations	Cancer type	Stage in clinic	Clinical trial number / References
Direct repair	MGMT	Lomeguatrib	TMZ	Metastatic colorectal cancer	Phase II	[137]
BER	PARP	Olaparib	paclitaxel	Gastric cancer	Phase II	NCT01063517
	APE1	TRC102	pemetrexed	Advanced or metastatic solid cancer	Phase I	NCT00692159
NER	ERCC1	Cetuximab	Oxaliplatin/5-FU/ FA/Irinotecan	Metastatic colorectal cancer	Phase II	NCT00422773
DNA damage signalling	Chk1	LY2603618	Pemetrexed and Cisplatin	Non Small Cell Lung Cancer	Phase I/II	NCT01139775
	Chk1/Chk2	AZD7762	Gemcitabine	Advanced Solid Malignancies	Phase I	NCT00413686
	p53	APR-246	Carboplatin	Ovarian cancer	Phase I/II	NCT02098343

Table 4: Examples of completed clinical trials of DDR inhibitors

2 DNA mismatch repair

2.1 DNA mismatch repair pathway

MMR is the pathway responsible for the repair of base-base mismatches (G:T, G:A, G:G, C:A, C:T, A:A and T:T) and IDLs that occur during DNA replication [138]. The recognition of base-base mismatches and short IDLs is carried out by MutSα, an MSH2-MSH6 heteroduplex, while the recognition of large IDLs is carried out by MutSβ, an MSH2-MSH3 heteroduplex [139]. MutSα and MutSβ have distinct functions but have also redundant roles [140]. When MutS (α or β) binds to the DNA, it forms a sliding clamp, able to translocate in either direction on the DNA until it recognizes a mismatch [141]. This recognition alters the MutS conformation in an ATP-dependent manner, allowing recruitment of MutL to form an ATP-dependent ternary complex. MutL, another MMR-associated heteroduplex, is always composed of MLH1 with another protein: either PMS2 (MutLα), PMS1 (MutLβ) or MLH3 (MutLγ). MutLα is the most prominent MutL complex and plays the most important role in MMR. MutLβ function is not yet known but it might play a backup role with MutLγ for MutLα [142, 143]. MutLγ is the only MutL complex with a role in meiotic recombination [144]. In the MMR pathway, when MutLα is complexed with MutS, it acts as an endonuclease [145]. MutLα recognizes the lagging strand from the leading strand. The mechanism by which MutLα discriminate the lagging strand is not fully understood. In prokaryotes, the newly synthesized strand is methylated by deoxyadenine methylase (Dam) at the position N6 of adenine in GATC sites which can be recognised by MutLα homolog [146]. Eukaryotes lack methylation in GATC sites therefore the mechanism of discrimination must be different. MutL might recognise the lagging strand by the Okazaki fragments or by the free 3'-terminus on the leading strand. However, pre-existing nicks in the two strands have unequal incidence [142]. Studies have also shown a role for ribonucleotide incorporation into the leading strand as entry sites for MMR; therefore ribonucleotide processing might contribute to the discrimination signal but other mechanisms remain to be elucidated [147-149]. MutL is able to recognize the lagging strand and excise it 5', but also 3', from the mismatch. Exonuclease 1 (Exo1) is recruited to excise nucleotides in a 5'→3' direction [150]. In the case of 3' excision, Exo1 recruits replication factor C (RFC) to perform a 3'→5' excision. Replication protein A (RPA), a binding-factor, stabilizes the single-stranded DNA

and inhibits Exo1 to prevent further degradation [151]. After removing the mismatch, the final step is to resynthetize the excised-DNA by DNA pol δ and to ligate the remaining nick by DNA ligase I. PCNA, required during DNA synthesis for the processivity of the DNA pol, is also required during MMR for mismatch recognition by interacting with MutS [152] and activation of the endonuclease [153] (Figure 4).

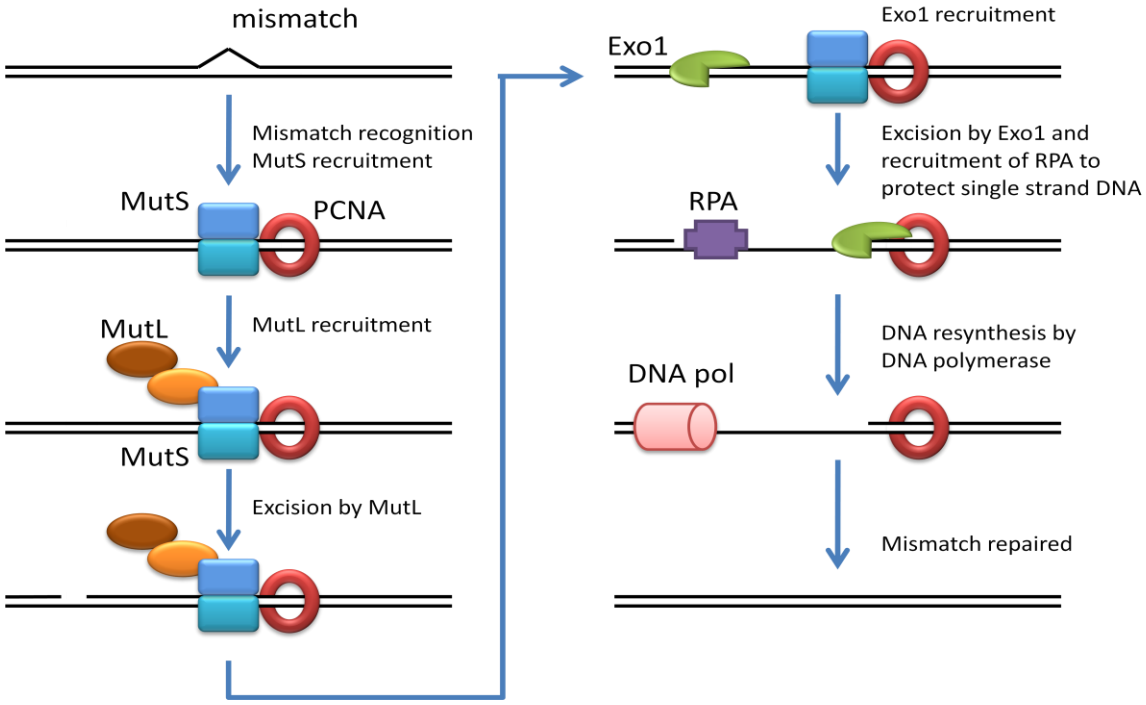

MutSα	MSH2 MSH6	Recognises base-base mismatches and small IDLs
MutSβ	MSH2 MSH3	Recognizes IDLs bigger than 2 nucleotides
MutLα	MLH1 PMS2	repair of base-base mismatches and IDLs; back-up for MutLγ
MutLβ	MLH1 PMS1	unknown
MutLγ	MLH1 MLH3	meiotic recombination; back-up of MutLα
PCNA		Role in initiation and DNA resynthesis steps of MMR
Exo1		exonuclease
RPA		Stabilizes single-strand DNA and inhibits Exo1
DNApol		Resynthesises DNA strand after excision by Exo1

Figure 4: DNA mismatch repair mechanism and role of proteins implicated

2.1.1 DNA mismatch repair mediated apoptosis

MMR is the pathway to repair base-base mismatches and IDLs that occur during replication. MMR can also recognize DNA lesions such as 5-FU and alkylating agents-induced DNA lesions [46, 154]. The MMR pathway is not always able to repair the lesions and subsequently triggers apoptosis. In this case, after recognition of a lesion, MutS recruits MutL, followed by the recruitment of ATM and ATR [155]. These proteins, once activated, recruit DNA damage repair proteins that cause cell cycle arrest with a delay in S-phase progression and an arrest in G2-phase leading to apoptosis via stabilization of p53 [156]. There are currently two models to explain ATM/ATR recruitment by MutS. The first model, called the direct signalling model, proposes that the MutS-MutL complex, after recognition of a lesion, directly recruits ATM/ATR. The alternate model, called the futile cycle model, suggests that MMR can recognize and excise the lesion. However, the continued exposure to DNA damaging agents such as 5-FU or alkylating agents, leads to further damage accumulation due to continuous excision of the adducts during the DNA resynthesis step of MMR, which leads to repeated cycles of MMR. The accumulation of lesions into DNA, and therefore, the initiation of the MMR process results in the formation of DNA strand breaks, that initiate the recruitment of ATM/ATR (Figure 5) [157]. Cell cycle arrest has been shown to occur during the first cell cycle after 5-FU and alkylating treatment; furthermore, a direct interaction between MSH2 and ATR has been identified [46, 158, 159]. These results support the direct signalling model, however, it is likely that both models are not mutually exclusive and might be compensatory to ensure apoptosis is initiated [156].

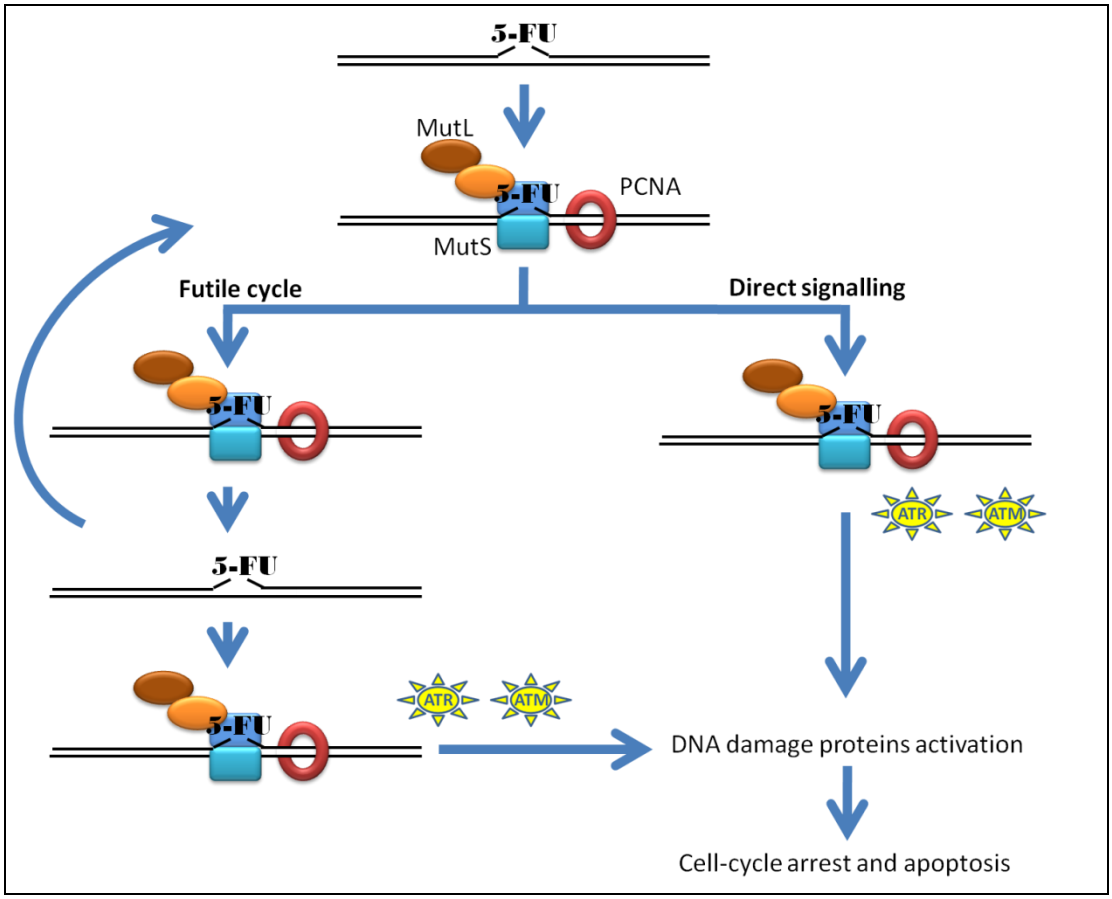

Figure 5: DNA lesions recognized but unrepaired by MMR pathway trigger apoptosis

When MMR pathway is not able to repair a lesion it recruits ATR/ATM through two possible mechanisms: either by direct recruitment or futile cycles of MMR. In both cases, ATR/ATM recruitment initiates cell cycle arrest and apoptosis.

2.2 MutSα structure and function

MutSα is the main complex of the MMR pathway required to recognize DNA damage. MSH6 protein was first described as an MSH2 partner in 1995 [160]. MSH6 and MSH2 have similar structures divided in 5 domains with the exception of an additional N-terminal disordered domain for MSH6 [139, 161]. MutSα dimerizes as an asymmetric mirror image with each domain (1-5) juxtaposed. Domain 1 is the DNA mismatch binding domain; domain 2 is a connector; domain 3 is a lever; domain 4 is a clamp region for unspecific DNA binding and domain 5 is an ATP binding domain (Figure 6). The precise mechanistic role of ATP binding and hydrolysis is not yet completely understood, however, the domain 5 is likely involved in altering MutSα structural conformation and DNA binding activity [162].

The N-terminal disordered domain of MSH6 contains 389 amino acids upstream of domain 1. Several activities dependent on this N-terminal domain unique to MSH6 have been identified but are still not fully understood [162]. It contains three nuclear localization sequences (NLSs). Transport to the nucleus is believed to occur only after dimerisation of MutSα in the cytosol as MSH2 does not contain an NLS and the level of MSH2 in the nucleus decreases in cells lacking MSH6 [163]. The N-terminus of MSH6 also has a motif allowing interaction with PCNA. PCNA is an essential DNA replication sliding clamp for various DNA replication and repair pathways. PCNA is required for MMR at the pre-excision step and during DNA resynthesis [164]. It initiates MMR by coordinating the MutSα directionality at the replication fork in an N-terminal MSH6 dependent manner [165].

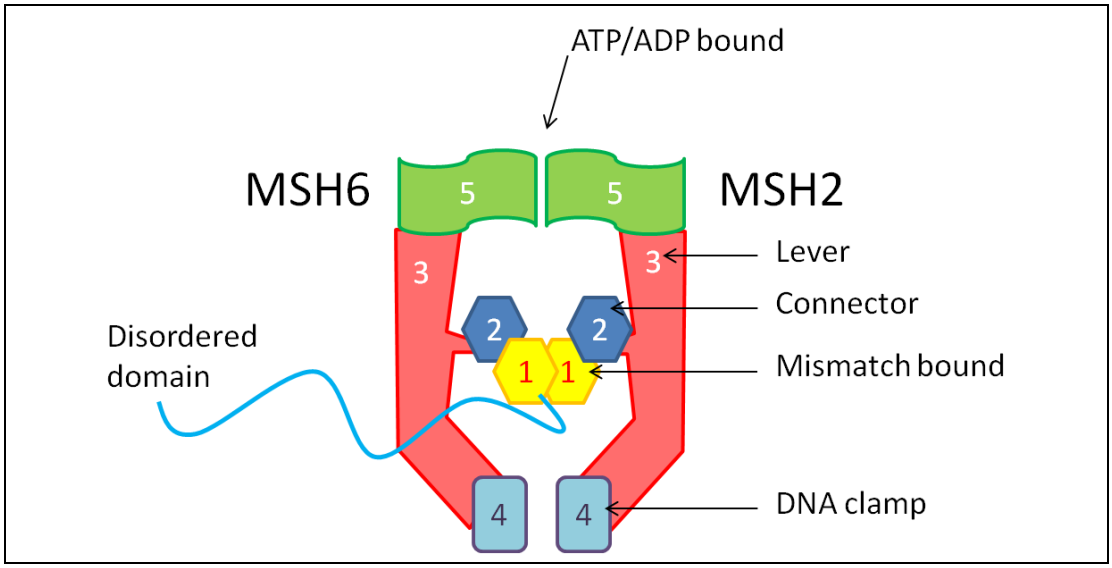

Figure 6: Structure of MutSα heterodimer
MSH2 and MSH6 proteins have 5 domains: domain 1 is the DNA mismatch binding domain; domain 2 is a connector; domain 3 is a lever; domain 4 is a clamp region for unspecific DNA binding and domain 5 is an ATP binding domain. MSH6 also have an N-terminal disordered domain.

2.3 Non-canonical role for DNA mismatch repair

We have previously detailed the canonical mechanism of MMR pathway in repairing replicating errors. In addition, a number of non-canonical roles for the MMR pathway have been identified. Such that, MMR has been implicated for example in

oxidative DNA damage, O^6meG, ICLs and DSBs repairs but also in chromatin assembly and immunoglobulin diversification (Figure 7) [166].

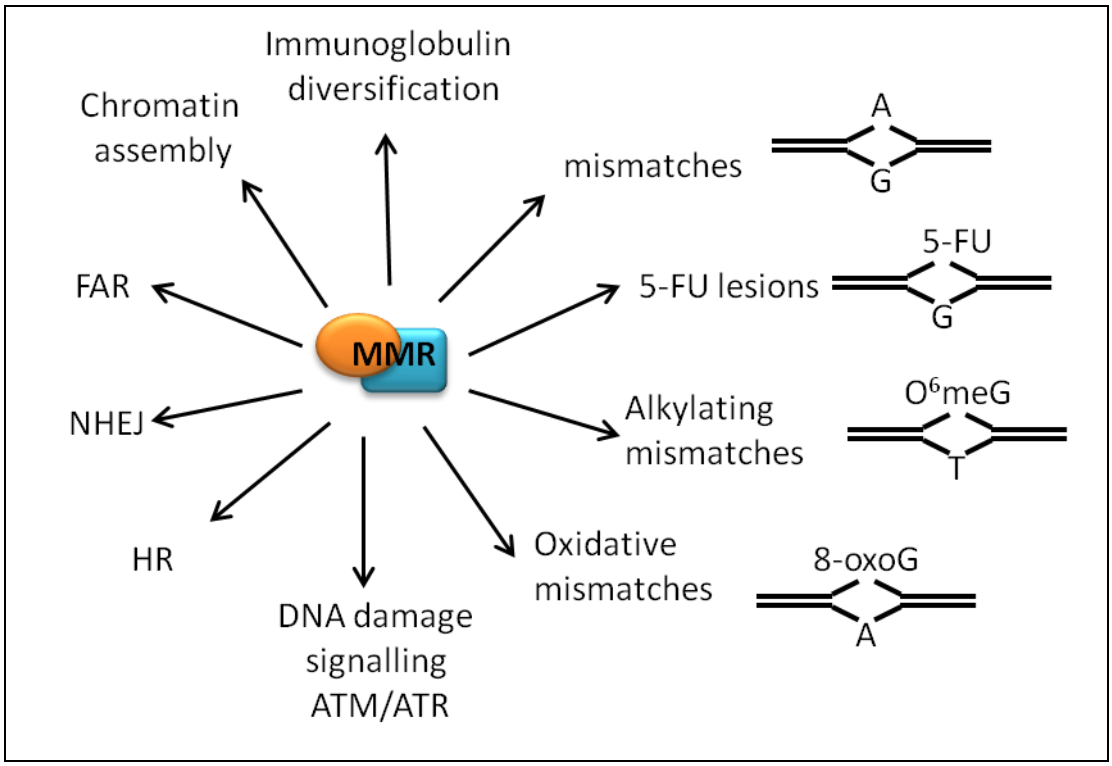

Figure 7: Different roles for MMR pathway
MMR is the pathway responsible for the repair of base-base mismatches and IDLs that occur during DNA replication. It also recognizes 5-FU lesions, alkylating and oxidative mismatches. MMR has non-canonical roles in DNA damage signalling, HR, NHEJ and FAR pathways; in chromatin assembly and in immunoglobulin diversification.

2.3.1 DNA mismatch repair and oxidative stress

Oxidative DNA damage is the primary cause of endogenous DNA damage. It is repaired by BER, NER but also MMR. Numerous studies report a link between oxidative DNA damage and MMR. The baseline 8-oxoG levels were shown to be higher in DNA extracted from MSH2 and MLH1 deficient cell lines compared to MMR proficient cell lines [167]. It has also been shown that MSH2 deficient embryonic stem (ES) cells treated with low doses of IR, accumulated more ROS-induced damage (8-oxodG and thymine glycol) compared to the wild type control [168]. The role for MMR in 8-oxodG repair has been further elucidated. MutSα but not MutSβ can recognize 8-oxodG mismatches. MutSα has a high affinity for 8-

oxodG mismatches and no affinity for 8-oxodG:C. MutSα evaluated affinity for 8-oxodG mismatches was 8-oxodG:T > 8-oxodG:G > 8-oxodG:A > 8-oxodG:C ≈ G:C [169, 170]. 8-oxodG mismatches, if not repaired can lead to the mutagenic T:A transition. Earley *et al.* observed that the mutation rate associated with MMR deficiency could be reduced by growing *S. Cerevisiae* under anaerobic conditions. These observations suggest a role for oxidative stress and more precisely for the mismatches occurring opposite oxidized bases in MMR associated mutation rate [171]. As previously mentioned, MUTYH plays a role in the repair of 8-oxodG:A mismatches. Evidence has been reported that MUTYH interacts with MSH6 [172] and that silencing MSH2, MUTYH or both have the same effect on 8-oxodG levels in comparison with the wild type mouse embryo fibroblasts (MEF) suggesting a shared pathway for MMR and MUTYH in 8-oxodG:A repair [173]. Therefore MUTYH and MMR can repair 8-oxodG:A mismatches to 8-oxodG:C, that can then be recognized and repaired by OGG1. Another important enzyme for the detoxification of oxidative DNA bases is MTH1. Over-expression of MTH1 has been shown to decrease genomic 8-oxodG. It has also been shown that MTH1 can decrease oxidative DNA damage with a greater extent in MSH2 deficient cells compared to MSH2 proficient cells, triggering a decrease in spontaneous mutation rate [167, 168]. Moreover, MMR also have a specific role for the recruitment of TLS polymerases to bypass oxidative damage during replication. Monoubiquitinated PCNA and TLS polymerase η recognize oxidative DNA damage in a BER independent and MutSα dependent manner [174]. Therefore, MMR pathway is important in the repair of oxidative stress-induced DNA damage.

2.3.2 DNA mismatch repair and direct repair

Cells proficient in MMR and deficient in MGMT, the main enzyme for the direct repair of O^6meG, are highly sensitive to alkylating agents by undergoing MMR dependant lethal G2-phase arrest. Cells deficient in MGMT are not able to directly repair O^6meG lesions which leads to an accumulation of O^6meG:T mismatches recognized by the MMR pathway, leading to apoptosis. Cells that are MGMT and MMR deficient have a high tolerance for O^6meG lesions and high mutation rate due to O^6meG:C → O^6meG:T → A:T transitions. Therefore, MMR is required for the

repair of O^6meG:T into O^6meG:C, to enable cells to enter another cell cycle in order to repair O^6meG adducts [175, 176].

2.3.3 DNA mismatch repair and DNA double strand breaks repair

In addition, MMR proteins have been implicated in DSB repair. After IR treatment, MSH6 interacts with KU70, a NHEJ repair protein, and colocalizes with γH2AX [177]. Defects in MSH6 result in an impaired NHEJ repair pathway and an accumulation of IR-induced DSBs, therefore suggesting a potential role for MSH6 in NHEJ dependent DSBs repair [177]. MutSα also has a role in HR-dependent IR-induced DSBs repair by suppressing recombination with mismatched DNA [178, 179]. In *S. cerevisiae*, the MMR pathway plays a role in the RAD51-dependent recombination fidelity. Therefore, MMR plays an important role in the high fidelity associated with HR. However, the detailed mechanism is still unclear [178-181].

2.3.4 DNA mismatch repair and Fanconi anemia

MSH2 and MLH1 have been found to interact with FAR proteins such as FANCD2 [182]. MMR deficient cells exhibit an ICL repair defect, through the inhibition of FAR recruitment. Unexpectedly, defects in both MSH2 and MLH1, restore the FAR pathway and can confer resistance to ICLs. One report has measured MMR and FAR proteins in 206 CRC patients and identified that only 5 % of the cohort had a defect in both FAR and MMR pathways [182]. FANCD2 or MLH1 knockout mice are viable but FANCD2/MLH1 double knockout mice displayed embryonic lethality [183]. Taken together, these reports suggest a vital cross-talk between the MMR and FAR pathway and a key role of the interactions between MMR and FAR proteins in these pathways [184, 185].

2.3.5 DNA mismatch repair and immunoglobulin diversification

Our immune system constantly develops new antibodies to combat antigens. Low affinity antibodies are diversified when exposed to antigens through the activation-induced deaminase (AID) which converts cytosines to uracils followed by mutagenic process involving the TLS DNA pol η, BER, MMR and NHEJ. The G:U mismatches are recognised by BER and MMR; if repaired, DNA pol η introduces further

mutations during the resynthesis step; if not repaired, BER and MMR generate DSBs that are repaired with the low fidelity NHEJ pathway creating recombination. Mutations in MMR pathway have been shown to affect the immunoglobulin diversification process [166, 186].

2.3.6 DNA mismatch repair and chromatin assembly

A crosstalk between chromatin assembly and MMR pathway has been proposed to extend the time-frame for MMR after replication [162]. This crosstalk is through the interaction of the histone chaperone chromatin assembly factor 1 (CAF1) and the N-terminal domain of MSH6, in S-phase of the cell cycle [187]. The histone mark H3K36me3 can also interact and recruit MSH6, via its N-terminal domain, to chromatin in early S-phase before DNA replication [188]. Furthermore, data suggest that histone acetylation and deacetylation cooperate with MMR in mutation and chromosome rearrangement avoidance [189]. In addition, inhibition of SET domain containing 2 (SETD2), the enzyme responsible for H3K36 trimethylation, has shown conflicting data with regards to induction of MSI in clear-cell renal carcinomas [190, 191]. A first report identified that cells lacking SETD2 displayed MSI *in vitro* [190]. More recently, a bioinformatic study did not validate a correlation between SETD2 mutations and MSI in renal cancer tumours which might be explained by an *in vivo* adaptation mechanism to prevent MSI induced by SETD2 [191]. Therefore, MSH6 has a potential role in the crosstalk between MMR pathway and chromatin assembly and further investigations to understand better this crosstalk is necessary.

2.3.7 DNA mismatch repair and cell cycle

There is emerging evidence for role of the MSH6 N-terminal domain in MMR-dependent cell cycle progression [192]. In the MSH6 N-terminal domain, 22 distinct phosphorylation sites of MSH6 were identified, including cyclin-dependent kinase 2 (CDK2), ATM/ATR and Aurora kinases binding sites [192]. CDK2 is a member of the cyclin-dependent kinase family essential for the G1/S transition of the cell cycle [193]. Aurora kinase family is composed of AURKA, AURKB and AURKC and plays an important role during the different phases of the mitosis [194]. These phosphorylation sites in MSH6 suggest a potential crosstalk between cell cycle proteins and MSH6.

Taken together, we reported the canonical and non-canonical roles for MMR pathway. MMR is implicated in the repair of mismatches, in other repair pathways and signalling, in chromatin assembly and in immunoglobulin diversification.

2.4 Epidemiology of DNA mismatch repair deficiency

Loss of expression of one of the MMR proteins (MSH2, MSH6, MSH3, MLH1, and PMS2) leads to MMR deficiency. This loss can be due to mutation, methylation or a combination of both. Germline mutations in any of the MMR genes can give rise to the autosomal dominant condition referred to as Lynch syndrome (LS), also called hereditary nonpolyposis colon cancer (HNPCC) [131]. This syndrome is one of the most prevalent hereditary cancer-prone syndromes. LS represents 1-5 % of all CRCs. It is associated with an increased predisposition to cancer, with an 80 % risk of developing CRC; and a 60 % risk in female patients of developing endometrial cancer. LS is also associated with cancers of the ovary, urologic tract, glioblastomas, small bowel, stomach, pancreas, breast and prostate [195-203]. In LS, only one mutated allele of an MMR gene is inherited. Loss of the second allele occurs somatically either by mutation or methylation. The rare case where both inherited alleles are mutated is called the constitutional MMR deficiency syndrome and leads to cancer during childhood [204]. The contribution of each MMR gene to LS is variable. MLH1 is the most common MMR protein found silenced, it represents 42 % of all LS cases; 10-20 % of MLH1-deficent LS cases are due to MLH1 methylation. MSH2, MSH6 and PMS2 are also notably important (mutated in 33, 18 and 7.5 % of LS cases respectively), while MSH3 mutations are moderately implicated in LS. MSH2 has been estimated to be lost due to methylation in 17-24 % of MSH2-deficient LS cases, 29 % of PMS2 deficient LS cases were associated with methylation and no case of MSH6 methylation has been reported (Table 5) [205, 206]. Cancer development and expression in LS is variable. MLH1 and MSH2 mutations are associated with a higher penetrance and earlier mean age of cancer onset compared to MSH6 and PMS2 mutations. MSH6 mutations have a higher risk of endometrial cancer [207]. MMR loss can be inherited but can also be somatic which represents 10-15 % of all CRC. All MMR genes can be somatically lost, however loss of MLH1 is identified in 60 % of cases, mainly due to hypermethylation of the MLH1 promoter [208]. No case of MSH2 and MSH6

methylation in sporadic cancers with somatic defect in MMR has been reported [209, 210]. Overall, data suggest that MMR deficient tumours have a better disease free survival rate in comparison to MMR proficient tumours. A meta-analysis estimated a hazard ratio of 0.65 for MSI which means tumours with MSI have a significantly better prognosis than microsatellite stable tumours [211]. One of the hypotheses to explain this better disease survival rate is a differential immune response in the MMR deficient tumours compare to the MMR proficient tumours [212]. MMR deficient tumours accumulate mutations that can trigger the generation of potentially immunogenic peptides recognized by the immune system [213]. However, MMR deficient tumours are not eliminated due to potential immune evasion strategies. Further investigations are necessary to understand the role for the immune system in MSI tumours development (see section 3.2.3.3) [214, 215].

Affected genes	Contribution to LS cases	Proportion due to gene methylation
MLH1	42 %	10-20 %
MSH2	33 %	17-24 %
MSH6	18 %	0 %
PMS2	7.50 %	29 %

Table 5: MMR genes associated with Lynch syndrome

Knockout mouse models have been developed to study MMR genes [155]. All models were cancer-prone, except MSH3 deficient mice [140]; and all models except MSH6 deficient mice had MSI [216]. MLH1, MSH2 and PMS2 knockout mice showed cancer susceptibility primary to lymphoma, not CRC as in humans, and secondary to gastrointestinal tumours, skin neoplasms and sarcomas [217]. The phenotype of MSH6 knockout mice is similar to MSH2 knockout mice except for the MSI [216, 218]. Double knockout for MSH6 and MSH3 have identical phenotype as MSH2 knockout mice [140].

2.5 Identification of DNA mismatch repair deficiency

The diagnosis of MMR deficiency is based on the Revised Bethesda Guidelines [219]. The diagnosis consists of either evaluation of MMR deficiency by sequencing or immunohistochemistry (IHC), or evaluation of MSI [220]. Microsatellites are 1-6 base pairs tandem repeated (most commonly dinucleotide CA repeats) present

throughout the whole genome. DNA polymerases can slip over the tandem repeats leading to replication length errors and MSI [221]. These errors can be repaired by MMR but, in MMR deficiency, the errors remain fixed. Five microsatellite markers (BAT26, BAT25, D5S346, D2S123 and D17S250) have been identified as good predictors of MMR deficiency and are used to analyze MSI [222, 223]. High MSI (MSI-H) is defined by two or more of the markers showing instability; MSI-low (MSI-L) is the term when one of the markers is instable; and microsatellite stability (MSS) when no marker shows instability [222, 223]. Loss of MMR is known to give rise to MSI-H. 25 % of all MSI-H are caused by inherited MMR deficiency and are diagnosed as LS, 75 % are due to somatic loss of MMR. MSI-L has, to date, an unclear clinical significance. It is sometimes classified as MSI and sometimes as an independent group. In this case, another method of diagnosis may be required to classify patients [224].

The other method is to diagnose MMR deficiency is by sequencing or IHC. Sequencing is a fast, reliable and low cost experiment. However, it detects only MMR mutations and not methylation. Therefore, this technique needs to be used in complement with another one [225, 226]. IHC consists of the assessment of loss of expression of MMR proteins in tumour samples. This is a good complement to MSI analysis as not all MMR deficiency give rise to MSI-H. For example, in the case of MSH6 deficiency, only 25 % of patients have MSI-H, although instability specifically at mononucleotide repeat sequences was consistently observed [207]. This is thought to be due to MSH3 compensation as MSH6 and MSH3 can both complex with MSH2 to form MutS α and β, and are both implicated in mismatch recognition. IHC is actually the best technique to diagnose MSH6 deficiency, but it cannot be the only technique clinically used as its sensitivity is around 90 %. This can be explained by the lack of standardization in this technique and the interpretation of the IHC staining results. In summary, MSI testing is cost effective and the best standardization in the technique but it does not identify all MMR deficiency (identify only 25 % MSH6 deficient tumours). IHC testing identifies mutations and methylation in all MMR genes but it is not well standardized. Sequencing allows a panel-based testing rather than a syndrome-based testing which means sequencing allows to test for mutation in MMR genes as well as other

oncogenes, but it does not identify methylation in MMR genes [227]. Therefore, these three techniques are, to date, complementarily used in the clinic [228].

2.6 Secondary mutations and DNA mismatch repair deficiency

Unsurprisingly, due to its role in genome stability, MMR deficiency can lead to a mutator phenotype, which is characterized by an accumulation of mutations in the DNA. The mutation rate is evaluated to be 100-1000-fold increased in MMR deficient cells [49]. This mutator phenotype is primarily due to MSI [229]. Many oncogenes and tumour suppressor genes contain microsatellites; therefore, MMR deficiency can give rise to mutations in many genes implicated in tumorigenesis (Table 6). For example, the Transforming Growth Factor-β type II Receptor (TGFβR2), a signal transduction gene, was the first MSI-H target gene reported in 1995 [230]. Later, BCL2-associated X protein (BAX), a gene involved in apoptosis; adenomatous polyposis coli (APC), a gene involved in cell adhesion; and insulin-like growth factor 2 receptor (IGF-IIR), a gene involved in signal transduction, were also identified [231-233]. Further secondary mutations to MMR deficiency, such as DSB repair genes including MRE11 and RAD50 have all been identified to have mutations in their microsatellite regions upon MMR loss and are thought to drive the tumourigenic phenotype. Therefore, it is thought that the cancer phenotype in MMR deficient tumours may be further driven by secondary mutations in cancer-associated genes [134, 234].

Pathway	Genes affected	mutational frequency in tumours
DNA repair	MRE11	74 %
	RAD50	21-46 %
	DNA-PKcs	34 %
	BRCA2	2 %
	Ligase III	13 %
	XRCC2	3 %
Damage signalling	CDC25	11 %
	ATR	44 %
	Chk1	10 %
Apoptosis	BAX	24-54 %
Signal transduction	BRAF V600E	31-83 %
	PTEN	19 %
	TGF2R	61-100 %
	IGF2R	6-36 %
Transcription regulation	E2F4	35 %
	HDAC2	20 %
	TCF4	34-53 %

Table 6: List of MSI-containing genes and their mutation frequency in MMR deficient tumours

2.7 DNA mismatch repair deficiency and drug response

Numerous studies agree that MMR deficient tumours are more resistant to a wide range of chemotherapeutic agents [132-134]. These include alkylating agents, platinum compounds and fluoropyrimidine agents.

2.7.1 DNA mismatch repair deficiency and alkylating agents response

Alkylating agents, such as TMZ, modify predominantly the ring nitrogen atom of purines. TMZ is the standard of care for patients with newly diagnosed glioblastoma tumours. In glioblastoma patients, resistance to TMZ in up to 40 % of patients is due to an acquired mutation in MSH6 [133, 235]. Long-term exposure to TMZ treatment can result in acquisition of an MSH6 mutation in glioblastoma cells, which mediates resistance to the drug [235, 236]. These observations are not surprising knowing that MMR pathway plays an important role in response to alkylating agents by repairing O^6meG:T mismatches [175, 176]. Acquired MSH6 mutations in the human lymphoblastoid cell line (A-to-T transversion at codon 1145, G-to-A transition at codon 1192) after MNNG treatment has also been reported and associated with

MNNG resistance [237]. MSH6 is not the only protein implicated in alkylating agent response. Loss of MLH1, MSH2 and PMS2 also confers resistance to alkylating agents [238, 239].

2.7.2 DNA mismatch repair deficiency and platinum compounds response

Platinum compounds, such as Carboplatin and Cisplatin, are the most effective treatments for endometrial, ovarian and testicular cancer. They act by crosslinking into DNA [240]. It has been well studied in patients and cell lines that MMR deficiency confers resistance to Cisplatin [133]. An *in vitro* study, comparing MMR proficient and deficient matched paired cell lines identified a role for MLH1 and MSH2 deficiency in Cisplatin resistance [241]. Resistance to platinum agents in ovarian and endometrial cancers has also been shown to be due, in part, to an acquired loss of MMR, primarily due to MLH1 methylation [242]. A study compared the MSI and MMR status of 24 primary resected tumours, prior and after Cisplatin treatment. They evaluated that all cases with MSS (72.5 %) exhibited MSI after Cisplatin treatment, from which 73.3 % acquired a loss in MLH1 protein [243]. A study on 38 ovarian cancer patients reported that 66 % of tumours had a loss of MLH1 after platinum based therapy which was associated with treatment resistance [244]. A study on 20 ovarian cancer patients correlated MSH2, but not MSH6 deficiency, with resistance to Cisplatin treatment [245]. Samimi *et al.* confirmed the significant decrease in MLH1 and MSH2 protein expression after treatment with platinum-based therapy. However, they did not confirm the correlation between MMR deficiency and treatment response [246]. One possible mechanism of resistance in MMR deficiency is the interaction between MLH1, MSH2 and FANCD2, a protein of FAR pathway implicated in ICLs repair which causes, in MMR deficient cells an inhibition of FAR leading to an ICLs repair defect [184].

2.7.3 DNA mismatch repair deficiency and IR response

The role of the MMR pathway in IR response is not completely understood and is particularly important for the treatment of MMR-deficient endometrial, glioblastoma and rectal cancers. IR has been shown to induce a wide range of DNA damage, for example, 1 Gy have been estimated to induce 1000 base damage, 1000 SSBs, 40 DSBs and 20 ICLs, and IR-induced DSBs are thought to be the main event in IR-

induced cell cytotoxicity [247]. In order to understand the role for MMR in IR-induced damage, Martin *et al.* have carried out meta-analysis on published reports regarding IR response in MMR deficiency. They concluded that following high-dose IR, MMR deficient cells appear to be more sensitive to IR whilst following low-dose rate IR, MMR deficient cells have been shown to be more resistant compared to MMR proficient cells [247]. We previously mentioned that MMR pathway plays a role in the RAD51-dependent recombination fidelity [178-181]. Loss of MSH2 induces aberrant RAD51 focus formation. Therefore, IR sensitivity in MMR deficient cells might be due to MMR dependent regulation of HR pathway [248, 249]. IR induces DSBs but also other lesions such as methylation and oxidative DNA damage [250]. MMR pathway is known to be implicated in the repair of those lesions which could also explain IR sensitivity in MMR deficient cell lines [166].

2.7.4 DNA mismatch repair deficiency and topoisomerase inhibitor response

Topoisomerase inhibitors, such as Irinotecan and Etoposide, induce stalled replication forks or SSBs and ultimately DSBs [251]. Studies examining their response in MMR deficiency are conflicting. It is known that MRE11 and RAD50 genes contain microsatellites in their DNA and therefore MMR tumours often have secondary mutations in these genes (Table 6). It is also known that cells with a defect in DSB repair pathways are sensitive to topoisomerase inhibitors [252]. Therefore, Irinotecan sensitivity in MSI compared to MSS tumours could be due to secondary mutations in RAD50 or MRE11 [253, 254]. However, an *in vitro* study, comparing MMR deficient and proficient matched paired cell lines that differ only due to their MMR status, showed resistance to topoisomerase inhibitors in MMR deficient cell lines [255]. Taken together, these reports showed that secondary mutations due to MMR deficiency, and not MMR deficiency itself, cause sensitivity to topoisomerase inhibitors.

2.7.5 DNA mismatch repair deficiency and nucleoside analogue response

2.7.5.1 Mechanism of action of 5-Fluorouracil (5-FU)

The nucleoside analogue, 5-FU is currently standard of care for many cancers, including CRC [256]. Developed in 1957 by Charles Heidelberger, 5-FU is a member of the fluoropyrimidine agents [257]. Presently, 5-FU remains an active

agent against CRC but its treatment response rate is only 10-15 % alone or 20-25 % in combination [256]. 5-FU is primarily catabolised in the liver into dihydrofluorouracil (DHFU) which account for 80 % of its catabolism [258]. 5-FU is converted into different cytotoxic metabolites which have different modes of action. FdUrd-5'monophosphate (FdUMP) blocks the activity of thymidylate synthase (TS) causing imbalance in deoxyribonucleotide (dNTP) pool triggering DNA damage; FdUrd-5'-triphoshate (FdUTP) is incorporated into DNA and causes DNA damage; and 5-fluorouridine-5'-triphosphate (FUTP) is incorporated into RNA triggering cytotoxicity [256] (Figure 8).

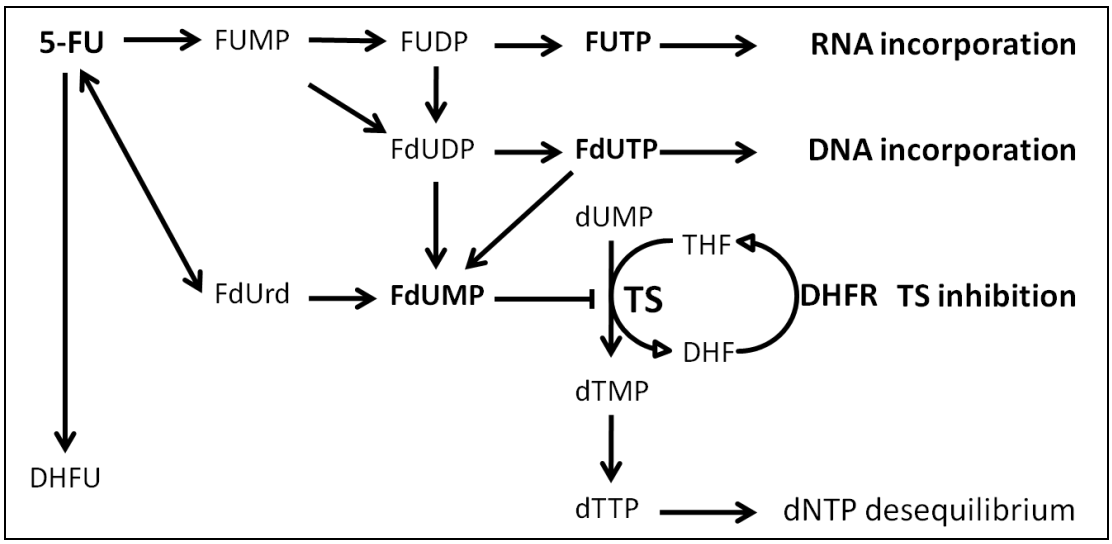

Figure 8: Mechanisms of action of 5-FU
In the liver, 80 % of 5-FU is catabolised into DHFU. 5-FU is also converted into different metabolites including FUTP which is misincorporated into RNA, FdUTP which is misincorporated into DNA and FdUMP which inhibits TS activity.

2.7.5.2 Resistance to 5-FU in MMR deficiency

Conflicting studies have been reported with regards to MMR deficiency and resistance to 5-FU treatment [259] potentially due to differences in study design, different adjuvant chemotherapies and the secondary mutations associated with MSI [211]. However, the majority of studies suggest that MMR deficient CRCs are more resistant to 5-FU than MMR proficient CRCs [260]. *In vitro*, where the resistance can be studied with a better control of parameters, MMR deficient cell lines have been shown to be 18-fold more resistant to 5-FU in comparison to MMR proficient cell lines [261, 262]. MMR is the first and predominant pathway to recognize DNA

misincorporation by 5-FU. It has been shown that MutSα and, with a lower affinity, MutSβ can recognize 5-FU lesions [263, 264]. In the absence of MMR, 5-FU lesions cannot be recognized, therefore ATM/ATR cannot be recruited and apoptosis cannot be triggered; thus leading to 5-FU resistance [134, 157]. FdUTP and FdUMP are the metabolites implicated in 5-FU mediated DNA misincorporation, so the resistance mediated by loss of MMR is thought to be due to FdUTP and FdUMP rather than FUTP [265]. To date, no case of acquired mutations in MMR genes in response to 5-FU treatment has been reported.

2.7.5.3 5-FU modulators

The treatment regime in CRC has evolved over time but primarily depends on the cancer stage [266]. Small tumours (stages I and II) are treated with surgical resection only; larger tumours with no metastases (stage III) are treated with surgery followed by chemotherapy treatment; and metastatic CRC (stage IV) are treated with an adapted chemotherapy regime. After surgical resection, 20-30 % experience disease recurrence or develop metastatic disease [267]. Adjuvant treatments in addition to 5-FU have been rapidly developed. Ullman *et al.* in 1978 reported that Leucovorin (LV), a reduced folate, could significantly enhance 5-FU cytotoxicity *in vitro*. A large number of phase I and II clinical trials have tested and validated LV as an modulator of 5-FU [268, 269]. A meta-analysis reported 11 % response rate with 5-FU alone and 21 % response rate with the combination 5-FU/LV [270]. In the early 2000s, Irinotecan and oxaliplatin were included in the 5-FU/LV combination treatment for stage III and metastatic CRCs. One study showed a 39 % response rate with Irinotecan/5-FU/LV compared to 21 % with 5-FU/LV [271]. The response rate with oxaliplatin/5-FU/LV compared to 5-FU/LV was also significantly increased (45 % and 31 % respectively) [272]. However, the comparison of Irinotecan/5-FU/LV with oxaliplatin/5-FU/LV did not show any difference in response rate (56 % and 54 % respectively) [273, 274]. The combination of these chemotherapy combinations with an anti-vascular endothelial growth factor-A antibody, bevacizumab, was tested in clinical trial to improve the treatment for metastatic CRCs. Better response rate were shown with bevacizumab/Irinotecan/ 5-FU/LV and bevacizumab/oxaliplatin/5-FU/LV treatments comparison with Irinotecan/5-FU/LV (44.8 % vs. 34.8 %) and oxaliplatin/5-FU/LV (22.7 % vs.

8.6 %) respectively [275, 276]. The different clinical trials have shown differences in response rate for the same treatment regime which might be dependent on the patients and/or cancer heterogeneity [267]. However, they all converged toward a better response rate with the different combined chemotherapy regimens compared to 5-FU alone. If the combined chemotherapy regimens showed better response rate, they also showed increased toxicity [277]. This is why 5-FU is still intensely studied and novel therapeutic strategies are investigated. Moreover, with a MMR loss in 10-15 % of CRCs, 5-FU resistance associated with MMR deficiency represents a major clinical concern.

3 Synthetic lethality

Ideally, an efficient chemotherapeutic treatment should be tumour cell specific. However, where loss of gene function is the determinant of disease, it is difficult to determine a therapeutic target as it is often technically difficult to recapitulate gene function efficiently. Recently, the concept of synthetic lethality has been proposed as a potential therapeutic approach for cancer treatment. Two genes are said to be synthetically lethal when a loss of function or mutation of either gene alone is compatible with viability but loss of both causes cell death (Figure 9) [278, 279]. Genetic changes that give rise to tumorigenesis, like MMR deficiency, are a potential target to identify genes or compounds that are synthetically lethal in order to identify new therapeutic strategies. Synthetic lethal relationship with DDR pathways have been identified and exploited in the clinic. High-throughput screens, using libraries of clinically-approved drugs, is a widely used technique to identify novel synthetic lethal relationships. The main advantage of this type of compound screen is the reposition of a drug already previously used in clinic and is therefore ready to be translated into clinical trial. it leads to faster drug approval by minimizing the risk of failure in late stage clinical trials [280]. Other screens, such as shRNA and siRNA screens using a library targeting genes of one specific pathway/mechanism, are also often used to identify novel therapeutic synthetic lethal targets. For example, the use of a kinome targeted siRNA library would be highly relevant as kinases play a key

role in many biological processes and have an inherent pharmacological tractability, and therefore often make good drug targets.

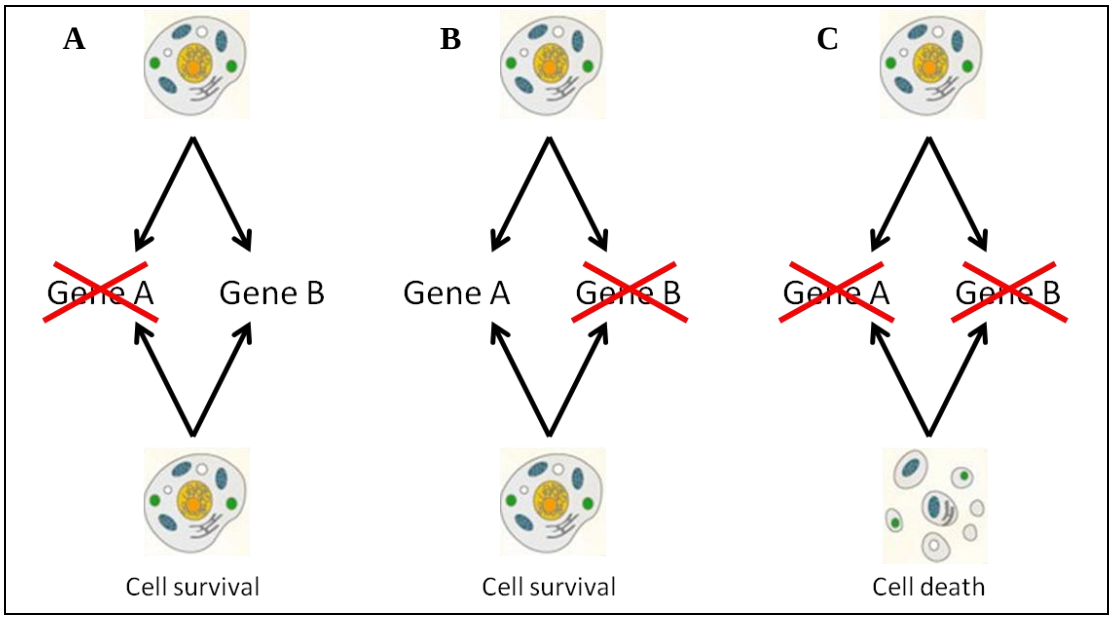

Figure 9: The mechanism of Synthetic lethality
Schematic of how synthetic lethality occurs. **A:** Loss of gene A alone, such as a mutation in a DDR gene, is compatible with cell viability. **B:** Loss of gene B alone is compatible with cell viability. **C:** A combined loss of both gene A and B, causes cell death.

3.1 Synthetic lethality within DDR pathways

3.1.1 Base excision repair and homologous recombination

Synthetic lethal relationships have been shown with regards to HR and BER. BRCA1 and BRCA2 are part of the HR pathway responsible for DSBs repair [281] and a mutation in either BRCA1 or BRCA2 genes highly increases the risk of developing breast and ovarian cancer [282]. PARP is a polymerase involved in BER by recognizing SSBs generated by APE1 and recruiting proteins for their repair [283, 284]. Inhibition of PARP leads therefore to unrepaired SSBs which, at the stalled replication fork, would generate DSBs. In the absence of BRCA1 or BRCA2, these DSBs cannot be repaired. Therefore, in BRCA1/2 deficient tumours, the inhibition of PARP gives rise to unrepaired SSBs leading to DSBs and ultimately cell death. Therefore, PARP and BRCA1/2 are involved in complementary pathways and are synthetically lethal [285]. This synthetic lethal relationship has been translated into

the clinic and Olaparib, a PARP inhibitor, is currently FDA-licensed and approved for the treatment of BRCA mutated ovarian cancers (FDA-3675412). Unrepaired DSBs can be caused by BRCA1/2 deficiency but also by a HR defect in general [286]. Phosphatase and tensin homolog (PTEN), a gene well known for its role in the phosphoinositide 3 kinase (PI3K) pathway, has been recently identified to play a role in HR by regulating levels of RAD51 and to be synthetically lethal with PARP inhibitors [287-289]. PTEN mutations are present in a wide range of tumours making this synthetic lethal relationship extremely clinically relevant [287]. APE1, another important enzyme in BER has been recently shown to be synthetically lethal with DBSs repair proteins: BRCA1/2, ATM and DNA-PKcs deficiency through the same mechanism as PARP inhibition in HR deficiency [290]. Therefore there is not only synthetic lethal relationship between PARP and BRCA1/2 but more broadly between the BER and the HR pathway.

3.1.2 Limitations in BRCA1/2 and PARP synthetic lethality

Treatment with PARP inhibitors in BRCA1/2 deficient tumours is a promising therapeutic strategy. However, a substantial fraction of BRCA1 deficient cancers are resistant to PARP inhibitors agents either by acquired or inherent resistance [291-293]. Different mechanisms of resistance have been proposed [294-296]. One of the mechanisms of resistance to PARP inhibitor is through the reactivation of HR pathway. The reversion of BRCA1/2 mutation, by acquired secondary mutation in the genes, results in restoration of the gene function, and has been identified as a mechanism of acquired resistance to PARP inhibitor, as well as platinum agents [297-300]. An inherent resistance to PARP inhibitors in HR deficiency due to loss of 53BP51 has been identified in different laboratories and is characterized by the rescuing of HR function in cells with a mutation in 53BP51 [301-304].

3.1.3 RAD52 and RAD51-dependent homologous recombination

They are two alternative pathways in HR: the RAD51-dependant pathway through the recruitment of the BRCA1-BRCA2-PALB2 complex and the RAD52-dependent pathway. The inactivation of RAD52 has been recently shown to be synthetically lethal with the BRCA1-BRCA2-PALB2 complex [305, 306]. Deficiency in either of the proteins of the complex leads to an alternative RAD51-independent pathway for

the repair of DSBs. This alternative pathway depends on RAD52. Therefore, inhibition of RAD52 in BRCA1/2 or PALB2 deficient cells may lead to inhibition of the alternative repair pathway, and therefore to cell death.

3.1.4 Fanconi anemia and other DNA damage signalling and repair proteins

FAR is implicated in the NER and HR pathways. FANCD2, a protein of the FAR pathway, can be phosphorylated by ATM, ATR and Chk1 [307-309]. Synthetic lethality has been shown between ATM and FAR proteins, FANCG and FANCC [310]. A proposed explanation is that in FAR deficiency, stalled replication folks can collapse and form a DSB which will activate an ATM dependent DDR. Therefore, inhibition of ATM in Fanconi anemia will leave no alternative pathway leading to cell death [15]. The FAR pathway is also synthetically lethal with PARP and Chk1 [311]. FAR is implicated in HR, therefore it is not surprising that defects in FAR and PARP are synthetically lethal. Chk1 inhibition and Cisplatin treatment were previously shown to be synergistic through Chk1-dependent G2 checkpoint regulation [311]. FAR is implicated in ICLs repair which can be induced by Cisplatin treatment. This suggests the role for Chk1-dependent G2 checkpoint in Chk1 and FAR synthetic lethality. There is, to date, no clinical trial to evaluate these synthetic lethal relationships.

3.1.5 ATR and p53

Another recent study identified ATR as being synthetically lethal with TP53 deficiency [312]. This synthetic lethal relationship was dependant on a novel non-canonical function for ATR. ATR was shown to phosphorylate and stabilise ETV1, a transcription factor for TERT, a catalytic subunit of telomerase implicated in proliferation maintenance [313]. TP53 is known to be mutated or inactivated in the majority of tumours [128]. Therefore TP53 is a potential critical target in cancer therapy [129, 314]. The preclinical synthetic lethal relationship between ATR, ETV1 and TP53 is a novel and promising discovery for new chemotherapy development.

3.2 Synthetic lethality with DNA mismatch repair pathway

MMR deficient cells have a high-predisposition to cancer and an inherent drug resistance. Secondary mutations upon MMR loss can greatly influence cellular

response to drugs, such as topoisomerase inhibitors. Therefore, there is a clinical need to identify new therapeutic strategies to target MMR loss, also considering secondary mutations [136].

3.2.1 Synthetic lethal with DNA mismatch repair deficiency and oxidative stress

Several studies have applied a synthetic lethal approach and more recently, have identified new regulators of the MMR pathway, which may provide alternate means of treating MMR deficient patients, other than standard chemotherapies. Martin *et al.* have previously shown that inhibition of specific polymerases is synthetically lethal with MMR deficiency, through the accumulation of oxidative DNA damage. More precisely, MSH2 deficiency is synthetically lethal with inhibition of DNA pol β, the main DNA polymerase that catalyzes nuclear BER; and that MLH1 deficiency is synthetically lethal with inhibition of DNA pol γ, the only polymerase specific to mitochondrial DNA [315]. Interestingly, the MLH1/DNA pol γ synthetic lethality is characterised by an accumulation of mitochondrial oxidative DNA lesions, whereas the MSH2/DNA pol β synthetic lethality leads to an increase in oxidative lesions in nuclear DNA. The requirement for MLH1 in mitochondrial genome stability has also been confirmed in retinal endothelial cells, showing a role for MLH1 in the development and progression of diabetic retinopathy [316]. Furthermore, MSH2 deficiency specifically, is cytotoxic with the drug, Methotrexate, through the accumulation of nuclear, but not mitochondrial, oxidative DNA damage [317]. No cytotoxicity was observed in MLH1 deficient cells upon treatment with Methotrexate, suggesting that synthetic lethal interactions with MLH1 loss, requires mitochondrial oxidative DNA damage. A randomized phase II clinical trial using Methotrexate treatment in MSH2 deficient colorectal cancer (NCT00952016) is currently underway which includes measurement of the oxidative DNA lesion, 8-oxoG as a biomarker. In addition, further synthetic lethal interactions upon oxidative DNA damage and MMR mutations have been identified. Using a high-throughput siRNA screen, inhibition of PTEN-induced putative kinase 1 gene (PINK1), a gene limiting oxidative-induced apoptosis, was identified to be synthetically lethal with MMR deficiency [318]. MMR deficient cells have also been shown to be sensitive to cytosine-based analogues through the induction of oxidative

stress [319]. Taken together, inducing oxidative DNA damage may be a promising therapeutic strategy for the treatment of MMR deficient cancers (Figure 10).

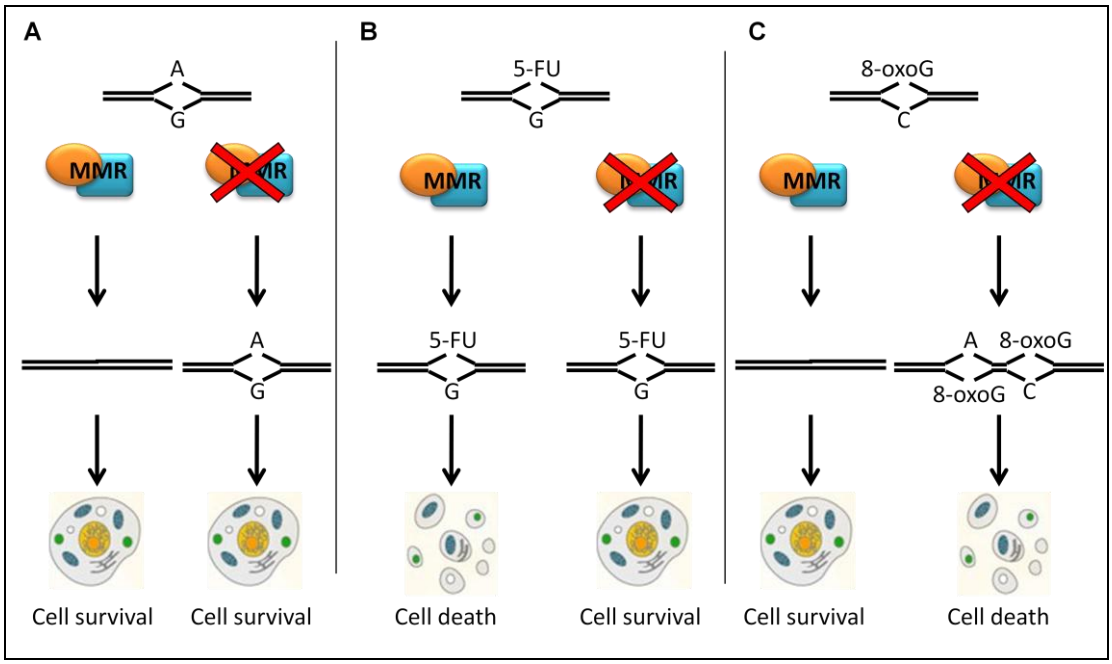

Figure 10: Role of MMR in response to 5-FU treatment and oxidative stress
A: Mismatches, naturally occurring during DNA replication, can be recognised and repaired by MMR pathway. In the absence of MMR, these mismatches accumulate in the DNA resulting in a "mutator phenotype". **B:** Chemotherapeutic treatment, including 5-FU, can be recognized by MMR pathway and lead to apoptosis. In the absence of MMR, the lesions are not recognized and the cells become resistant to the drug treatment. **C:** Upon oxidative stress, 8-oxodG lesions are recognized and repaired by MMR proteins. In the absence of MMR, these lesions accumulate ultimately resulting in cell death.

3.2.2 Targeting MMR-associated secondary mutations

Secondary mutations to MMR deficiency are essential to consider with regards to drug response. I previously mentioned the role for secondary mutations in MMR deficiency in Irinotecan response (see section 2.7.2) [253]. Therefore, secondary mutations associated with MMR deficiency need to be taken into consideration with regards to response to treatment and as potential therapeutic targets. Mutations in DSB repair genes, such as MRE11, ATR, PTEN and RAD50, are associated with MMR deficiency (Table 6) [142, 234]. Due to their role in HR pathway, the loss of these genes is synthetically lethal with PARP inhibitors [289, 320]. Therefore MMR

deficient tumours with secondary mutations in these genes could be treated with Olaparib, a PARP inhibitor currently used in clinic. Oxidative DNA damage, if unrepaired, can accumulate and lead to lethal DSBs. However, MMR deficiency mediated secondary mutations in DSB repair genes could potentially lead to oxidative stress resistance. Therefore a combination treatment with Methotrexate and Olaparib, targeting both primary and secondary mutations, might be an efficient strategy to overcome this potential mechanism of resistance. A phase II clinical trial is currently evaluating the effect of Olaparib on MSI CRCs (NCT00912743) and a phase II clinical trial is evaluating the effect of a PARP inhibitor in inoperable advanced endometrial cancers (NCT02127151). In this trial, MRE11, PTEN and MSI will be evaluated. Both clinical trials should give us answers about PARP inhibitor response in MMR deficient tumours with or without secondary mutations in MRE11 and/or PTEN. Another phase I clinical trial is evaluating the benefit of the combination PARP inhibitor and TMZ treatment in relapsed glioblastoma patients (NCT01390571) where, amongst others, MSI, MMR, MGMT and PTEN status will be measured. This trial should determine the role for MMR deficiency and secondary mutations in Olaparib/TMZ treatment response.

Another secondary mutation frequently present in MMR deficient tumours is the BRAF V600E activating mutation. Patients with metastatic melanoma with a BRAF V600E mutation can be treated with Vemurafenib, a BRAF inhibitor [321]. However, this drug has low response in BRAF V600E mutated CRCs due to a feedback activation of the epidermal growth factor receptor (EGFR). Therefore, the combination of Vemurafenib and an EGFR inhibitor has shown promising results for the treatment of BRAF V600E mutated CRCs [322]. Interestingly, EGFR has been shown for its role in Cisplatin and IR repair through DNA-PKcs binding [323]. To date, Vemurafenib has not been tested as a potential treatment of MSI tumours.

3.2.3 Other clinical strategies in MMR deficient tumours

3.2.3.1 Re-expression of MMR genes

MMR deficiency confers resistance to numerous chemotherapeutic agents. Researchers have focused on attempts to reactivate methylated MLH1 by treatment with a demethylating agent, 2'-deoxy-5-azacytidine. Preclinical data were promising but adverse reactions was shown in a terminated phase II clinical trials

(NCT00748527) [324]. Another strategy to reexpress MMR proteins is by targeting the microRNA miR-155. An inverse correlation between miR-155 expression and the MMR proteins MLH1 and MSH2 was observed in CRC tumours. Moreover, tumours with MSI not associated with MMR deficiency were shown to highly express miR-155. Therefore, silencing miR-155 might be a promising novel strategy for the treatment of MSI tumours.

3.2.3.2 MMR and aspirin

A recent preclinical study identified a chemo-preventive effect of aspirin in a LS mouse model [325]. A cohort of 1 000 LS-carrier patients from 43 countries were selected to measure the effect of a daily dose of aspirin on the predisposition to cancer development. They observed patients who took aspirin were 59 % less likely to be diagnosed with CRC compared to the placebo group [326, 327]. Based on the same approach, a phase I clinical trial is currently testing the effect of naproxen, a non-steroidal anti-inflammatory alternative to aspirin, in LS CRC patients (NCT02052908). They will test naproxen as a potential CRC preventive and they will measure, amongst other criteria, the microRNA profiles of the tumours. It will be interesting to know if naproxen treatment regulates miR-155 expression. A role for MMR proteins in inflammation has previously been reported [328]. More precisely an epigenetic repression of MLH1 has been observed after colitis induced by G-protein alpha subunit Giα2 in mice which leaded to MSI tumours [328]. Therefore, it would be interesting to correlate the aspirin chemo-preventive effect and the somatic loss of MLH1 following inflammation. Aspirin has also an antioxidant activity [329-331]. As mentioned previously oxidative stress plays a role in tumour progression and in mutator phenotype associated with MMR deficiency (see sections 1.4 & 2.3.1). Therefore, aspirin might prevent LS associated CRC development through ROS scavenging.

3.2.3.3 MMR deficiency and immunotherapy

It has been shown that MSI tumours have a better outcome than MSS tumours [211]. It has been speculated that this was due to a better immune response. Immune response was measured in 100 MSI or MSS CRCs. Interestingly, the T helper type 1 (Th1) response was found higher in MSI compared to MSS CRCs [213]. However, it

has been shown than despite their active Th1 microenvironment, MSI CRCs are not eliminated by the immune system. A possible explanation was the significant up-regulation of immune checkpoint molecules (PD-1, PD-L1, CTLA-4, LAG- 3, and IDO) leading to an immunosuppressive microenvironment in MSI tumours [214, 215]. Clinical trials are currently exploiting this immune microenvironment specific to MSI tumours. A phase II clinical trial is testing MK-3475, a T-cell inhibitor in MSI tumours (NCT01876511). Another phase I/II clinical trial is exploiting the role for MMR in frameshift peptides (FSP) generation by testing the efficacy of a vaccination with FSP antigens in MSI tumours (NCT01461148) [332]. These studies are recent and therefore there is yet no published investigation on a potential synthetic lethal relationship between immune checkpoint molecules and MMR deficiency.

3.2.3.4 DNA mismatch repair and cell cycle

The cell cycle related genes Cyclin D1 and AURKA have been associated with an early onset of CRCs in LS [333]. Cyclin D1 regulates G1/S transition. Polymorphisms in Cyclin D1 result in alternative splicing of Cyclin D1 mRNA and gives rise to two protein variants. The variants have been associated with differential onset of CRCs in LS (11 years difference) [334]. This has been confirmed by Talseth *et al.* in another study measuring the incidence of Cyclin D1 and AURKA polymorphisms on the onset of CRCs in LS [335]. However, other studies have not confirmed this correlation [336, 337]. In the Talseth *et al.* study, they found that the onset of CRCs in LS was correlated with polymorphisms in Cyclin D1 but not in AURKA, a regulator of G2/M transition of the cell cycle [335]. However, other studies have associated AURKA polymorphisms with a later onset of CRCs in LS [333, 338]. The differences in these studies might result from the difference in the cohort and the range of MMR genes affected. However it would be interesting to understand the role for AURKA and Cyclin D1 in the development of CRC associated with LS. To date, there is no preclinical or clinical study to exploit the potential role for Cyclin D1 and AURKA in the development of CRC in patients with LS.

3.2.3.5 DNA mismatch repair and antifolates

Dihydrofolate reductase (DHFR), methylene tetrahydrofolate reductase (MTHFR) and TS are key enzymes of the folate pathway (Figure 11). DHFR converts dihydrofolate (DHF) into tetrahydrofolate (THF) which is converted into 5,10-methylene THF (commonly referred as THF). TS produces dUTP and recycles DHF, and MTHFR produces 5-methylene THF for the methyl cycle. THF is a substrate for both enzymes. Polymorphisms in MTHFR and TS have been associated with an increased CRC risk; conversely, polymorphisms in DHFR have been associated with decreased CRC risk [339-342]. In LS associated CRCs, studies have found that polymorphisms in MTHFR had a protective effect on the disease onset [343, 344]. One study found a correlation between MTHFR 677TT mutation, low folate levels and MSI [345]. The association between MTHFR 677TT and MSI has been confirmed in a study by Hubner *et al.* [346] whilst others showed an inverse correlation between MTHFR 677TT and MSI in patients with adequate folate intake and no correlation in patients with low folate intake [347]. More investigations are necessary to understand whether any correlation exists between MTHFR polymorphisms, folate levels and MSI. No study has evaluated a possible correlation between DHFR and TS polymorphisms and onset of LS associated CRC.

Antifolates have been developed and translated into clinic in order to inhibit the key enzymes of the folate pathway and thereby trigger inhibition of nucleotide biosynthesis leading to cell death [348]. The antioxidant role of the folate pathway has been described but is not well understood [349]. There is a potential role for the MMR pathway in antifolate response. Both Methotrexate, a DHFR inhibitor, and 5-FU, a TS inhibitor, have been associated with oxidative stress which is known to be cytotoxic in MMR deficient cells [350]. However, MMR deficient cells are resistant to 5-FU, due to misincorporation of FdUTP and dUTP into DNA (see section 2.7.5). Raltitrexed, another TS inhibitor, competes with THF in the formation of the dUMP-TS-THF active complex. It is used as a treatment in CRCs and in malignant pleural mesothelioma [351]. Raltitrexed response has not been associated with MMR status [265]. No publication has measured cell viability in MMR deficient and proficient cell lines upon TS silencing (by siRNA or shRNA transfection). Therefore, the role of MMR pathway in TS activity is not clear. Methotrexate, a DHFR inhibitor used for the treatment of breast, bladder and head and neck cancers, has been shown to be

synthetically lethal in MSH2 deficient tumours specifically [317]. One study suggests that only 5 % of DHFR activity is necessary for the production of THF required for TS activity and therefore, high concentrations of DHFR inhibitors are necessary to inhibit TS activity through the decrease in the THF pool, the rate-limiting factor for TS activity [352]. Pemetrexed is a multitargeted antifolate. It inhibits both the TS and DHFR enzymes. It is prescribed in combination with Cisplatin for the treatment of malignant pleural mesothelioma, non-squamous and non-small cell lung cancers [353, 354]. Pemetrexed has been shown to give better response in MSH2 deficiency in lung cancer [355] Therefore, there is a potential role for the MMR pathway in the cellular response to antifolates which is still unclear except for the synthetic lethal relationship between DHFR and MSH2 [317]. The role of MMR pathway in the folate pathway would require further investigation as it represents a potential novel therapeutic strategy for the treatment of MMR deficient tumours.

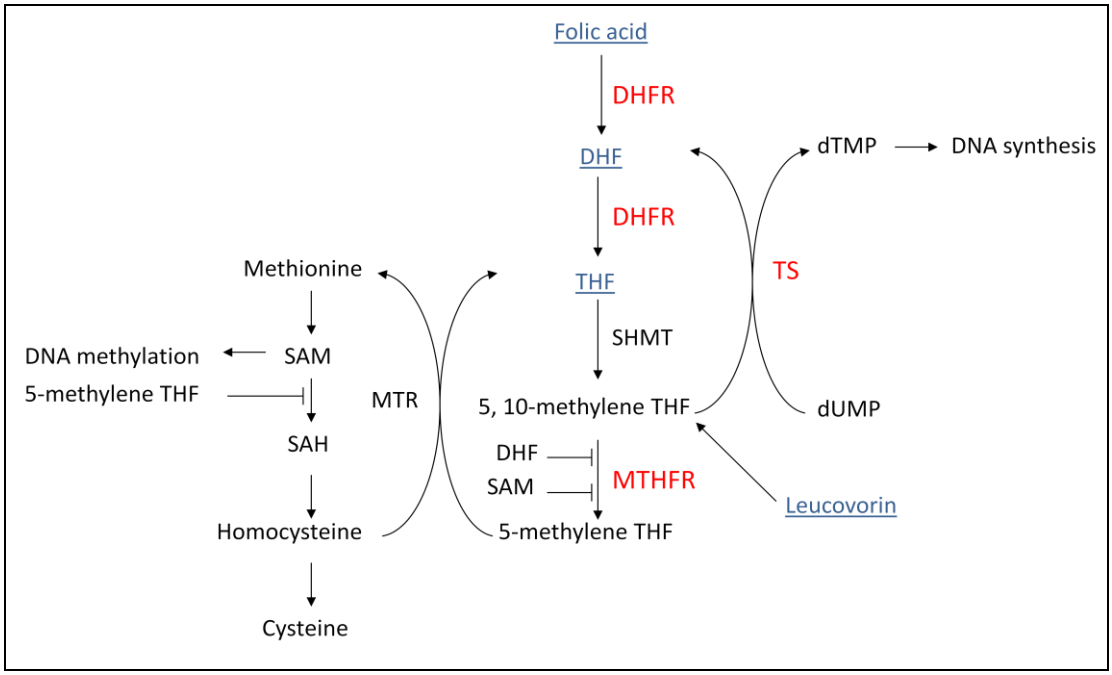

Figure 11: Folate pathway

The folate pathway plays a crucial role in DNA synthesis and DNA methylation. Folic acid is reduced to DHF which is then reduced to THF by DHFR. THF is converted into 5,10-methylene THF by serine hydroxymethyltransferase (SHMT). 5,10-methylene THF is the rate limiting factor for TS activity to produce dTMP and DHF recycle into THF by DHFR. 5,10-methylene THF is also the substrate for MTHFR activity to produce 5-methylene THF, itself a substrate, with homocysteine for 5-methyltetrahydrofolate-homocysteine methyltransferase (MTR) activity to produce methionine catabolised into SAM. SAM is a cosubstrate in methyl transfer essential for DNA methylation.

3.3 General remarks

MMR deficiency is present in 15 % of CRCs and in a wide range of cancers. It leads to a mutator phenotype and to resistance to a wide range of chemotherapies. Therefore, further investigations are necessary to overcome MMR deficiency associated chemotherapy resistance. The synthetic lethal relationship between MMR and oxidative stress represents a promising novel therapeutic strategy for the treatment of MMR deficient tumours. However, further studies are necessary to understand the role for MMR deficiency and secondary mutations in this synthetic lethal relationship. The MMR pathway has been described to have diverse canonical and non-canonical roles (Figure 7). Therefore, the MMR pathway represent a promising target to identify novel synthetic lethal relationships in order to develop new therapeutic strategies for the treatment of MMR deficient tumours.

Aims of the PhD project

Genomic instability can be caused by deficiency in DNA repair pathways [13, 14]. MMR, is a DNA repair pathway that repairs base-base mismatches and insertion deletion loops that occur during DNA replication [12]. Deficiency in MMR, which can be inherited (LS) or somatic, highly increases the predisposition to a wide range of cancers with, for example, results in an 80 % increased risk of developing CRC [131]. It has been shown that, in comparison to MMR proficient tumours, MMR deficient tumours are more resistant to a range of chemotherapies such as 5-FU, the major treatment for CRCs [134]. Synthetic lethality is a novel therapeutic strategy under investigation used to identify personalized treatment for tumours with DNA repair deficiencies [278]. To date, accumulating data has identified promising synthetic lethal interactions between MMR deficiency and oxidative stress [136].

My PhD project aimed to identify, via high-throughput screens, new potential therapeutic targets and drugs for the treatment of MMR deficient tumours and ultimately investigate the mechanisms of the identified synthetic lethality.

To this end, we aimed to:

- Identify drugs currently in clinical use that can modulate the resistance to 5-FU for the treatment of MMR deficient tumour cells using a high-throughput compound screen containing a library of 1120 drugs currently in clinical use.
- Identify synthetic lethal relationships with MMR deficiency, using a high-throughput siRNA screen containing an siRNA library targeting 779 human kinases and kinase-associated genes. Identification of new synthetic lethal relationship with MMR might allow better understanding of the non-canonical roles for MMR and/or identify new ones.

Materials and methods

1 Cell culture

1.1 Cell lines

The human colon cancer cell lines DLD1 and DLD1+chr2 were a kind gift from Dr. T. Kunkel (National Institute of Environmental Health Sciences (NIEHS), Research Triangle Park, NC, USA). DLD1 and DLD1+chr2 cells were grown in Roswell Park Memorial Institute medium (RPMI 1640) supplemented with fetal bovine serum (FBS; 10 % v/v), L-glutamine, penicillin (5X v/v) and streptomycin (5X v/v). The human colon cancer cell line HCT116 and HCT116+chr3 were a kind gift from Dr. A. Clark (NIEHS) and were grown in Dulbecco's modified Eagle's medium (DMEM) supplemented with FBS (10 % v/v), L-glutamine, sodium pyruvate, penicillin (5X v/v) and streptomycin (5X v/v). The human endometrial cell lines HEC59 and HEC59+chr2 were a kind gift from Dr. T. Kunkel (NIEHS), and were grown in DMEM supplemented with FBS (10 % v/v), L-glutamine, sodium pyruvate, penicillin (5X v/v) and streptomycin (5X v/v). The human ovarian cancer cell lines A2780cp70A2 and A2780cp70E1 were a kind gift from Dr. R. Brown (Institute of Cancer Research (ICR), London, UK) and were grown in RPMI 1640 supplemented with FBS (10 % v/v), L-glutamine, penicillin (5X v/v) and streptomycin (5X v/v). The glioblastoma cell lines U251 and U251.TR3 were a kind gift from Dr. D. Louis (Massachusetts general hospital, MA, USA). U251 and U251.TR3 cells were grown in DMEM supplemented with FBS (10 % v/v), L-glutamine, sodium pyruvate, penicillin (5X v/v) and streptomycin (5X v/v). DLD1+chr2, HCT116+chr3 and HEC59+chr2 cells were maintained under selective pressure of 400 µg/mL geneticin (G418 sulfate, Roche). A2780cp70E1 cells were maintained under selective pressure of 200 µg/mL of hygromycin (Calbiochem). U251.TR3 cells were maintained in 100 µM TMZ.

1.2 Cell growing conditions

Early passage cells were stored in 10 % Dimethyl sulfoxide (DMSO)/FBS in liquid nitrogen and at -80˚C. All cell lines were cultured in T75 flasks (Corning) at 37˚C in 5 % CO_2. Every 3 days, cells were washed with 1X phosphate buffered saline (PBS) and cultured in fresh media. When cells were 70-90 % confluent, they were split by firstly washing them with 5 mL 1X PBS and then trypsinizing them with 4 mL 1X

Trypsin. Cells were incubated in Trypsin until completely detached. To inactive the Trypsin, 12 mL complete media was added and a portion of the cells (depending on the confluency required the following days) was diluted in media for a final volume of 10 mL and was transferred to a new flask. No cell line was cultured at passage higher than 10. All cell lines were authenticated on the basis of STR-profile, viability, morphologic inspection, and were routinely mycoplasma tested.

1.3 Cell seeding conditions

All experiments were performed in triplicate with cells of passage less than 10. When cells were 70-90 % confluent in a T75 flask, they were seeded in either 96, 12 or 6-well plates or 10 cm petri dishes (Corning), according to the experiments carried out, and in T75 flask for further experiments. Cells were washed with 5mL 1X PBS followed by addition of 4 mL 1X trypsin to allow the cells to detach and then 12 mL complete media was added to inactivate the trypsin. The cells were centrifuged at 1200 rpm for 3 mins and the pellet was resuspended in fresh media. Cells were counted using a Cell counter (TC20, BioRad) in order to plate the appropriate cell density for experiments.

2 High-throughput screens

2.1 High-throughput compound screen

The Prestwick compound library was a kind gift from Prof. Alan Ashworth (ICR, London, UK). This library was composed of 1120 small molecules which include 90 % that are marketed drugs and 10 % that are bioactive alkaloids. This library was at a concentration of 10 mM, in 14*96-well plates, with no drug in the first and last columns. The library was diluted in media at a concentration of 200 µM the day before use. The first and last columns of each plate contained either media or 200 µM 5-FU. DLD1 and DLD1+chr2 cells were plated in 96-well plates at a density of 1000 cells/well. The following day, cells were treated with either 2 µM 5-FU or media alone. On day 4, cells were exposed to 10 µM of each of the library compounds (5 µL of the 200 µM library stock into 95 µL of media). Cell viability was measured on day 7, using the CellTiter-Glo assay according to the manufacturer's instructions (refer to section 3.3) (Figure 12).

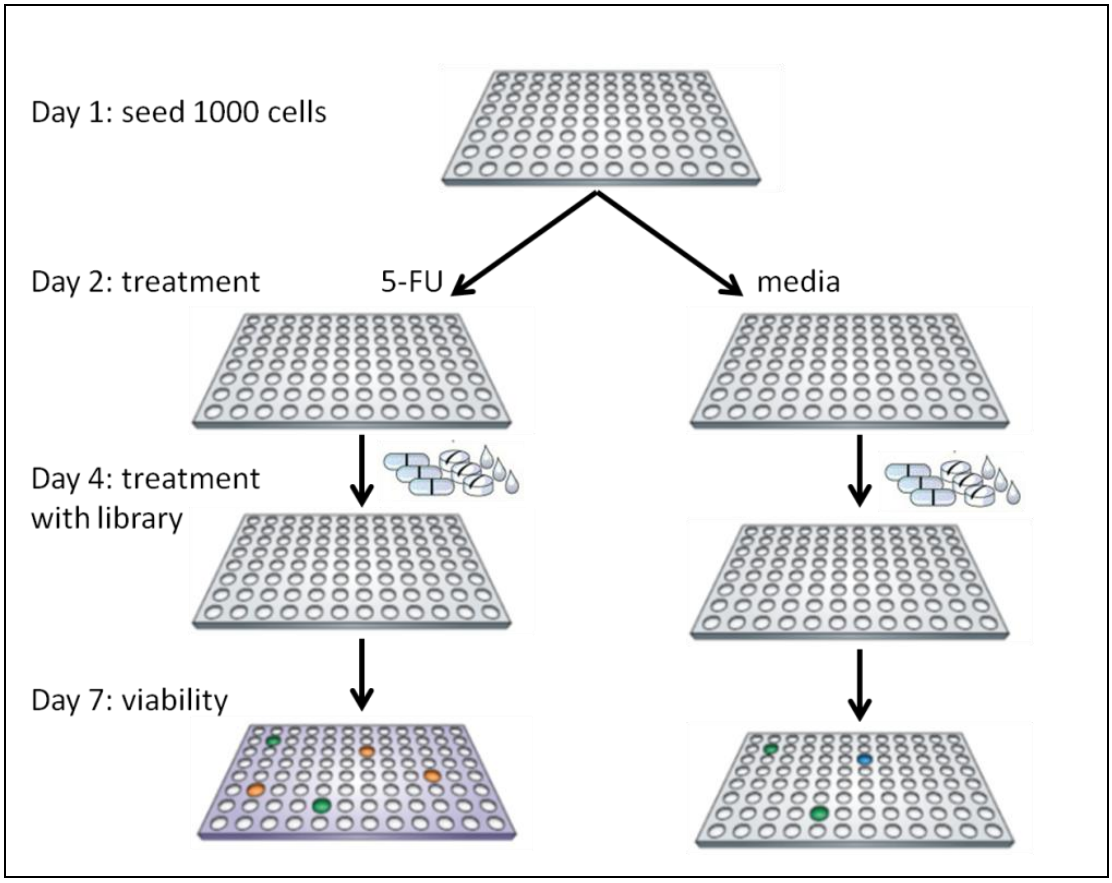

Figure 12: High-throughput compound screen

DLD1 and DLD1+chr2 cells were plated at the density of 1000 cells per well in 28*96-well plates each and treated, the following day, with the optimized concentration of 5-FU (2 µM) or media. After 2 days, cells were treated with 10 µM of each of the library compounds. After 3 days, cell viability was measured using an ATP-based luminescent assay. The library, after dilution in media, was stored at 4˚C and used after 24 and 48 hrs for replicate 1 and 2 respectively.

Luminescence readings from each well were log transformed and normalized according to the median signal on each plate and then standardized by use of a Z-score statistic, using the median absolute deviation (MAD) to estimate the variation in each screen (Figure 13) [356]. Z-score analysis has been described as a reliable method to analyse high-throughput screens [356]. In our case, a Z-score represented the magnitude of difference between one compound and the rest of the screen. This was based on the assumption of a normal distribution of cell viability upon treatment in a specific cell line. The standardization and normalization of the data in each cell line allowed comparing the 4 conditions (with or without 5-FU treatment in both DLD1 and DLD1+chr2 cell lines). A Z-score = 0 represented a compound that was

not cytotoxic and a Z-score < 0 represented a compound that was cytotoxic for the cells. We considered as potential hits the compounds with a Z-score lower than -1.5 and selected 5 compounds. A heatmap graph was generated using R software to represent the Z-scores of our selected compounds.

$$Z_{score} = X - \frac{median(sample)}{MAD(sample)} \qquad MAD(sample) = median_i\left(\left|X_i - median_j\left(X_j\right)\right|\right)$$

Figure 13: Z-score equation

2.2 Compound screen validation

Validation experiments were carried out with the following compounds: Triamterene, Clotrimazole, Quinacrine, Disulfiram and Astemizole (Table 7). Cells were plated in 96-well plates at a density of 1000 cells/well. The following day, cells were treated with either 2 µM 5-FU or increasing concentrations of the compound (from 1 nM to 10 µM). On day 4, 5-FU pre-treated cells were exposed to increasing concentrations of the compound (from 1 nM to 10 µM), and the media was replaced for cells previously treated with the hits compounds. Cell viability was measured on day 6, using the CellTiter-Glo assay. Luminescence data were normalized to the average luminescence reading of the untreated or the 5-FU treatment alone conditions to obtain the surviving fraction.

2.3 High-throughput siRNA screen

The siKinome SMARTpool library (Thermo-Fisher) used for this screen was composed of 779 SMARTpool siRNAs targeting protein kinases and kinase-related genes. This library was used at a concentration of 50 nM, with 5 µL of each siRNA (2 µM) in 9*96-well plates, no siRNA in the first and last columns. In the first and last columns of each plate media, 5 µL non-targeting control siRNA (siCtrl), or polo-like kinase 1 (PLK1) targeting siRNA (siPLK1) at 2 µM concentration were added. DLD1 and DLD1+chr2 cells were plated in 96-well plates at a density of 1800 cells/well. The following day, cells were transfected with the siKinome library using lipofectamine RNAiMAX transfection reagent (TR) (Invitrogen) according to the manufacturer's instructions (refer to section 6.1). Media was changed 24 hrs after transfection. Cell viability was measured after 4 days, using the CellTiter-Glo assay

(Figure 14). Luminescence readings from each well were normalized as described for the high-throughput compound screen (see section 2.1). Data were log transformed, normalized to the median signal on each plate, and standardized to Z-scores using the MAD (Figure 13) [356]. In our case, a Z-score represents the magnitude of difference between one siRNA compared to the rest of the screen. This was based on the assumption of a normal distribution of cell viability upon siRNA library transfection in a specific cell line. The standardization and normalization of the data in each cell line permit to compare the 2 cell lines using ΔZ-scores:

$$\Delta\text{Z-scores} = \text{Z-score}_{(\text{DLD1 cells})} - \text{Z-score}_{(\text{DLD1+chr2 cells})}$$

Negative ΔZ-scores represent genes synthetically lethal in DLD1 compared to DLD1+chr2 cells. We enforced a threshold of ΔZ-score <-1.5 to select 5 potential hits.

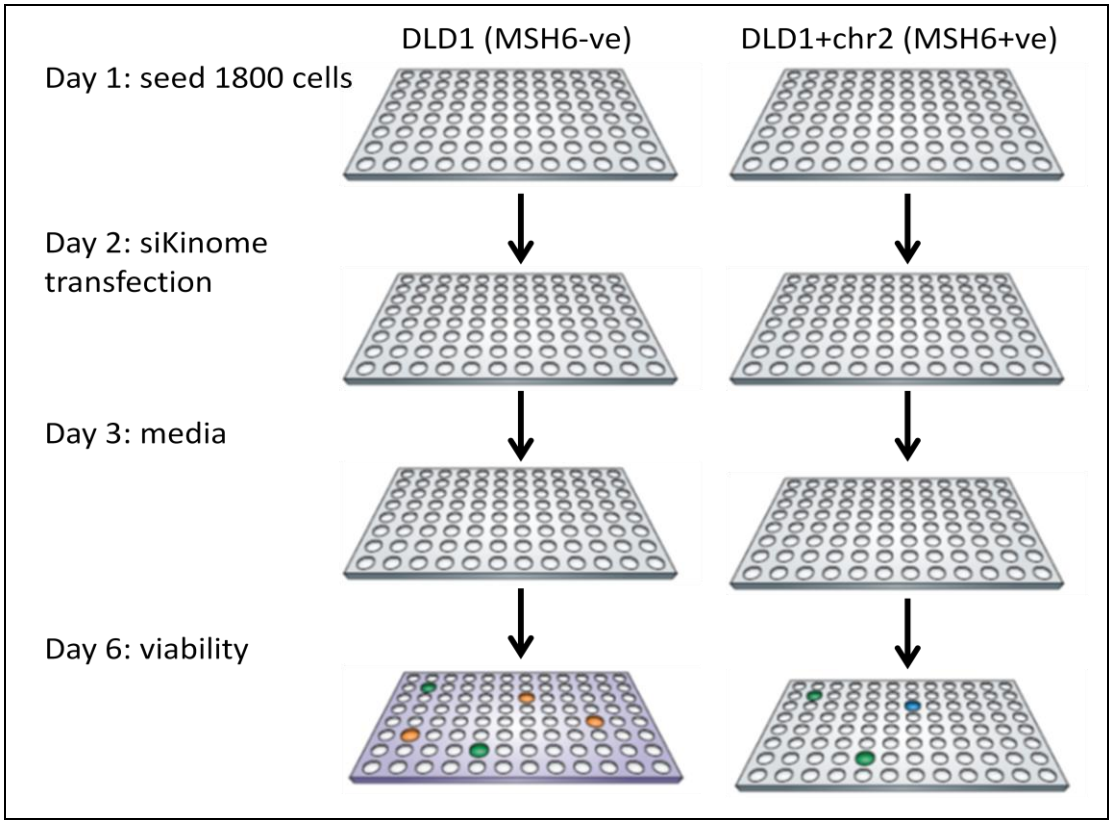

Figure 14: High-throughput siRNA screen

1 800 DLD1 and DLD1+chr2 cells were plated in 9*96-well plates and transfected with the siKinome library using RNAiMAX TR according to the manufacturer's instructions. We included 6*siCtrl and 4*siPLK1 in each plate for transfection controls. 24 hrs after transfection, the media was changed. Four days after transfection, cell viability was measured using the CellTiter-Glo ATP luminescence assay.

2.4 siRNA screen validation

After analysing the siRNA screen ΔZ-score data, 5 genes were selected for validation. A 96-well plate (GE Healthcare), containing one siRNA SMARTpool (the same as in the original siRNA screen) and 4 single siRNAs (deconvoluted from the SMARTpool siRNA) per hit gene, as well as 3* siCtrl and 2* siPLK1 was used following the same protocol as for the screen. In brief, 1800-2000 cells were seeded on day 1, followed by siRNA transfection using RNAiMAX TR, the media was replaced 24 hr after transfection and the cell viability was measured by an ATP-luminescence assay, 4 days after transfection.

3 Cell viability upon compound treatment

3.1 Compounds

All compounds were diluted according to manufacturer's instructions (Table 7). The compounds were stored in -20˚C except 5-FU, which was stored at room temperature.

Compounds	Catalogue number	Company	Stock concentration
5-FU	sud-5fu	Invivogen	70 mM (water)
Alisertib MLN8237	M76000	Epigentek	10 mM (DMSO)
Amiloride	sc-3578	Santa Cruz	10 mM (DMSO)
Astemizole	SIH-302	StressMarq	10 mM (DMSO)
Clotrimazole	2735	Sigma-Aldrich	10 mM (DMSO)
DHF	sc-214895	Santa Cruz	10 mM (DMSO)
Disulfiram	sc-205654	Santa Cruz	10 mM (DMSO)
Folate	sc-204758	Santa Cruz	10 mM (DMSO)
Leucovorin	sc-205701A	Santa Cruz	10 mM (DMSO)
NAC	sc-202232A	Santa Cruz	100 mg/mL (PBS)
Quinacrine	Q3251	Sigma-Aldrich	10 mM (water)
Raltitrexed	R9156	Sigma-Aldrich	10 mM (DMSO)
THF	sc-215955	Santa Cruz	100 mM (DMSO)
TMZ	sc-203292	Santa Cruz	100 mM (DMSO)
Triamterene	T4143	Sigma-Aldrich	10 mM (DMSO)

Table 7: Compounds

3.2 Short-term experiment

For short-term experiments, we carried out two different experiment scheduling. In general, i) Day 1, cells were plated in 96-well plates at a density of 1000 cells/well; day 2, cells were treated with the compound of interest (or a combination); day 6, cell viability was measured using the CellTiter-Glo assay. Alternatively, ii) Day 1, cells were plated in 96-well plates at a density of 1000 cells/well; day 2, cells were treated with the appropriate, indicated concentration of 5-FU or increasing concentrations of the compound of interest; day 4, the 5-FU pre-treated cells were treated with increasing concentrations of the compound of interest and the media was replaced on the previously drug-treated cells; day 6, cell viability was measured using the CellTiter-Glo assay. Luminescence data were normalized to the average luminescence reading of the untreated condition to obtain the surviving fraction. In the case of combination treatment, luminescence data were normalized to the average luminescence reading of the cells treated with the compound used at a constant concentration only.

3.3 Cell viability

Cell viability was measured using the ATP-based luminescent CellTiter-Glo assay (Promega). The luciferase reaction of this assay is:

$$\text{Beetle luciferin} + \text{ATP} + O_2 \rightarrow \text{Oxyluciferin}$$

CellTiter-Glo reagent was diluted 1:4 in 1X PBS prior to use. The media was removed from the cells and 100 µL of diluted CellTiter-Glo was added. The plates were mixed for 2 mins using a plate shaker (Grant-bio) and incubated for 10 mins at room temperature. Luminescence was read using a Wallac 1420 plate reader (PerkinElmer). Luminescence data were normalized to the average luminescence reading of the untreated condition to obtain surviving fractions.

3.4 Long-term clonogenic assay

Approximately 100-500 cells were seeded in 6-well plates in duplicate and treated with Triamterene every 3-4 days. Once cells had formed clear and distinct colonies (10-14 days), they were washed in 1X PBS, fixed with cold methanol for 10 mins and stained with 0.057 % Sulforhodamine B (SRB). Colonies were then washed with 1 % acetic acid prior to counting using a counter-pen (Fisherbrand). The number of

colonies counted per well was normalized to the average number of colonies in the untreated condition to obtain the surviving fraction.

4 Protein expression analysis

4.1 Protein extraction

Cells were lysed in 50-150 µL NP-40 lysis buffer (20 mM Tris [pH 8.0], 200 mM NaCl, 0.5 % NP-40, 10 % glycerol, 1 mM EDTA) and protease inhibitors cocktail (Roche). After 10 mins incubation, lysed cells were scraped off and transferred in 1.5 mL tubes (Eppendorf). After 15 mins incubation, lysed cells were centrifuged for 20 mins at 12 000 rpm at 4˚C. The supernatant was transferred in a new 1.5 mL tube and used fresh or stored at -80˚C. Protein concentration was measured using the Bradford protein assay (Sigma). 2 µL of protein lysates and 5 µL of standard dilutions of bovine serum albumin (BSA) (0, 0.1, 0.25, 0.5, 1, 1.5 mg/mL) were incubated with 250 µL Bradford reagent in triplicates in a 96-well plate. Plates were shaken and read at 560 nm using the microplate reader (Opsys MR, Dynex Technologies) and protein concentration was estimated using the BSA standard curve.

4.2 Western blot

Protein lysates (10-40 µg) were prepared in 10 % dithiothreitol (DTT) in 4X NuPage LDS sample buffer (Invitrogen) to a final volume of 25 µL. Lysates were incubated for 5 mins at 95˚C in order to denature the higher order structure. Boiled lysates were then electrophoresed on 4-12 % Novex precast gels (Invitrogen, UK) for 1 hr 30 mins at 120V and transferred onto nitrocellulose membrane (Thermo Scientific) using a wet-transfer method for 2 hrs at 20V. Membranes were blocked in 5 % milk/0.1 % Tween/1X PBS for 1 hr to prevent non-specific binding and then immunoblotted using primary antibodies overnight, using the indicated dilution (Table 8). This was followed by 1 hr incubation with secondary antibodies (mouse or rabbit depending on host animal for the primary antibody), diluted in 5 % milk/0.1 % Tween/1X PBS (Table 8). Before and after incubation with the secondary antibodies the membranes were washed 3 times for 5 mins in 0.1 % Tween/1X PBS. Protein expression was detected by chemiluminescence (SuperSignal West Pico

Chemiluminescent Substrate, Pierce, UK). Immunoblotting for β-actin was used as a loading control.

Antibody	Catalog number	Company	Dilution
alexa 488	A11034	Invitrogen	1:1000
β-actin	5125	Cell signalling	1:1000
DHFR	sc-377091	Santa cruz	1:1000
FLAG	F1804	Sigma	1:1000
γH2AX	05-636	Millipore	1:1000
MLH1	4256	Cell signalling	1:1000
MSH2	2017	Cell signalling	1:1000
MSH3	sc-11441	Santa Cruz	1:1000
MSH6	5424	Cell signalling	1:1000
PMS2	sc-618	Santa Cruz	1:1000
Thymidylate synthase	9045	Cell signalling	1:1000
anti-rabbit IgG	7074	Cell Signalling	1:4000
anti-mouse IgG	7076	Cell Signalling	1:4000

Table 8: Antibodies

5 Quantification of mRNA level

5.1 RNA extraction

Cells were plated in 6-well plates. After appropriate drug treatment or siRNA transfection, cells were washed in 1X PBS and 1 mL Trizol was added to lyse the cells and maintain the RNA integrity. Samples were transferred in 1.5 mL tubes, 200 µL chloroform was added and the tubes were centrifuged for 15 mins at 12 000 rpm at 4˚C to separate proteins, DNA and RNA. The aqueous phase containing RNA was transferred to a new tube and precipitated with 1 mL isopropyl alcohol for 10 mins at room temperature, centrifuged for 10 mins at 12 000 rpm at 4˚C and then washed with 1 mL 75 % ethanol and centrifuged for 5 mins at 7 000 rpm at 4˚C. RNA, after purification, was resuspended in water. Concentration and purity was measured with a ND-1000 NanoDrop.

5.2 Multiplexed Real-time PCR

To measure mRNA expression, we performed a reverse transcription quantitative polymerase chain reaction (RT-qPCR). The mRNA was firstly reversely transcribed to cDNA for better stability using the omniscript RT kit, according to manufacturer's instructions (Qiagen). In brief, 1 µg of RNA was incubated with 2 µL oligodT (10 µM), 2 µL dNTP pool (5 mM each dNTP), 0.25 µL RNAse inhibitor (40 units/µL) and 1 µL reverse transcriptase (4 units/µL) for a final volume of 20 µL in Buffer RT. The reaction was incubated for 1 hr at 37˚C. The cDNA was then incubated on ice to stop the reaction. The diluted cDNA was used to measure the mRNA expression levels. For each sample replicate, 1.2 µL GAPDH probes/primers (4310884E) and 1.2 µL gene specific Taqman DNA probes/primers (SOD1: Hs00533490_m1; SOD2: Hs00167309_m1; NRF1: Hs00192316_m1 and NRF2: Hs0095961_g1 from Applied Biosystems) were added to 10 µL 2X Taqman mastermix (Applied Biosystems). In a 96-well plate, 12 µL probes/primers/maxtermix was added to 8 µL cDNA (diluted 1:8 in water) and the gene specific sequence of cDNA was amplified and measured by real-time qPCR (750 real-time PCR system, Applied Biosystems). The PCR program used to amplify the cDNA was 2 mins at 50˚C, 10 mins at 95˚C followed by 40 cycles of 15 sec at 95˚C and 1 min at 60˚C. The fluorescence was read at the end of each cycle. In a Taqman qPCR, a fluorophore-bounded probe recognizes and binds single stranded DNA of a specific gene. During DNA synthesis of this specific gene (using specific primer), the fluorophore probe is degraded and fluoresces. Therefore, the fluorescence is proportional to the DNA synthesis. The quantification of cDNA was calculated by measuring the number of PCR cycles (Ct) necessary to reach a defined quantity of cDNA. The Ct results for each gene of interest were normalized to GAPDH mRNA level. Results were expressed in relative quantity (RQ) according to the following equation:

$$RQ=2^{-(Ct\ (cDNA\ interest)\ -\ Ct\ (cDNA\ GAPDH))}$$

Samples were run in triplicate and experiments were carried out in triplicate. Results were normalized to the untreated condition of the MMR deficient sample.

6 Transfection

6.1 siRNA transfection

In order to silence gene expression, cells were transfected with individual small interfering RNA (siRNA) (Table 9; Qiagen) using lipofectamine 2000 or RNAiMAX according to manufacturer's instructions (Invitrogen). Briefly, cells were seeded in 96-well plates or 6-well plates at 1000-2000 cells/well and 100 000-150 000 cells/well, respectively. The following day, cells were transfected and the media was replaced after 24 hrs post transfection. For transfection in 96-well plates, each siRNA was transfected into the two paired cell lines using the same transfection reaction as follows; 0.4 µL TR and 50 µL OptiMEM media (Invitrogen) were incubated in a 50 mL tube for 5 mins. In a clear 96-well plate, 50 µL of TR in OptiMEM was added to 5 µL of siRNA (2 µM). After 20 mins incubation, 155 µL complete media was added. The media of the cells was then replaced by 100 µL of the siRNA/TR/OptiMEM mix for a final siRNA concentration of 50 nM. In the case of transfections in 6-well plates, for each siRNA transfected in two cell lines, 10 µL TR and 500 µL OptiMEM media (Invitrogen) were incubated in a 50 mL tube for 5 mins; In a 1.5 mL tube, 500 µL of TR in OptiMEM was added to 10 µL of siRNA (20 µM) and incubated for 20 mins. The media of the cells was changed and 250 µL of the siRNA/TR/OptiMEM mix was added for a final siRNA concentration of 100 nM.

Cells were transfected with siCtrl or siPLK1. The cell viability of cells transfected with siCtrl was compared to the cells grown in media alone to assess whether the transfection itself did not affect cell viability. Transfection with siPLK1 was used as a positive control for transfection efficiency. PLK1 was a polo-like kinase implicated in mitosis and apoptosis, its silencing causes cell death in most cell lines [357]. It was expected to have 80-100 % cell viability in siCtrl transfected cells and 0-20 % in siPLK1 transfected cells in comparison to un-transfected cells.

In case of a combination of siRNAs, the final siRNA concentration was the same in all conditions. For example, for a combination of 3 siRNAs in 96-well plates, we used 50 nM of each siRNA (i.e. with siRNA targeting the subunits (α, β and γ) of the epithelial sodium channel (ENaC), 50 nM siENaCα, 50 nM siENaCβ and 50 nM siENaCγ) which correspond to a 150 nM final concentration. To compare this

combination of 3 siRNAs to a single siRNA, we used a combination of 50 nM of a single siRNA (i.e. siENaCα) and 100 nM of siCtrl in order to have the same final concentration of 150 nM siRNA and the same 50 nM concentration of the siRNA of interest (i.e. siENaCα). Similarly, to compare a combination of 3 siRNAs to a combination of 2 siRNAs, we used a combination of 50 nM of both siRNAs (i.e. 50 nM siENaCα and 50 nM siENaCβ) and 50 nM of siCtrl.

Name	Target sequence
Ctrl	5'-CATGCCTGATCCGCTAGTC-3'
PLK1	5'-CCGGATCAAGAATGAATA-3'
ENaC_α	SMARTpool
ENaC_β	SMARTpool
ENaC_γ	SMARTpool
DHFR_1	5'-TACGGAGAAACTGAACTGAGA-3'
DHFR_2	5-'AACCTCCACAAGGAGCTCATT-3'
TYMS_1	5'-CCAAACGUGUGUUCUGGAA-3'
TYMS_2	SMARTpool

Table 9: siRNAs

6.2 Plasmid transformation and transfection

In order to over-express a protein, cells were transfected with a plasmid using Fugene HD TR (Section 6.3; Promega). DHFR plasmid (#RC200089) and its corresponding empty vector (#PS100001) were purchased from OriGene. TYMS plasmid was cloned from a cloning library (see 6.2.1) into the pIREShyg3 empty vector (#631620 ClonTech).

6.2.1 TYMS plasmid construction

To generate a TYMS expression construct we ligated the amplified TYMS gene insert into the pIREShyg3 empty vector. The insert was amplified by PCR from the MegaMan cDNA library (Agilent) using 2 primers targeting TYMS:

Fwd 5'-ATCTAGCTAGCATGCCTGTGGCCGGCTCG-3'

Rev 5'-TCGCGGATATCAGCACCCTAAACAGCCATTTC-3'

For each PCR reaction: 10 µL 5X HF buffer; 2.5 µL Fwd primer (10 µM); 2.5 µL Rev primer (10 µM); 1 µL dNTPs (10 mM); 0.5 µL Phusion polymerase and 0.5 µL

MegaMan library were mixed to a final volume of 50 µL in water. The PCR was run for 2 min at 98˚C; followed by 35 cycles of 1 min at 98˚C, 30 sec at 64˚C and 1 min at 72˚C; and 7 mins at 72˚C. The PCR product was electrophoresed for 1 hr at 150 V in a 1 % agarose gel (containing 1:2000 GelRed; Biotiom) and the appropriate band was extracted and purified with a Qiagen Gel Extraction kit according to the manufacturer's instructions. 41 µL PCR product was then digested with 2 µL NheI and 2 µL EcoRV restriction enzymes (20 000 units/mL; BioLabs) in 5 µL CutSMART buffer for 2 hrs in a water-bath at 37˚C. The digested PCR product was purified using a Qiagen PCR Clean up kit according to the manufacturer's instructions and electrophoresed for 1 hr at 150 V on a 1 % agarose gel (containing 1:2000 GelRed; Biotiom) to validate the digestion. The last step was the ligation of the pIREShyg3 empty vector with the digested PCR product. To this end, 10 µL PCR product, 1 µL vector, 2 µL 10X ligase buffer, 1 µL ligase, 2 µL PEG 4000 and 4 µL water were incubated for 1 hr at room temperature.

6.2.2 Plasmid transformation

All plasmids (empty vectors, DHFR plasmid and TYMS plasmid) were primarily transformed into NEB-5α competent E. *Coli* bacteria by heat shocking 25 µL of bacteria in presence of 1-5 µL of plasmid for exactly 30 seconds at 42˚C. 650 µL Lysogeny broth (LB) was added to the transformed bacteria and incubated and shaken at 3000 rpm for 1-2 hrs at 37 ˚C. Bacteria were spread on two LB agar plates complemented with the appropriate antibiotic (100 µg/mL Ampicillin or 30 µg/mL Kanamycin). In order to be able to select an individual colony in the case of either low or high transformation rate, 90 % bacteria were spread on one plate and 10 % on the other plate. One colony of each transformation was selected and grown in liquid LB for 12-18 hrs. Glycerol stocks were generated by mixing 1:1 ratio of bacterial culture with 50 % glycerol and stored at -80˚C. Plasmid DNA was extracted from the remaining bacterial culture using the Qiagen Plasmid Miniprep kit according to the manufacturer's instructions. The DNA concentration and purity was measured with a ND-1000 NanoDrop.

6.3 Plasmid transfection

Plated cells were transfected the following day with plasmids using Fugene HD TR. For transfections in 96-well plates, 100 ng/well of plasmid DNA was diluted in optiMEM to a total volume of 5 µL. After adding 0.6 µL Fugene, 5 µL of the transfection mix was added to the cells. In 6-well plates, 1 µg/well of plasmid was diluted in optiMEM for a total volume of 50 µL. After adding 6 µL Fugene, 50 µL of the transfection mix was added to the cells. The media was replaced 24 hrs after transfection.

6.4 Qiagen kits protocols

We used a number of Qiagen kits: Gel extraction kit, PCR Clean up kit and miniprep kit according to the manufacturer's instructions. They all follow the same steps: sample preparation, DNA isolation, washes and elution. Samples for bacterial DNA extraction (miniprep kit) were prepared using an alkaline lysis buffer; DNA was isolated from an agarose gel and from the PCR enzymatic reaction by using a buffer containing chaotropic salts, a denaturating agent (Gel extraction kit and PCR Clean up kit). For all samples, DNA was absorbed onto a silica membrane in presence of high concentration of salts. The membranes were then washed with a buffer composed of 10 mM Tris-Cl [pH 7.5] and the DNA was eluted in water.

7 DNA and RNA concentration

The concentration and quality of DNA and RNA samples were measured using the ND-1000 NanoDrop. RNA and DNA absorb light at 260 nm, solvents at 230 nm and proteins at 280 nm. Therefore, to validate the quality, we looked at the absorbance ratio 260/230 and 260/280. A solvent contamination of our samples was observed by a ratio 260/230 lower than 1.7. A protein contamination of our samples was observed by a ratio 260/280 lower than 1.7.

8 Antioxidant Response Element (ARE) reporter assay

The antioxidant response was measured using an ARE reporter assay kit (Qiagen) according to the manufacturer's instructions. This kit includes different reporter plasmids: an ARE reporter to measure the activity of the ARE promoter (a firefly luciferase construct regulated by ARE); a negative control to measure the background (a firefly luciferase construct with no regulation promoter); and a positive control to measure the transfection efficiency (a firefly luciferase construct regulated by CMV). Each reporter plasmid contained an internal control (a renilla luciferase construct regulated by cytomegalovirus (CMV)) to measure cell viability (Table 10).

Components	Constructs
ARE reporter	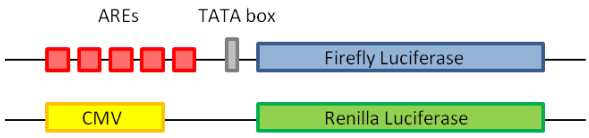
Negative control	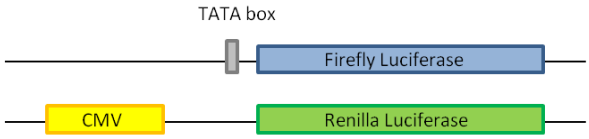
Positive control	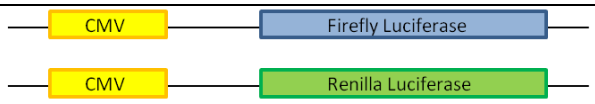

Table 10: ARE reporter assay constructs

In our experiment we combined siRNA transfection, ARE reporter plasmid transfection and drug treatments (Figure 15). The experiment schedule for this experiment was: on day 1, we plated 150 000 cells in 6-well plates; on day 2, we transfected the cells with siCtrl, siPLK1 and siTS as described previously (section 6.1); on day 3, cells were washed with 1 mL 1X PBS incubated in 250 µL Trypsin at 37 ˚C, when the cells were detached, 2 mL complete media was added and the cells were transferred in 15 mL tubes and centrifuged at 3 200 rpm for 3 mins. Cells were counted and seeded at the density of 3,000 cells/well into 96-well plates; on day 4, we transfected the cells with the ARE reporter assay using Fugene HD TR. We added per well 5 µL of a mix of 1 µL of the ARE reporter, negative control or

positive control (100 ng/µL), 0.6 µL Fugene and 5 µL of optiMEM; on day 5, we treated the cells with DMSO or 10 µM Triamterene; and on day 6, we measured ARE promoter activity using a dual luciferase assay (Promega) according to the manufacturer's instructions. In brief, we removed the media, washed the cells with PBS and added 20 µL of lysis buffer. Plates were mixed for 15 mins using a plate shaker (Grant-bio). In order to quantify the firefly luciferase activity, 100 µL Luciferase Assay Substrate was added and the luminescence was read using a Wallac 1420 plate reader (PerkinElmer). After the first reading, 100 µL Stop&Glo Substrate was added and the luminescence read on the same plate reader to measure the Renilla luciferase activity. The firefly luciferase activity was normalized to the Renilla luciferase activity.

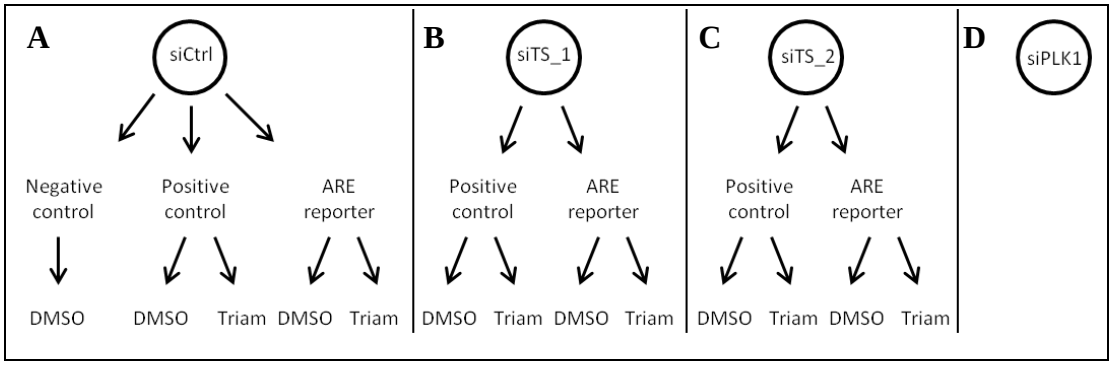

Figure 15: ARE reporter assay scheduling experiment
A: Cells transfected with siCtrl were then transfected with the negative control, positive control and ARE reporter from the ARE reporter assay; **B, C:** cells transfected with siTS are then transfected with the positive control and ARE reporter; **D:** cells transfected with siPLK1 are kept in 6-well plates to control the siRNA transfection efficiency. **A-C:** One day after ARE reporter assay, cells were treated in triplicates with DMSO or 20 µM Triamterene (Triam).

9 DHFR activity assay

DHFR activity was measured with a DHFR assay kit (Sigma, CS3040), according to the manufacturer's instructions. Cells were plated in 10 cm dishes. After 5 and 10 µM Triamterene treatment, proteins were extracted and the concentration was measured as indicated previously (section 4.1). All samples were diluted to 1 mg/mL in the assay buffer provided to a final volume of 1 mL. After addition of 5 µL DHF

and 6 µL NADPH, the optical density (OD) at 340 nm was measured every 15 sec for 4 mins using a BioPhotometer plus (Eppendorf). Absorbance was normalized in ΔOD/min using the equation: $\Delta OD/min = \frac{OD(4\,min) - OD\,(0min)}{4min}$.

10 Reactive oxygen species assay

Cellular ROS was measured using DCFDA-Cellular Reactive Oxygen Species Detection Assay Kit (Abcam, ab113851) according to the manufacturer's instructions. 2',7'-dichlorofluorescein diacetate (DCFDA) - non fluorescent - was converted in DCF - fluorescence - by ROS (H_2O_2, •OH, $ONOO^-$ and $•O_2^-$) [358-360]. To measure ROS levels in our cells, we plated 3 000 cells in one 96-well plate for cell viability, and one clear bottom black 96-well plate for the ROS assay. For a dose dependent experiment, cells were treated with the appropriate concentrations of Triamterene for 48 hrs. For a time course experiment, cells were treated with the appropriate concentration of Triamterene at different time points identically for both plates (24 hrs treatment corresponded to cells treated 24 hrs prior DCF measurement). After appropriate treatment in both plates identically, cells in the clear bottom black 96-well plate were washed in 1X PBS and treated with 20 µM DCFDA or incubated in assay buffer as a negative control. After 30 mins incubation at 37˚C, cells were washed with 1X PBS and incubated for 4 hrs in fresh assay buffer at 37˚C in a 5 % CO_2 incubator. Fluorescence was measured, using the Wallac 1420 plate reader (PerkinElmer), in the clear black bottom 96-well plate and cell viability was measured in the other 96-well plate using the CellTiter-Glo assay. Fluorescence data were normalized to the cell viability luminescence data and to the average of the normalized fluorescence of the untreated MMR deficient condition.

11 Immunofluorescence

Cells were seeded on coverslips coated in Poly-L-Lysine (Corning) in 6-well plates at a density of 75 000 DLD1 and DLD1+chr2 cells/well or 100 000 U251 and U251.TR3 cells/well. After 48 hrs treatment with 10 µM Triamterene in the DLD1 and DLD1+chr2 cells, or 24 hrs treatment with 20 µM Triamterene in the U251 and U251.TR3 cells treatment; cells were fixed in 4 % Paraformaldehyde and permeabilised in 0.2 % 100X Triton. Cells were then blocked in 5 % BSA/1X PBS for a minimum of 30 mins. Coverslips were incubated in 50 µL γH2AX primary antibody (1:1000 in 5 % BSA) overnight at 4˚C. The coverslips were washed in 1X PBS and incubated with 50 µL Alexa Fluor® conjugated secondary antibody (1:1000 in 5 % BSA) for 1 hr in the dark (Table 8). Coverslips were then washed in 4 % DAPI/1X PBS and mounted on a slide with 3 µL ProLong® gold antifade mounting solution (Invitrogen). When dry, the coverslips were stored at 4˚C and analysed using the confocal LSM 510 microscope (Zeiss). For the DLD1 and DLD1+chr2 cells, we used a 40x objective and captured at least 3 images per condition using the same settings. Images were analysed and cells positive for >5 γH2AX foci were counted using the cell counting software available using ImageJ. For U251 and U251.TR3 cells, cells positive for >5 γH2AX foci were counted directly on the confocal using a 40x objective. Images were captured with the same conditions as for DLD1 and DLD1+chr2 cells. Results were normalized to the total number of cells counted per cell line.

12 *In vivo* experiments

12.1 Drug preparation

For *in vivo* experiments, Triamterene was used at concentrations of 25 mg/kg and 50 mg/kg. The average weight for a mouse was 27.2 g therefore 25 mg/kg and 50 mg/kg corresponded to 6.8 mg/mL and 13.6 mg/mL Triamterene, respectively. Triamterene was diluted in folate-free RPMI media (Sigma) and stored in aliquots in 1.5 mL tubes at -20˚C. The vehicle used as a control for all the *in vivo* experiments was folate-free RPMI media, stored in aliquots in 1.5 mL tubes at -20˚C. A fresh aliquot was used for each treatment.

12.2 *In vivo* pilot experiment

Cells were resuspended in 1X PBS at the density of 16 million cells per mL. We injected subcutaneously 100 µL of cells using 22 gauge needles, into both flanks of adult (~10 weeks old) male NOD-SCID mice (Charles-River Laboratories) [361]. When the tumours were all measurable, the mice were treated 3 times a week by gavage or intraperitoneal (IP) injection, with either 25 mg/kg, 50 mg/kg Triamterene or vehicle (only by IP, no gavage) (Figure 16). Tumours were measured twice weekly. Using callipers, we measured the width and the length of the tumours. The tumour growth was calculated as follows [362]: area (mm^2) =width (mm) * length (mm).

Each tumour measurement was normalized to the tumour size obtained on the first day of treatment. Results were analysed by calculating the slope linear regression using GraphPad Prism software, assuming the tumour growth was linear.

12.3 *In vivo* experiment

Cells were resuspended in 1X PBS at the appropriate number ($1.6x10^6$ cells for the first experiment on 20 mice; $0.6x10^6$ DLD1 cells, $0.8x10^6$ DLD1+chr2 cells for the second experiment on 40 mice). We injected subcutaneously 100 µL of cells, into one flank of adult (~10 weeks old) male NOD-SCID mice. When the tumours were measurable, the mice were treated 3 times a week by gavage, with 25 mg/kg Triamterene or vehicle. Tumours were measured twice weekly. The mice were sacrificed in case of sickness or when the tumours reached 1.44 cm^2. Tumours from each mouse were harvested on the day of sacrifice. The measurements were normalized to the size of the tumour on the first day of treatment.

In the case of U251 and U251.TR3 xenografted mice, $2.5x10^6$ or $1x10^6$ cells in 1X PBS or $1x10^6$ cells in matrigel (1:1) were injected subcutaneously. No tumour was visible 4 weeks after injection; therefore, the mice did not receive treatment and were sacrificed.

For all mice experiment, animals were sacrificed in the event of sickness or when the tumours reached 1.44 cm^2. All animal procedures were carried out as per the Animals Scientific Procedures Act 1986, under the Home Office approval licences (PPL 70/7275 and PIL – 70/23444).

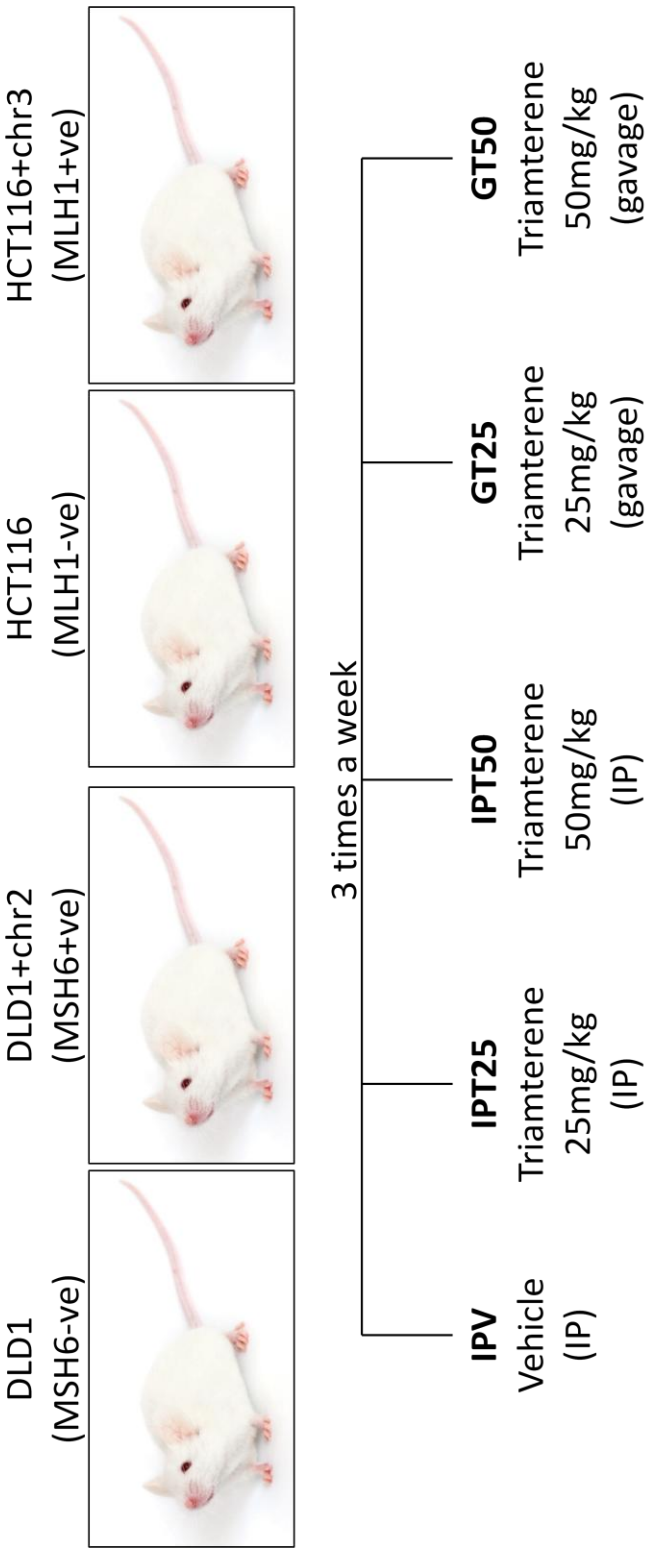

Figure 16: *In vivo* pilot experiment

DLD1, DLD1+chr2, HCT116 and HCT116+chr3 cells were injected in both flanks of each mouse at the density of $1.6x10^6$ cells per tumour (5 mice per cell line). Mice were treated 3 times a week with either 25 mg/kg (T25) or 50 mg/kg (T50) Triamterene, by IP or by gavage (G); and with vehicle (V) by IP. Tumours were measured twice a week.

12.4 RNA extraction from tumours

All the tumours were harvested on the day of sacrifice and stored at -80˚C. We extracted RNA from all the tumours from the second repeat experiment in DLD1 and DLD1+chr2 xenografted mice. We incubated a section of frozen tumour in 1 mL Trizol reagent. The frozen tumour was homogenized for 10 seconds using the cell homogenizer (Ultra Turrax T25basic, Labortechnik) and placed on dry ice. RNA from all the homogenized tumours was extracted following the RNA extraction protocol described previously (section 5.1).

13 Data analysis and representation

For data analysis, values unless otherwise stated were normalized to the average of the untreated condition in the cell line concerned. All graphs were generated using Graphpad Prism software except the heatmap which was generated using R software. All experiments were carried out in triplicate and error bars represent standard error of the mean (SEM). Statistics for data significance were measured using Graphpad Prism software. Stars were used to represent significance on graphs with:

NS p-value > 0.05; * p-value < 0.05; ** p-value < 0.01; *** p-value < 0.001

Results were considered non-significant (NS) when the p-value > 0.05. The test used to calculate the p-values was dependant on the conditions compared and was stipulated in the legend for each graph. The most frequently used statistical test was a 2way ANOVA, to compare surviving curves and time course experiments; and 1way ANOVA to compare 2 conditions among a multi-condition test (often represented with a histogram). Both tests were followed by Bonferroni correction test which was considered the simplest and most conservative method to counteract the problem of multiple comparisons [363].

For the mice experiment, it was not possible to use a 2way ANOVA as all the mice did not survive until the end of the experiment (2way ANOVA cannot be used in case of missing values). We did not want to assess the significance of the last measurement only as we considered it would be biased as not all mice survived until then. Therefore, we used a two-tailed paired t-test which has been previously used in other studies to evaluate differential tumours growth *in vivo* [364-367].

Results

Chapter 1: Identification of novel therapeutics for the treatment of MMR deficient tumours

Chapter 2: Investigation into Triamterene as a synthetic lethal drug for the treatment of MMR deficiency

Chapter 3: High-throughput siRNA screen to identify synthetic lethal interactions with MSH6 deficiency

Chapter 1: Identification of novel therapeutics for the treatment of MMR deficient tumours

The MMR pathway is responsible for the repair of base-base mismatches and insertion/deletion loops, formed during DNA replication. Mutations in MMR genes significantly increase the predisposition to cancer with MMR deficiency estimated to be present in 15-17 % of all CRCs. 5-FU is the main treatment for advanced CRC, however the majority of studies suggest that MMR deficient tumours are more resistant to 5-FU than MMR proficient tumours. Therefore, there is a critical clinical need to identify novel therapeutics to treat these tumours.

1 DNA mismatch repair deficient cell lines are resistant to 5-FU treatment

MMR deficient cells are reported to be more resistant to 5-FU treatment and this has critical clinical implications for the treatment of MMR deficient CRCs. In order to assess this resistance, we studied cell viability upon treatment with increasing concentrations of 5-FU in our panel of MMR deficient and MMR proficient paired-cell lines (Table 11). We firstly confirmed the MMR status of our panel by analysing the protein expression of MLH1, MSH2, MSH6, MSH3 and PMS2 by western blot (Figure 17A). As previously described [368], PMS2 expression levels were decreased in MLH1 deficient cells. We confirmed this in our MLH1 deficient HCT116 and A2780cp70 A2 cell lines with loss of MLH1 by mutation or methylation, respectively, leads to a decrease in PMS2 expression. Similarly, MSH6 and MSH3 expression levels have previously been shown to have decreased expression in MSH2 deficient cells [140]. Consequently, we observed that MSH3 and MSH6 expression were reduced in the MSH2 mutated HEC59 cells. This is because, PMS2 is unstable without heterodimerization with MLH1, and MSH3 and MSH6 are unstable without heterodimerization with MSH2. However, loss of MSH6

in DLD1 cell lines, or MSH3 in HCT116 and HCT116+chr3 cell lines, does not lead to loss of MSH2 expression as MSH2 can remain stable by complexing with either MSH3 or MSH6 [369]. We also have in our panel of paired cell lines, another MSH6 deficient and proficient paired cell lines, U251.TR3 and U251 glioblastoma cells. The U251.TR3 TMZ resistant cell lines were generated by continuous exposure of U251 cells to 100 µM of TMZ and were found to have generated a somatic MSH6 mutation (resulting in a $Thr^{1219}Ile$ substitution) [235], and decreased MSH6 expression was confirmed by western blot (Figure 17B).

In our panel of cell lines, three cell lines (DLD1, HCT116 and HEC59) harbour mutations in MMR genes. They are matched paired with proficient cell lines generated by the stable addition of a chromosome (chr2 for re-expression of MSH2 and MSH6, chr3 for re-expression of MLH1). The main advantage for these matched paired cell lines is that they only differ on the addition of a chromosome and therefore on the MMR status. They do not differ on secondary mutations that often occur in MMR deficiency [239, 370]. Our panel of cell lines is also composed of MMR deficient cell lines by other means. This is the case for U251.TR3 (MSH6 mutation acquired by continuous exposure to TMZ) and A2780cp70 A2 (MLH1 methylation acquired by continuous exposure to Cisplatin). Therefore the matched paired cell lines differ from MMR status and secondary mutations. Our panel is composed of matched paired cell lines representing a wide range of tumour types. Therefore, this panel represents a great tool for the study of MMR dependent mechanisms.

Origin	Cell line	MMR status	Reference
Colorectal	DLD1	MSH6 mutation	[370]
	DLD1+chr2	MMR proficient	
Colorectal	HCT116	MSH3 and MLH1 mutation	[239]
	HCT116+chr3	MSH3 mutation	
Ovarian	A2780cp70 A2	MLH1 methylation	[242, 315]
	A2780cp70 E1	MMR proficient	
Endometrial	HEC59	MSH2 mutation	[370]
	HEC59+chr2	MMR proficient	
Glioblastoma	U251.TR3	MSH6 mutation	[235]
	U251	MMR proficient	

Table 11: Matched paired cell lines panel

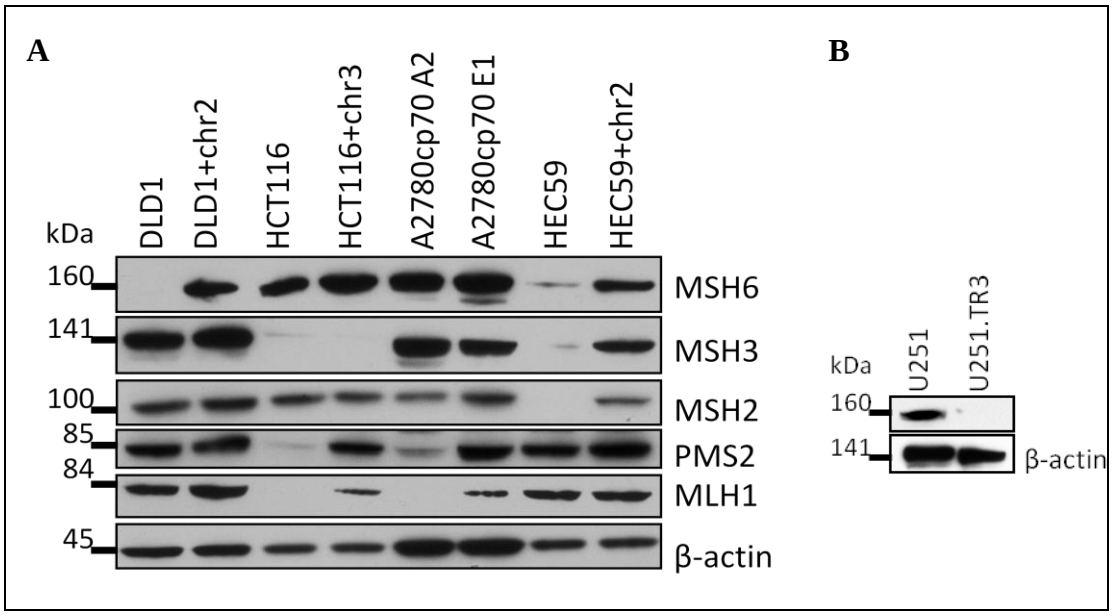

Figure 17: MMR status in our panel of cell lines

A: Cells were seeded in 6-well plates and proteins were extracted three days later. Protein expression was measured by western blot using MSH2, MSH3, MSH6, MLH1, PMS2 and β-actin antibodies. β-actin is used as a loading control. **B:** U251 and U251.TR3 cells were seeded in 6-well plates and proteins were extracted three days later. Protein expression was measured by western blot using MSH6 and β-actin antibodies. β-actin is used as a loading control.

In order to assess 5-FU resistance in MMR deficient cells, we treated our panel of MMR deficient and MMR proficient cell lines with 5-FU (increasing concentrations from 1 µM to 10 µM) to determine their sensitivity to 5-FU treatment. We observed that all MMR deficient cell lines were more resistant to 5-FU treatment in comparison to their MMR proficient matched paired cell lines (Figure 18 & Figure 19). Therefore, our results validate that MMR deficiency confers resistance to 5-FU treatment.

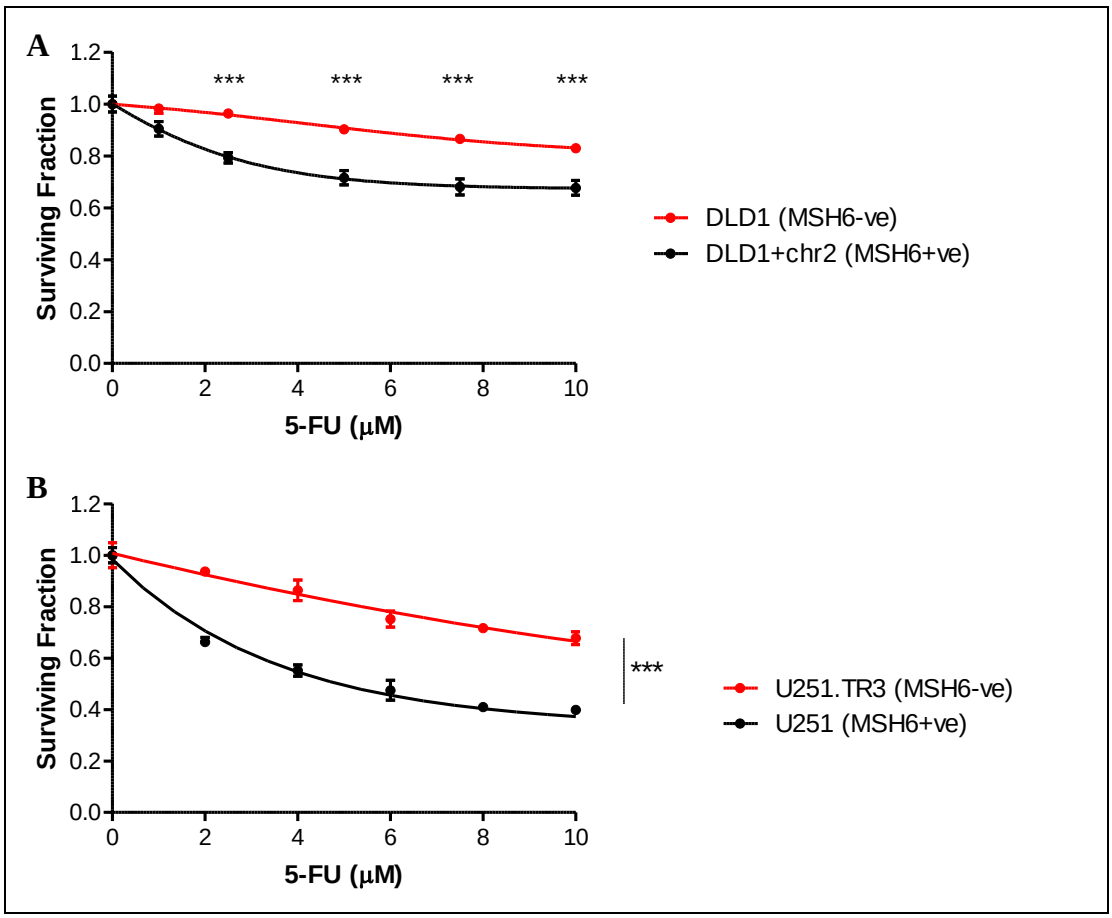

Figure 18: 5-FU response on our panel of MSH6 proficient and deficient cell lines

A, B: Cells were seeded in 96-well plates and treated with increasing concentrations of 5-FU (1, 2.5, 5, 7.5 and 10 µM in DLD1 and DLD1+chr2 cells; 2, 4, 6, 8 and 10 µM in U251 and U251.TR3 cells). After 4 days treatment, cell viability was assessed by ATP-luminescence assay. Experiments were carried out in triplicate and error bars represent SEM. P-values derived from 2way ANOVA (*** $p < 0.001$).

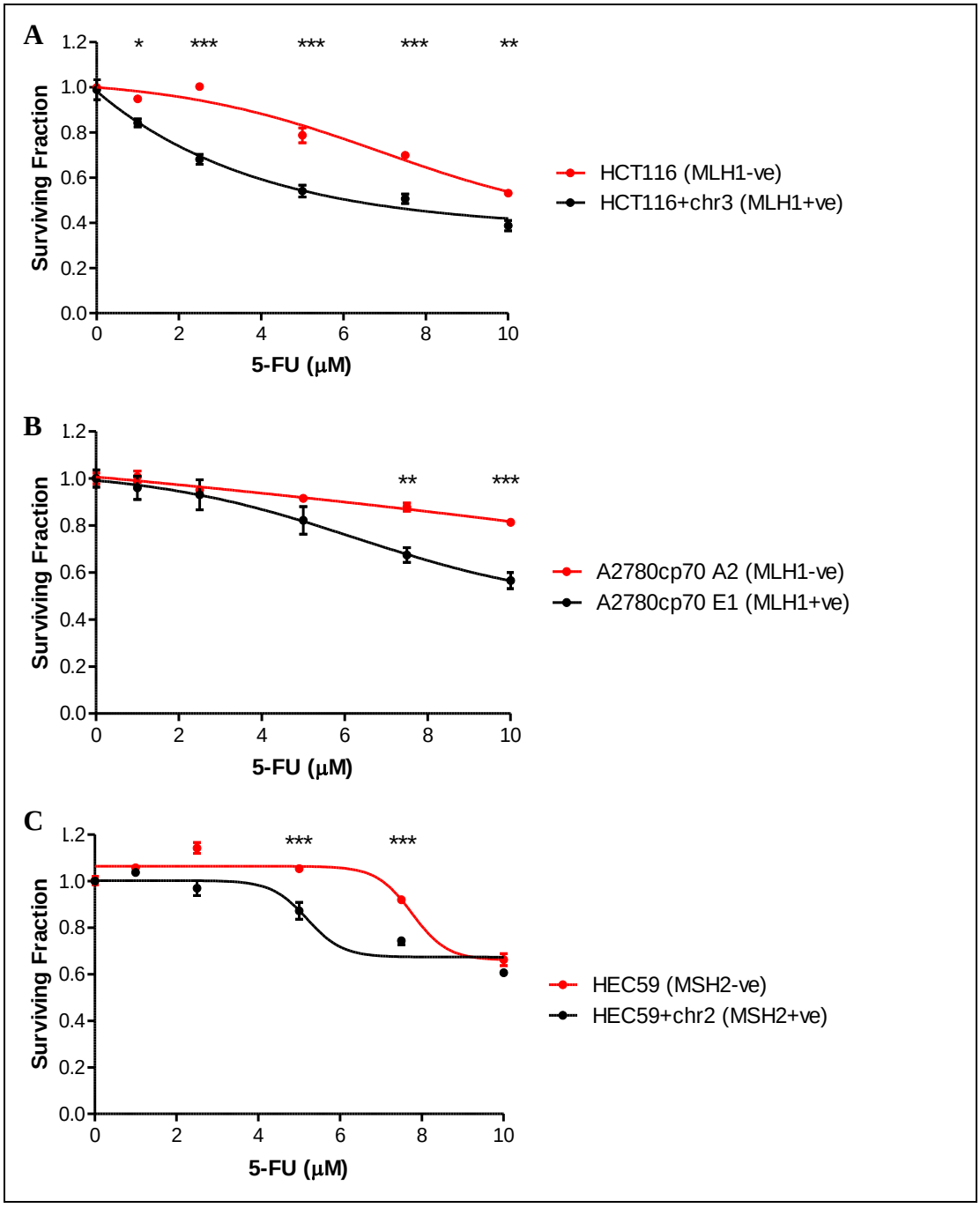

Figure 19: 5-FU response on our panel of MLH1 and MSH2 MMR proficient and deficient cell lines

A-C: Cells were seeded in 96-well plates and treated with increasing concentrations of 5-FU (1, 2.5, 5, 7.5 and 10 µM). After 4 days treatment, cell viability was assessed by ATP-luminescence assay. Experiments were carried out in triplicate and error bars represent SEM. P-values derived from 2way ANOVA (* $p < 0.05$, ** $p < 0.01$, *** $p < 0.001$).

2 High-throughput compound screen

2.1 High-throughput compound screen optimization

Our initial results confirm that a deficiency in the MMR pathway leads to a resistance to 5-FU treatment. The MSH6 deficient colorectal cell line DLD1 showed the most consistent resistance to 5-FU in comparison to the MSH6 proficient cell line DLD1+chr2 and therefore, these matched-paired cell lines were chosen to carry out a high-throughput compound screen in order to identify modulators of this resistance. Initially, we carried out a series of optimization experiments to determine an appropriate schedule of treatment, 5-FU concentration and cell number to perform the compound screen. We firstly determined the experiment scheduling: day 1, cell seeding; day 2, 5-FU treatment; day 4, compound library treatment; and day 7, cell viability assay. Our previous experiments to confirm 5-FU resistance in MMR deficient cell lines, helped us to determine that, to have cells at 90 % confluency on day 7, we needed to seed 1000 cells per well. We also previously determined that 2 µM 5-FU was the lowest concentration to have the highest difference between DLD1 and DLD1+chr2 cell viability (Figure 18A). The compound library was successfully used in previous studies at the concentration of 10 µM and 100 µM [317, 319]. We decided to carry out our screen with a compound library diluted at 10 µM in order to identify modulators of 5-FU that are active at a lower concentration and therefore are potentially less toxic. We determined that the optimized schedule to carry out the high-throughput compound screen was to treat 1000 DLD1 and DLD1+chr2 cells with either DMSO or 2 µM of 5-FU followed by 10 µM 5-FU, which correspond to the concentration of the compound library (Figure 20). Therefore, to perform the compound screen, 1000 DLD1 and DLD1+chr2 cells were plated in 28*96-well plates each and treated, the following day, with either DMSO or the optimized concentration of 5-FU (2 µM). After 2 days, all cells were treated with 10 µM of each of the library compounds. Cell viability was measured using an ATP-based luminescent assay after 72 hrs treatment with the library (Figure 12). The high-throughput screen was carried out using a compound library of 1120 drugs previously used in the clinic, 90 % of which were marketed drugs, the remaining 10 % being bioactive alkaloids. The screen included one well per compound and we carried out the screen in duplicate.

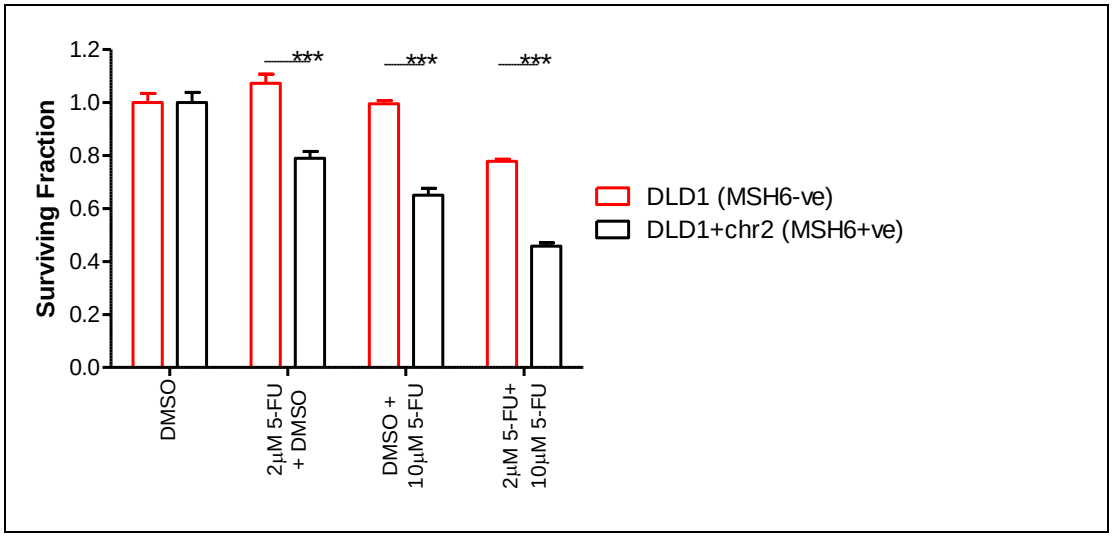

Figure 20: High-throughput compound screen

DLD1 and DLD1+chr2 cells were plated in 96-well plates at the density of 1000 cells/well and treated with either DMSO or 2 µM 5-FU the following day. After 2 days treatment, cells were treated with either DMSO or 10 µM 5-FU which corresponds to the drug library concentration. After 3 days, cell viability was measured using an ATP-based luminescent assay. Experiments were carried out in triplicate and the error bars represent the SEM. P-values derived from 2way ANOVA (*** $p < 0.001$).

2.2 High-throughput compound screen analysis

In order to be able to analyse the compound screen results, the cell viability luminescent readings were normalized into Z-scores (Figure 21A & Appendix 1). Luminescence readings from each well were log transformed and normalized according to the median signal on each plate and then standardized by use of a Z-score statistic, using the median absolute deviation (MAD) to estimate the variation in each screen (Figure 13). Z-score analysis has been described as a reliable method to analyse high-throughput screens [356]. In our case, a Z-score represented the magnitude of difference between one compound and the rest of the screen. This was based on the assumption of a normal distribution of cell viability upon treatment in a specific cell line. The standardization and normalization of the data in each cell line enabled us to compare the 4 conditions with or without 5-FU in both MMR deficient and proficient cell lines. A Z-score = 0 represented a compound that was not cytotoxic to the cells and a Z-score < 0 represented a compound that was cytotoxic for the cells. We enforced a threshold of hit identification based Z-scores

lower than -1.5. Based on this threshold, we identified a number of compounds which either: 1) caused synthetic lethality in the MSH6 deficient cell lines, 2) modulated resistance to 5-FU in the MSH6 deficient cell lines, or 3) modulated 5-FU treatment response regardless of MMR status. Methotrexate has been previous identified for its synthetic lethal relationship with MSH2 deficiency [317]. In this screen, Methotrexate was cytotoxic regardless of MSH6 status. This is in agreement with the previous study which showed selectivity for Methotrexate with MSH2 deficiency only and not other MMR genes. From the screen results, we selected 5 drugs, Quinacrine, Disulfiram, Clotrimazole, Astemizole and Triamterene, which showed synthetic lethality in MSH6 deficiency and a potential re-sensitization of MSH6 deficiency mediated 5-FU resistance. Quinacrine is an antimalarial treatment. Its mechanism of action against protozoa is uncertain, however, a role for Quinacrine in the inhibition of NFκB and activation of p53 in mammalian cells has been reported [371, 372]. Disulfiram inhibits the enzyme acetaldehyde dehydrogenase which plays a key role in alcohol degradation and therefore, Disulfiram is a prescribed treatment of alcoholism [373]. It has been previously shown that Disulfiram and Quinacrine can synergize with 5-FU treatment [371, 373]. Clotrimazole is an antifungal treatment which alters the permeability of the fungus membrane; it has also been described as a Calmodulin antagonist [374, 375]. Astemizole is an anti-histaminic treatment which is metabolized by CYP3A4 and inhibits CYP24A1, two members of the cytochrome P450 family of oxidizing enzymes [376, 377]. Triamterene is an epithelial sodium channel (ENaC) antagonist and an antifolate [378, 379]. All the selected compounds apart from Triamterene had previously been shown to induce an anticancer activity. No study has been published connecting the selected drugs with MMR deficiency (Table 12). The screen results from both replicates showed variability, which was expected as the screen includes only one well per compound (Figure 21B). Therefore further validation experiments were necessary. Taken together, we identified 5 potential compounds synthetically lethal with MSH6 and/or modulators of MMR deficiency mediated 5-FU resistance.

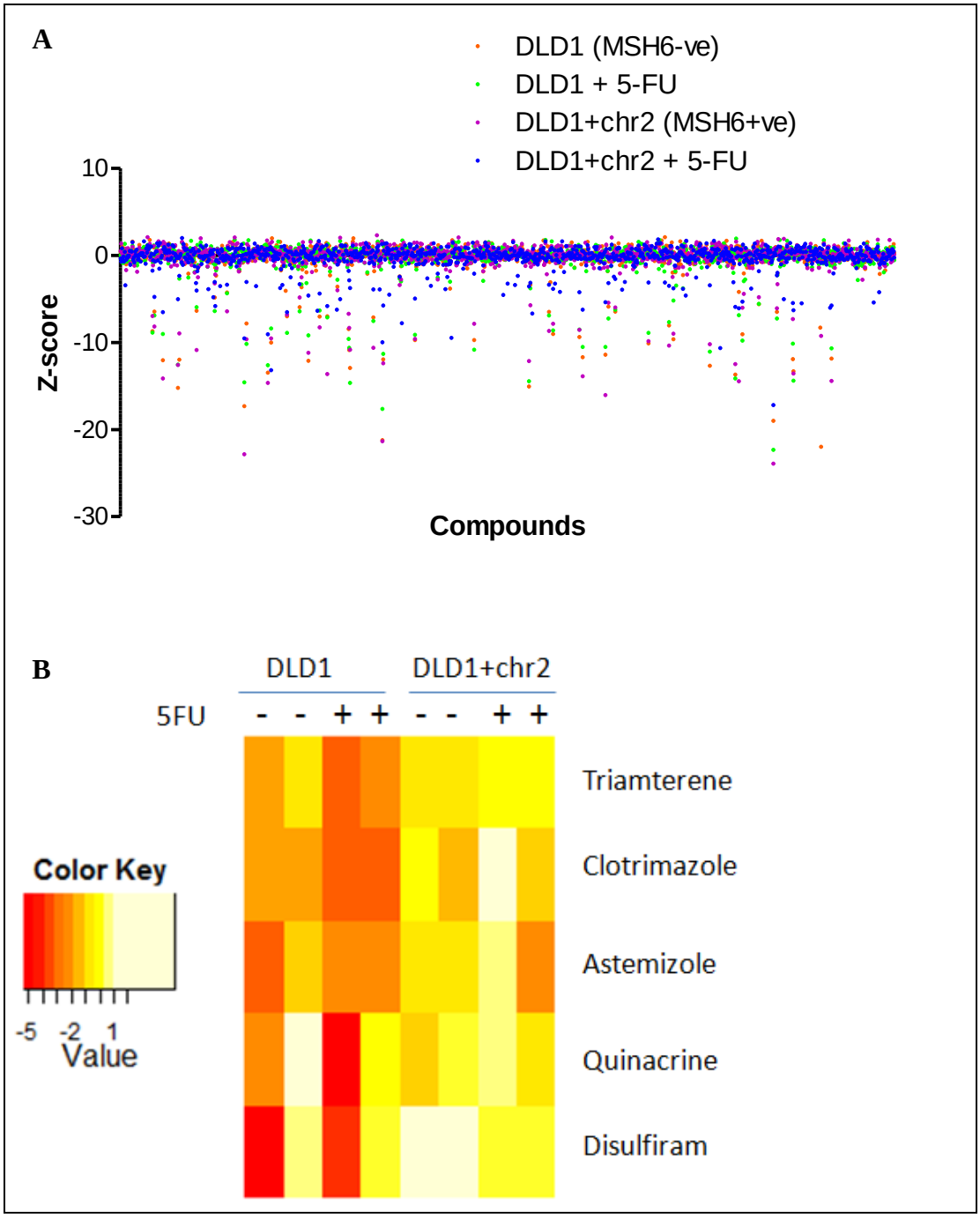

Figure 21: Z-scores obtained from the compound screen data analysis

A: Z-score for each compound in the 4 conditions (DLD1 and DLD1+chr2 with or without 5-FU pre-treatment). **B:** The cell viability results from the compound screens were normalized to Z-scores. Z = 0: no effect of the drug compared to the control; Z < 0: cell sensitivity to the drug. The heatmap represents the screen results for the selected compounds. The colour key represents the Z-scores of the compound effects in the different conditions in each replicate.

	Activity	Previously reported anti-cancer activity	Mechanism of action
Quinacrine	Antimalarial	√	inhibits topoisomerase activity; activates p53, p21; inhibits NFκB [371, 372]
Disulfiram	Sensitivity to alcohol	√	inhibits topoisomerase activity; activates p53 and inhibits NFκB [373]
Clotrimazole	antifungal	√	Calmodulin antagonist [374, 375]
Astemizole	anti-histaminic	√	Inhibits Eag1 potassium channel; inhibits CYP24A1 [376, 377]
Triamterene	hypertension	x	blocks epithelial sodium channel, folate antagonist [378, 379]

Table 12: Clinical use and known mechanisms of action for the selected drugs

2.3 Validation of selected drugs on DLD1 and DLD1+chr2 cells

We previously carried out a high-throughput compound screen in DLD1 and DLD1+chr2 cells in order to identify modulators of 5-FU resistance and/or compounds synthetically lethal in MMR deficient cells. We selected 5 compounds which showed synthetic lethality and a potential re-sensitization to 5-FU resistance in MSH6 deficient cells (Figure 21B). As mentioned previously, the results from both replicates were variable and the selected compounds were tested at the one concentration of 10 µM; therefore, validation experiments are required to further investigate these compounds. We performed validation experiments with the selected drugs in short-term cell viability assays (Figure 22 & Figure 23). DLD1 and DLD1+chr2 cells were treated with either 2 µM 5-FU or increasing concentrations of the hit compound alone (from 1 nM to 10 µM). After 48 hrs, 5-FU pre-treated cells were exposed to the hit compound (from 1 nM to 10 µM), and the media was replaced on the cells previously treated with the hit compound. After 48 hrs, cell viability was measured using an ATP-luminescence assay. Our results showed that treatment with both Triamterene and Clotrimazole could re-sensitize the 5-FU pre-treated cells (Figure 22A, B). More precisely, 5 µM Triamterene treatment sensitized specifically the 5-FU pre-treated DLD1 cells; 10 µM Triamterene sensitized both 5-FU pre-treated cell lines but with significant higher toxicity in the 5-FU pre-treated DLD1 cells than in the 5-FU pre-treated DLD1+chr2 cells. Clotrimazole re-sensitizes the cells to 5-FU treatment in DLD1 cells specifically with 1, 5 and 10 µM

Clotrimazole; 5 and 10 µM Clotrimazole alone were synthetically lethal in DLD1 compared to DLD1+chr2 cells. No re-sensitization was observed with Disulfiram, Quinacrine and Astemizole (Figure 23). Based on these results, we confirmed the modulation of the 5-FU resistance in MMR deficient cells by Triamterene and Clotrimazole. The other selected drugs, Disulfiram, Quinacrine and Astemizole were not validated by this experiment and previously gave varying results in the screen analysis (differences between the duplicates). Quinacrine and Disulfiram were previously described to modulate 5-FU response [371, 373]. Both of these published studies assessed DLD1 cell viability after 72 or 96 hrs treatment with a combination of Disulfiram and 5-FU or Quinacrine and 5-FU. We carried out our experiments by treating the cells first with 5-FU followed by Disulfiram or Quinacrine treatment. The difference in experiment scheduling might explain why we did not validate Disulfiram and Quinacrine as modulators of 5-FU resistance in our MMR deficient cell lines. Further validation experiments could be done using these drugs, by testing different drug scheduling regimes. However, in this project, we decided to focus on Clotrimazole and Triamterene as the most promising modulators of 5-FU resistance in MMR deficient cells.

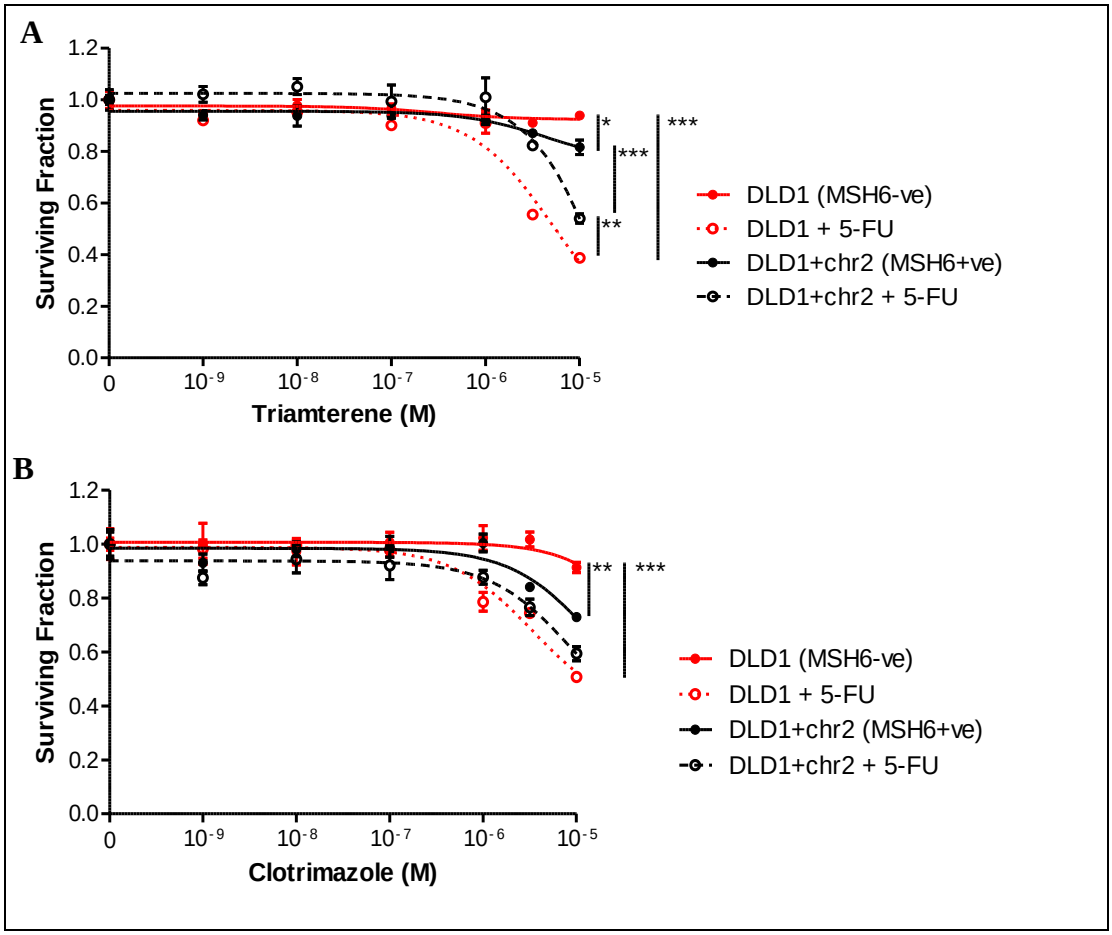

Figure 22: Triamterene and Clotrimazole are apparent modulators of 5-FU resistance in the MMR deficient DLD1 cell line

A, B: DLD1 and DLD1+chr2 cells were treated with either DMSO, 2 µM 5-FU or with 10-fold-diluted concentrations of Triamterene (**A**) or Clotrimazole (**B**). After 48 hrs, the 5-FU pre-treated cells were treated with 1 nM to 10 µM of the selected drugs and the media was replaced on the other drug-treated cells. After 48 hrs, cell viability was measured using an ATP-luminescence assay. Experiments were carried out in triplicate and the error bars represent the SEM. P-values derived from 2way ANOVA (*** $p < 0.001$, ** $p < 0.01$, * $p < 0.05$).

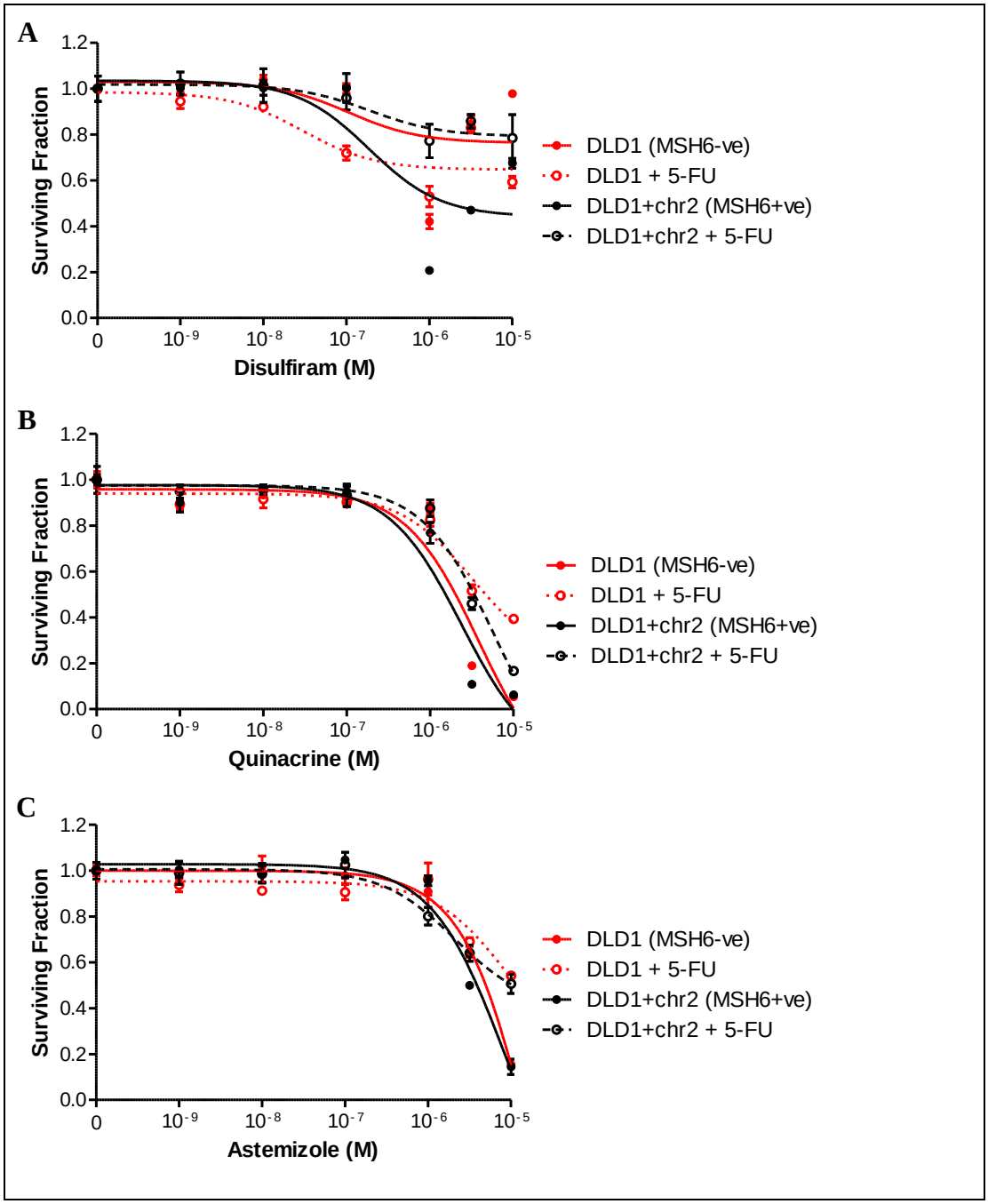

Figure 23: Disulfiram, Quinacrine and Astemizole were not validated in short term cell viability assays

A-C: DLD1 and DLD1+chr2 cells were treated with either DMSO, 2 µM 5-FU or with 10-fold-diluted concentrations of the selected drugs. After 48 hrs, the 5-FU pre-treated cells were treated with 10^{-5} to 10^{-9} M of the selected drugs and the media was replaced on the other drug-treated cells. After 48 hrs, cell viability was measured using an ATP-luminescence assay. Experiments were carried out in triplicates and the error bars represent the SEM.

3 Clotrimazole modulates 5-FU response in DLD1 cells

Clotrimazole was identified and validated to be a modulator of 5-FU resistance in DLD1 and DLD1+chr2 cells. To investigate this modulation, we treated our panel of paired MMR deficient and proficient cell lines with Clotrimazole and 5-FU. Cells were treated with either 5 µM 5-FU or increasing concentrations of Clotrimazole (from 1 nM to 10 µM). After 2 days, 5-FU pre-treated cells were exposed to increasing concentrations of Clotrimazole (from 1 nM to 10 µM), and the media was replaced for the remaining cells. Cell viability was then measured after 2 days, using the ATP-luminescence assay (Figure 24). Our results did not suggest that Clotrimazole can modulate 5-FU resistance in other MMR deficient cell lines compared to their MMR proficient matched paired cell lines. Based on these results, our data suggests that Clotrimazole is a modulator of 5-FU resistance specifically in the MSH6 deficient DLD1 cells. We did not measure the Clotrimazole mediated re-sensitization of 5-FU in our other MSH6 proficient and deficient matched paired cell lines (U251 and U251.TR3 cells). Therefore, we cannot conclude if the modulation observed in DLD1 is specific to this cell line or if it is MSH6 specific. Taken together, we identified Clotrimazole as a novel modulator of 5-FU resistance in the colorectal DLD1 cell line. Further investigations are necessary to further validate the role for MSH6 in Clotrimazole response and to understand the mechanism of Clotrimazole as a modulator of 5-FU response in MSH6 deficient cell lines. We would primarily measure the Clotrimazole response in the U251 and U251.TR3 cells pre-treated with 5-FU and we would investigate the role for the experiment scheduling in this cytotoxicity by testing different treatment regimes such as a combination of 5-FU and Clotrimazole in a longer-term experiment.

From our high-throughput compound screen, we validated Clotrimazole and Triamterene as modulators of 5-FU resistance in DLD1 compared to DLD1+chr2 cells. Due to the specific nature of the Clotrimazole re-sensitization in DLD1 cells only, we therefore decided to carry out our further experiments to investigate Triamterene in our panel of cell lines.

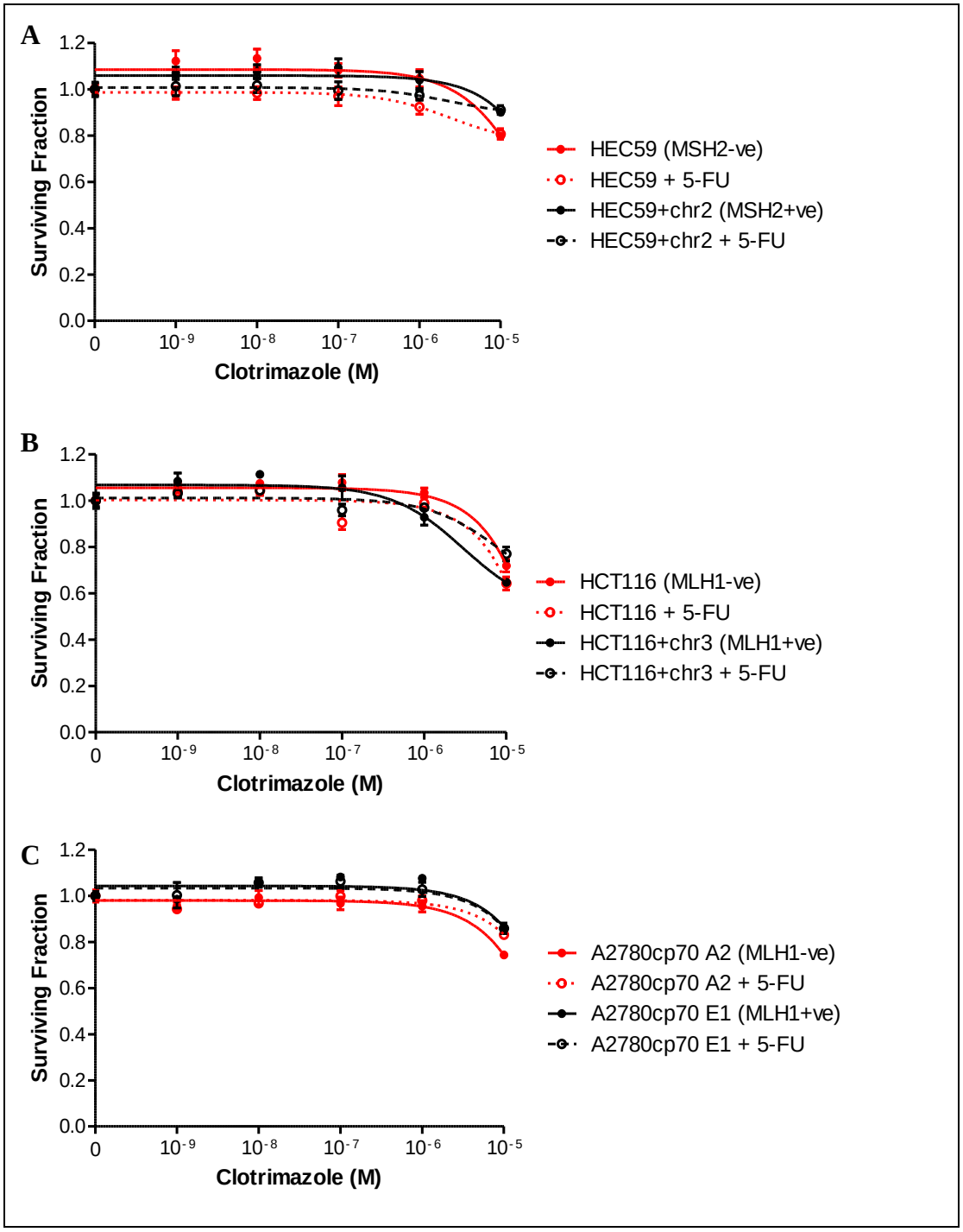

Figure 24: Clotrimazole response on a panel of cell lines

A-C: Cells were treated with either DMSO, 5 µM 5-FU or with increasing concentrations of Clotrimazole (from 1 nM to 10 µM). After 2 days treatment, 5-FU pre-treated cells were treated with Clotrimazole (from 1 nM to 10 µM) and media was replaced on the remaining cells. After 2 days, cell viability was measured using an ATP-based luminescence assay. Experiments were carried out in triplicate and the error bars represent the SEM. P-values derived from 2way ANOVA, no significant different observed by comparing the different conditions.

4 Triamterene is synthetically lethal with MMR deficiency

4.1 Triamterene alone is synthetically lethal in DLD1 cells

From our high-throughput compound screen, we validated Triamterene as a modulator of 5-FU resistance in DLD1, compared to DLD1+chr2 cells. We next carried out further experiments to validate Triamterene as a modulator of 5-FU resistance. Our initial results identified Triamterene as a modulator of 5-FU response in DLD1 and DLD1+chr2 cells, at 5 and 10 µM concentrations. In order to further validate these results, we tested the effect of 0, 2, 4, 6, 8 and 10 µM of Triamterene alone or upon 5-FU treatment in DLD1 and DLD1+chr2 cells (Figure 25A). This experiment validated the specific modulation of Triamterene upon 5-FU treatment in DLD1 cells compared to DLD1+chr2 cells in the range of 4 to 10 µM concentration of Triamterene.

To further investigate the requirement of 5-FU in the Triamterene-induced cytotoxicity, we repeated a short-term experiment with Triamterene only; we treated the cells for 4 days with Triamterene (instead of 2 days in drug followed by 2 days in media, as in previous validation experiments). Interestingly, we observed reduced cell viability in the MSH6 deficient DLD1 cells compared to DLD1+chr2 cells with Triamterene independently of 5-FU, suggesting a potential synthetic lethality with Triamterene treatment upon MSH6 deficiency (Figure 25B). Our initial validation experiments showed no cytotoxicity of Triamterene alone (Figure 25A); however, further validation showed a selective cytotoxicity of Triamterene alone in MSH6 deficient DLD1 cells (Figure 25B). These contradictory results can be explained by the difference in experiment scheduling: in the initial validation experiment, we either treated the cells for 2 days with Triamterene, followed by 2 days in media which triggered no cytotoxicity; or we treated the cells 2 days with 5-FU and 2 days with Triamterene which triggered cytotoxicity compared to 5-FU alone. In this experiment, we treated the cells for 4 days with Triamterene, which triggered cytotoxicity in the absence of 5-FU. These results suggest that Triamterene is synthetically lethal in DLD1 cells, when the cells are kept in treatment for longer. This result will be explained in greater detail in chapter 2, section 1.3. The aim of this project was to identify modulators of 5-FU resistance mediated by MMR deficiency; however, it would be clinically relevant to identity novel compounds

synthetically lethal with MMR deficiency. Further experiments are required to investigate Triamterene as a potential synthetic lethal agent for the treatment of MMR deficient tumours.

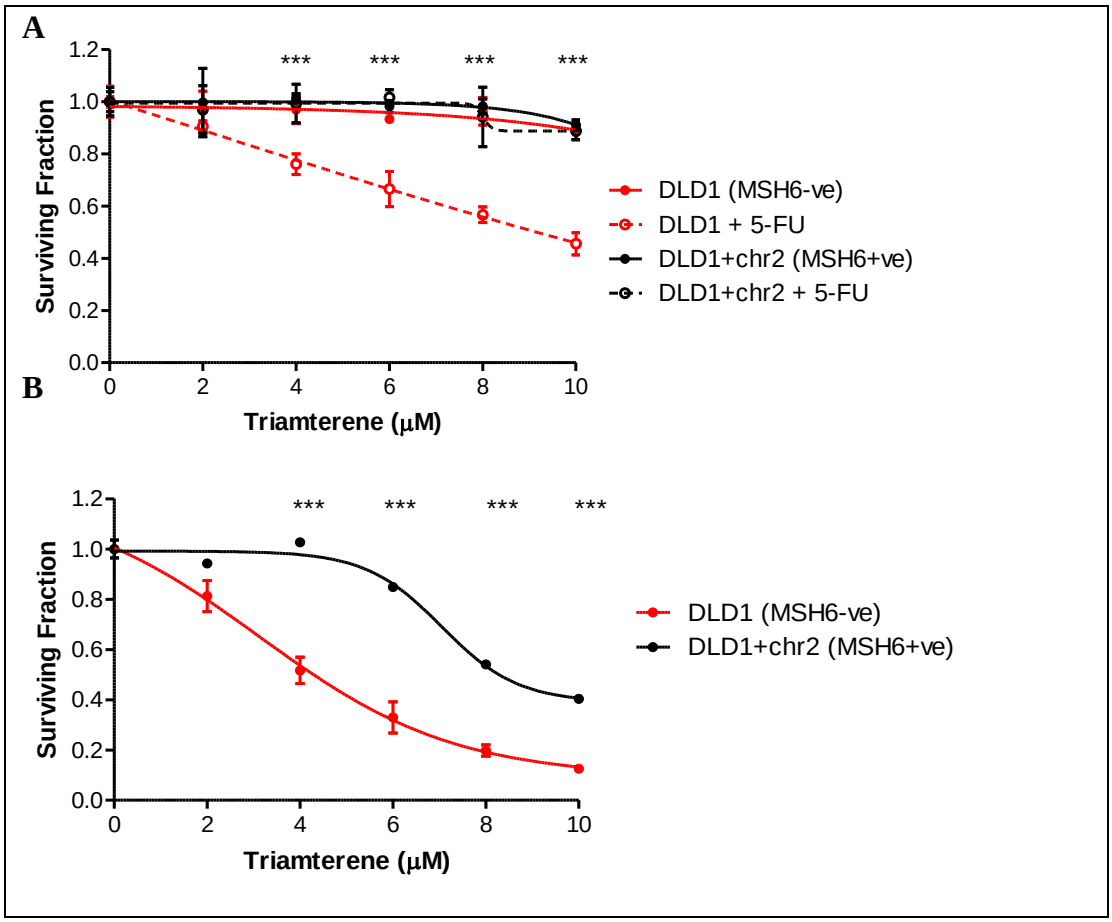

Figure 25: **Triamterene alone is synthetically lethal in DLD1 cells**
A: Cells were treated with either DMSO, 2 µM 5-FU or with increasing concentrations of Triamterene (0, 2, 4, 6, 8 and 10 µM). After 48 hrs treatment, the 5-FU pre-treated cells were treated with increasing concentrations of Triamterene (0, 2, 4, 6, 8 and 10 µM) and the media was replaced for the remaining cells. After 48 hrs, cell viability was measured using an ATP-luminescence assay. **B:** Cells were treated with increasing concentrations of Triamterene (0, 2, 4, 6, 8, and 10 µM). After 4 days treatment, cell viability was measured using an ATP-based luminescence assay. **A, B:** Experiments were carried out in triplicate and the error bars represent the SEM. P-values derived from 2way ANOVA (*** $p < 0.001$).

4.2 Triamterene is synthetically lethal in MSH6 deficient cell lines

We previously showed that Triamterene alone was synthetically lethal in DLD1 cells. To further validate this Triamterene-induced synthetic lethality in MSH6 deficient cell lines, we performed longer-term clonogenic assays in DLD1 and DLD1+chr2 cells treated with increasing concentrations of Triamterene (0, 2, 4, 6, 8 and 10 μM) alone. After 14 days treatment, we observed an inhibition of colony formation in the MSH6 deficient DLD1 cells upon Triamterene treatment, compared to DLD1+chr2 cells (Figure 26A). These results further suggest that Triamterene alone is synthetically lethal in DLD1 cells. We also performed longer-term clonogenic assays in the MSH6 deficient and proficient, U251 and U251.TR3 cells treated with increasing concentrations of Triamterene (0, 4, 8, 12, 16 and 20 μM) alone. After 14 days treatment, we also observed an inhibition of colony formation specifically in the MSH6 deficient U251.TR3 cells upon Triamterene treatment, compared to U251 cells (Figure 26B). Taken together, these results suggest that Triamterene alone is synthetically lethal in MSH6 deficient cell lines.

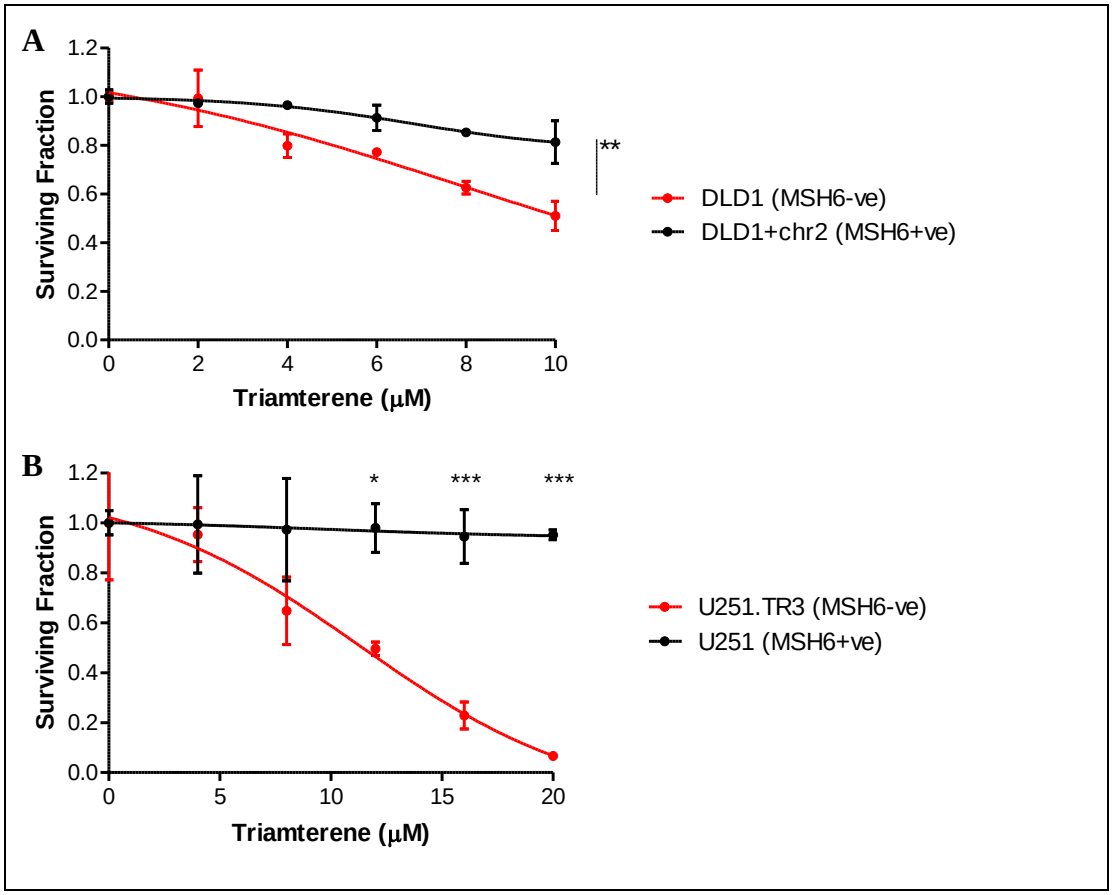

Figure 26: Long-term clonogenic assay of Triamterene treatment in MSH6 deficient and proficient matched paired cell lines

A: DLD1 and DLD1+chr2 cells were plated at low density (300 and 350 cells per well respectively) in 6-well plates and treated every 3 days with increasing concentrations of Triamterene (0, 2, 4, 6, 8 and 10 µM). After 14 days, colonies were fixed, stained with SRB and counted. **B:** U251 and U251.TR3 cells were plated at low density (350 and 400 cells per well respectively) in 6-well plates and treated every 3 days with increasing concentrations of Triamterene (0, 4, 8, 12, 16 and 20 µM). After 14 days, colonies were fixed, stained with SRB and counted. **A, B:** Experiments were carried out in triplicate and error bars represent the SEM. P-values derived from 2way ANOVA t-test, (* $p < 0.05$; ** $p < 0.01$; *** $p < 0.001$).

4.3 Triamterene is synthetically lethal in a panel of MMR deficient cell lines

We previously showed that Triamterene was synthetically lethal in MSH6 deficient cell lines. To establish whether the Triamterene is synthetically lethal in MSH6 deficiency specifically or in MMR deficiency in general, we tested this compound on our panel of MMR deficient and proficient paired cell lines described previously (Figure 17A; Table 11). Significantly, treatment with Triamterene caused a selective cytotoxic effect in all MMR deficient cell lines compared to their paired MMR proficient cells, regardless of tumour type (Figure 27). These results suggest a potential role for Triamterene as a synthetic lethal compound for the treatment of MMR deficient tumour cells.

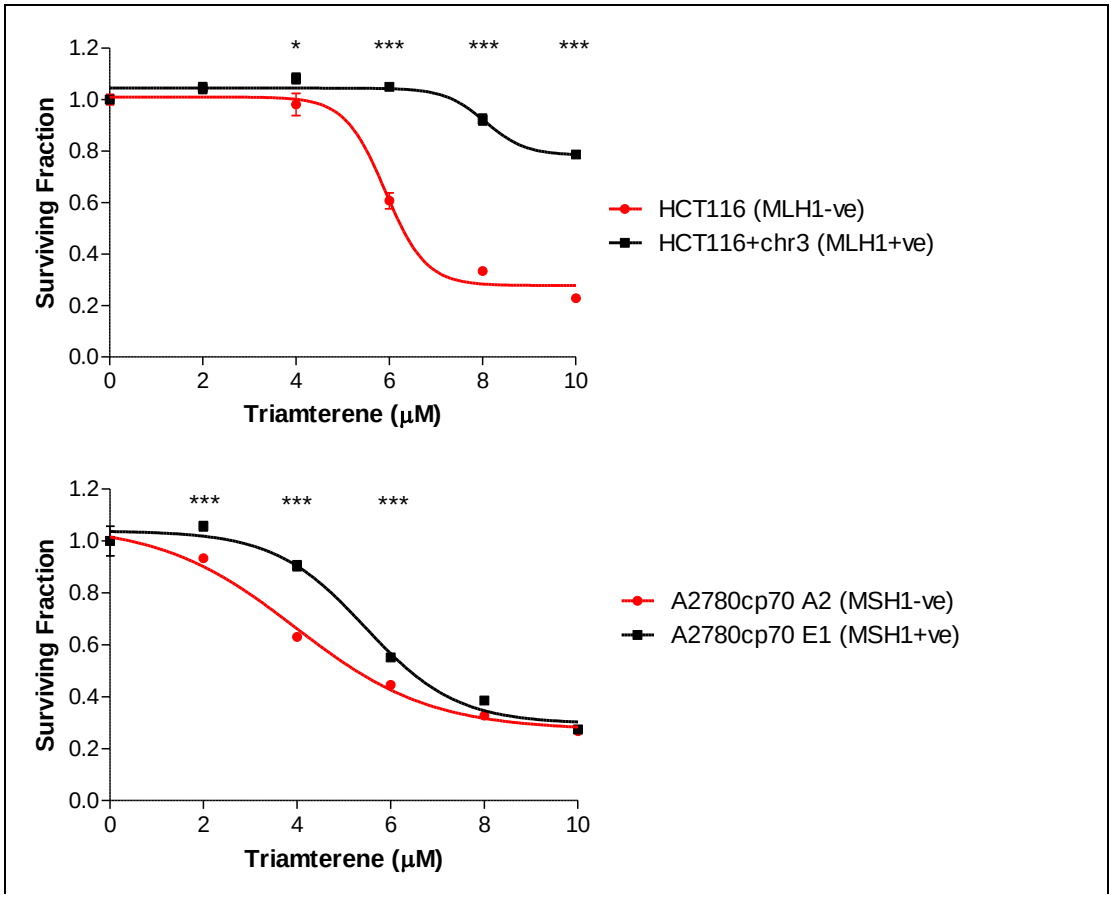

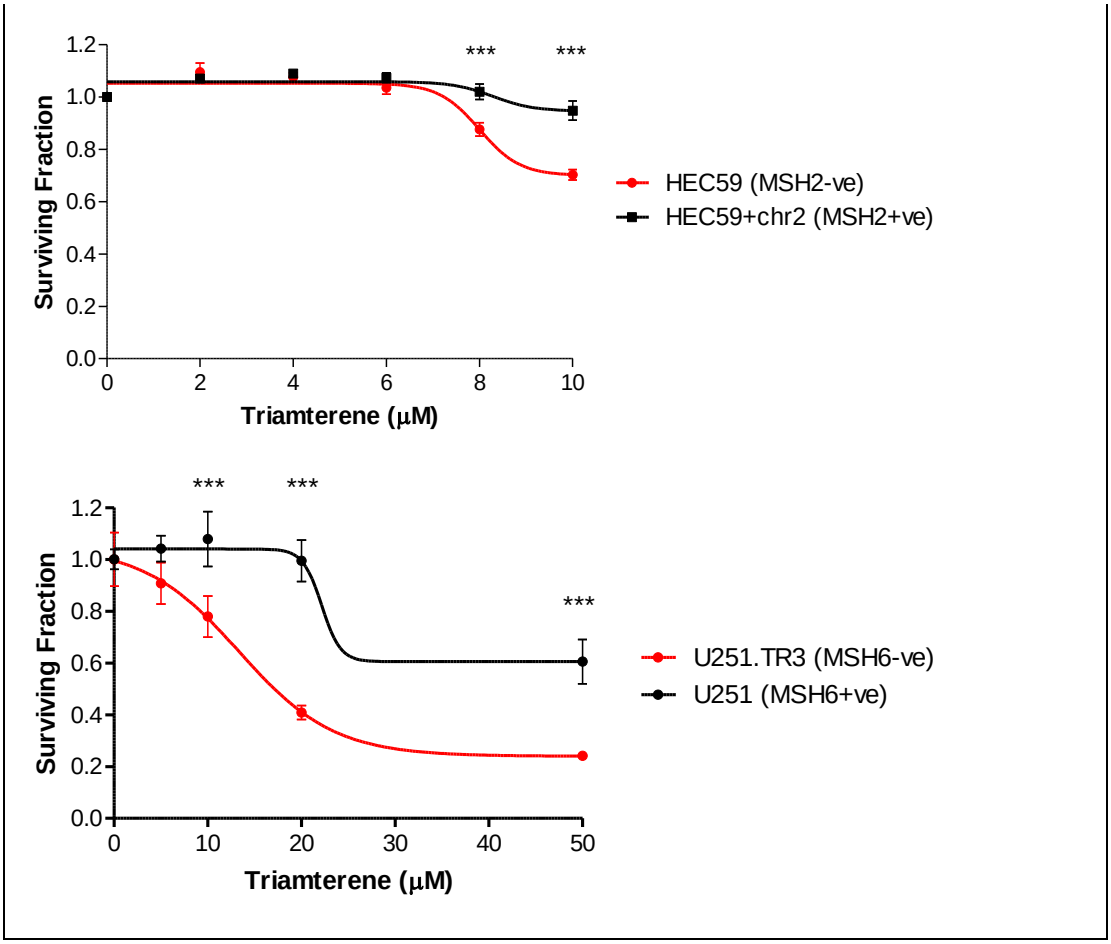

Figure 27: **Triamterene response in our panel of MMR deficient and proficient matched paired cell lines**

A: A panel of MMR proficient and deficient matched paired cell lines was treated with Triamterene (0, 2, 4, 6, 8 and 10 μM in HEC59, HEC59+chr2, HCT116, HCT116+chr3, A2780cp80 A2 and A2780cp80 E1 cells; and 0, 5, 10, 20 and 50 μM in U251 and U251.TR3 cells). Cell viability was measured after 4 days treatment. Experiments were carried out in triplicate and error bars represent the SEM. P-values derived from 2way ANOVA (* $p < 0.05$, *** $p < 0.001$).

5 *In vivo* experiment

5.1 Pilot experiment

5.1.1 Experiment set up

We have previously shown that Triamterene is synthetically lethal in MMR deficient cell lines *in vitro*. To assess Triamterene efficacy *in vivo*, we performed a pilot study on 20 mice to select the best experimental conditions for further xenograft studies. We carried out *in vivo* experiments using DLD1, DLD1+chr2, HCT116 and HCT116+chr3 cells. We injected 1.6 million cells in both flanks (2 tumours per mouse) into male NOD-SCID mice. Treatment was started as soon as the tumours were measurable in all mice. As illustrated in Figure 16, each mouse received, 3 times a week, the following treatment regimes: (1) vehicle (folate-free RPMI) by IP injection; (2) 25 mg/kg Triamterene by IP; (3) 25 mg/kg by gavage; (4) 50 mg/kg by IP and (5) 50 mg/kg by gavage [380, 381]. Triamterene is more soluble in media than in 1X PBS; therefore we decided to dilute the drug in media for the *in vivo* experiment. Furthermore, Triamterene has an antifolate activity [382], therefore, we decided to dilute the compound in folate-free RPMI to avoid any potential antagonist effect of the folate present in the media with Triamterene. The tumours were measured twice a week by measuring the width and the length using callipers. The mice were sacrificed when the tumour area reached 1.44 cm^2, in case of sickness or after 25 days treatment (Table 13).

	tumour size (mm^2) day 1				sacrifice (days)	
	DLD1		DLD1+chr2		DLD1	DLD1+chr2
IPV	32.7	53.72	41.95	54.35	10	25
GT25	52.42	67.2	16.32	36.86	23	>25
GT50	12.41	128.13	15.74	22.05	2	>25
IPT25	27.84	22.8	42.56	47.62	7 (sick)	23
IPT50	37.44	102.91	40.77	57.73	4	>25

	tumour size (mm^2) day 1				sacrifice (days)	
	HCT116		HCT116+chr3		HCT116	HCT116+chr3
IPV	40.67	82.88	22.58	39.01	23 (sick)	17 (sick)
GT25	61.09	25.48	20.38	56.23	4	14
GT50	37.9	24.2	13.44	18.72	23	4 (no tumour)
IPT25	55.14	29.4	17.47	58.61	4	17
IPT50	38.16	34.11	12.8	104.43	23	10 (sick)

Table 13: Tumour sizes on the first day of treatment and number of days of treatment before sacrifice

IPV: vehicle (folate-free RPMI) by IP injection; GT25: 25 mg/kg by gavage; GT50: 50 mg/kg by gavage; IPT25: 25 mg/kg Triamterene by IP; and IPT50: 50 mg/kg by IP.

5.1.2 Pilot experiment results and analysis

As explained in the previous section, we started treating the mice when all the tumours were measurable. The tumour sizes on the first day of treatment were heterogeneous and the majority of tumours grew rapidly which limited the interpretation of this experiment on treatment efficacy (Table 13, Figure 28 & Figure 29). All tumour sizes were normalized to the first tumour measurements in order to analyse the tumour growth. As a linear tumour growth was expected and observed, and to make the interpretation easier, we represented the slope linear regression for each condition (Figure 30A, B). Our results showed no interpretable results in the HCT116 and HCT116+chr3 mice, probably due to the limited number of mice analysed and the variability between them. Also during the experiment, two HCT116+chr3 xenografted mice became sick and one HCT116+chr3 xenografted mouse did not grow tumour. Therefore, we could not interpret the results from the HCT116 and HCT116+chr3 xenografted mice and decided not to carry out more mice experiment using HCT116 and HCT116+chr3 cells (Table 13, Figure 29 & Figure 30B). One DLD1 xenografted mouse showed signs of sickness; this mouse

was smaller than the others (19 grams vs 27 grams in average) which might explain why it was sick (Table 13). The DLD1 and DLD1+chr2 xenografted mice treated with 25 mg/kg Triamterene by gavage gave us the most conclusive and significant results ($p < 0.0001$) (Figure 28 & Figure 30A, C). Therefore, for further *in vivo* experiment, we selected the concentration of 25 mg/kg Triamterene by gavage in DLD1 and DLD1+chr2 cells xenografted into NOD-SCID mice.

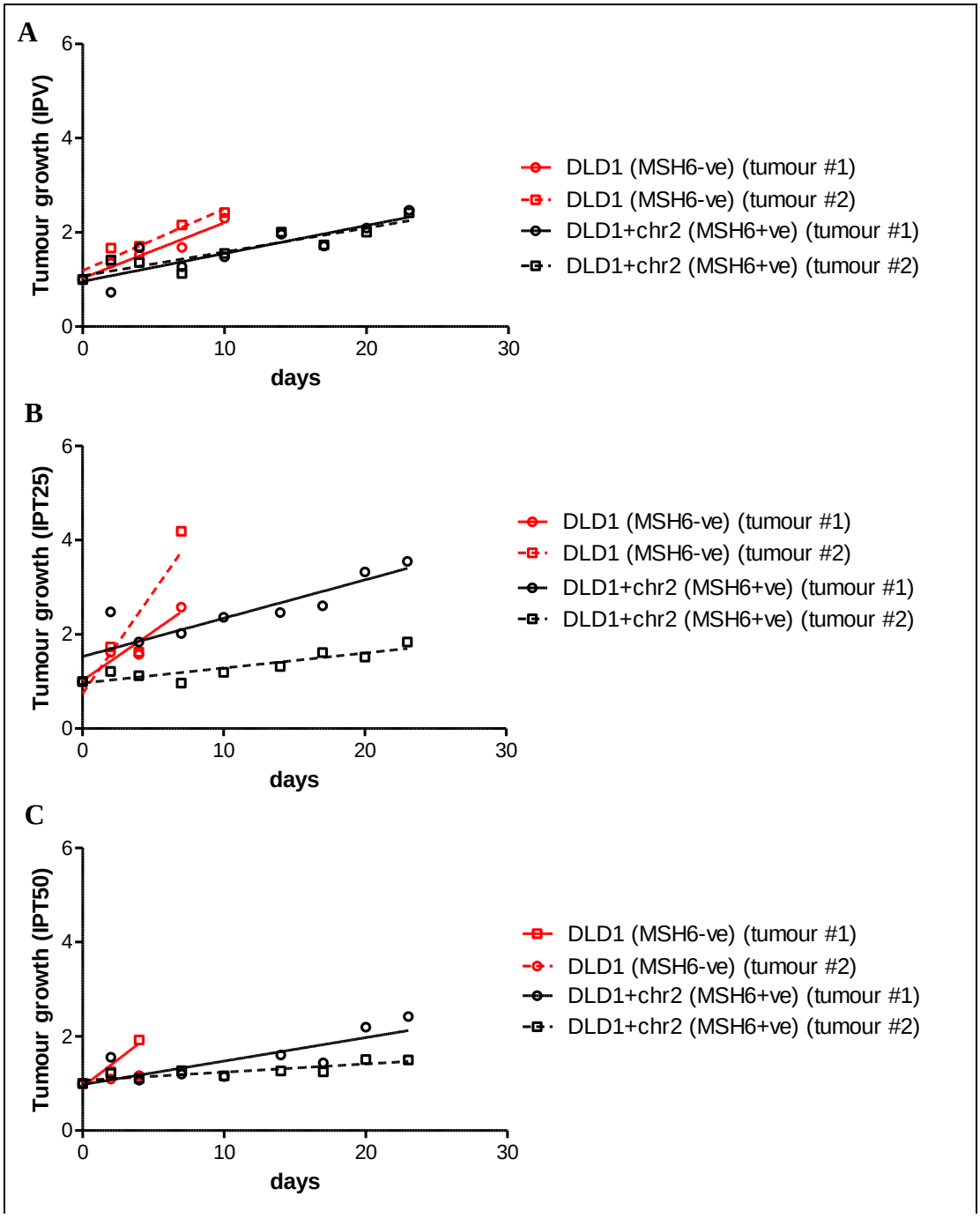
A
Tumour growth (IPV)
days
DLD1 (MSH6-ve) (tumour #1)
DLD1 (MSH6-ve) (tumour #2)
DLD1+chr2 (MSH6+ve) (tumour #1)
DLD1+chr2 (MSH6+ve) (tumour #2)
B
Tumour growth (IPT25)
days
DLD1 (MSH6-ve) (tumour #1)
DLD1 (MSH6-ve) (tumour #2)
DLD1+chr2 (MSH6+ve) (tumour #1)
DLD1+chr2 (MSH6+ve) (tumour #2)
C
Tumour growth (IPT50)
days
DLD1 (MSH6-ve) (tumour #1)
DLD1 (MSH6-ve) (tumour #2)
DLD1+chr2 (MSH6+ve) (tumour #1)
DLD1+chr2 (MSH6+ve) (tumour #2)

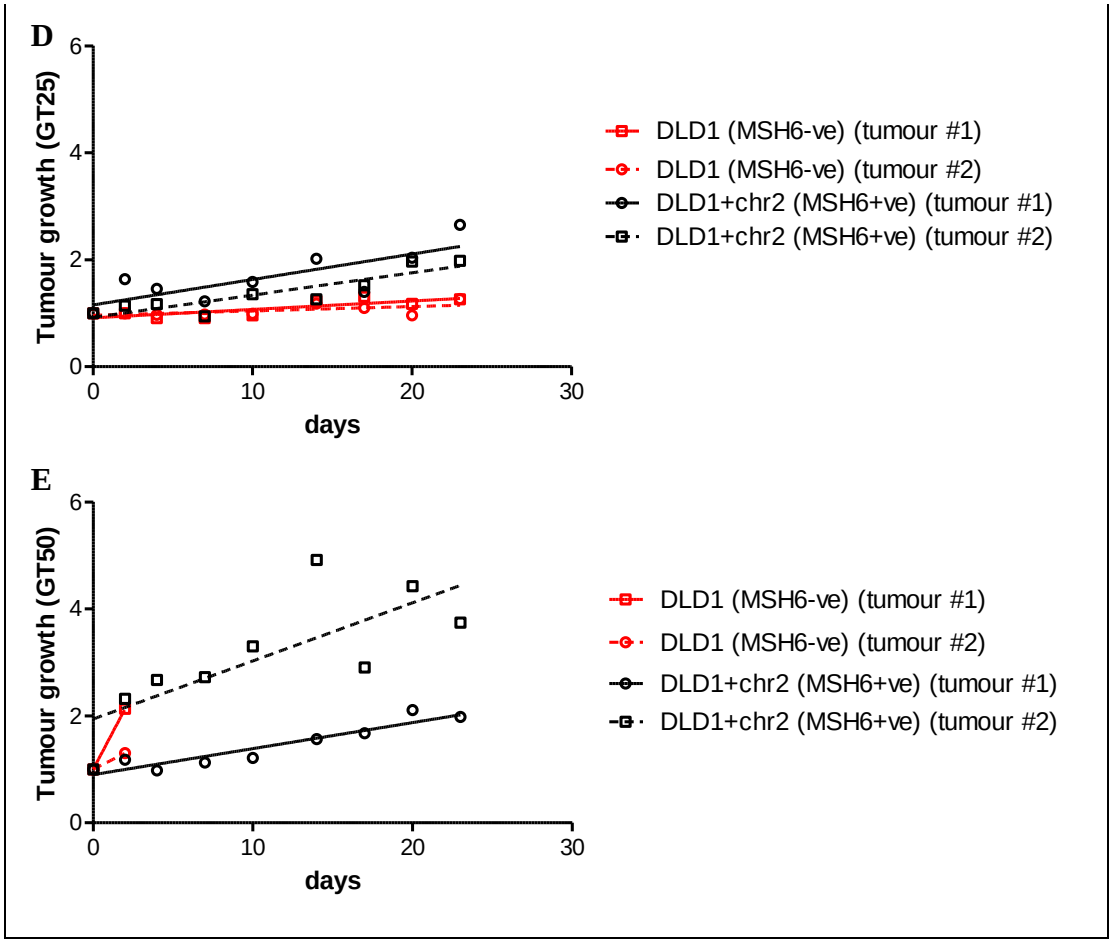

Figure 28: *In vivo* pilot experiment on DLD1 and DLD1+chr2 xenografted mice

A-E: Tumour growth measurements upon treatments with IPV: vehicle (folate-free RPMI) by IP injection; IPT25: 25 mg/kg Triamterene by IP; GT25: 25 mg/kg by gavage; IPT50: 50 mg/kg by IP; or GT50: 50 mg/kg by gavage of the DLD1, DLD1+chr2 xenografted mice. Each mouse had 2 tumours. Tumours were measured twice a week and normalized to the first day treatment measurements.

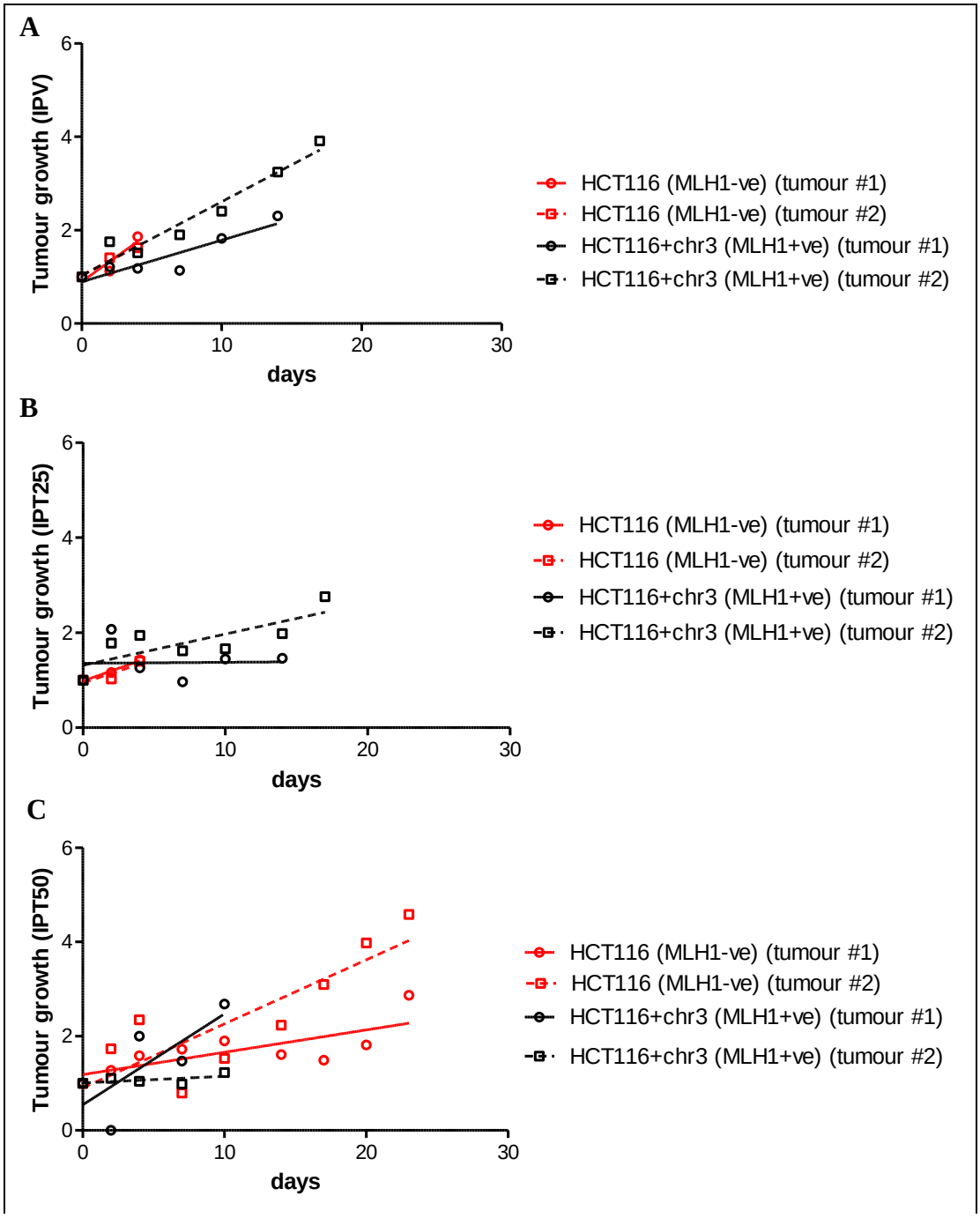
A
Tumour growth (IPV)
0
2
4
6
0
10
20
30
days
HCT116 (MLH1-ve) (tumour #1)
HCT116 (MLH1-ve) (tumour #2)
HCT116+chr3 (MLH1+ve) (tumour #1)
HCT116+chr3 (MLH1+ve) (tumour #2)
B
Tumour growth (IPT25)
0
2
4
6
0
10
20
30
days
HCT116 (MLH1-ve) (tumour #1)
HCT116 (MLH1-ve) (tumour #2)
HCT116+chr3 (MLH1+ve) (tumour #1)
HCT116+chr3 (MLH1+ve) (tumour #2)
C
Tumour growth (IPT50)
0
2
4
6
0
10
20
30
days
HCT116 (MLH1-ve) (tumour #1)
HCT116 (MLH1-ve) (tumour #2)
HCT116+chr3 (MLH1+ve) (tumour #1)
HCT116+chr3 (MLH1+ve) (tumour #2)

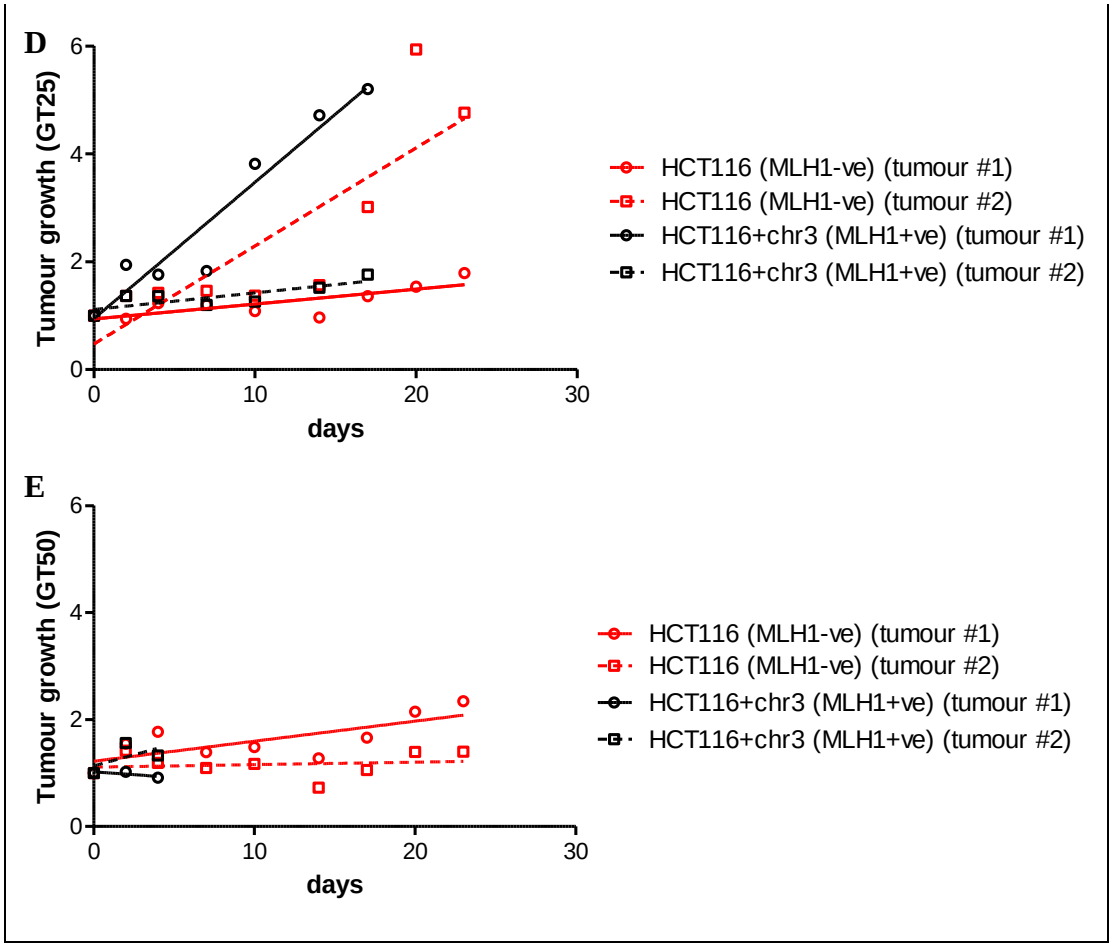

Figure 29: *In vivo* pilot experiment on HCT116 and HCT116+chr3 xenografted mice

A-E: Tumour growth measurements upon treatments with IPV: vehicle (folate-free RPMI) by IP injection; IPT25: 25 mg/kg Triamterene by IP; GT25: 25 mg/kg by gavage; IPT50: 50 mg/kg by IP; or GT50: 50 mg/kg by gavage of the HCT116, HCT116+chr3 xenografted mice. Each mouse had 2 tumours. Tumours were measured twice a week and normalized to the first day treatment measurements.

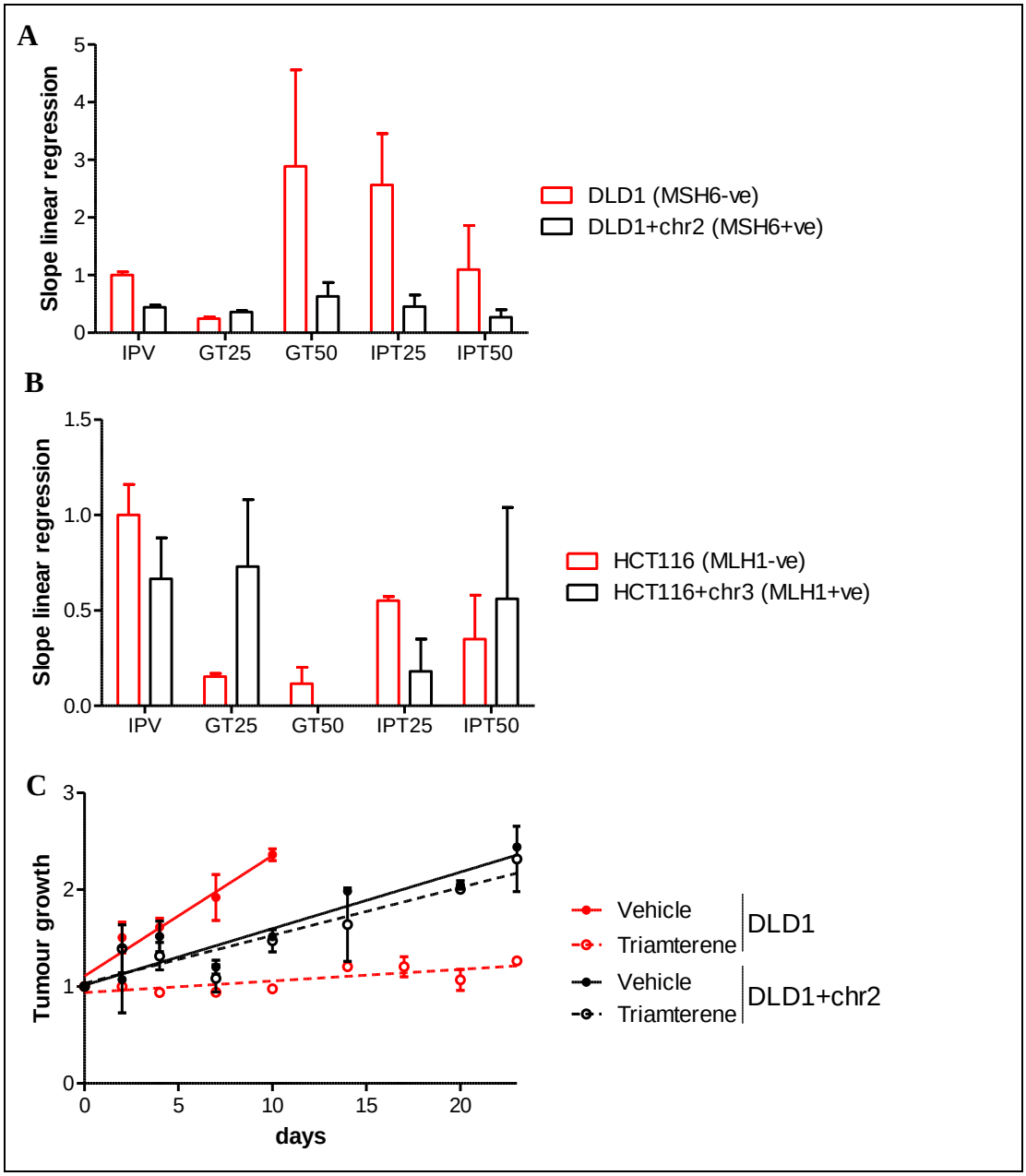

Figure 30: *In vivo* pilot experiment

A, B: Slope linear regression as a representation of tumour growth for the DLD1, DLD1+chr2, HCT116 and HCT116+chr3 xenografted mice. **C:** Tumour growth in DLD1 and DLD1+chr2 xenografted mice treated with vehicle by IP injection or 25 mg/kg Triamterene by gavage. Error bars represent SEM.

5.2 *In vivo* experiment in DLD1 and DLD1+chr2 cells

5.2.1 *In vivo* experiment on 20 NOD-SCID mice with DLD1 and DLD1+chr2 cells

We previously selected the concentration of 25 mg/kg Triamterene by gavage in DLD1 and DLD1+chr2 cells xenografted into NOD-SCID mice for further *in vivo* experiments. We next carried out an *in vivo* experiment in 20 NOD-SCID mice xenografted with DLD1 and DLD1+chr2 cells. We injected $1.6x10^6$ cells in both flanks (2 tumours per mouse) by gavage, with 25 mg/kg Triamterene or vehicle. The width and the length of the tumours were measured twice a week using callipers. The mice were sacrificed in case of sickness or when the tumours reached 1.44 cm^2. Our results showed a significant tumour growth reduction ($p < 0.01$) in DLD1 xenografted mice treated with Triamterene compared to the vehicle treated mice (Figure 31A). However we did not observe any significant tumour growth difference in the DLD1+chr2 xenografted mice treated with Triamterene or vehicle (Figure 31B). We observed a faster tumour growth in DLD1 xenografted mice compared to the DLD1+chr2 xenografted mice. These results were expected as we observed, *in vitro*, a slower growth for DLD1+chr2 compared to DLD1 cells. These results suggest a Triamterene-induced decrease in tumour growth in the MSH6 deficient DLD1 xenografted mice specifically, which further validates Triamterene as synthetically lethal in MMR deficiency.

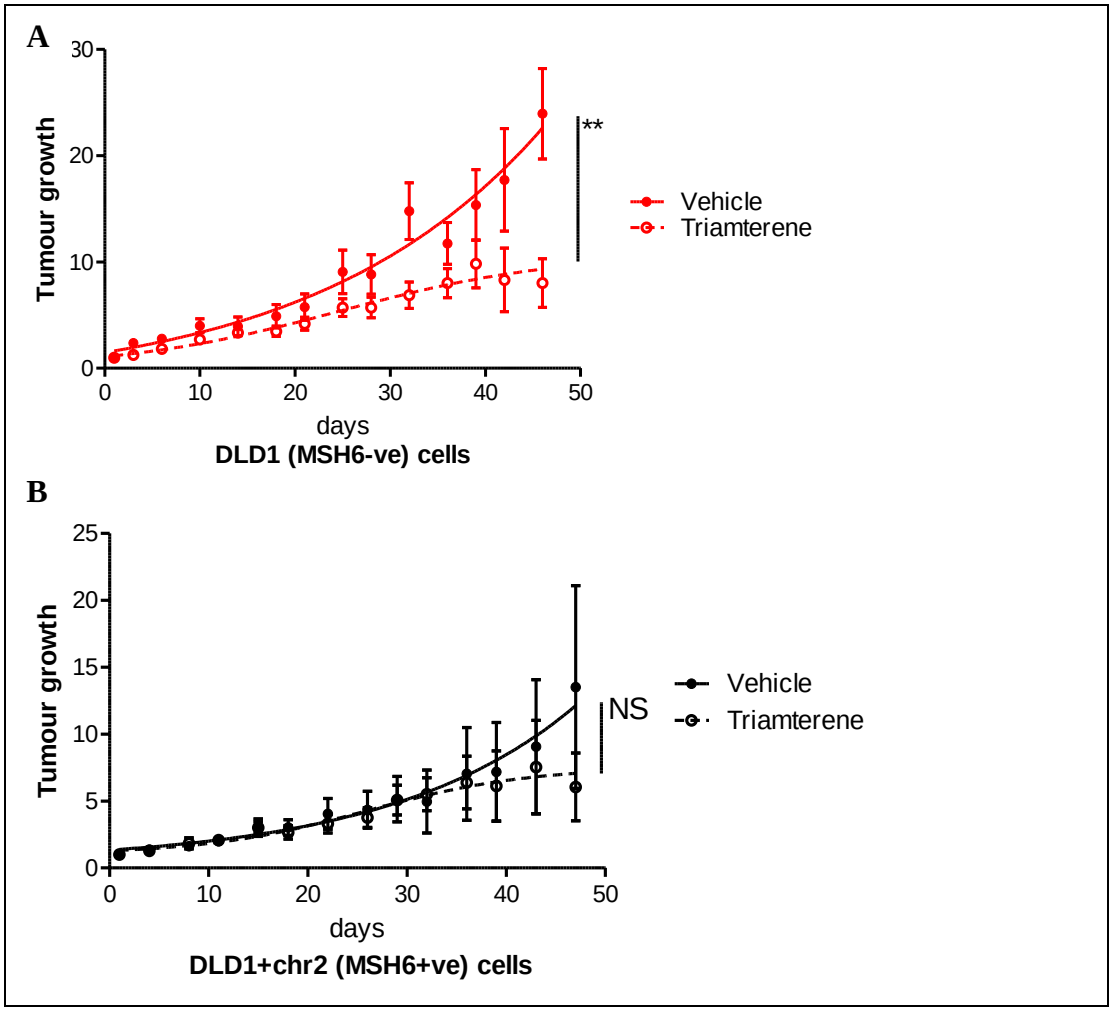

Figure 31: *In vivo* experiment on 20 NOD-SCID mice with DLD1 and DLD1+chr2 cells treated with Triamterene

A, B: Initial *in vivo* mouse experiment on 20 NOD-SCID mice injected in both flanks with DLD1 or DLD1+chr2 cells ($1.6x10^6$ cells per flank). Mice were treated 3 times a week by gavage with 25 mg/kg Triamterene or vehicle. Tumours were measured twice a week and normalized to the first day treatment measurements. Error bars represent SEM. P-values derived from paired two-tailed t-test (** $p < 0.01$, NS $p > 0.05$).

5.2.2 *In vivo* experiment on 40 NOD-SCID mice with DLD1 and DLD1+chr2 cells

Our previous experiment showed a Triamterene-induced decrease in tumour growth in the DLD1 xenografted mice specifically. However, we observed a difference in tumour growth in the vehicle treated DLD1 compared to the DLD1+chr2 xenografted mice. To further confirm that the effect of Triamterene observed *in vivo* is not due to the tumour growth but to MSH6 deficiency, we repeated this experiment with an adjusted number of cells injected. We injected either $0.6x10^6$ DLD1 cells or $0.8x10^6$ DLD1+chr2 cells in only one flank of 40 NOD-SCID mice. The treatment regime and tumour measurements were done as previously. In this experiment, we observed again a slower growth in DLD1+chr2 xenografted mice compared to DLD1 xenografted mice. We also confirmed a significant decrease in tumour growth in mice treated with Triamterene compared with mice treated with vehicle ($p < 0.05$) in the DLD1 xenografted mice only (Figure 32A, B). These results further suggest a Triamterene-induced decrease in tumour growth in the MSH6 deficient DLD1 xenografted mice specifically.

The treatment regime and tumour measurements for both experiments were similar. Therefore, we compared both experiments and observed similar tumour growth for the vehicle treated DLD1 xenografted mice from the first experiment (Figure 31A) and for the vehicle treated DLD1+chr2 xenografted mice from the second experiment (Figure 32B). We observed a decreased tumour growth in DLD1 xenografted mice but not in DLD1+chr2 xenografted mice by comparing the Triamterene treated mice to the vehicle treated mice. This further suggests that the Triamterene effect observed is not due to a greater tumour cell proliferation, but rather to MSH6 deficiency. Taken together these results confirm a synthetic lethal interaction between Triamterene treatment and MSH6 deficiency *in vivo*.

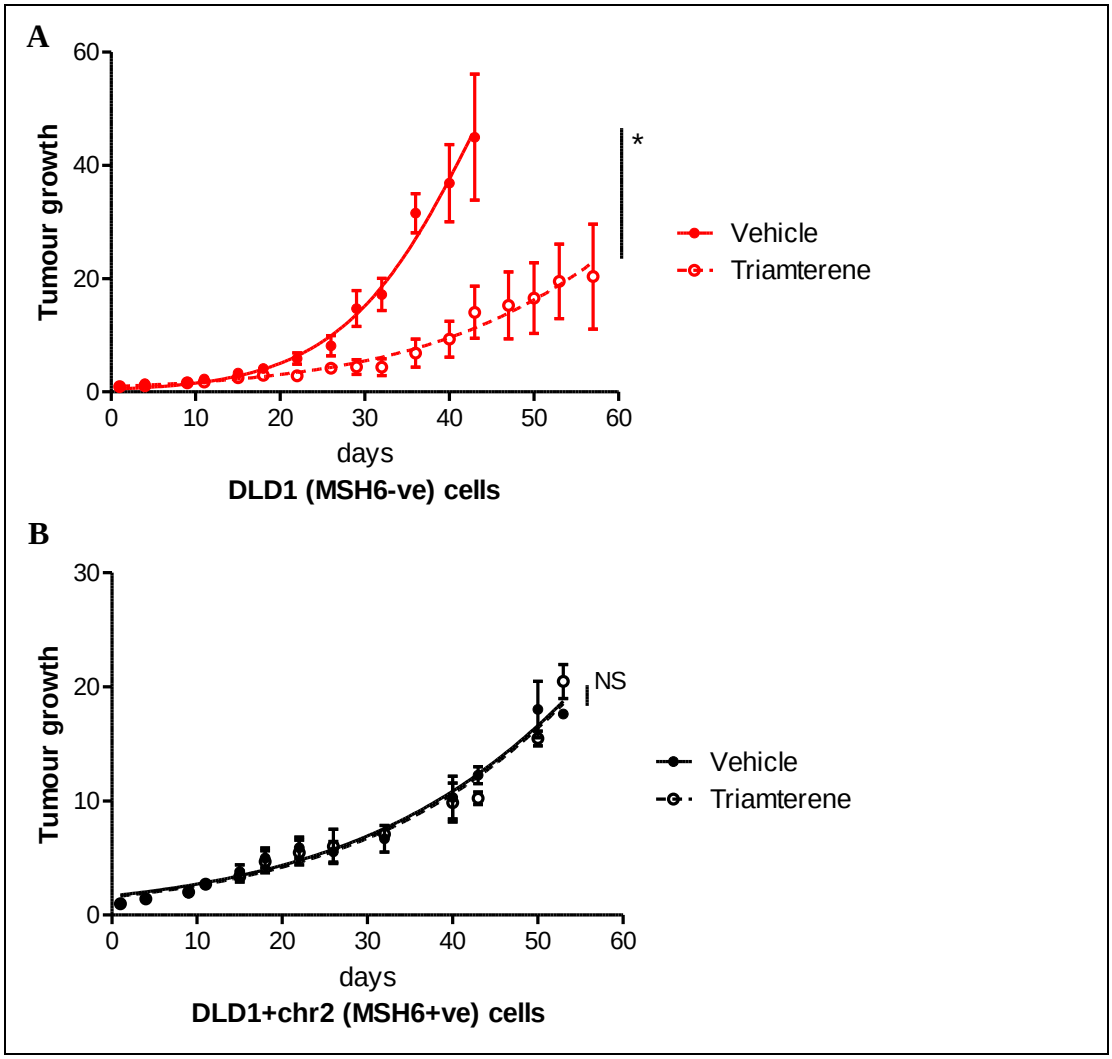

Figure 32: *In vivo* experiment on 40 NOD-SCID mice with DLD1 and DLD1+chr2 cells treated with Triamterene

A, B: Second *in vivo* mouse experiment on 40 NOD-SCID mice injected in one flank with DLD1 or DLD1+chr2 cells ($0.6x10^6$ cells and $0.8x10^6$ cells respectively). Mice were treated 3 times a week by gavage with either vehicle or 25 mg/kg Triamterene. Tumours were measured twice a week and normalized to the first day treatment measurements. Error bars represent SEM. P-values derived from paired two-tailed t-test (* $p < 0.05$, NS $p > 0.05$).

5.2.3 *In vivo* experiment with U251 and U251.TR3 cells

Our previous results confirm a synthetic lethal interaction between Triamterene treatment and MSH6 deficiency *in vivo*. To further validate that the effect observed *in vivo* was due to MSH6 deficiency rather than increased tumour growth; we carried out an *in vivo* experiment on U251 and U251.TR3 xenografted mice. We previously observed that the MSH6 proficient U251 cells have a higher proliferation rate than U251.TR3 cells *in vitro,* the opposite to the DLD1 and DLD1+chr2 cells. Therefore, any decrease in tumour growth upon Triamterene treatment in U251.TR3 compared to U251 xenografted mice, would confirm a proliferation-independent synthetic lethality between Triamterene and MSH6 deficiency *in vivo*. To determine cell number, we carried out a pilot experiment on 6 NOD-SCID mice. We injected the mice subcutaneously with U251 and U251.TR3 cells at different densities: $2.5x10^6$ or $1x10^6$ cells in PBS or $1x10^6$ cells in matrigel (1:1). None of the mice grew tumours after 4 weeks; therefore due to technical constraints we could not conclude the selectivity *in vivo* experiment, using these cells.

Taken together, we have identified, using a high-throughput compound screen, Clotrimazole and Triamterene as modulators of 5-FU resistance in the MSH6 deficient DLD1 cells. We observed that Clotrimazole is a specific modulator of 5-FU resistance in DLD1 cells, rather than MMR deficient cell lines in general. Our data also suggest a synthetic lethal relationship between Triamterene treatment and MMR deficiency, in the absence of 5-FU. Our results confirmed this synthetic lethality *in vitro* and *in vivo*. Therefore, using a high-throughput compound screen, we have identified a novel agent, Triamterene for use in the treatment of MMR deficient tumours. Further investigations are necessary to understand the mechanism of synthetic lethality upon Triamterene treatment and MMR deficiency.

Chapter 2: Investigation into Triamterene as a synthetic lethal drug for the treatment of MMR deficiency

1 Triamterene synthetic lethality is through its antifolate activity

1.1 The known mechanisms of action of Triamterene

Our previous results showed a novel synthetically lethal relationship between Triamterene and MMR deficient tumours. To understand the mechanism by which Triamterene is cytotoxic in MMR deficient cell lines, we first needed to understand the known mechanisms by which Triamterene has been reported to act. Triamterene (6-phenylpteridine-2,4,7-triamine) was first described in 1962 for its pteridine structure and its diurectic activity [383-385]. Triamterene has been used in clinic since 1963 for the treatment of oedemas, ascites, hypertension and congestive heart failure [386-389]. Triamterene has been shown to share the same mechanism of action as Amiloride by direct inhibition of the ENaC [378]. It has also been reported to be a regulator of DHFR activity. Conflicting studies have been published with regards to this regulation, therefore, it is not clear if Triamterene increases or decreases DHFR activity [390-392]. However, it is clear that Triamterene has an antifolate activity due to its pteridine structure (Figure 33) [382].

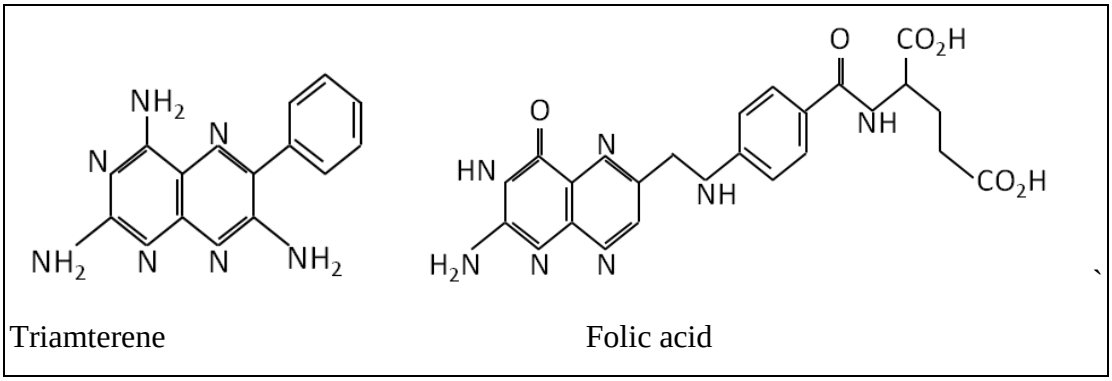

Triamterene Folic acid

Figure 33: Triamterene has an antifolate activity due to its pteridine structure

1.2 Triamterene cytotoxicity in MMR deficient cells, is not due to its role as a sodium channel antagonist

1.2.1 Amiloride is not synthetically lethal in MMR deficient cells

We identified Triamterene, a potassium-sparing diuretic, to be synthetically lethal with MMR deficiency. We firstly wanted to determine if Triamterene was synthetically lethal through its diuretic action by the inhibition of the ENaC. Amiloride is a drug known to inhibit the ENaC through the same mechanism as Triamterene [393]. Kellenberger *et al* previously showed that mutations in the different subunits of the ENaC could induce a comparable reduction of the ENaC inhibition mediated by Triamterene and Amiloride treatment. Therefore, they concluded that these two compounds have the same binding sites on the ENaC [394]. In the clinic, Triamterene is prescribed as an alternative to Amiloride for the treatment of hypertension [394, 395]. We hypothesised that if Triamterene was synthetically lethal through the inhibition of the ENaC, Amiloride, which shares the same mechanism of action, would also be synthetically lethal in MMR deficient cell lines. We treated DLD1 and DLD1+chr2 cells with increasing concentrations of Amiloride (0, 0.5, 5, 10 and 50 µM) and measured cell viability after 4 days. As shown in Figure 34, only at high concentrations of Amiloride (50 µM) we observe cytotoxicity for the cells and Amiloride does not show selective lethality in the MMR deficient DLD1 cells, compared to DLD1+chr2 cells. These results suggest that Triamterene is not synthetically lethal in MMR deficient cells through its shared mechanism of action with Amiloride, as a sodium channel antagonist.

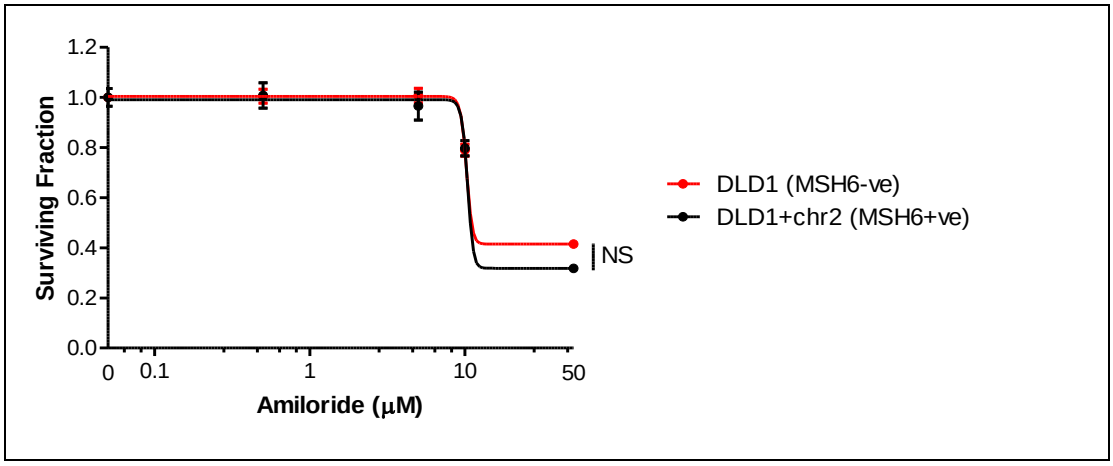

Figure 34: Amiloride, another ENaC inhibitor, is not synthetically lethal in MMR deficient cells

Cells were seeded in 96-well plates and treated with increasing concentrations of Amiloride (0, 0.5, 5, 10 and 50 µM). After 4 days treatment, cell viability was assessed by ATP-luminescence assay. Experiments were carried out in triplicate and error bars represent SEM. P-values derived from 2way ANOVA (NS $p > 0.05$).

1.2.2 Silencing of the different subunits of the ENaC is not synthetically lethal in MMR deficient cell lines

Our results suggest that Triamterene is not synthetically lethal in MMR deficient cells through its shared mechanism of ENaC inhibition with Amiloride. The ENaC is composed of 2 x α, 1 x β and 1 x γ subunits [396]. In order to further investigate the role of ENaC inhibition in Triamterene synthetic lethality in MMR deficient cells, we silenced the three different subunits of ENaC (α, β and γ) by siRNA transfection in a range of MMR deficient and proficient matched paired cell lines (Figure 35). We silenced the different subunits individually or in combination using the same final siRNA concentration to allow the comparison of the different conditions (see the material and methods section 6.1). We validated siENaC transfection efficiency with internal siRNA controls (siCtrl and siPLK1). In DLD1 and DLD1+chr2 cells, the inhibition of the ENaC subunits was not lethal for the cells, with higher toxicity observed upon silencing of the ENaC γ subunit. However, we did not observe any selective lethality in the MSH6 deficient DLD1 cells compared to the MSH6 proficient DLD1+chr2 cells (Figure 35A). In HCT116 and HCT116+chr3 cells, the inhibition of the ENaC subunits was not lethal. Again, we did not observe any selective lethality in the MLH1 deficient HCT116 cells compared to the MLH1

proficient HCT116+chr3 cells (Figure 35B). In U251 and U251.TR3 cells, again the inhibition of the ENaC subunits were not selective lethality in the MSH6 deficient U251.TR3 cells compared to the MSH6 proficient U251 cells. We observed higher toxicity upon silencing of the ENaC β subunit (Figure 35C). Taken together, our results suggest a cell line dependent toxicity upon inhibition of the different ENaC subunits. Moreover, silencing of the ENaC subunits either alone or in combination was not synthetically lethal in MMR deficient cell lines and therefore suggests that ENaC inhibition is not the mechanism by which Triamterene induces synthetic lethality in MMR deficient cells.

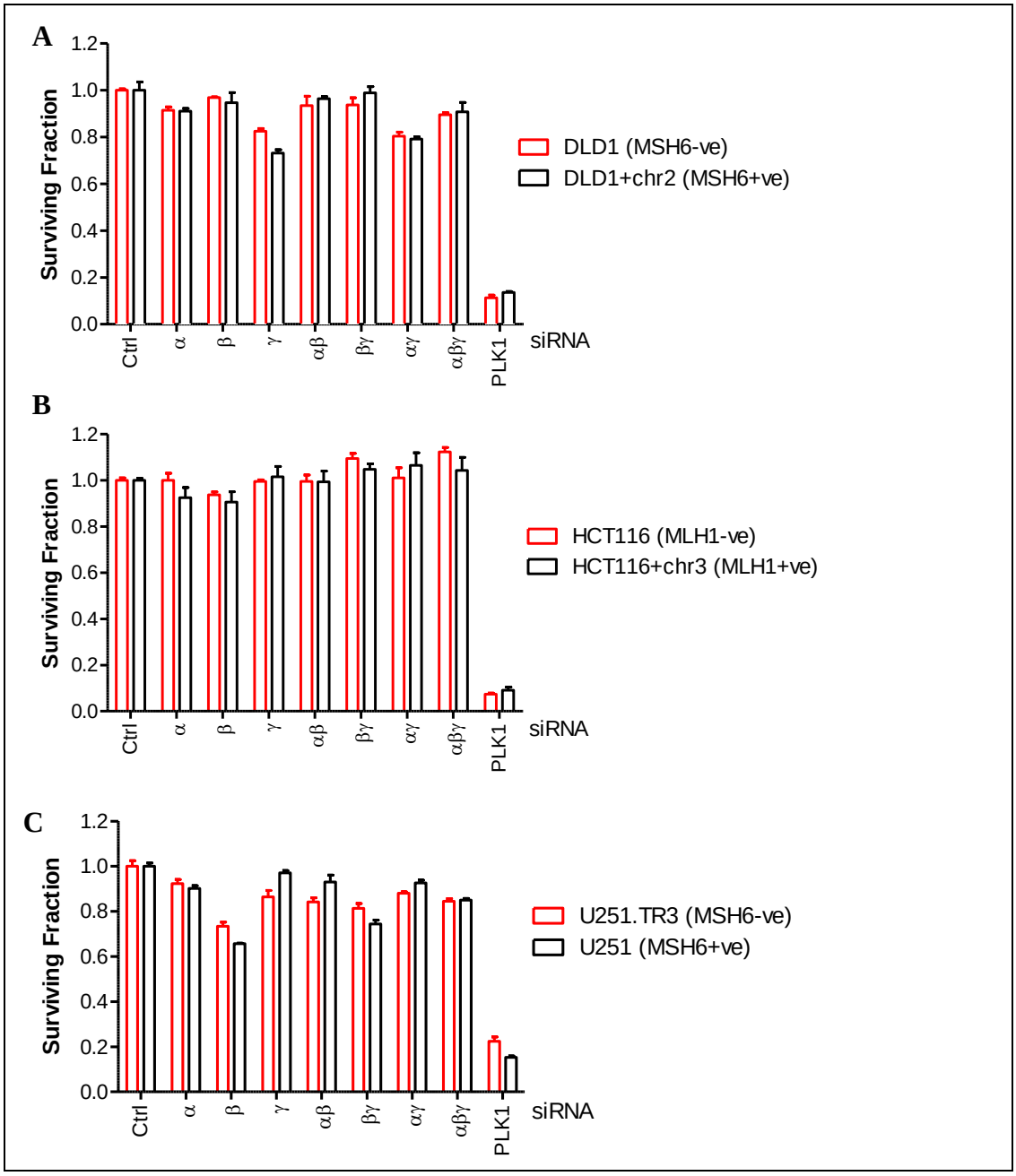

Figure 35: Triamterene is not cytotoxic through the inhibition of the ENaC

A-C: Cells were transfected with siCtrl, siPLK1 or siRNAs targeting the different subunits of the ENaC (α, β and γ), individually or in combination. To be able to compare the different silencing conditions, we used the same siRNA concentration and the same final concentration for each condition (50 nM of each siRNA in addition of the appropriate concentration of siCtrl for a final concentration of 150 nM). After 24 hrs transfection, the media was replaced and after 5 days transfection, cell viability was measured, by an ATP-luminescence assay. Experiments were carried out in triplicate, data were normalized to the siCtrl condition and error bars represent SEM. P-values derived from 2way ANOVA (NS $p > 0.05$).

1.3 Triamterene cytotoxicity is due to its antifolate activity

Our data suggested that the synthetic lethality observed upon Triamterene treatment in MMR deficient cells is not due to its role as an ENaC inhibitor; therefore we investigated the other reported roles of the compound. Structural analysis and previous studies have shown that Triamterene shares the same structure as a folate and therefore can compete with folate binding and function as an antifolate, which may regulate DHFR activity (Figure 33) [397].

1.3.1 Addition of folates can rescue Triamterene synthetic lethality in MMR deficient cells.

To investigate if Triamterene was synthetically lethal in MMR deficient cell lines through its antifolate activity, we hypothesised that the addition of folic acid could rescue Triamterene selective cytotoxicity. We treated DLD1 and DLD1+chr2 cells, grown in folate-free media (folate-free RPMI supplemented with 10 % dialysed FBS), with 10 µM Triamterene and increasing concentrations of folic acid (0, 0.01, 0.1, 1, 2, 10 µM) (Figure 36A). Our results showed that 4 days folate starvation was not cytotoxic in DLD1 and DLD1+chr2 cells. The residual levels of folates present in the dialysed FBS may be sufficient to retain cell viability. In the presence of 0.1 µM folic acid or less, Triamterene was cytotoxic in both cell lines. With higher concentration of folic acid (1, 2 and 10 µM), we observed a folic acid concentration dependant rescuing effect of Triamterene cytotoxicity. With 2 µM folic acid, we observed a selective cytotoxicity upon Triamterene treatment in the DLD1 cells. With 10 µM folic acid, we observed a rescued Triamterene-induced cytotoxicity. Our results suggest that addition of folic acid can rescue the Triamterene selective effect in MMR deficient cells. However folate-free media is not cytotoxic to the cells and Triamterene treatment can induce cytotoxicity in folate-starved media. We hypothesize that this may be due to residual folate remaining in the media due to addition of dialysed FBS. Furthermore, we previously showed that Triamterene is cytotoxic alone, only when the cells are kept in drug and not if the media is replaced with fresh drug-free media after 2 days treatment (Figure 25). To know if this was due to the presence of folate in the replaced media, we treated the cells with Triamterene for 2 days and either replaced the media with media containing Triamterene, folate-free media or complete media containing folate (Figure 36B).

We observed the same selective cytotoxicity in MMR-deficient cells treated with Triamterene alone or treated with Triamterene followed by folate-free media. However, we observed a rescuing effect of the Triamterene cytotoxicity in cells treated with Triamterene followed by normal media containing folate. Taken together, these results suggest a critical role for the folate pathway in Triamterene synthetic lethality in MMR deficient cells.

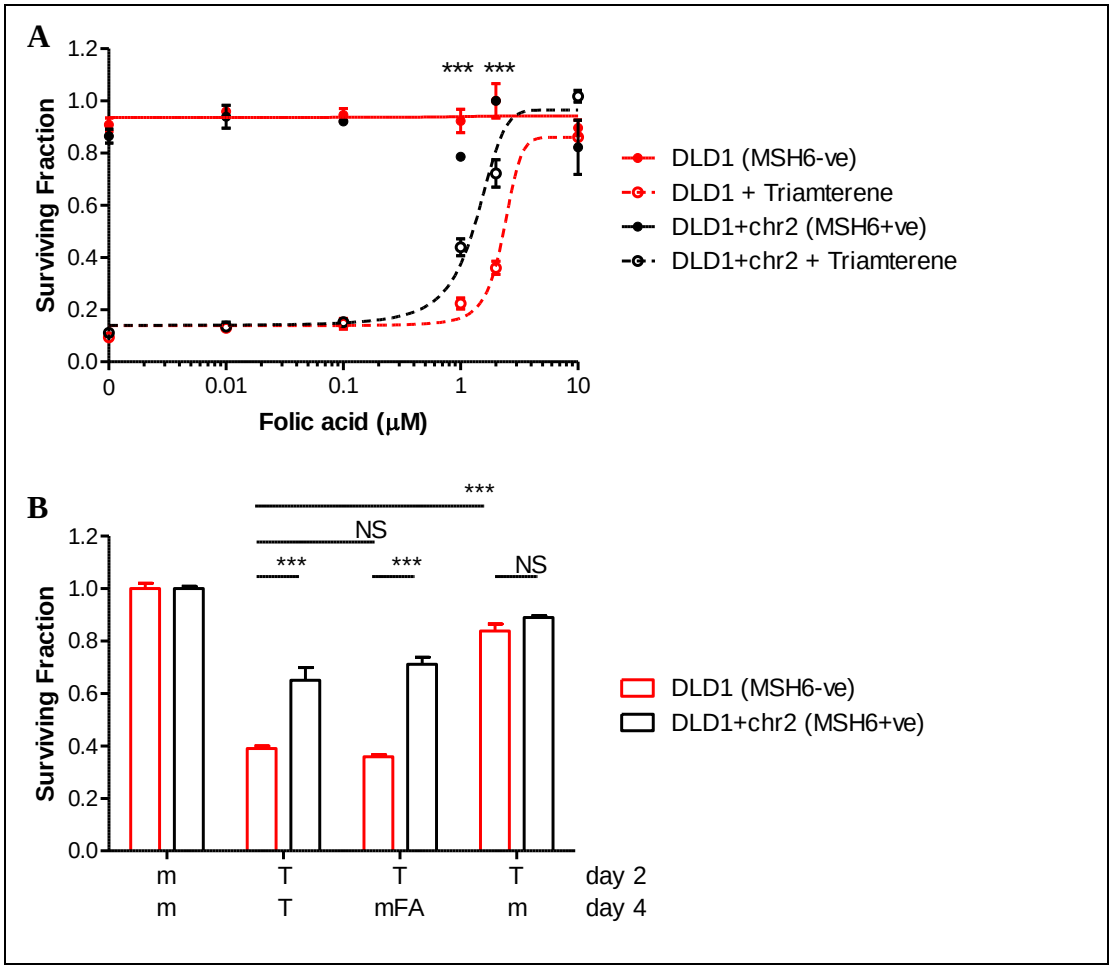

Figure 36: Addition of folic acid and media containing folate can rescue Triamterene synthetic lethality in MMR deficient cells

A: Cells were treated in folate-free media with increasing concentrations of folic acid (0, 0.01, 0.1, 1, 2, 10 µM) alone or in addition of 10 µM Triamterene. Cell viability was measured after 4 days treatment by an ATP-luminescence assay. Data were normalized to the cell viability upon 10 µM folic acid alone in order to see a potential folate-free-induced cytotoxicity. Experiments were carried out in triplicate and error bars represent SEM. P-values derived from 2way ANOVA representing the difference between DLD1 and DLD1+chr2 cells treated with Triamterene (*** $p < 0.001$). **B:** On day 1, cells were plated in a 96-well plate; on day 2 cells were treated with 10 µM Triamterene (T) or media (m); on day 4, cells were treated with 10 µM Triamterene (T), media (m) or folate-free media (mFA); Cell viability was measured using an ATP-luminescence assay on day 6. Experiments were carried out in triplicate and error bars represent SEM. P-values derived from 2way ANOVA (NS $p > 0.05$, *** $p < 0.001$).

1.3.2 Triamterene synthetic lethality in MMR deficient cell lines could be rescued by a range of different folates

We previously showed that the addition of folic acid or folate-containing media could rescue Triamterene cytotoxicity in the MMR deficient cell lines. We investigated any specificity for the requirement of folates to reverse the cytotoxicity, by using a range of different folates (folic acid (FA), dihydrofolate (DHF), tetrahydrofolate (THF) and Leucovorin (LV)) implicated in the folate pathway (Figure 11). We wanted to understand whether different folates could have different rescuing effect on Triamterene selective cytotoxicity, leading us to a better understanding of the role of Triamterene in the folate pathway.

To this end, we treated cells with 10 µM or 20 µM Triamterene, in addition to 10 µM or 50 µM of a range of different folates (DHF, THF, FA and LV) in the DLD1, DLD1+ch2 cells and U251, U251.TR3 cells respectively, and measured cell viability after 4 days treatment. In the DLD1 and DLD1+chr2 cells, the addition of FA, DHF, THF and LV could completely rescue Triamterene selective lethality (Figure 37A). In the U251 and U251.TR3 cells, the addition of DHF and LV could partially rescue the MSH6 deficient U251.TR3 cells from Triamterene cytotoxicity. However the addition of FA and THF could completely rescue Triamterene selective lethality (Figure 37B). We observed a greater reduction in cell viability upon Triamterene treatment in the U251.TR3 cells (58 %) in comparison to the DLD1 cells (30 %). This difference may explain the only partial rescuing of the Triamterene cytotoxic effect in the U251.TR3 compared to the DLD1 cells, upon addition of DHF and LV. Taken together, our results showed that Triamterene cytotoxicity in MMR deficient cells could be rescued by the addition of a range of different folates. These results suggest that Triamterene is synthetically lethal in MMR deficiency through its antifolate activity. However, as we observed the ability of all of the folate compounds tested to rescue the cytotoxic effect of Triamterene, this data did not enable us to elucidate a specific role for Triamterene in the folate pathway.

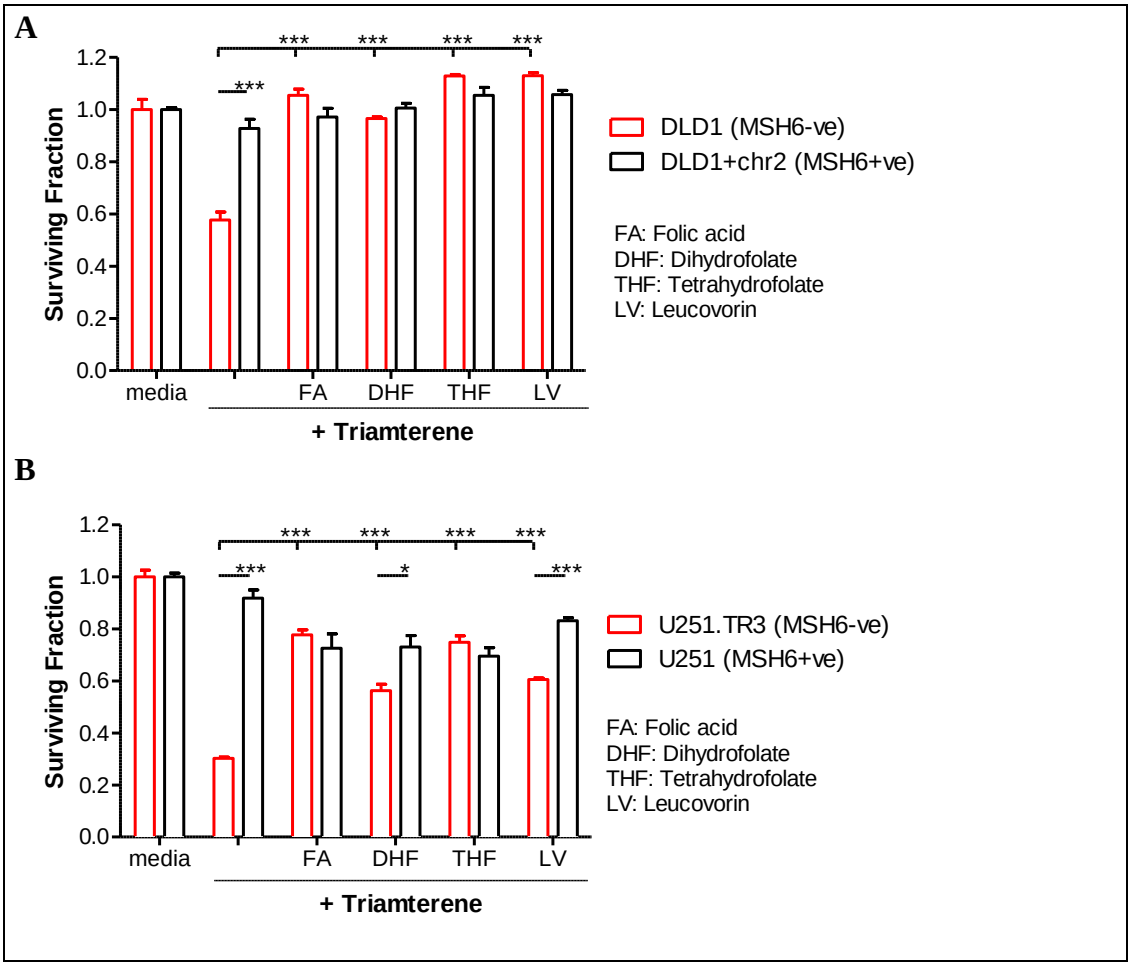

Figure 37: Addition of a range of different folates can rescue Triamterene synthetic lethality in MMR deficient cells

A: Cells were treated with 10 µM Triamterene combined with either 10 µM folic acid (FA), dihydrofolate (DHF), tetrahydrofolate (THF) or Leucovorin (LV). Cell viability was measured after 4 days treatment by ATP-luminescence assay. **B:** Cells were treated with 20 µM Triamterene combined with either 50 µM FA, THF, DHF or LV. Cell viability was measured after 4 days treatment by ATP-luminescence assay. **A, B:** Experiments were carried out in triplicate and error bars represent SEM. P-values derived from 2way ANOVA (* $p < 0.05$, *** $p < 0.001$).

1.4 Triamterene cytotoxicity is not due to the DHFR up-regulation

1.4.1 Triamterene induces an up-regulation of DHFR

Structural analysis and previous studies have shown that Triamterene shares the same structure as a folate and therefore can function as an antifolate which may regulate DHFR activity (Figure 33) [397]. DHFR is the main enzyme required for the folate pathway. It converts folate into DHF, and DHF into THF which is the rate limiting factor of TS activity and therefore, for dTMP synthesis (Figure 11) [398]. We next investigated whether Triamterene was synthetically lethal in MMR deficiency through the regulation of DHFR. In order to investigate the potential role for DHFR in Triamterene synthetic lethality in MMR deficient cells, we measured DHFR protein expression by western blot upon Triamterene treatment in a range of MMR deficient and proficient matched paired cell lines (DLD1 and DLD1+chr2; U251 and U251.TR3 cells). DHFR expression was similar in the MMR deficient cells when compared with their matched-paired MMR proficient cells (Figure 38A&B). Interestingly, the Triamterene-induced DHFR up-regulation was higher in the MSH6 deficient DLD1 and U251.TR3 cells in comparison to the MSH6 proficient DLD1+chr2 and U251 cells. However, we observed an increase in DHFR protein expression upon Triamterene treatment, independent of drug concentration and in both MMR deficient and proficient cell lines. We measured DHFR protein levels in DLD1 and DLD1+chr2 cells upon 0, 2, 4, 6, 8 and 10 µM Triamterene (Figure 38C). We confirmed that DHFR up-regulation was independent of Triamterene concentration and also observed that it was independent of Triamterene cytotoxicity if compared to the cell viability and clonogenic assays (Figure 25B & Figure 26A). We next investigated if the observed Triamterene-induced up-regulation of DHFR expression was correlated with an increase in DHFR activity. We measured DHFR activity, by measuring the DHFR dependent consumption of NADPH, in the protein lysates used for western blotting (Figure 38A). As shown in Figure 38D, Triamterene treatment induced an increase in DHFR activity in DLD1 and DLD1+chr2 cell lines. However, the difference in DHFR regulation in the DLD1 cells compared to the DLD1+chr2 cells was not significant. We also observed, in DLD1 and DLD1+chr2 cells that the DHFR protein expression correlated with the DHFR activity (Figure 38A & D). Taken together, our data suggest that the differential increase in DHFR expression and activity upon

Triamterene treatment in the MSH6 deficient cells may contribute to the synthetic lethal interaction we observe.

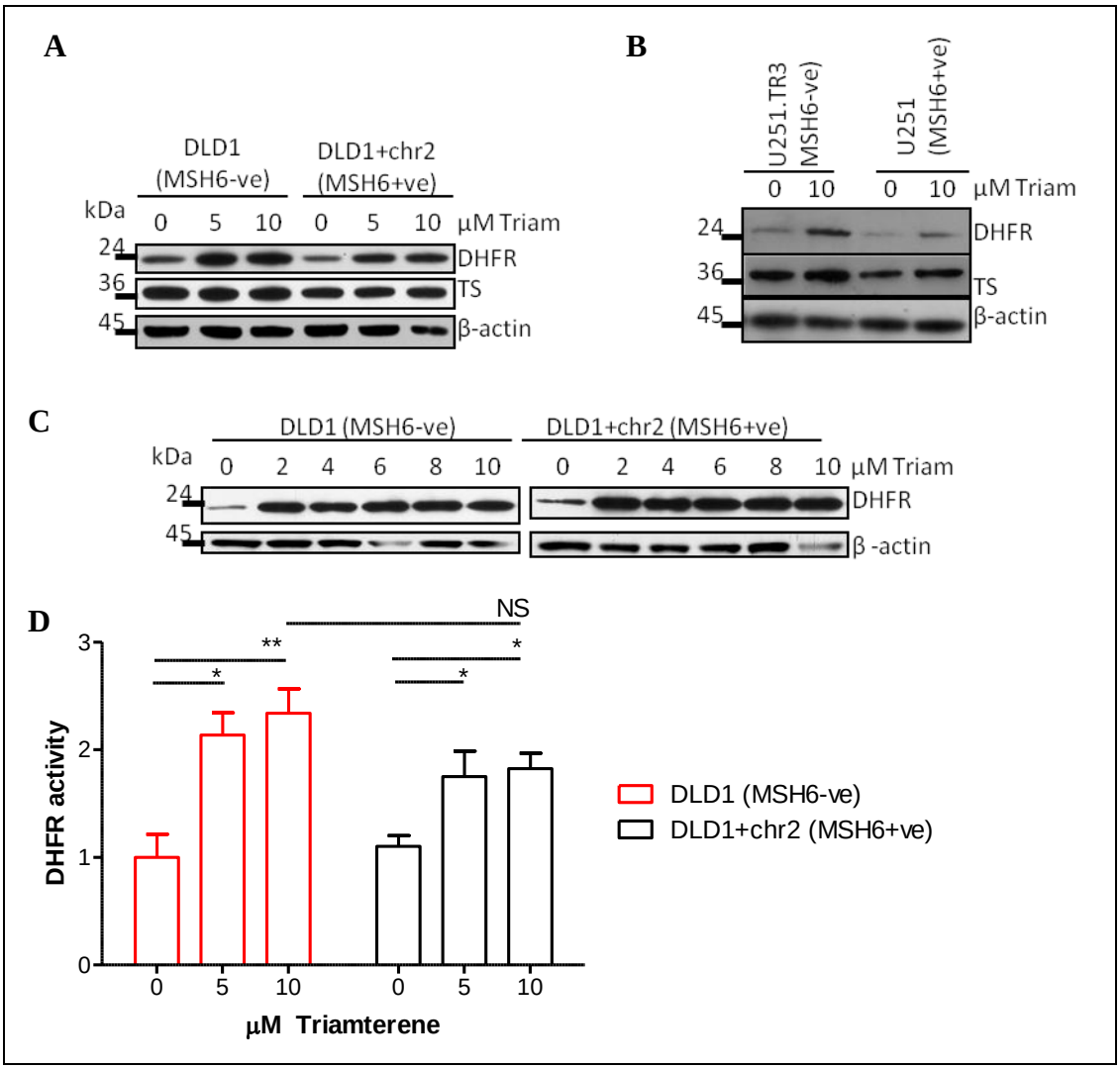

Figure 38: Triamterene induces a DHFR up-regulation

A, C: Cells were plated in 10 cm dishes and were treated with either media, 5 µM or 10 µM Triamterene. After 48 hrs treatment, protein was extracted. **B:** Cells were plated in 6-well plates and were treated with 10 µM Triamterene. After 48 hrs treatment, protein was extracted. **A, B:** DHFR and TS expression were measured by western blot using DHFR, TS and β-actin antibodies. β-actin is used as a loading control. **C:** Cells were plated in 6-well plates and were treated with 0, 2, 4, 6, 8 and 10 µM Triamterene. After 48 hrs treatment, protein was extracted. DHFR expression were measured by western blot using DHFR and β-actin antibodies. β-actin is used as a loading control. **D:** DHFR activity was measured by measuring the DHFR-dependant consumption of NADPH by monitoring the decrease in absorbance at 340 nm. Experiments were carried out in triplicate and error bars represent SEM. P-values derived from 1way ANOVA (NS $p > 0.05$, * $p < 0.05$, ** $p < 0.01$).

1.4.2 Triamterene is not synthetically lethal through DHFR up-regulation

We previously observed that Triamterene was synthetically lethal in MMR deficient cells lines through its antifolate activity. We also showed that Triamterene treatment induced a greater, but not significant, increase in DHFR expression and activity in MMR-deficient cells. We hypothesised that if Triamterene was synthetically lethal with MMR deficiency, through DHFR up-regulation, DHFR silencing would rescue the cells from Triamterene cytotoxicity and DHFR over-expression would induce synthetic lethality in MMR deficient cells. To assess the role of DHFR up-regulation in Triamterene cytotoxicity, we treated cells transfected with siDHFR or siCtrl, with increasing concentrations of Triamterene (0, 2, 4, 6, 8, 10 μM) and measured cell viability after 2 days treatment (Figure 39). We firstly validated that the transfection using siRNAs targeting DHFR was efficiently reducing DHFR protein expression in DLD1 and DLD1+chr2 cells by western blot (Figure 39B). We observed that silencing DHFR increased Triamterene cytotoxicity in both cell lines regardless of their MMR status (Figure 39A). These results suggest that the Triamterene-induced up-regulation of DHFR activity and expression is not mediating the synthetic lethality in MMR deficient cells. To further investigate this, we over-expressed DHFR by plasmid transfection with an empty or DHFR-expression construct and measured the effect of DHFR over-expression alone or in combination with Triamterene treatment on DLD1 and DLD1+chr2 cell viability (Figure 40). Over-expression of DHFR was not cytotoxic in DLD1 and DLD1+chr2 cells in comparison with the control plasmid. Moreover, DHFR over-expression did not modulate Triamterene selective lethality (Figure 40A). We validated DHFR over-expression by western blotting (Figure 40B); however, we did not validate the correlation between DHFR over-expression and DHFR activity and cannot conclude on the role of DHFR over-expression in Triamterene synthetic lethality. DHFR activity might depend on the substrates availability in the cells and therefore, DHFR over-expression alone might not be correlated with an up-regulation of DHFR activity. We did not include a positive control such as Methotrexate, a well known inhibitor of DHFR activity, in the assay and therefore, we cannot be assured that the DLD1 and DLD1+chr2 cells had an increased DHFR activity. Taken together, our results suggest that DHFR up-regulation is not the mechanism of cytotoxicity of Triamterene.

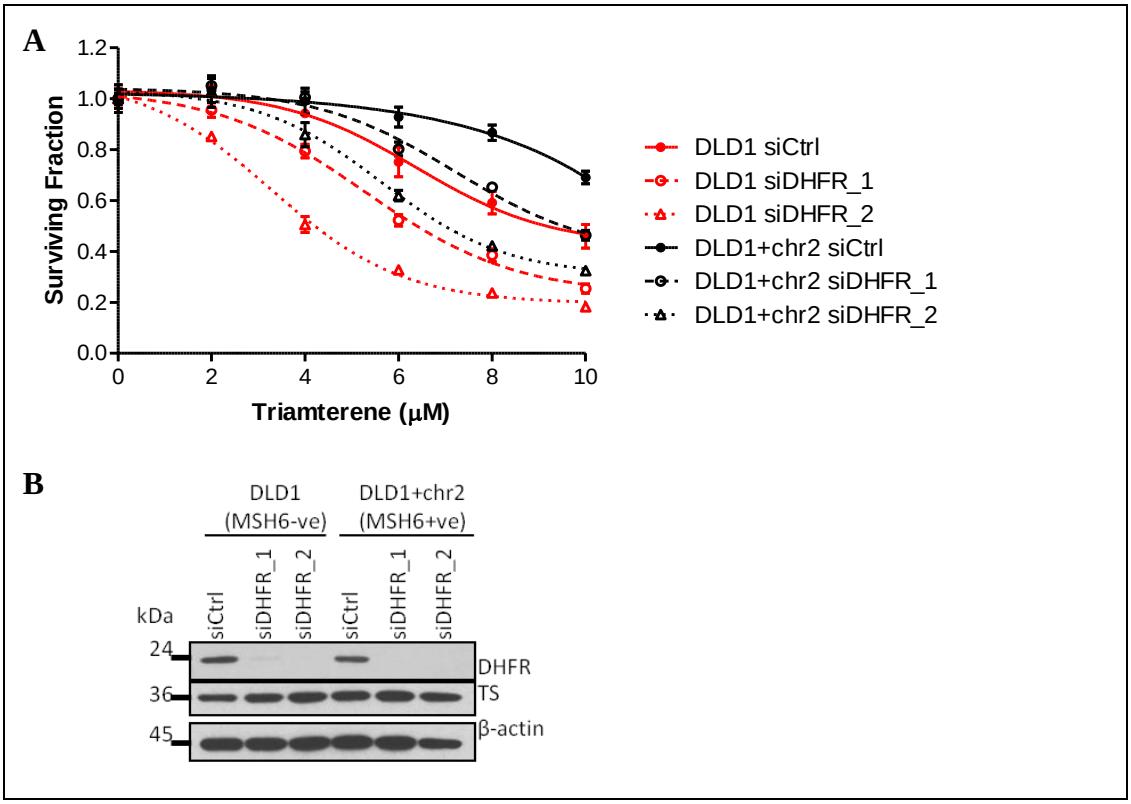

Figure 39: Triamterene is not synthetically lethal with MMR deficiency, through DHFR up-regulation

A, B: Cells were transfected in 6-well plates with a siCtrl or two different siRNAs targeting DHFR. **A**: The following day cells were counted, plated in 96-well plates and treated with increased concentration of Triamterene. After 2 days treatment, cell viability was measured using ATP luminescence assay. Experiments were carried out in triplicate and error bars represent SEM. **B**: The following day, cells were split in 6-well plates. After 2 days treatment, protein was extracted and DHFR expression was measured by western blot using DHFR and β-actin antibodies. β-actin is used as a loading control.

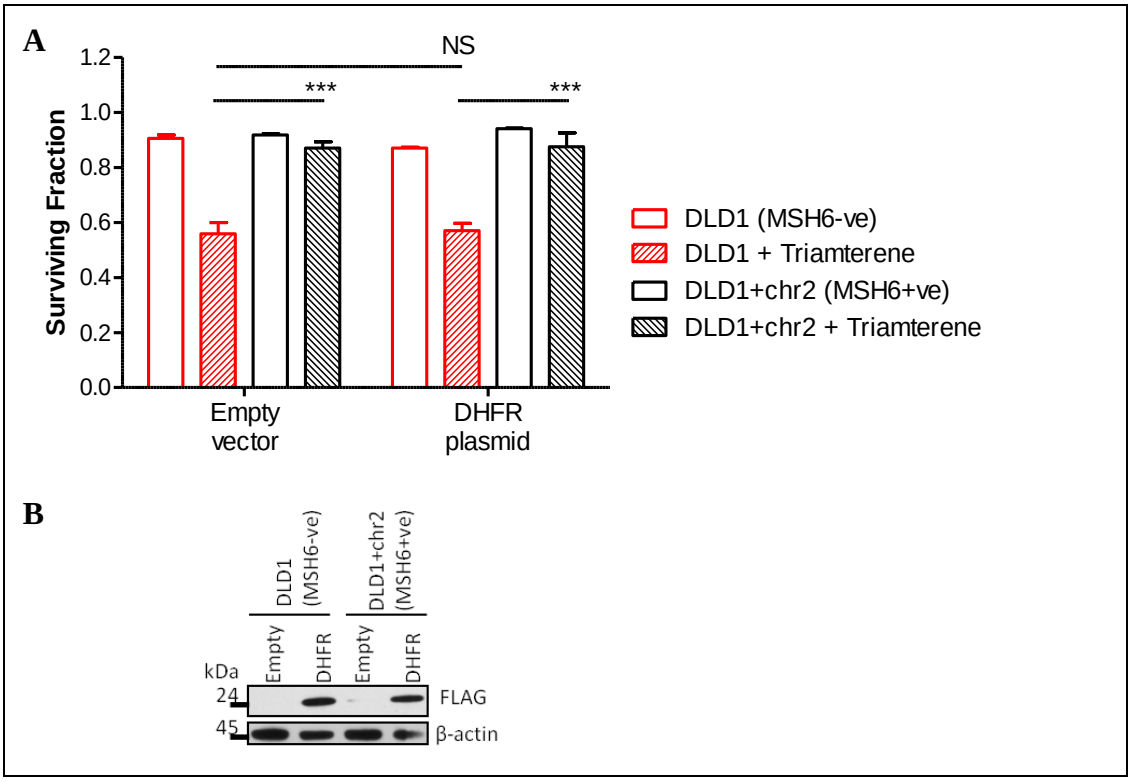

Figure 40: DHFR over-expression does not modulate cell viability alone or in combination of Triamterene treatment in DLD1 and DLD1+chr2 cells

A: Cells were transfected in 96-well plates with an empty vector or a DHFR plasmid. The following day, cells were treated with either DMSO or 10 µM Triamterene. After 4 days treatment, cell viability was measured using ATP luminescence assay. P-values derived from 1way ANOVA (NS $p > 0.05$ and *** $p < 0.001$). Experiments were carried out in triplicate and error bars represent SEM. **B:** Cells were transfected in 6-well plates with an empty vector or a DHFR-expressing vector. Two days after transfection, protein was extracted and DHFR over-expression was measured by western blot using FLAG and β-actin antibodies. β-actin is used as a loading control.

1.5 Triamterene cytotoxicity requires thymidylate synthase expression

1.5.1 Triamterene synthetic lethality requires thymidylate synthase expression

We previously showed that Triamterene treatment induced an increase in DHFR expression and activity, which is not required for the Triamterene synthetic lethality in MMR deficient cells. DHFR produces THF, the rate limiting factor of TS activity (Figure 11) [398]. We hypothesised that if treatment with Triamterene could up-regulate DHFR, it may also regulate TS activity, as TS activity depends on DHFR activity [399]. Therefore, we next measured TS protein expression by western blot upon Triamterene treatment in a range of MMR deficient and proficient matched paired cell lines (DLD1 and DLD1+chr2; U251 and U251.TR3 cells). As shown in Figure 38A & B, TS expression is similar in the MMR deficient cells in comparison to their matched-paired MMR proficient cells. TS protein expression was unchanged upon Triamterene treatment. Taken together, these results show no Triamterene-induced regulation of TS protein expression in our panel of cells. To further assess the role of TS in Triamterene cytotoxicity, we hypothesised that if Triamterene was synthetically lethal through TS regulation, TS silencing would rescue the cells from Triamterene selective lethality. DLD1 and DLD1+chr2 cells, transfected with two different siRNA targeting TS or siCtrl, were treated with increasing concentrations of Triamterene (0, 2, 4, 6, 8 and 10 µM) and cell viability was measured after 4 days treatment. We firstly validated that the transfection using siRNAs targeting TS-induced a decrease in TS protein expression in DLD1 and DLD1+chr2 cells by western blot (Figure 41A). Interestingly, we observed that TS silencing by siRNA transfection prevented the Triamterene-induced lethality in the MSH6 deficient DLD1 cells, suggesting the TS is required for Triamterene cytotoxicity in MSH6 deficient cells (Figure 41B). To further validate these results, we carried out the same experiment in the matched paired U251 and U251.TR3 cell lines (Figure 41C). We observed that TS silencing also prevented the Triamterene-induced lethality in the MSH6 deficient U251.TR3 cells. Taken together, these results strongly suggest the Triamterene synthetic lethality in MMR deficient cells, is dependent on TS expression.

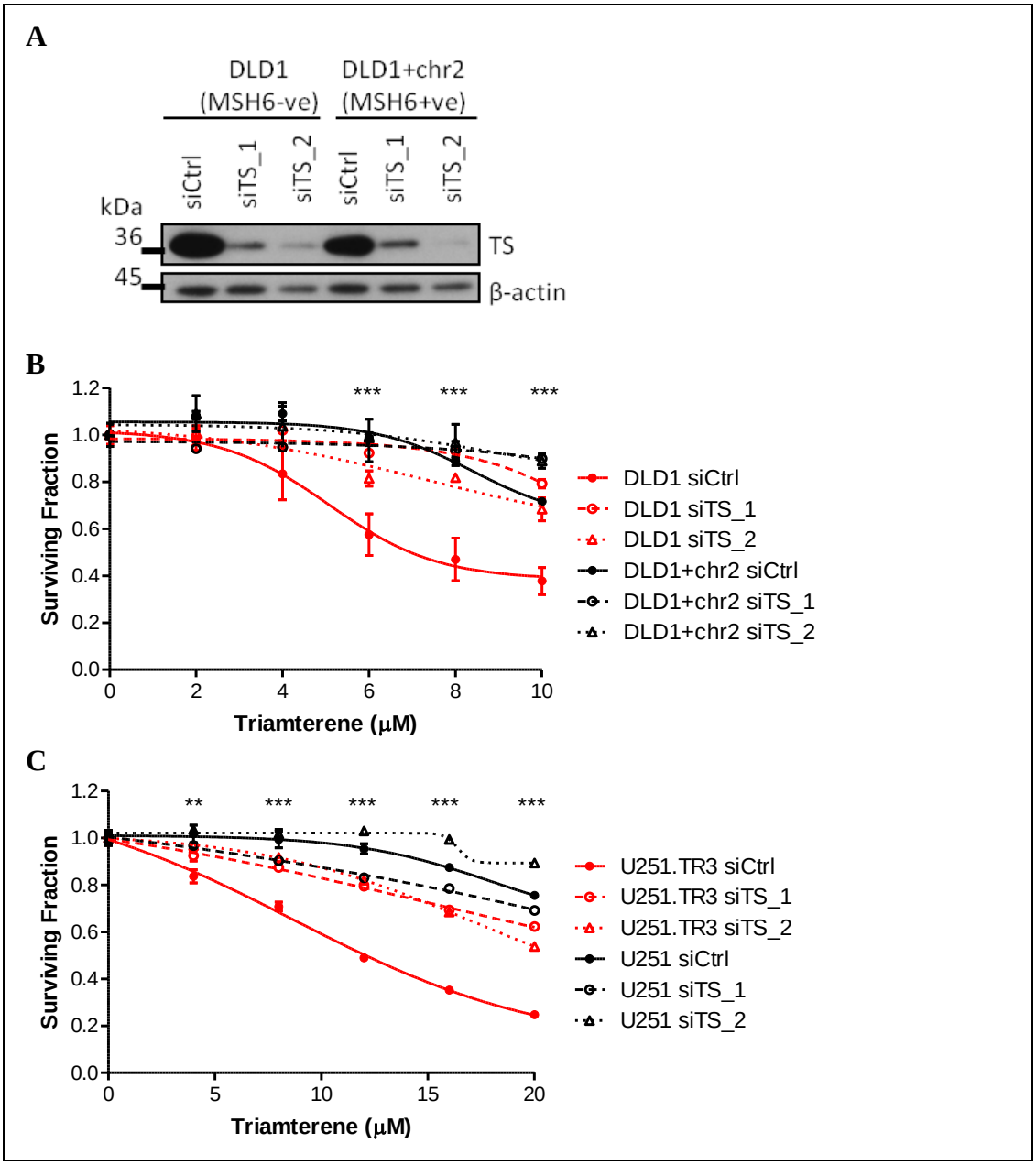

Figure 41: Triamterene synthetic lethality requires thymidylate synthase expression

A-C: Cells were transfected in 6-well plates with a siCtrl, siPLK1 or two siRNA targeting TS. The following day, cells were counted and seeded into either 6-well (**A**) or 96-well plates (**B, C**). **A**: Protein was extracted from DLD1 and DLD1+chr2 cells in 6-well plates after 2 days and TS expression was measured by western blot using TS and β-actin antibodies. β-actin is used as a loading control. **B, C**: Cells plated in 96-well plates were treated with increased concentration of Triamterene. After 4 days treatment, cell viability was measured using an ATP luminescence assay. Experiments were carried out in triplicate and error bars represent SEM. P-values derived from 2way ANOVA (** $p < 0.01$, *** $p < 0.001$).

1.5.2 Triamterene synthetic lethality can be rescued by TS inhibitors

We have previously shown that TS expression was required for the Triamterene-induced synthetic lethality in MMR deficient cell lines. Two widely used chemotherapeutic treatments in CRC, 5-FU and Raltitrexed, are TS inhibitors. They inhibit the active complex form of THF-TS-dUMP, either by competing with dUMP in the case of 5-FU or by competing with THF in the case of Raltitrexed. We hypothesised that, if TS expression was required for Triamterene cytotoxicity, 5-FU and Raltitrexed would be able to rescue the cytotoxic effect of Triamterene in MMR deficient cells. To investigate this, we treated cells with either 2 µM 5-FU or 1 nM Raltitrexed in addition to Triamterene treatment and measured cell viability after 4 days treatment. Our results indicate that Triamterene cytotoxicity can be rescued by addition of TS inhibitors in the DLD1 and U251.TR3 MSH6 deficient cells (Figure 42). Interestingly, we observed a greater rescuing effect of the Triamterene cytotoxicity, with Raltitrexed treatment compared to 5-FU. This difference may be explained by the fact that Raltitrexed has only one mechanism of action, the inhibition of TS; however, 5-FU has three known mechanisms of action: the inhibition of TS, the misincorporation of FdUTP into DNA and the misincorporation of FUTP into RNA (Figure 8). Taken together, these results suggest the requirement for TS for the Triamterene-induced synthetic lethality in MMR deficient cell lines.

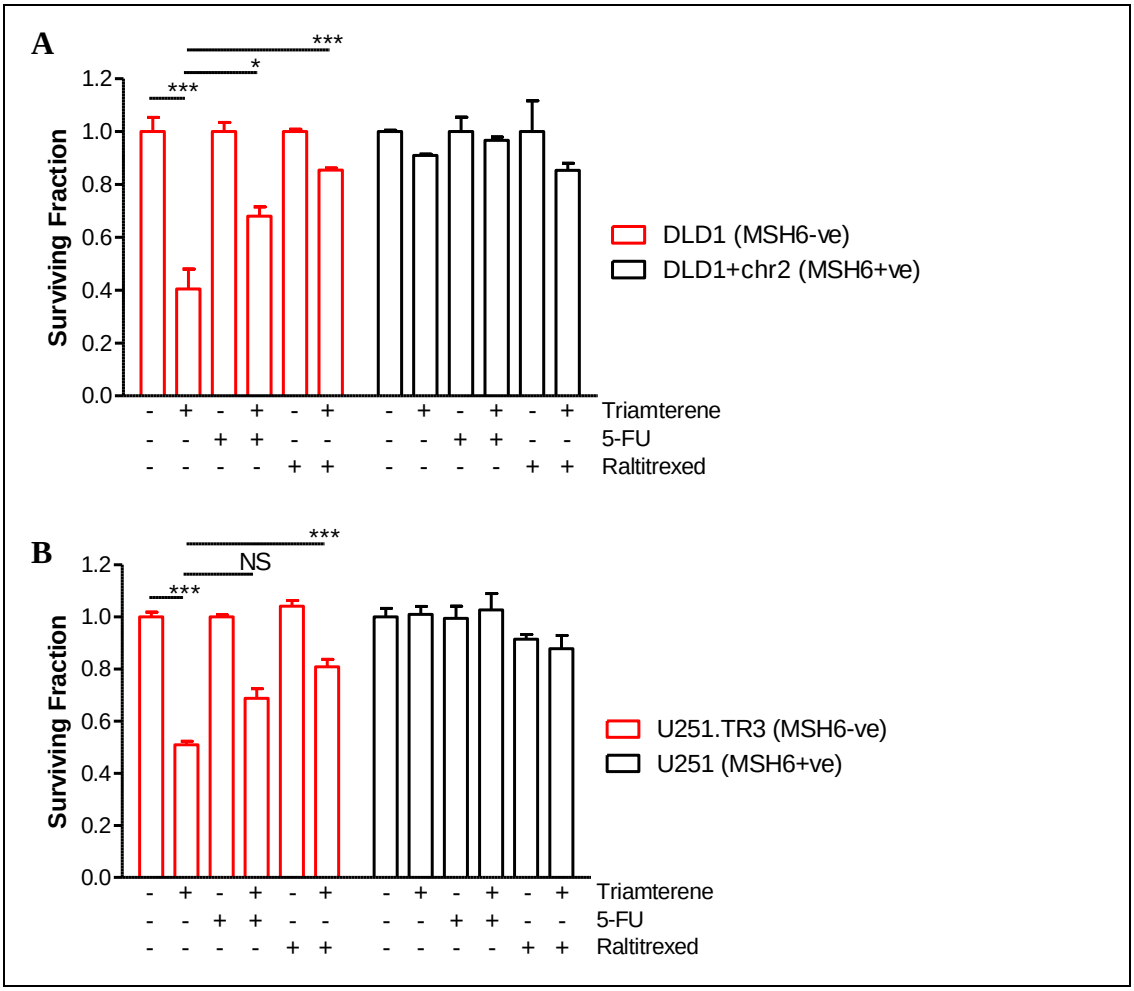

Figure 42: Triamterene synthetic lethality can be rescued by TS inhibitors

A, B: Cells were treated with either Triamterene (10 µM in DLD1 and DLD1+chr2 cells; 20 µM in U251 and U251.TR3 cells), 2 µM 5-FU, 1 nM Raltitrexed or a combination of Triamterene and 5-FU or Raltitrexed. Cell viability was measured 4 days after treatment by ATP-luminescence assay. Experiments were carried out in triplicate and error bars represent SEM. P-values are derived from 1way ANOVA (NS $p > 0.05$, * $p < 0.05$, *** $p < 0.001$).

1.5.3 Over-expression of TS does not affect Triamterene synthetic lethality

There is a requirement for TS activity for the Triamterene-induced synthetic lethality in MMR deficient cell lines. Therefore, we hypothesised that TS over-expression could modulate the Triamterene cytotoxicity in the MMR deficient cells. To this end, we over-expressed TS using a TS-expressing plasmid and transfected the cells with this construct or an empty plasmid as a control. We validated TS over-expression by western blotting (Figure 43A). 48 hrs after transfection, we measured the effect of TS over-expression alone or in combination with Triamterene treatment on DLD1 and DLD1+chr2 cell viability (Figure 43B). We observed that over-expression of TS was not cytotoxic in DLD1 and DLD1+chr2 cells in comparison with the control plasmid. Moreover, TS over-expression did not modulate the Triamterene selective lethality. We did not include a positive control such as 5-FU in the assay and therefore, we cannot be assured that TS over-expression is correlated with an increase in TS activity. THF is the rate-limiting factor of TS activity; therefore, over-expression of TS might not be correlated with an increase in TS activity. Taken together, our results suggest that up-regulation of TS does not mediate Triamterene synthetic lethality in MMR deficient cells.

We previously observed an up-regulation of DHFR expression and an increase in DHFR activity upon Triamterene treatment. In addition, we identified a dependency for TS expression in the Triamterene synthetic lethality with MMR deficiency. We speculated that over-expression of DHFR may produce an excess of THF and therefore, in combination with over-expression of TS, this may correlate with an increase in TS activity, which may induce Triamterene synthetic lethality in MMR deficient cells. We over-expressed TS and DHFR proteins by plasmid transfection and measured whether over-expression of both TS and DHFR together, either untreated or upon Triamterene treatment could induce synthetic lethality in DLD1 cells (Figure 43C). Over-expression of DHFR/TS was not cytotoxic in DLD1 and DLD1+chr2 cells in comparison with the control plasmid. In addition, over-expression of DHFR/TS together did not modulate Triamterene cytotoxicity. Taken together, our results suggest that TS over-expression is not the mechanism of Triamterene synthetic lethality in MMR deficient cells and that the over-expression of DHFR and TS, alone or in combination, do not modulate Triamterene synthetic lethality in MMR deficient cells.

We have shown that Triamterene induces a non toxic up-regulation of DHFR. We have also shown that Triamterene requires TS expression and activity to be synthetically lethal. However, over-expression of TS alone or in combination with DHFR, does not induce selective lethality and does not modulate Triamterene synthetic lethality in MMR deficient cell lines.

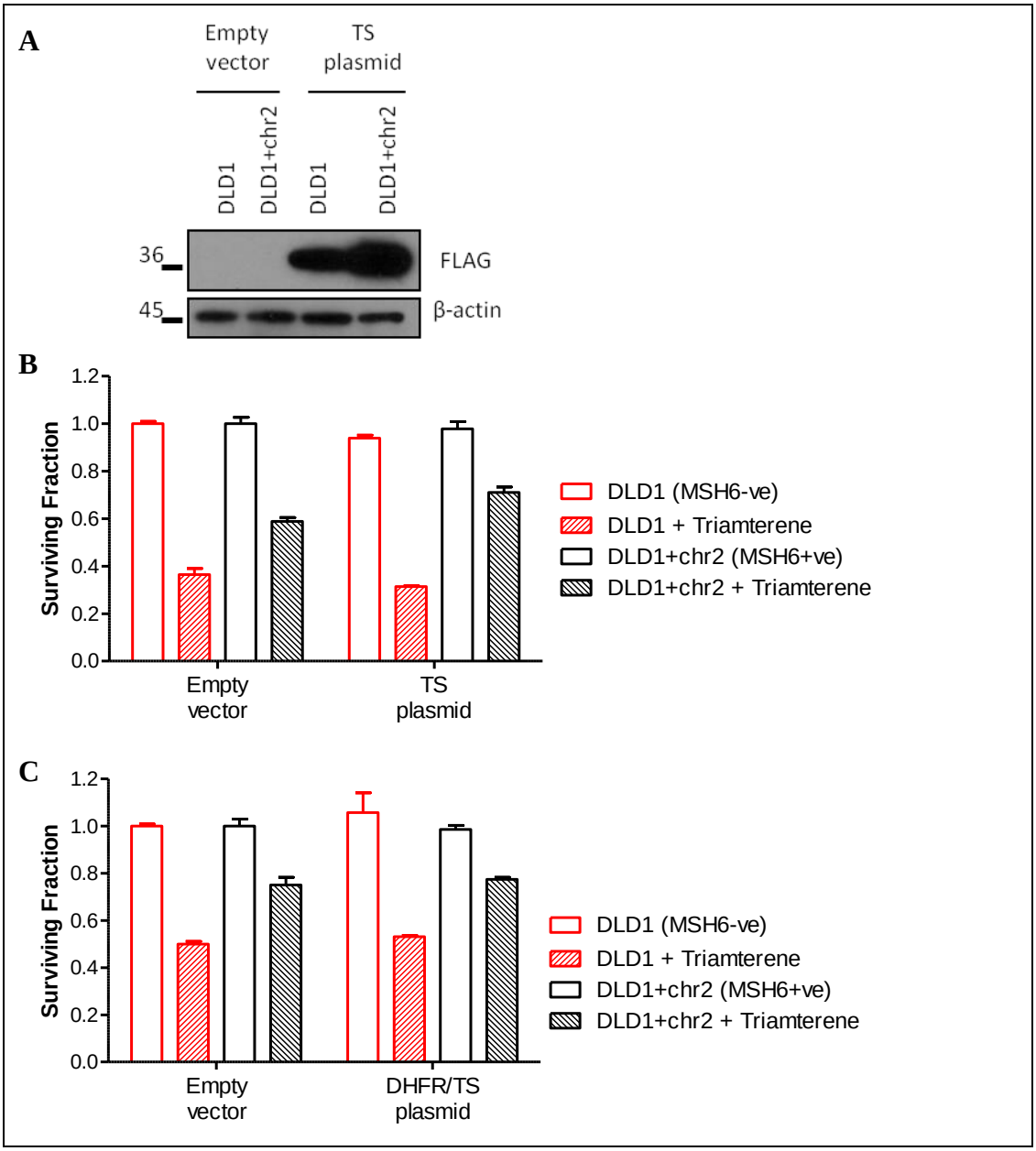

Figure 43: Over-expression of TS does not modulate Triamterene synthetic lethality

A: Cells were transfected in 6-well plates with an empty vector or a TS plasmid. After 2 days transfection, protein was extracted and TS over-expression was measured by western blot using FLAG and β-actin antibodies. β-actin is used as a loading control. **B:** Cells were transfected in 96-well plates with empty vector or TS-expressing plasmid. The following day, cells were treated with 10 µM Triamterene. Cell viability was measured on day 6 by ATP-luminescence assay. **C:** Cells were transfected in 96-well plates with empty vector or a combination of both the TS and DHFR-expressing plasmids. The following day, cells were treated with 10 µM Triamterene. Cell viability was measured on day 6 by ATP-luminescence assay. Experiments were carried out in triplicate and error bars represent SEM.

2 Triamterene is cytotoxic through an increase in reactive oxygen species

2.1 Triamterene induces an increase in ROS level

Previous studies have shown that MMR deficient tumours are sensitive to oxidative stress [315, 317-319]. Oxidative stress is caused by an imbalance between ROS production and degradation via the antioxidant response [21]. We investigated whether Triamterene was synthetically lethal in MMR deficient cell lines due to an increase in ROS levels. We treated the cells for 48 hrs with either 5, 10 or 20 µM Triamterene in a panel of MMR deficient and proficient matched paired cell lines and measured ROS levels (Figure 44). ROS was measured using an DCFDA-Cellular ROS Detection Assay. DCFDA is converted in DCF by ROS. DCF, which is proportional to ROS levels, can be measured by fluorescence. Our results showed a dose-dependent increase in ROS levels in the MMR deficient cell lines, whilst ROS was not significantly induced in the matched paired MMR proficient cell lines upon treatment with increasing concentrations of Triamterene. Therefore our results suggest that Triamterene treatment induces an increase in ROS levels, specifically in MMR deficient cells lines.

To further investigate this Triamterene-induced increase in ROS levels, we measured ROS levels over time (after 2, 6, 24 and 48 hrs) following Triamterene treatment in both of our MSH6 proficient and deficient matched paired cell lines (Figure 45). Our results show an accumulation of ROS levels over-time in the MMR deficient DLD1 and U251.TR3 cell lines compared to their matched-paired MMR proficient DLD1+chr2 and U251 cell lines, respectively. Taken together, our results show a differential accumulation of ROS levels upon Triamterene treatment in the MMR deficient cell lines.

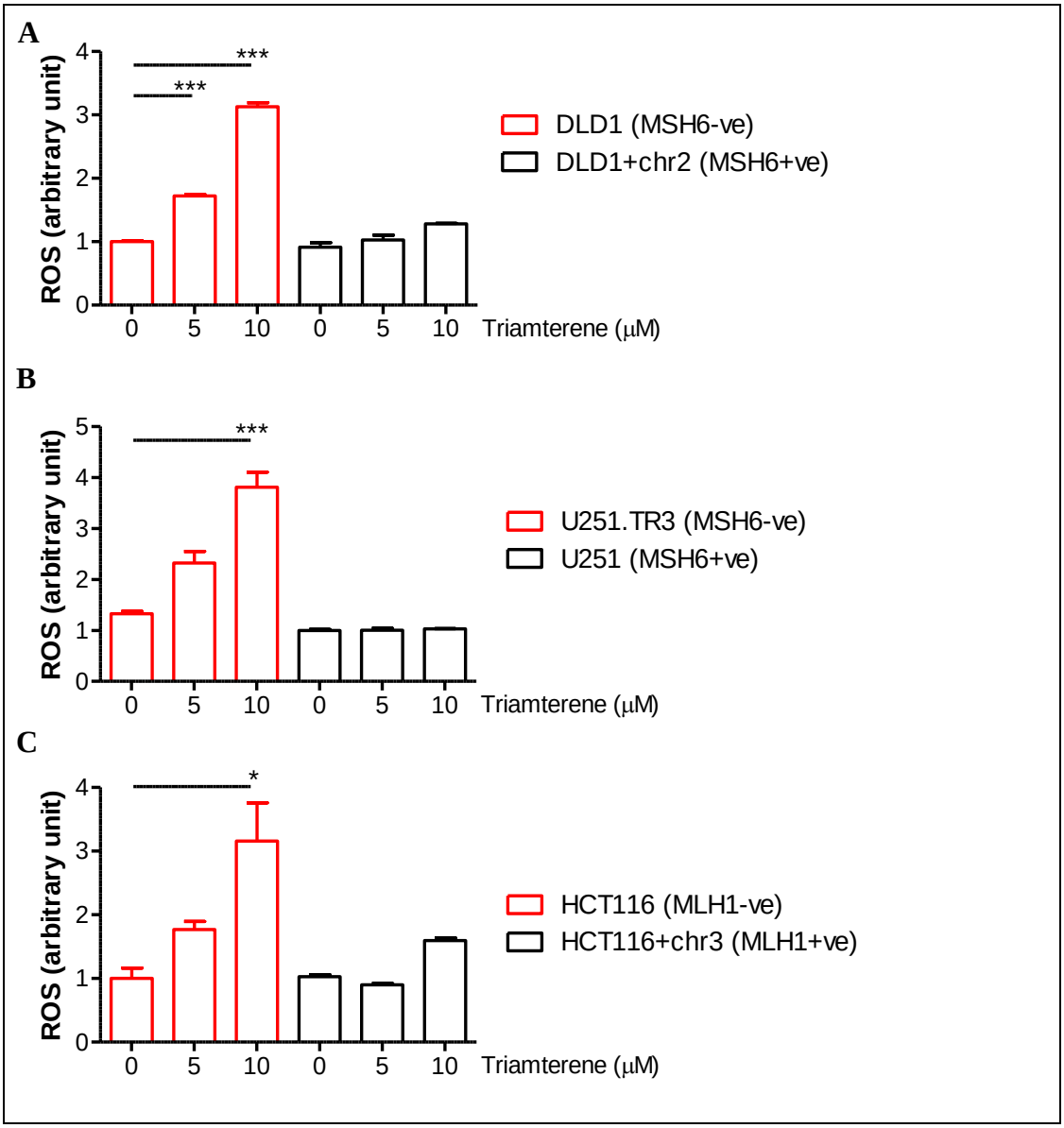

Figure 44: Triamterene induces an increase in ROS levels in MMR deficient cells

A-C: DLD1, DLD1+chr2; HCT116, HCT116+chr3; and U251, U251.TR3 cells were plated in 2 x 96-well plates (one to measure ROS levels, and one to measure cell viability). The following day cells, from both plates, were treated with either DMSO, 5 μM, 10 μM or 20 μM Triamterene. After 48 hrs treatment, cell viability was measured by ATP-luminescence assay and ROS levels were measured by quantifying the conversion of DCFDA into DCF by fluorescence. Fluorescence data were normalized to the cell viability values. Experiments were carried out in triplicate and error bars represent SEM. P-values derived from 1way ANOVA (* $p < 0.05$, *** $p < 0.001$).

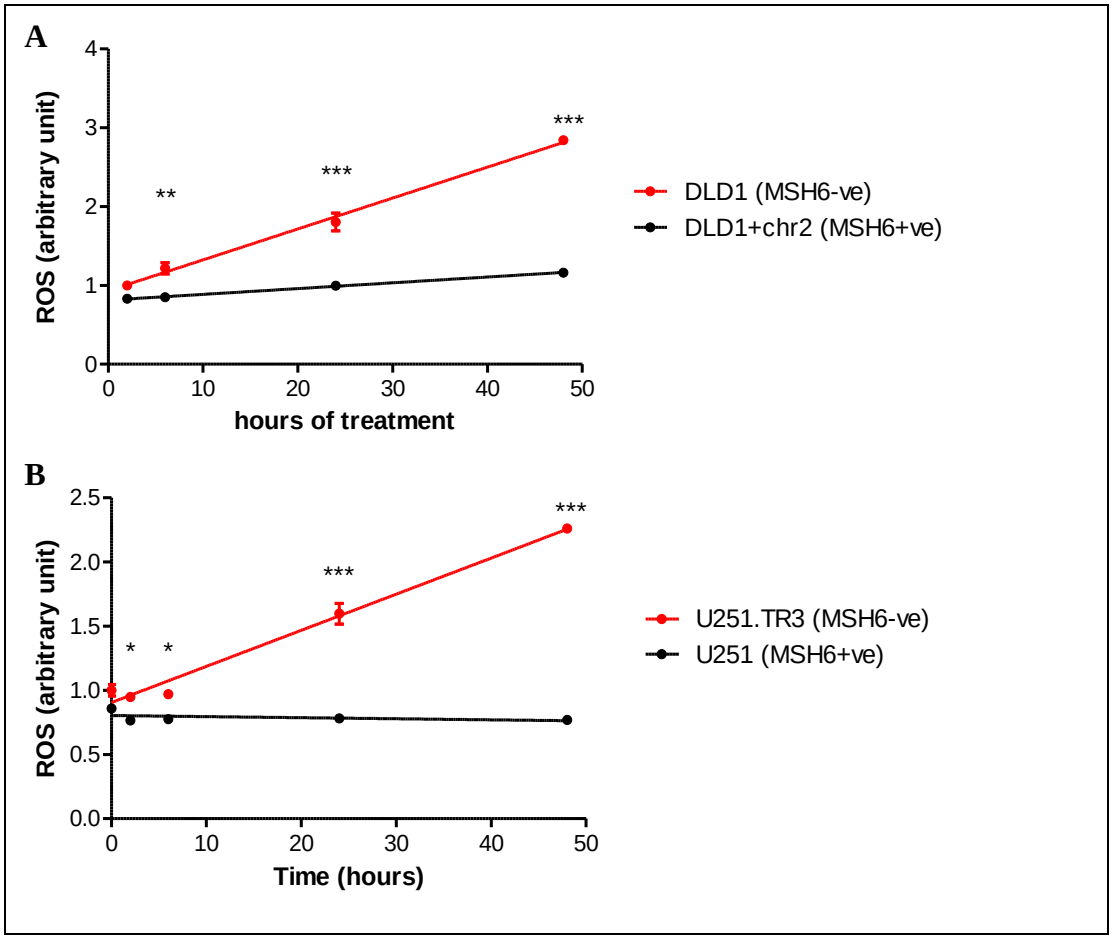

Figure 45: Triamterene-induced an accumulation in ROS levels over time in MMR deficient cells

A-B: DLD1, DLD1+chr2 and U251, U251.TR3 cells were plated in 2 x 96-well plates (one to measure ROS levels, and one to measure cell viability). Cells from both plates were treated with Triamterene (10 μM in DLD1 and DLD1+chr2 cells or 20 μM in U251 and U251.TR3 cells) at different time points (2, 6, 24 and 48 hrs from the end of the assay). At the end of the different time points, cell viability was measured by ATP-luminescence assay and ROS levels were measured by quantifying the conversion of DCFDA into DCF by fluorescence. Fluorescence values were normalized to the cell viability values. Experiments were carried out in triplicate and error bars represent SEM. P-values derived from 2way ANOVA (* $p < 0.05$, ** $p < 0.01$, *** $p < 0.001$).

2.2 The Triamterene-induced synthetic lethality in MMR deficient cell lines can be rescued by the addition of a ROS scavenger

We previously shown a differential accumulation of ROS levels upon Triamterene treatment in MMR deficient cell lines. In order to investigate if the increase in ROS levels was the mechanism of Triamterene synthetic lethality in these cells, we treated the DLD1, DLD1+chr2, HCT116 and HCT116+chr3 cells with increasing concentrations of Triamterene (0, 2, 4, 6, 8 and 10 µM) alone or in combination with 1 mg/mL N-acetylcysteine (NAC), a ROS scavenger (Figure 46). Our results showed a complete rescuing of Triamterene synthetic lethality with the addition of NAC in DLD1 cells compared to DLD1+chr2 cells and a partial rescuing of Triamterene synthetic lethality with the addition of NAC in HCT116 cells compared to HCT116+chr3 cells (Figure 47). Our results suggest that increased ROS levels are at least in part the mechanism of lethality upon Triamterene treatment in MMR deficient cell lines.

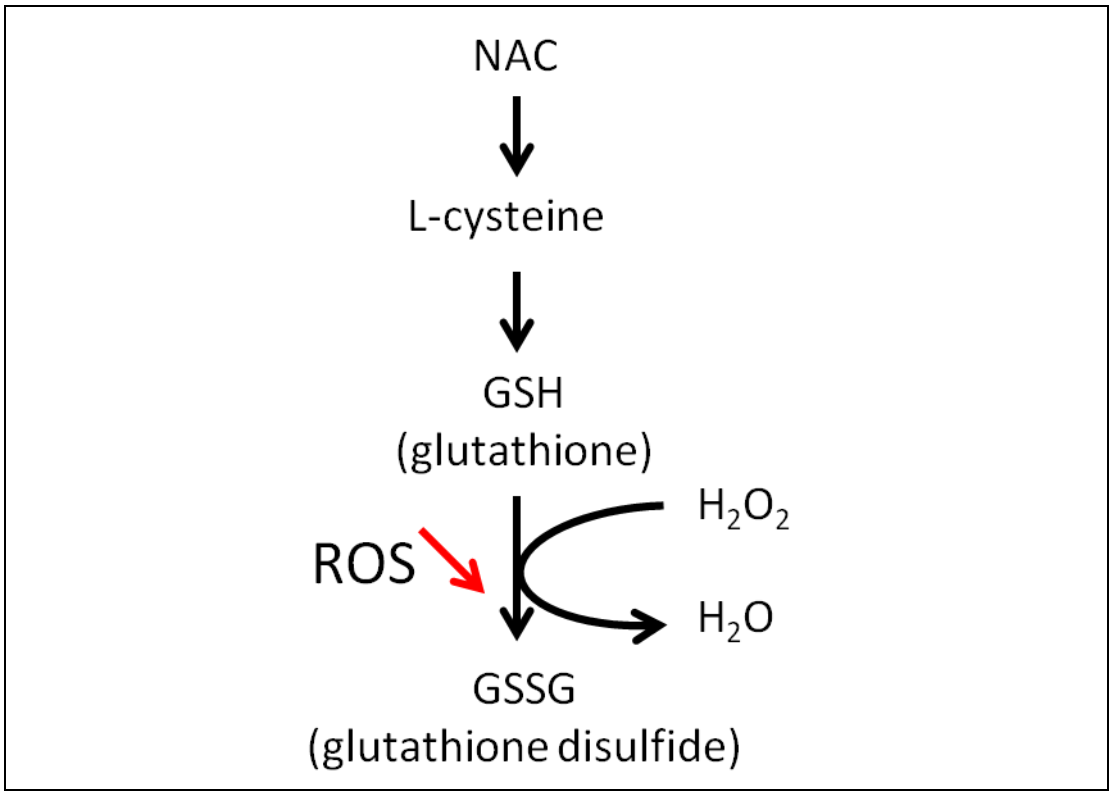

Figure 46: Mechanism of action of NAC, a ROS scavenger

NAC is converted into L-cysteine, itself converted into glutathione (GSH). GSH reduces H_2O_2 into H_2O therefore reduces ROS levels.

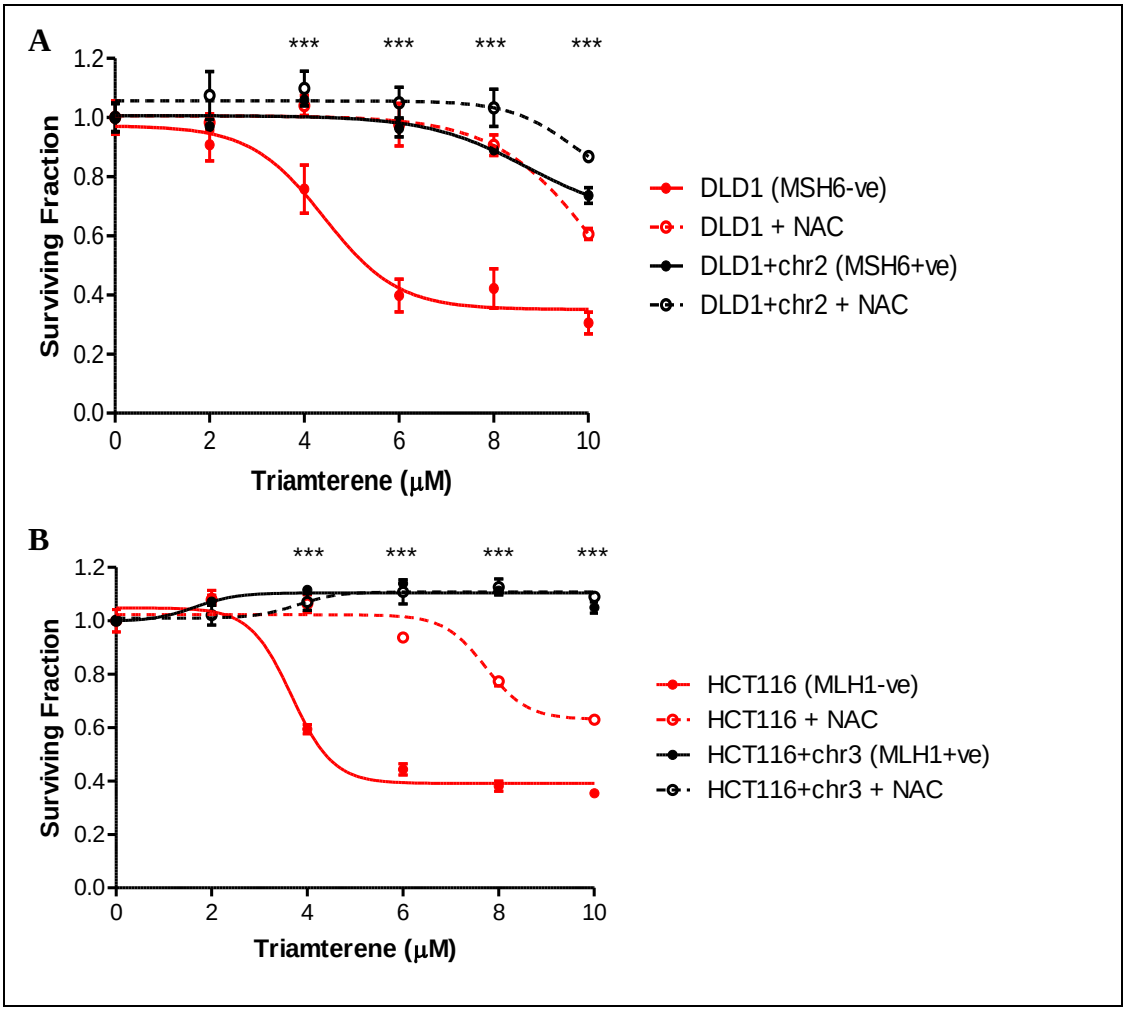

Figure 47: The Triamterene-induced synthetic lethality can be rescued by the addition of the ROS scavenger, NAC

A, B: Cells were treated with increasing concentrations of Triamterene (0, 2, 4, 6, 8 and 10 μM) alone or in combination with 1 mg/mL NAC. After 4 days treatment, cell viability was measured by ATP-luminescence assay. Experiments were carried out in triplicate and error bars represent SEM. P-values derived from 2way ANOVA (*** $p < 0.001$).

2.3 Thymidylate synthase expression is required for the Triamterene-induced accumulation of ROS levels in MMR deficient cells

The Triamterene-induced synthetic lethality was by an accumulation of ROS levels in MMR deficient cells. We showed that this synthetic lethality required TS expression. Therefore, we investigated whether TS expression was required for the Triamterene-induced accumulation of ROS levels. DLD1 and DLD1+chr2 cells, transfected with siTS or siCtrl, were treated with 10 µM Triamterene and, ROS levels were measured 48 hrs after treatment (Figure 48A). As expected, we observed an increase in ROS levels upon Triamterene treatment specifically in the DLD1 cells transfected with the siCtrl. However, in the TS-silenced DLD1 cells treated with Triamterene, we observed no increase in ROS levels. These results suggest a TS dependent-accumulation of ROS levels upon Triamterene treatment in MMR deficient cells. To further validate these results, we repeated the same experiment in the U251 and U251.TR3 matched paired cell lines (Figure 48B). Significantly, we also observed no increase in ROS levels upon Triamterene treatment in the cells transfected with siRNA targeting TS. Taken together, these results suggest that Triamterene is synthetically lethal in MMR deficient cells through the accumulation of ROS, which requires expression of TS.

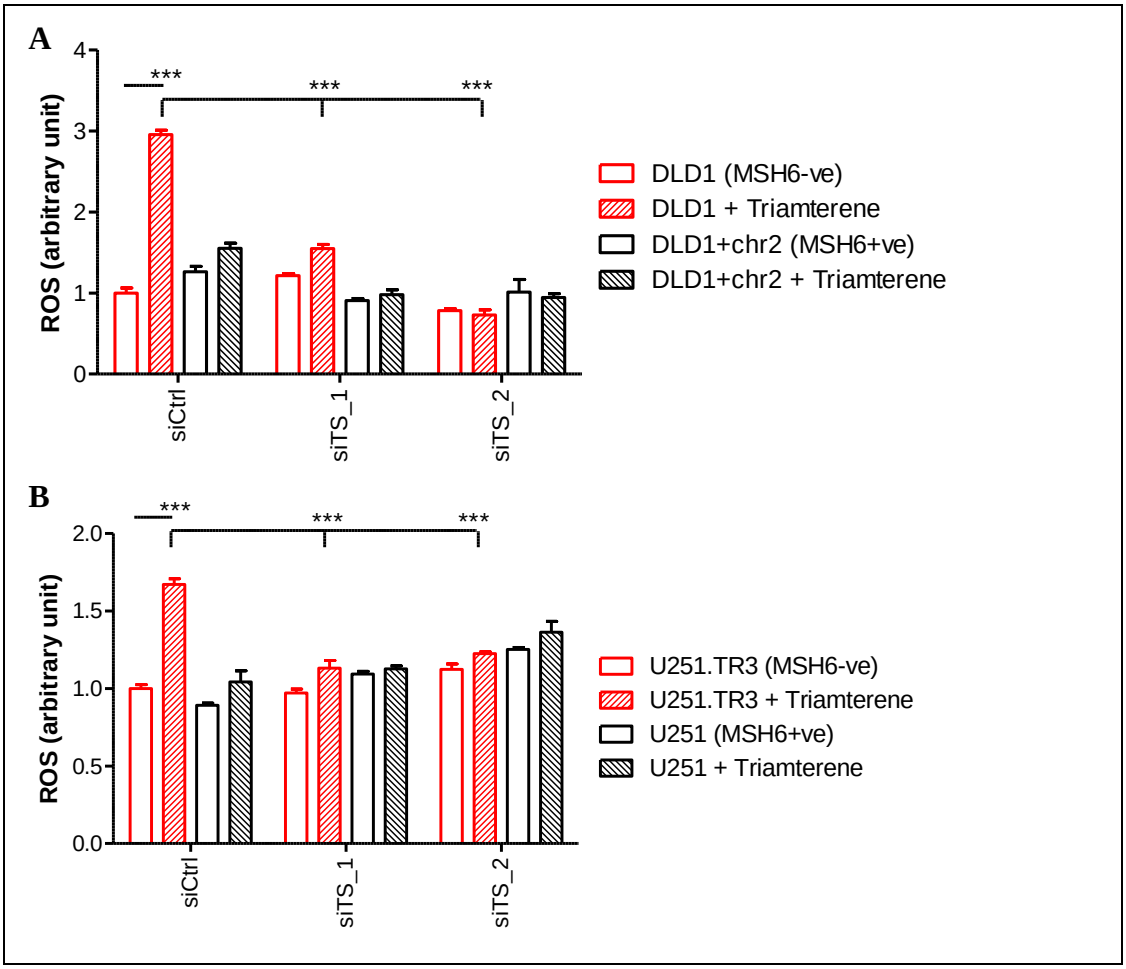

Figure 48: Thymidylate synthase expression is required for Triamterene-induced accumulation of ROS levels in MMR deficient cells

A, B: Cells were transfected in 6-well plates with siCtrl, siPLK1 or 2 x siTS. The following day cells were counted and plated in 2 x 96-well plates and treated with 10 µM Triamterene (in DLD1 and DLD1+chr2 cells) or 20 µM Triamterene (in U251.TR3 and U251 cells). After 48 hrs treatment, cell viability was measured by ATP-luminescence assay and ROS levels were measured by quantifying the conversion of DCFDA into DCF by fluorescence. Fluorescence data were normalized to the cell viability values. Experiments were carried out in triplicate and error bars represent SEM. P-values derived from 1way ANOVA (*** $p < 0.001$).

2.4 Triamterene-induced accumulation of ROS levels induces DNA double strand breaks

We have previously shown that Triamterene is synthetically lethal in MMR deficient cells through the accumulation of ROS. An increase in ROS level can lead to oxidative DNA damage [43]. It is known that an accumulation of oxidative DNA damage is synthetically lethal in MMR deficient cell lines ultimately leading to an accumulation of DSBs triggering cell death [317-319]. We hypothesised that Triamterene was synthetically lethal in MMR deficient cells through an accumulation of DSBs induced by an increase in ROS levels. To assess this hypothesis, we measured γH2AX foci by confocal microscopy after treatment with Triamterene, NAC or a combination of both in DLD1, DLD1+chr2, U251 and U251.TR3 cell lines (Figure 49 & Figure 50). It has been shown previously that the formation of γH2AX foci, which is the localized and focused phosphorylation at Ser 139 of H2A.X at the DSB, is a marker for measuring DSBs [400, 401]. It can be measured by confocal microscopy by counting the proportion of cells with more than 5 foci in the nucleus. Cells with a pan-nuclear staining of γH2AX rather than specific γH2AX foci, may represent apoptotic cells due to DNA fragmentation during apoptosis [402]. Therefore cells with pan-nuclear γH2AX are not counted as γH2AX positive cells. We treated DLD1 and DLD1+chr2 cells with either DMSO, 10 µM Triamterene, 10 mg/mL NAC or a combination of 10 µM Triamterene and 10 mg/mL NAC. After 48 hrs we observed a significant increase in γH2AX foci formation and a low pan-genomic γH2AX staining in DLD1 and DLD1+chr2 cells lines (Figure 49). We observed that 50 % DLD1 cells treated with Triamterene were positive for γH2AX foci; however, we did not observed an increase in γH2AX foci in DLD1+chr2 treated with Triamterene in comparison with the control. Upon treatment with NAC alone, we observed no difference in γH2AX foci formation, however upon treatment of the DLD1 and DLD1+chr2 cells with a combination treatment of NAC and Triamterene, we observed no increase in γH2AX foci in DLD1 cells. We confirmed these results in the MSH6 matched paired U251 and U251.TR3 cells lines by measuring γH2AX foci formation after 24 hrs treatment (Figure 50).We observed an accumulation of DSBs upon Triamterene treatment in the MSH6 deficient U251.TR3 cells and a rescuing effect of this accumulation with addition of NAC. Taken together, these results suggest that Triamterene treatment

can induce formation of DSBs, due to a TS-dependant ROS accumulation and these DSBs result in the reduced cell viability observed in the MMR deficient cells.

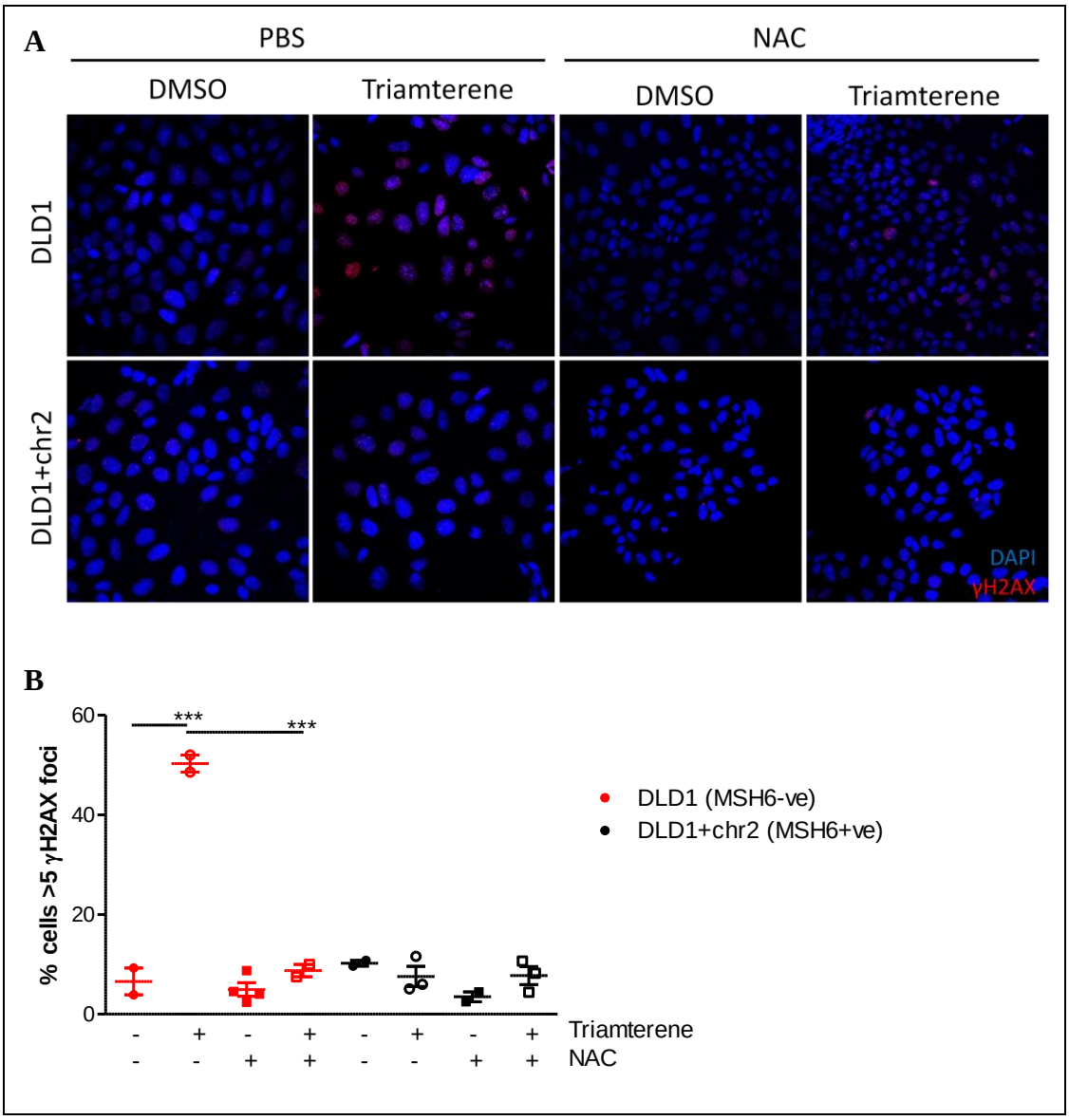

Figure 49: Triamterene induces a ROS-dependent increase in DSBs in the MSH6 deficient DLD1 cells

A, B: Cells were plated on coverslips in 6-well plates and were treated with either DMSO, PBS, 10 mg/mL NAC, 10 µM Triamterene or a combination of 10 µM Triamterene and 10 mg/mL NAC. After 48 hrs, coverslips were stained using γH2AX antibody and DAPI and observed by confocal microscopy (x40 objective). Per condition, a minimum of 100 cells, in a minimum of 3 images, were counted and quantified for γH2AX positive cells (> 5 foci per nucleus) using ImageJ. **A**: Representative images of γH2AX staining. **B:** Graph representing the quantification of cells positive for γH2AX. Experiments were carried out in triplicate and error bars represent SEM. P-values derived from 1way ANOVA (*** $p < 0.001$).

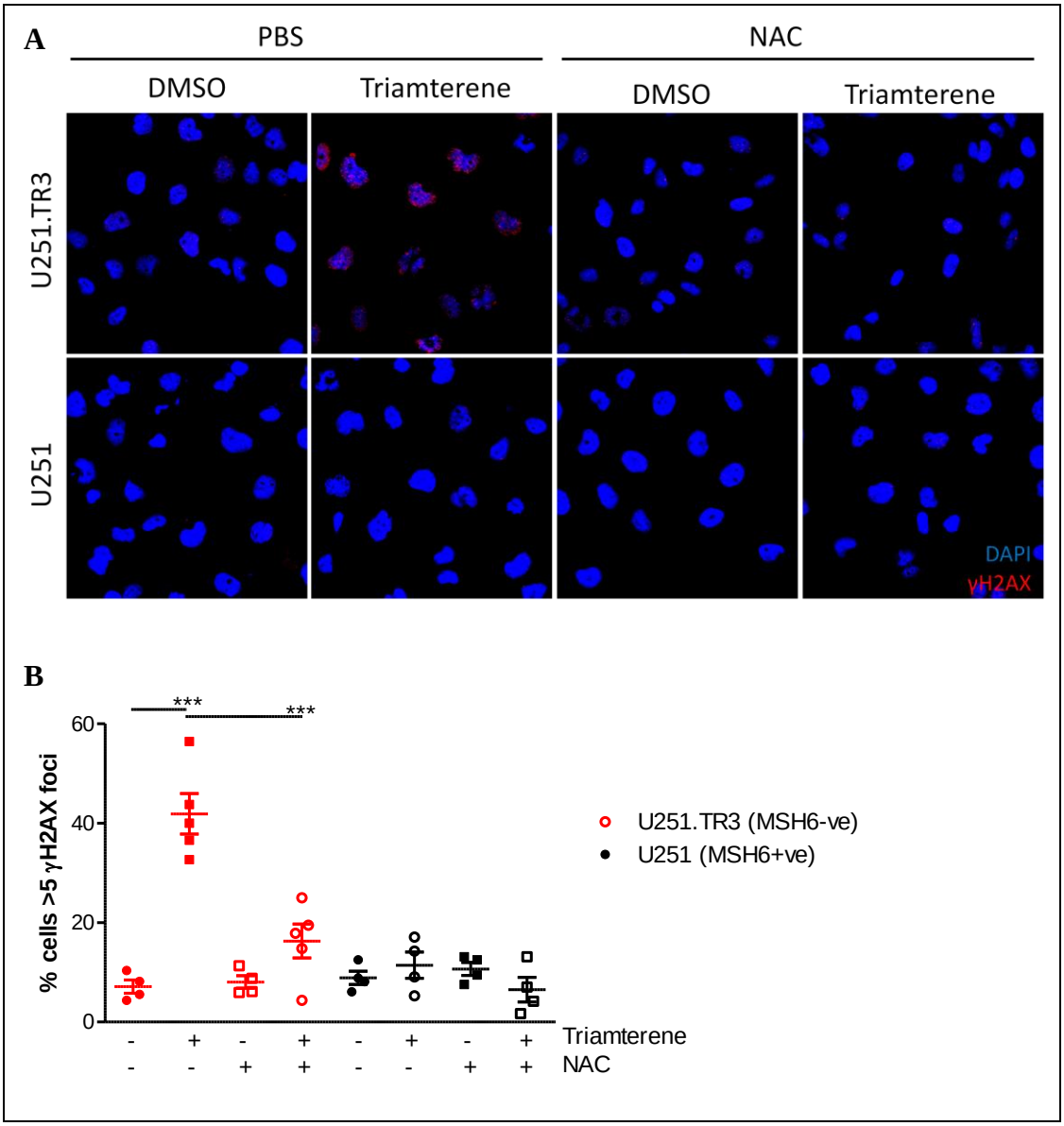

Figure 50: Triamterene induces a ROS-dependent increase in DSBs in the MSH6 deficient U251.TR3 cells

A, B: Cells were plated on coverslips in 6-well plates and were treated with either DMSO, PBS, 10 mg/mL NAC, 20 µM Triamterene or a combination of 20 µM Triamterene and 10 mg/mL NAC. After 24 hrs, coverslips were stained using γH2AX antibody and DAPI and observed by confocal microscopy (40x objective). Per condition, a minimum of 300 cells were counted and quantified for γH2AX positive cells (> 5 foci per nucleus). **A**: Representative images of γH2AX staining. **B:** Graph representing the quantification of cells positive for γH2AX. Experiments were carried out in triplicate and error bars represent SEM. P-values derived from 1way ANOVA (*** $p < 0.001$).

3 Triamterene induces antioxidant response

3.1 Antioxidant response induced by Triamterene treatment

We have observed a Triamterene-induced synthetic lethality in MMR deficient cell lines through an increase in oxidative stress. Oxidative stress can be caused by a greater induction of ROS, a decreased cellular antioxidant response or by a combination of both. To investigate the role of the antioxidant response in Triamterene cytotoxicity, we analysed mRNA expression of the antioxidant response genes, NRF1, NRF2, SOD1 and SOD2 in our MMR matched paired cell lines (Figure 51). NRF1 and NRF2 are two transcription factors, which bind to AREs and regulate genes involved in protecting cells from oxidative damage, such as SOD1 and SOD2. Interestingly, we observed a significant difference in the antioxidant profiles in the two matched-paired cell lines we analysed. We observed a significant decrease in NRF1 and SOD2 mRNA levels in the MSH6 deficient DLD1 cells in comparison to the MSH6 proficient DLD1+chr2 cells (this was not observed in the U251 and U251.TR3 cells). However, we observed a decrease in SOD1 and increase in SOD2 levels in the MSH6 deficient U251.TR3 cell line in comparison to the MSH6 proficient U251 cell line (this was not observed in the DLD1 and DLD1+chr2 cells). These results potentially suggest cell line specific antioxidant responses. However, we consistently observed, in both MMR deficient and proficient matched-paired cell lines, an up-regulation of NRF2 levels upon Triamterene treatment in the MSH6 deficient cell lines compared to their paired MSH6 proficient cell lines. Taken together, our results suggest a Triamterene mediated NRF2 up-regulation in the MSH6 deficient cell lines.

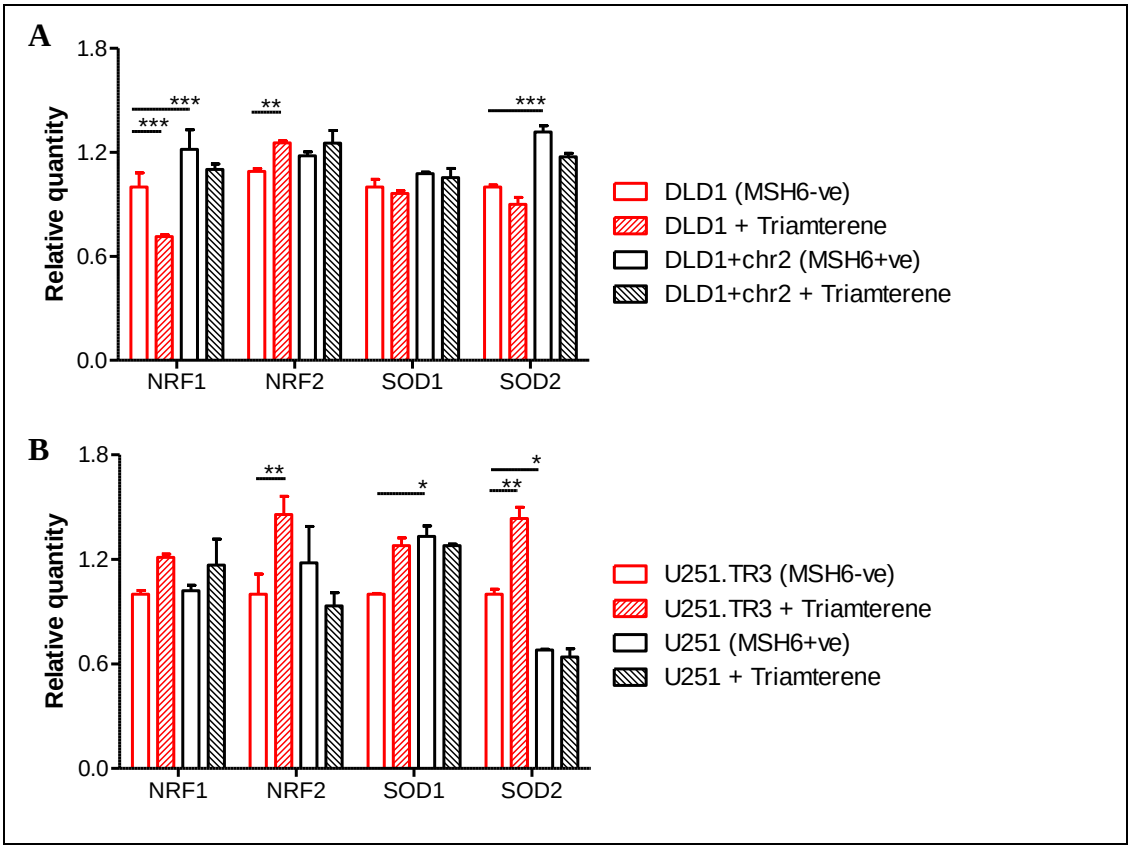

Figure 51: Antioxidant response induced by Triamterene treatment

A, B: Cells were plated in 6-well plates and treated with either DMSO or 10 µM Triamterene (in DLD1 and DLD1+chr2 cells) or 20 µM Triamterene (in U251.TR3 and U251 cells). After 48 hrs treatment, RNA was extracted and measured by RT-qPCR using NRF1, NRF2, SOD1 and SOD2 primers. Data were normalized in relative quantity to GAPDH mRNA level. Experiments were carried out in triplicates and error bars represent SEM. P-values derived from 1way ANOVA (* $p < 0.05$, ** $p < 0.01$, *** $p < 0.001$).

3.2 Thymidylate synthase regulates NRF2 expression

We previously showed that the Triamterene mediated increase in ROS levels required TS expression. We next investigated whether TS expression was also required for the up-regulation of NRF2 mRNA levels observed in MSH6 deficient cells. To investigate this hypothesis, we silenced TS in our cells, followed by 48 hrs treatment with 10 μM Triamterene (in DLD1 and DLD1+chr2 cells) or 20 μM Triamterene (in U251.TR3 and U251 cells), and measured NRF2 mRNA levels (Figure 53). We observed similar results in the DLD1 and DLD1+chr2 and in the U251 and U251.TR3 matched paired cell lines. As expected, we observed an up-regulation of NRF2 in the MSH6 deficient cell lines upon Triamterene treatment. We observed an increase in NRF2 mRNA level in the TS-silenced cell lines compared to the siCtrl transfected cells, regardless of treatment and MMR status. Interestingly, silencing TS further increased the Triamterene mediated up-regulation of NRF2. Taken together, our results suggest a TS dependent regulation of NRF2 that may be the mechanism for TS requirement in Triamterene MSH6 specific cytotoxicity.

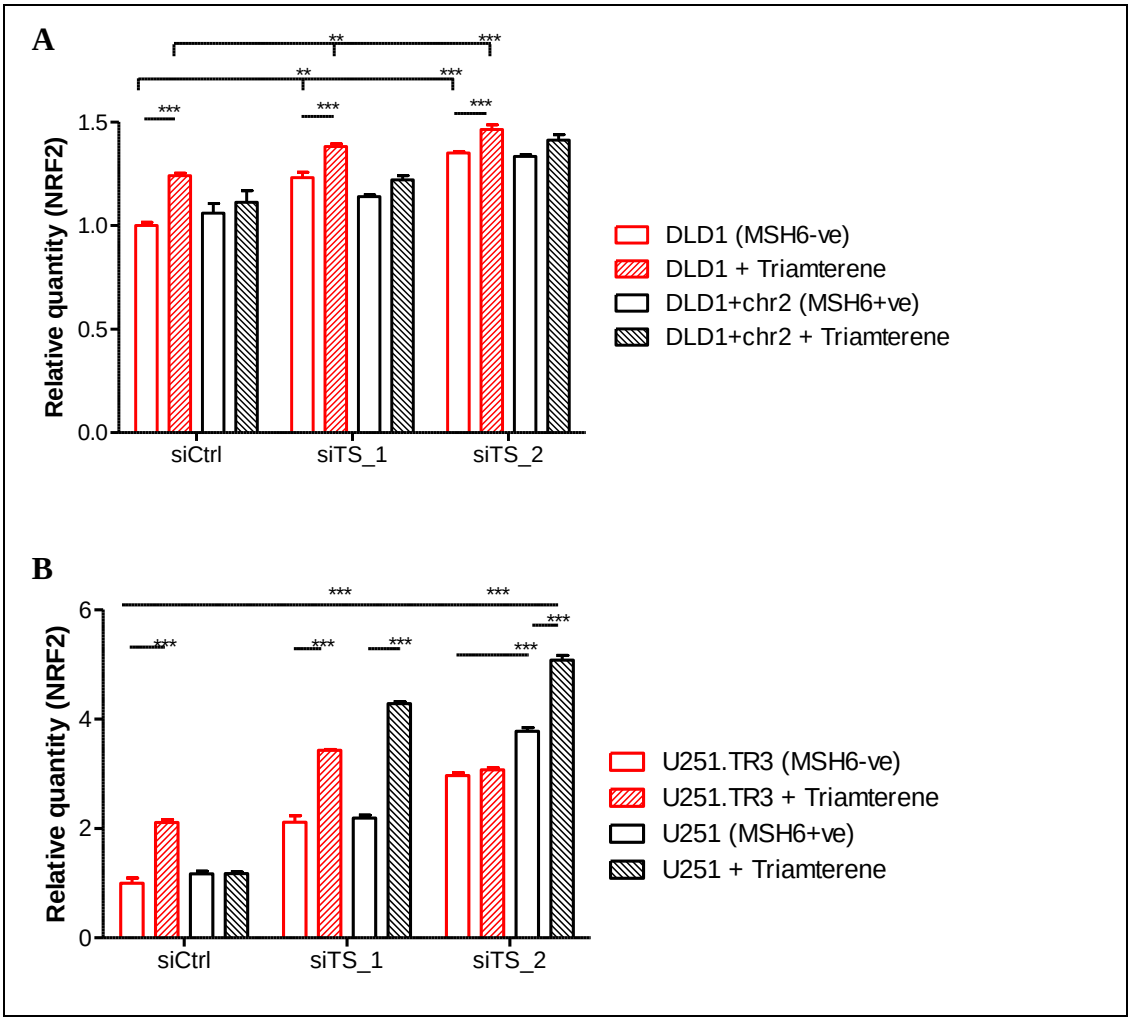

Figure 52: Thymidylate synthase regulates NRF2 mRNA expression

A, B: Cells were plated in 6-well plates and transfected with siCtrl, siPLK1 or siTS. The following day, cells were plated in 12-well plates and were treated with either DMSO or Triamterene (10 µM in DLD1 and DLD1+chr2 cells or 20 µM in U251 and U251.TR3 cells). After 48 hrs of treatment, RNA was extracted and measured by RT-qPCR using NRF2 primers. Data were normalized in relative quantity to GAPDH mRNA level. Experiments were carried out in triplicates and error bars represent SEM. P-values derived from 1way ANOVA (** $p < 0.01$, *** $p < 0.001$).

3.3 Triamterene and the Antioxidant response

We showed that treatment with Triamterene and silencing TS could induce an increase in NRF2 mRNA expression. NRF2, when active, binds to the AREs in the promoter region of many antioxidant genes and initiates their transcription [29-31]. To analyse the functional cellular consequences of increased NRF2 levels, we transfected U251.TR3 and U251 cells with luciferase reporter constructs that measures the transcriptional activity of NRF1 and NRF2 through binding to AREs, and consequently the activity of the cellular antioxidant pathway. The luciferase reporter constructs are a firefly luciferase construct regulated by ARE and a renilla luciferase construct regulated by CMV, to measure cell viability. We used a positive control to measure transfection efficiency. It is a firefly luciferase construct and a renilla luciferase both regulated by CMV (Table 10). We transfected our cells with either control or TS siRNA, followed by the ARE luciferase reporter transfection and treatment with 20 μM Triamterene (Figure 15). After 48 hrs treatment, we measured by luminescence, the activity of the antioxidant pathway. Firefly luciferase measurements were normalized to the renilla luciferase data (cell viability) and to the positive control (transfection efficacy) (Figure 53). We observed a significant higher antioxidant response in the MSH6 deficient U251.TR3 cells compared to the MSH6 proficient U251 cells which increased upon Triamterene treatment. These results were not expected as we did not observe a significant difference in ROS levels and NRF1 and NRF2 mRNA levels in U251 compared to U251.TR3 cell lines. This suggested a higher basal oxidative stress in the MMR deficient cells. We showed previously that Triamterene treatment induced an up-regulation of NRF2 mRNA expression in MMR deficient cell lines. We observed here, that Triamterene treatment highly increased the antioxidant pathway in the MSH6 deficient U251.TR3 cells specifically; suggesting that the Triamterene-induced up-regulation of NRF2 can trigger an increase in the antioxidant response. However, the up-regulation of NRF2 observed upon TS silencing was not correlated with an increase in antioxidant response. Significantly, we observed a significant decrease in antioxidant response in TS silenced cells treated with Triamterene compared to the siCtrl transfected cells treated with Triamterene. Taken together, these results indicate that there was an increase in the antioxidant response in the MSH6 deficient cells compared to the MSH6 proficient cells. Upon Triamterene treatment we observed a greater increase

in the antioxidant response in the MSH6 deficient cells, which is significantly decreased upon silencing of TS. These results further suggest that Triamterene is cytotoxic in MSH6 deficient cells through an increased oxidative stress.

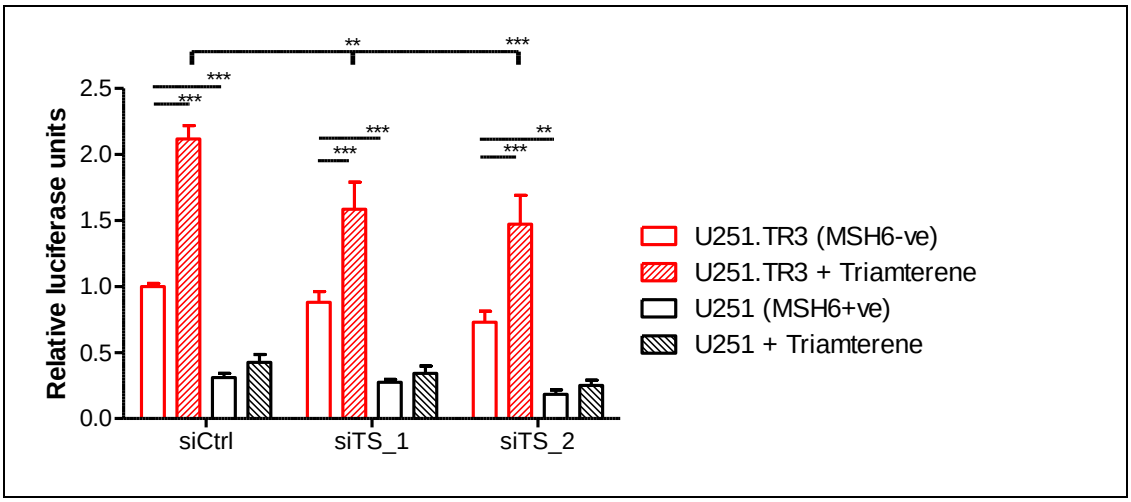

Figure 53: Increased antioxidant response in MMR deficient cells
Cells were plated in 6-well plates and transfected with siCtrl, siPLK1 or siTS. The following day, cells were plated in 96-well plates and were transfected with the luciferase reporter construct and then treated with either DMSO or 20 µM Triamterene. After 48 hrs treatment, the luminescence was measured and normalized to the controls. Experiments were carried out in triplicates and error bars represent SEM. P-values derived from a 1way ANOVA (** $p < 0.01$, ** $p < 0.001$).

3.4 Antioxidant response *in vivo*

We have previously shown that Triamterene treatment induced an up-regulation of NRF2 mRNA level and an increased antioxidant response *in vitro* in MMR deficient cells. We also observed a Triamterene-induced synthetic lethality in MSH6 deficient xenografted tumours *in vivo*. In order to further investigate the role for the antioxidant response in Triamterene synthetic lethality in MMR deficiency *in vivo*, we measured NRF1, NRF2, SOD1 and SOD2 mRNA levels in the harvested xenografted MSH6 deficient and proficient tumours (Figure 54). We previously observed *in vitro* a decrease in NRF1 and SOD2 in DLD1 cells compared to DLD1+chr2 cells and a Triamterene-induced decrease in NRF1 and increase in NRF2 mRNA levels in the DLD1 cells specifically (Figure 51A). In this experiment, we observed a minor, although significant, decrease in NRF1 expression but no difference in SOD2 expression in DLD1 compared to the DLD1+chr2 xenografted

tumours (Figure 54A, D). We did not observe a Triamterene-induced regulation of NRF1, NRF2, SOD1 or SOD2 levels in the xenografted tumours (Figure 54). Taken together, these results validated the differential regulation of NRF1 levels observed *in vitro* in the MSH6 proficient and deficient cell lines. However, these results did not validate the Triamterene mediated regulation of NRF1 and NRF2 in the MSH6 deficient cells observed *in vitro*. Taken together, these results do not confirm the regulation of the antioxidant response upon Triamterene treatment in MSH6 deficiency *in vivo*. However, we could speculate the antioxidant response was an early mechanism of protection upon Triamterene treatment. The tumours were harvested when their sizes reached their maximum which therefore could explain the absence of NRF1/NRF2 regulation upon Triamterene in the xenografted tumours.

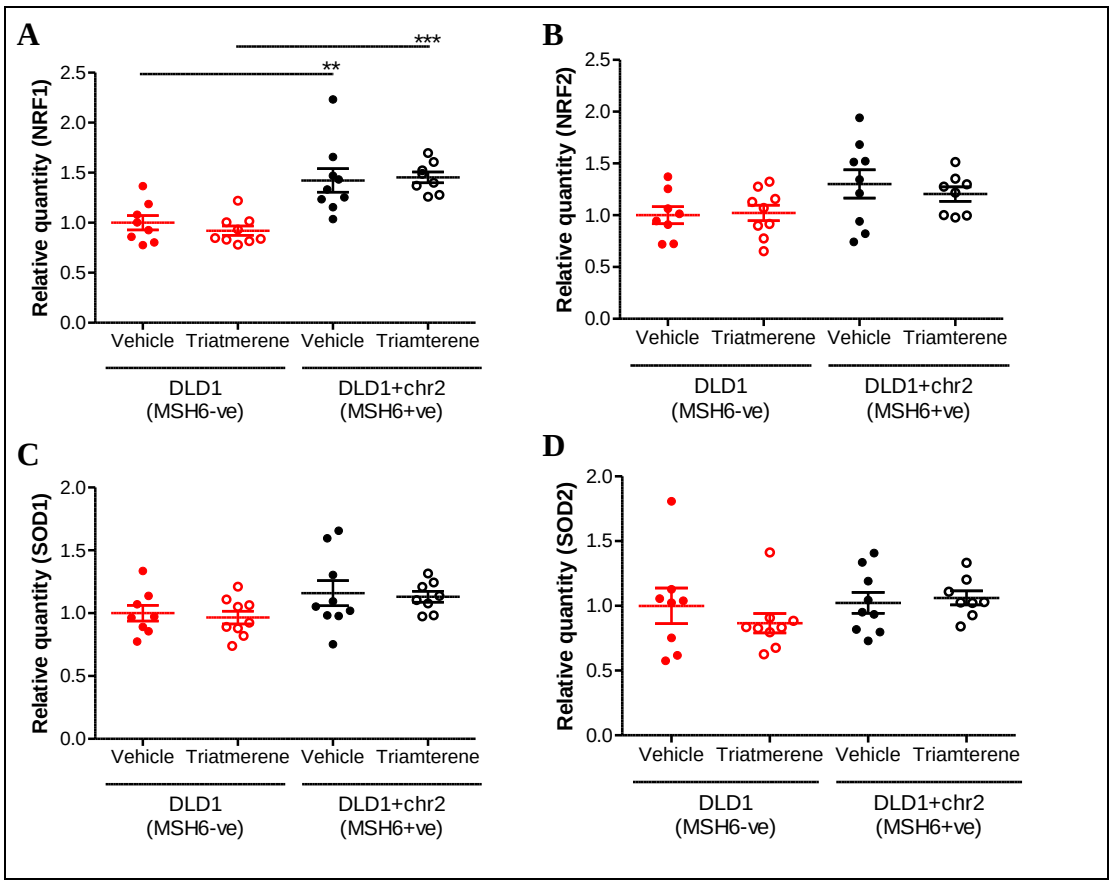

Figure 54: Antioxidant response *in vivo*

A-D: RNA was extracted from the harvested xenografted tumours and measured by RT-qPCR using NRF1, NRF2, SOD1 and SOD2 primers. Data were normalized in relative quantity to GAPDH mRNA level. Error bars represent SEM. P-values derived from a 1way ANOVA test (** $p < 0.01$; *** $p < 0.001$).

Our data showed that Triamterene is synthetically lethal in MMR deficient cells through its antifolate activity. Triamterene can induce a TS-dependent increase in ROS levels that triggers oxidative stress and ultimately lethal DSBs in the MMR deficient cell lines specifically. We also identified a Triamterene mediated up-regulation of NRF2 expression and an increase in the antioxidant response in the absence of MMR. We observed that TS silencing could rescue the cells from Triamterene cytotoxicity by inhibiting the increase in ROS levels and in antioxidant response, and also by up-regulating NRF2 expression (Figure 55). Therefore our data suggest a potential role for the antioxidant response in Triamterene cytotoxicity.

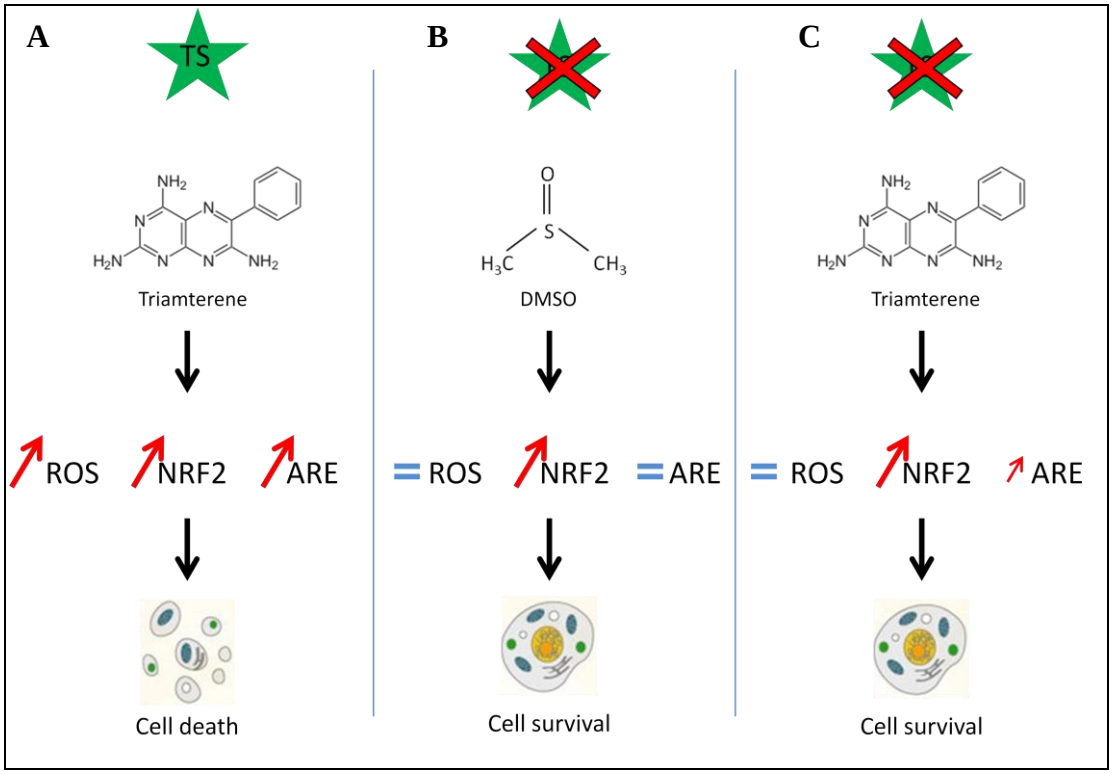

Figure 55: Effect of Triamterene treatment and/or TS silencing on ROS levels, NRF2 mRNA levels and antioxidant response in the U251.TR3 MSH6 deficient cells

A: Triamterene treatment in cells expressing TS leaded to cell death. It induced an increase in ROS and an increase in NRF2 mRNA levels leading to an increase in antioxidant response. **B:** Silencing TS did not lead to cell death. It increased increases NRF2 mRNA level but did not modulate ROS levels and the antioxidant response. **C:** Triamterene treatment in TS-silenced cells was not toxic for the cells. It induced no increase in ROS levels and an increase in NRF2 levels as well as a small increase in antioxidant response.

Chapter 3: High-throughput siRNA screen to identify synthetic lethal interactions with MSH6 deficiency

1 High-throughput siRNA screen

In order to identify genes and pathways that are synthetically lethal with MMR deficiency we carried out an siRNA screen on the DLD1 and DLD1+chr2 cells. We have chosen to carry out an siRNA screen targeting 779 siRNAs targeting protein kinases and kinase-associated genes successfully used previously. This library contains SMARTpool siRNAs which are a pool of 4 individual siRNAs targeting one gene of interest [318, 403]. Targeting kinases using the siKinome library is relevant to drug discovery as the kinase superfamily plays a key role in many biological processes and has an inherent pharmacological tractability. We carried out a series of optimisation experiments to determine the appropriate protocol to perform the siRNA screen. We tested different cell density (1 000, 2 000 and 3 000 cells per well) and two different TR (lipofectamine 2000 and RNAiMAX) (Figure 56). We validated the following protocol: day 1, seed 2 000 cells per well; day 2, transfect cells with RNAiMAX TR; day 3, change the media; day 6, measure cell viability with an ATP-luminescence assay (Figure 14). Transfection controls for each experiment were included which included transfecting cells with a non-targeting siCtrl and siRNA targeting PLK1. The cell viability of cells transfected with siCtrl was compared to the cells grown in media alone to validate that the transfection itself did not affect cell viability. Transfection with siPLK1 is used as a positive transfection control. PLK1 is a polo-like kinase implicated in mitosis and apoptosis [404], its silencing causes cell death in most cell lines.

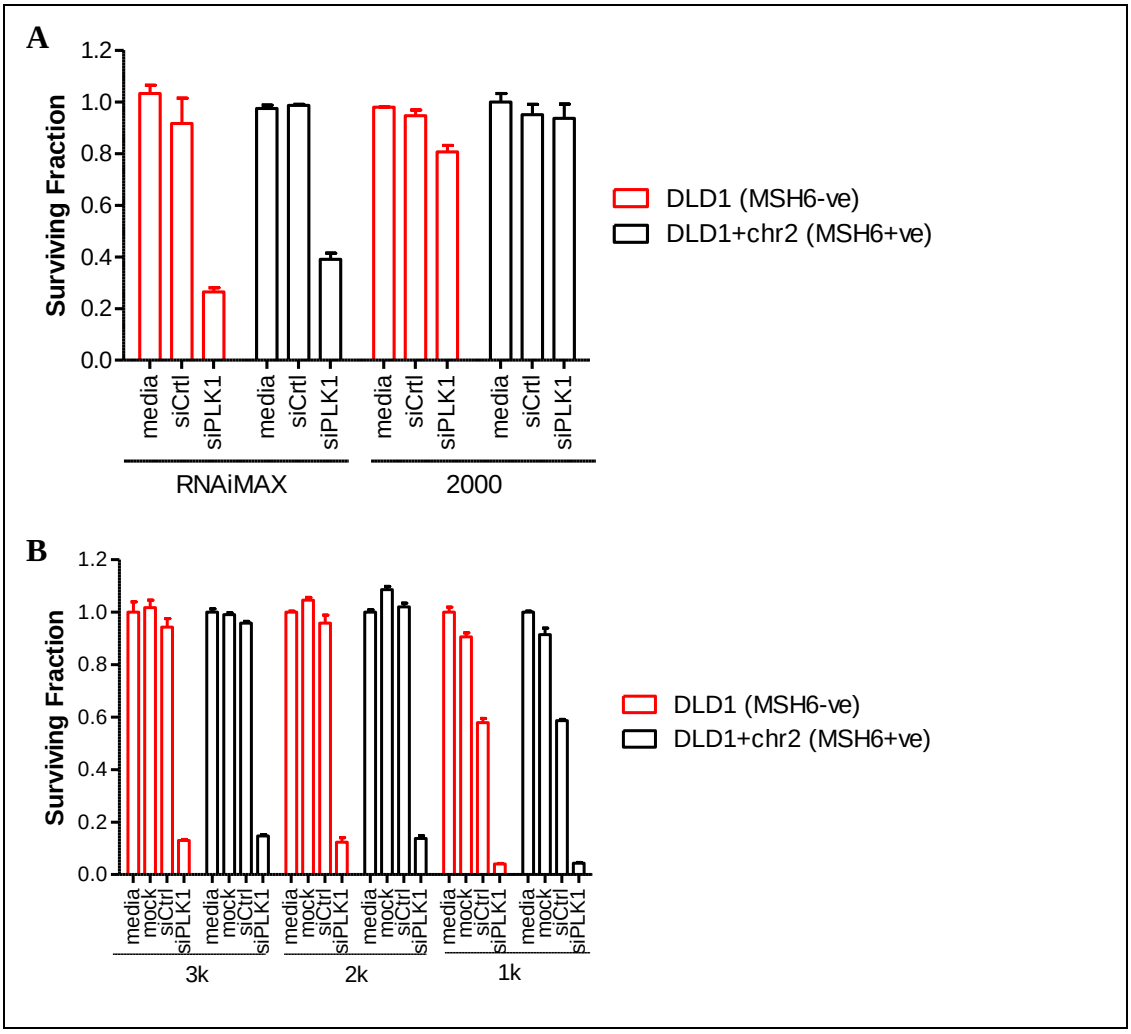

Figure 56: Optimization of the siRNA transfection protocol

A: 3 000 cells were seeded in 96-well plates. The following day, cells were transfected with either lipofectamine 2000 or RNAiMAX and the media was changed after 24 hrs. After 4 days transfection, we measured ATP-luminescence assay. **B:** Different densities were plated in 96-well plates (1 000, 2 000 and 3 000 cells/well). The following day, cells were transfected with lipofectamine RNAiMAX and the media was changed after 24 hrs. After 4 days transfection we measured ATP-luminescence assay. Experiments were carried out in triplicates and error bars represent SEM.

After an additional validation experiment for the protocol to carry out a high-throughput siRNA screen (Figure 57A), 1 800 DLD1 and DLD1+chr2 cells were plated in 9*96-well plates and transfected with the siRNA library. We included 6x siCtrl and 4x siPLK1 on each plate for transfection controls, and to allow us to determine the transfection efficiency across all plates and how it differed. After 24 hrs the media was changed and after 5 days transfection, cell viability was

measured by ATP luminescence assay. The cell viability results were normalized onto ΔZ-scores (Figure 57B). Luminescence readings from each well were log transformed and normalized according to the median signal on each plate and then standardized by use of a Z-score statistic, using the MAD to estimate the variation in each screen (Figure 13). Z-score analysis has been described as a reliable method to analyse high-throughput screens [356]. The Z-score represents the magnitude of difference between one siRNA compared to the rest of the screen. This is based on the assumption of a normal distribution of cell viability upon siRNA library transfection in a specific cell line. The standardization and normalization of the data in each cell line allow us to compare the 2 cell lines using ΔZ-scores. Negative ΔZ-scores represent genes synthetically lethal in the MSH6 deficient DLD1 cells compared to the MSH6 proficient DLD1+chr2 cells. We enforced a threshold of hit identification based ΔZ-scores lower than -1.5. Based on this threshold and on their known function, we selected 5 hit genes from the siRNA screen results for further validation. These include Janus kinase 2 (JAK2), Copine-III (CPNE3), RIOK2, 1,3,4,5,6-pentakisphosphate 2-kinase (IPPK) and AURKA (Table 14).

JAK2 is a non-receptor tyrosine kinase and intracellular signalling effectors of cytokine receptors. JAK2 is involved in a range of processes such as cell growth, differentiation or histone modifications. Previous preclinical and clinical reports have described the inhibition of JAK2 as a promising inhibitor of tumour growth [405-408]. Ruxolitinib is a FDA-approved JAK2 inhibitor used for psoriasis, myelofibrosis and rheumatoid arthritis treatment [409]. No report has associated JAK2 with MMR pathway. CPNE3 is a calcium-dependent phospholipid-binding protein which may function in membrane trafficking. It has been identified to promote cell migration and invasion in lung cancer and in breast cancer [410, 411]. RIOK2 is part of the RIO kinase family required for ribosome biogenesis and cell cycle progression [412]. Inhibition of RIOK2 accelerates mitotic progression [413]. RIOK2 silencing results in Akt pathway inhibition and cell cycle arrest and apoptosis in glioblastoma cells [414]. IPPK forms inositol-1,2,3,4,5,6-hexakisphosphate (InsP6) by phosphorylation [415]. InsP6 has various functions such as stimulation of DNA repair, mRNA export and endocytosis. For example, InsP6 binds to KU70 protein implicated in NHEJ in order to increase NHEJ activity [416]. The anticancer activity of InsP6 has been shown to be through a G1 phase arrest of the cell cycle

[417]. AURKA is a member of the Aurora kinase family. AURKA has a role in mitosis by maintaining the microtubule assembly; in other phases of the cell cycle and in HR by inhibiting BRCA1/2 and RAD51 [418]. AURKA is significantly up-regulated in solid tumours including CRC, breast, ovarian neuroblastoma and cervical cancer [419, 420]. AURKA inhibitors have been identified as potential anticancer agents [421, 422].

Although all the selected kinases have been described to play a role in cancer, only AURKA has been described to play a role in CRC onset in LS [333]. However, this role has not been confirmed in another study [335]. Therefore, our selected hit genes might be promising novel synthetic lethal kinases for the treatment of MMR deficiency.

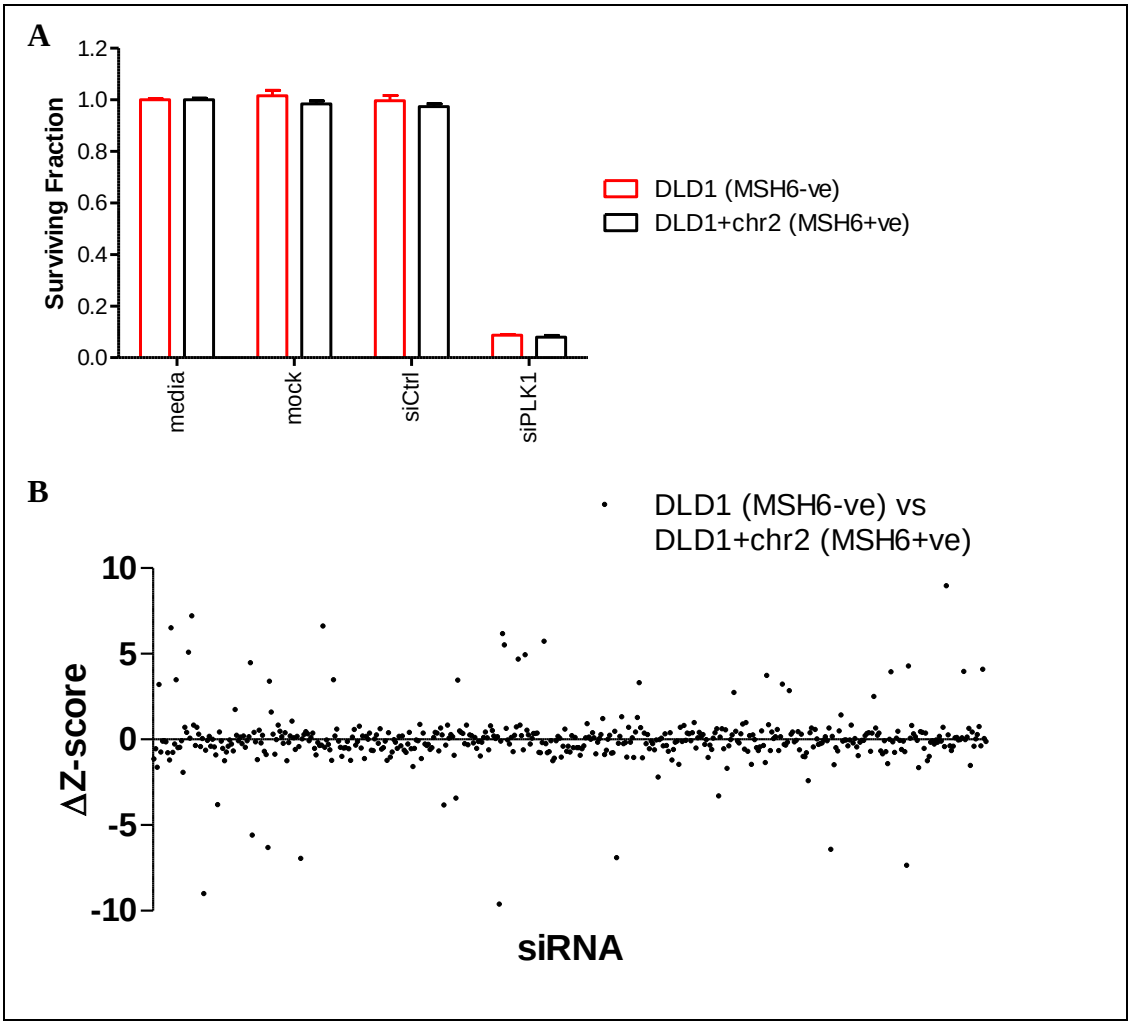

Figure 57: siRNAs screen validation and results

A: 1 800 cells were transfected with mock, siCtrl or siPLK1 and the media was replaced 24 hrs after transfection. Cell viability was measured, after 5 days transfection, by ATP-luminescence assay. Experiments were carried out in triplicate and error bars represent SEM. **B:** Dotplot representing the ΔZ-score for each siRNA of the library. ΔZ = 0: no difference in cytotoxicity between DLD1 and DLD1+chr2 cells, ΔZ > 0: DLD1+chr2 are more sensitive to the silencing than DLD1 cells and ΔZ < 0: DLD1 are more sensitive to the silencing than the DLD1+chr2 cells.

Gene	ΔZ-score	Role	Reference
JAK2	-9.6118	JAK/STAT pathway	[423]
CPNE3	-6.9372	membrane trafficking	[411]
RIOK2	-6.3989	cell cycle, mitotic progression	[413, 414]
IPPK	-3.8040	DNA repair, endocytosis, mRNA export, NHEJ	[415]
AURKA	-1.9110	microtubule formation, cell cycle	[424-426]

Table 14: siRNAs selected from the high-throughput siRNA screen

2 High-throughput siRNA screen validation

The performed siRNA screen allowed us to select 5 potential synthetic lethal genes in the MSH6 deficient DLD1 cells. In order to validate them, we carried out experiments in DLD1 and DLD1+chr2 cells using 5 siRNAs per selected gene (the SMARTPool siRNA originally used in the screen and the 4 individual siRNAs deconvoluted from the SMARTpool siRNA). As shown in Figure 58A, AURKA silencing showed, in 3 out of the 5 siRNA, to be selectively lethal in DLD1 cells compared to DLD1+chr2 cells. Only one siRNA targeting CPNE3, JAK2 and IPPK showed higher toxicity in DLD1 compared to DLD1+chr2 cells. Surprisingly, RIOK2 silencing showed higher toxicity in DLD1+chr2 compared to DLD1 cells with all siRNAs. Our experiments and validation may be limited due the fact that we performed the siRNA screen only once, and there was only one well per targeted gene in the library, which could explain the difference observed in the siRNA screen compared to the validation experiments. Our results however validate the cytotoxicity of silencing AURKA in the MSH6 deficient DLD1 cells compared to the MSH6 proficient DLD1+chr2 cells.

To determine whether this synthetic lethal effect was cell line specific to the DLD1 cells, we transfected the matched paired U251 and U251.TR3 cell lines, proficient and deficient in MSH6 respectively with siRNAs targeting the 5 selected kinases (Figure 58B). We measured the cell viability after 5 days transfection. The results in U251 and U251.TR3 cells suggest no selective cytotoxicity of siCPNE3, siIPPK and siJAK2 in the MSH6 deficient U251.TR3 cells compared to the MSH6 proficient U521 cells. We previously showed a significant increased selectivity for siRIOK2 in the MSH6 proficient DLD1+chr2 cells, in comparison with the MSH6 deficient DLD1 cells. However, this observation was not validated in the MSH6 proficient U251 cells. Silencing of AURKA gene showed a synthetic lethality in the MSH6 deficient DLD1 cells in comparison with the DLD1+chr2 cells and interestingly, our experiments in the U251 and U251.TR3 cells suggest comparable results. The siAURKA_pool, siAURKA_2 and siAURKA_4 showed higher cytotoxicity in the MSH6 deficient U251.TR3 cells, compared to the MSH6 proficient U251 cells, as observed in the DLD1 compared to the DLD1+chr2 cells (Figure 58A & B). These results suggest a synthetic lethal relationship between AURKA and MSH6.

To further validate whether this synthetic lethal interaction was due to MSH6 deficiency or to MMR deficiency in general, we transfected the MLH1 deficient HCT116 and MLH1 proficient HCT116+chr3 cell lines with siRNA targeting AURKA (Figure 58C). We did not observe any cytotoxic difference upon AURKA silencing in the MLH1 deficient and proficient cells. These results suggest no synthetic lethality upon AURKA silencing in the MLH1 deficient cell lines. Therefore perhaps AURKA inhibition is specific to MSH6 loss rather than MMR deficiency in general. Further experiments are required to determine whether this is truly the case as, due to lack of time, these experiments were only performed in triplicate, once. Further experiments are also required to determine whether AURKA silencing can cause synthetic lethality in cells with mutations in other members of the MMR pathway such as MSH2 and PMS2.

Taken together, the validation experiments, carried out in the different MMR proficient and deficient matched paired cell lines, suggest AURKA as a potential synthetic lethal interactor with MSH6 loss, specifically. However, further experiments in the U251, U251.TR3, HCT116 and HCT116+chr3 cells are necessary to confirm these observations.

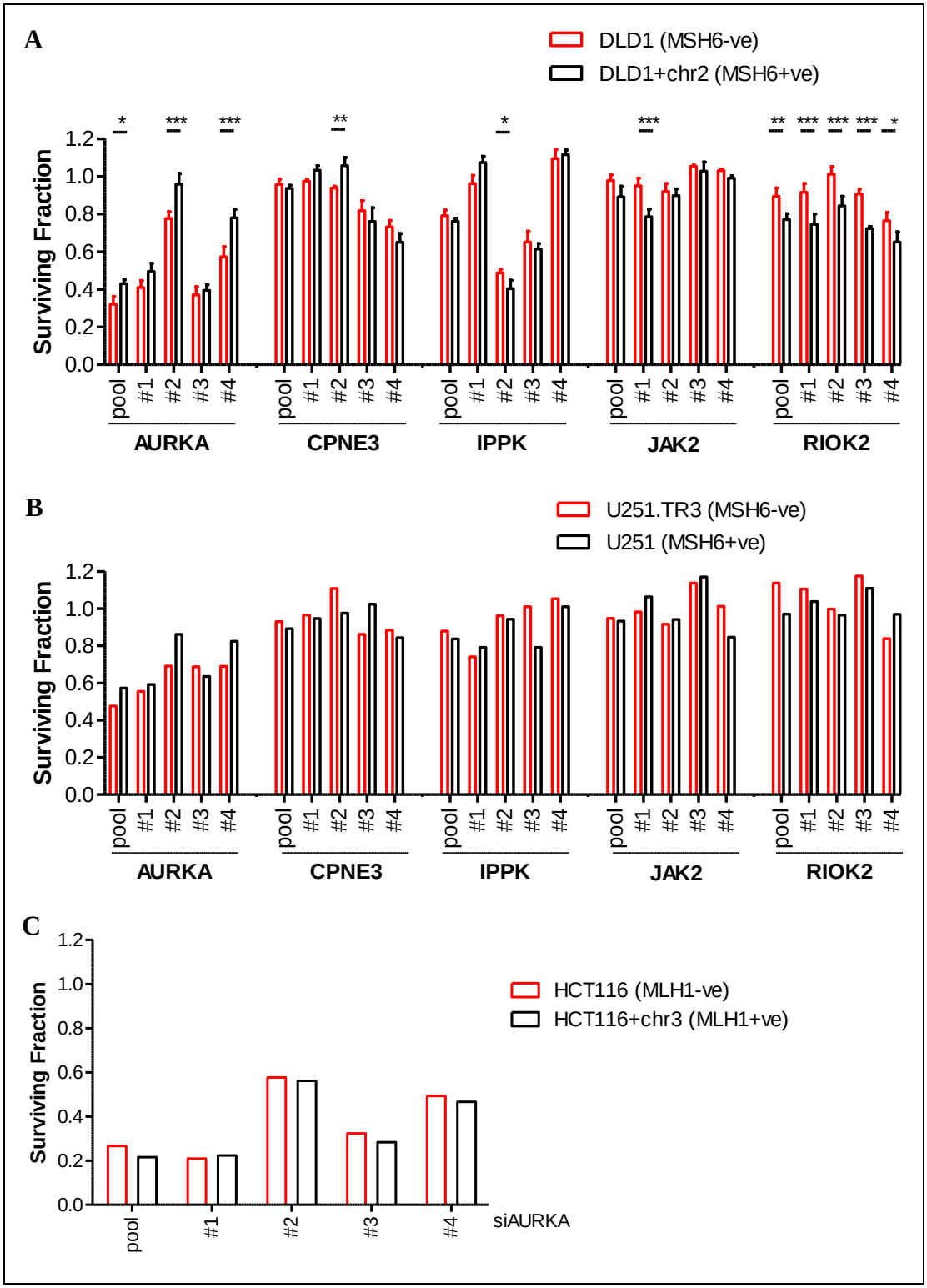

Figure 58: High-throughput siRNA screen validation

A-C: Cells were transfected with siCtrl, siPLK1 and siRNAs targeting the 5 genes selected from the screen and the media was changed after 24 hrs. After 5 days transfection, cell viability was measured by ATP-luminescence assay. **A:** The graph represents the mean of 3 independent replicates and error bars represent SEM. P-values derived from 2way ANOVA (* $p < 0.05$, ** $p < 0.01$, *** $p < 0.001$). **B, C:** Graph representative of one replicate. Experiments were carried out only once.

3 AURKA as a potential therapeutic target in MMR deficiency

To investigate the potential synthetic lethal interaction between loss of AURKA and MSH6 deficiency, we treated the MSH6 deficient and proficient cells with increasing concentrations (0, 40, 80, 120, 160 and 200 nM) of the AURKA inhibitor, Alisertib (MLN8237). Alisertib is an AURKA inhibitor currently in phase III clinical trial for treatment of patients with relapsed or refractory peripheral T-cell lymphoma (NCT01482962). This compound has the main advantage to be specifically inhibiting AURKA and not AURKB as it was the case with previous generations of AURKA inhibitors [427, 428]. As shown in Figure 59, we observed a greater and significant cytotoxicity of the increasing concentrations of AURKA inhibitor in the MSH6 deficient cell lines compared to their paired MSH6 proficient cell lines. These results suggest the inhibition AURKA as synthetically lethal in MSH6 deficient cell lines.

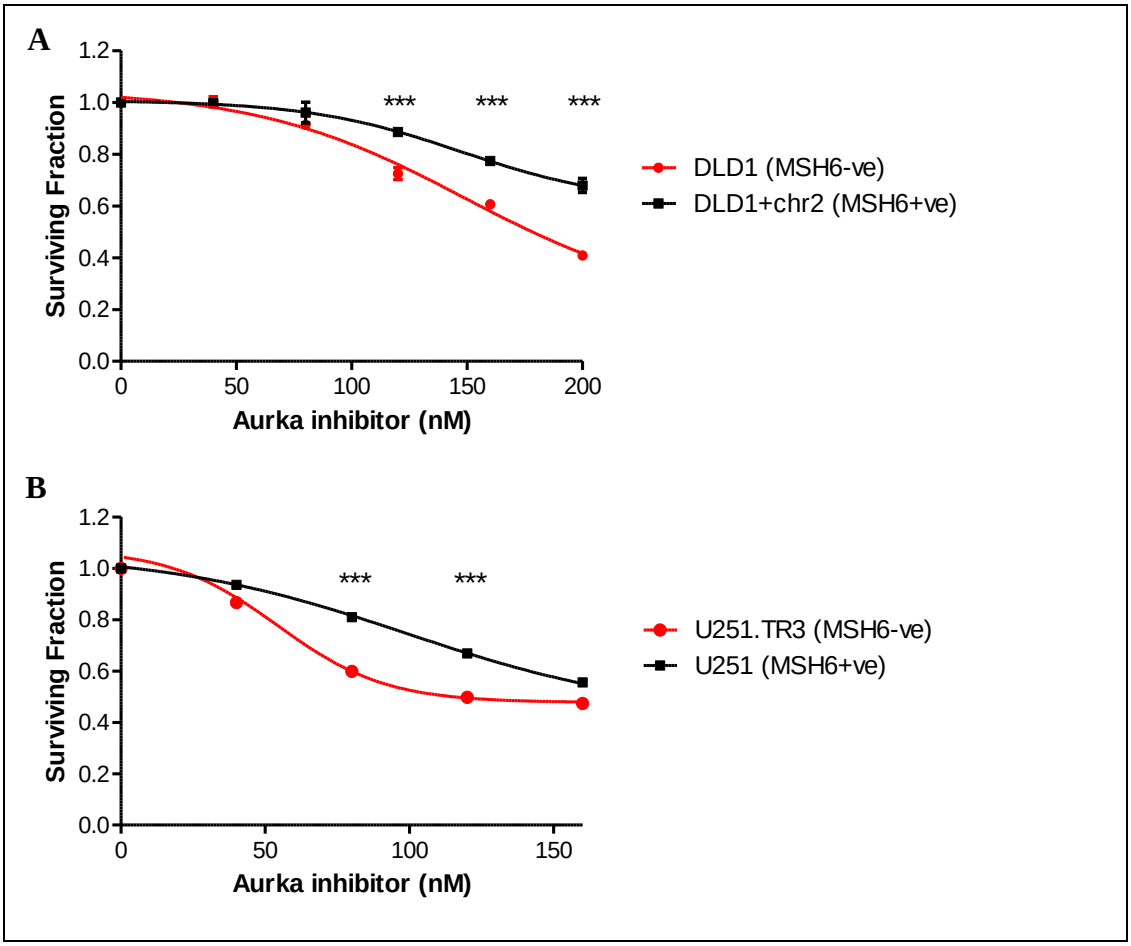

Figure 59: AURKA inhibition as a potential therapeutic target in MSH6 deficiency

A, B: Cells were treated with an increased concentration of the AURKA inhibitor Alisertib. After 4 days treatment, cell viability was measured by ATP-luminescence assay. Experiments were carried out in triplicate and error bars represent SEM. P-values derived from 2way ANOVA (*** $p < 0.001$).

AURKA is part of Aurora kinase family composed of AURKA, AURKB and AURKC. Aurora kinase family is responsible for microtubule formation. AURKA is required for the microtubule organisation, AURKB functions in the attachment of the microtubules to the centromere and AURKC function is not known [426]. AURKB was not present in the high-throughput screen data and AURKC was not synthetically lethal with MSH6 deficiency (ΔZ-score = 0.7062). We have previously mentioned the potential role for AURKA and Cyclin D1 in the onset for CRC in LS (see the introduction section 3.2.3.4) [333]. The siRNA library used for the screen is composed of kinases therefore there is no siRNA targeting Cyclin D1. The drug library used to carry out the high-throughput compound screen included two

compounds targeting microtubules, Colchicine and Paclitaxel, and one AURKB inhibitor, Hesperidin [429, 430]. Our data from the drug screen suggests that Colchicine and Paclitaxel were cytotoxic in both the MSH6 deficient and proficient cell lines and Hesperidin was not cytotoxic in any of the cells (Table 15). In the compound screen, compounds were used at a fixed concentration of 10 µM which might explain the lack of selectivity with these compounds. AURKB was not present in our siRNA screen, and the AURKB inhibitor Hesperidin, did not show cytotoxicity in the compound screen. Therefore, we cannot conclude on a possible synthetic lethality between the other Aurora kinases and MSH6 deficiency. In addition, these compounds, Colchicine and Paclitexel, are not inhibitors of AURKA and they have different mechanisms of action than AURKA inhibition on the microtubules. A synergistic relationship has been published between Alisertib and Paclitaxel in ovarian cancer cells *in vitro* and *in vivo*, and an over-expression of AURKA gene has been observed as a mechanism of resistance to Paclitaxel treatment [425]. These observations suggest complementary mechanism of action of Paclitaxel and Alisertib. Therefore, further experiments are required to deepen our understanding of AURKA as a novel synthetic lethal gene in MSH6 deficiency and/or MMR deficiency.

	DLD1 (MSH6-ve)		**DLD1+chr2 (MSH6+ve)**		
Compound	**Replicate 1**	**Replicate 2**	**Replicate 1**	**Replicate 2**	**Function**
Hesperidin	0.700	2.192	0.331	2.727	AURKB inhibitor
Colchicine	-11.791	-12.425	-10.544	-11.785	Inhibits microtubule assembly
Paclitaxel	-9.099	-6.980	-9.324	-11.353	Stabilises microtubules

Table 15: Z-score results from the high-throughput compound screen

We carried out an siRNA screen in order to identify novel synthetic lethal relationships with MMR deficiency. We identified and validated a potential synthetic lethal interaction between MSH6 deficiency and AURKA inhibition. A role for AURKA has been previously shown in the age of CRC development associated with LS; with a potential difference for MLH1 and MSH2 deficient LS [333]. The mechanism through which AURKA delays CRC onset in LS has not been further investigated. Therefore these results need further validation to understand the relationship between AURKA and MMR deficiency. The first step would be to further validate the synthetic lethal relationship between AURKA and MMR deficiency by measuring cell viability in our panel of matched paired cell lines upon Alisertib treatment or upon transfection with siAURKA. To understand why we validated the synthetic lethal relationship between AURKA and MSH6 with three out of five siRNAs only, we would measure AURKA protein levels in DLD1 and DLD1+chr2 cell lines transfected with siAURKA to investigate the inverse correlation between protein expression and cytotoxicity. In addition, to understand the mechanism of synthetic lethality, we would start by measuring cell cycle progression in MSH6 deficient and proficient cell lines upon Alisertib treatment to investigate the role for MSH6 in AURKA regulation of the cell cycle.

Taken together, we identified a promising synthetic lethal relationship between AURKA and MSH6 genes. Further investigations are necessary to better understand this synthetic lethal relationship.

Discussion

1 Using a high-throughput compound screen to identify novel therapeutics for the treatment of MMR deficient tumours

The MMR pathway, one of the major DNA repair pathways, repairs base-base mismatches and insertion deletion loops that occur during DNA replication [12]. Deficiency in MMR, highly increases the predisposition to a wide range of cancers with, for example, an 80 % risk of developing CRC [131]. It has been shown that, in comparison to MMR proficient tumours, MMR deficient tumours are more resistant to a range of chemotherapies such as 5-FU, the major treatment for CRCs [134]. In this PhD project we aimed to identify novel therapeutic strategies for the treatment of MMR deficient tumours using high-throughput compound and siRNA screens.

1.1 Panel of cell lines

In order to identify new therapeutic strategies in MMR deficient tumours, we used a panel of MMR deficient and proficient matched paired cell lines. Our panel of cell lines (Table 11 & Figure 17), represent a wide range of tumour types, and are MMR deficient due to number of different processes. To generate isogenic matched paired models of MMR deficiency, the parental cell lines that harbour mutations in MMR genes (DLD1, HEC59 and HCT116 cell lines) were matched paired with cell lines generated by the stable addition of a chromosome (DLD1+chr2, HEC59+chr2 and HCT116+chr3 cell lines). Alternatively, parental cell lines that were MMR proficient (U251 and A2780cp70 E1 cell lines) were compared to matched paired MMR deficient cell lines generated by acquired mutation due to continuous exposure to a drug (TMZ in the case of U251.TR3 cells and Cisplatin in the case of A2780cp70 A2 cells). The cell line panel is composed of matched paired cell lines that differ only from their MMR status (DLD1, DLD1+chr2, HCT116, HCT116+chr3, HEC59 and HEC59+chr2 cell lines) and matched paired cell lines that differ due to their MMR status and also their secondary mutations (U251, U251.TR3, A2780cp70 A2 and A2780cp70 E1 cell lines). The advantage for using matched paired cell lines that differ only due to their MMR status is a better identification of MMR dependent synthetic lethal relationships. However, the advantage for using matched paired cell lines that differ due to their MMR status, in addition to their secondary mutation is

that these cell lines are closer to a MMR deficient tumour phenotype in patients. MMR deficiency was first described in CRCs but is present in a wide range of cancers such as endometrial, ovarian and glioblastoma cancers, which are all represented in our panel of cell lines. Moreover, loss of MLH1 due to methylation represents a major proportion of tumours associated with MMR deficiency (see the introduction section 2.4) which is represented in our panel with the MLH1 methylated A2780cp70 A2 cell line. Therefore, this panel represents a great tool for the study of MMR dependent mechanisms.

1.2 5-FU resistance in MMR deficiency

There is controversy with regards to 5-FU resistance in MMR deficiency [259]. *In vitro*, where the parameters can be better controlled, MMR deficient cell lines have shown 5-FU resistance in comparison to MMR proficient cell lines [261]. With our panel of cell lines, we validated that 5-FU resistance strongly associates with MMR deficiency. A previous study reported the MLH1 deficient HCT116 cells were 18-fold more resistant to 5-FU than the MLH1 proficient HCT116+chr3 cells [262]. In our experiments, the difference observed with these matched paired cell lines was not as high as reported. However, they carried out a long-term clonogenic assay to measure 5-FU response which might explain why we observed a smaller difference in our short-term experiment. The MSH6 deficient cell lines showed the most consistent resistance to 5-FU in comparison to their matched paired MSH6 proficient cell line. This result was not expected as, in MSH6 mutated cells, MSH3 can complex with MSH2 to form the heterodimer MutSβ which can also recognize 5-FU, but with lower affinity than MutSα [264]. No previous study has demonstrated a greater 5-FU resistance in MSH6 deficiency compared to deficiency in the other MMR genes.

1.3 High-throughput compound screen

To identify modulators of the MSH6-mediated 5-FU resistance, we performed a high-throughput compound screen composed of 1120 compounds previously in clinical use, 90 % of which were marketed drugs, the remaining 10 % being bioactive alkaloids. This compound library has been successfully screened in previous studies [317, 319]. Each study used the compound library at different

concentrations: 10 µM and 100 µM. The concentration of 100 µM would potentially be more toxic to the cells than 10 µM in both MSH6 proficient and deficient cell lines, therefore limiting hit selection. We decided, in this study to carry out the screen with compounds at a concentration of 10 µM. The advantage of using this compound library is that this library is composed of drugs previously used in the clinic therefore enabling them to progress quickly to clinical trial. We performed the compound screen in duplicate with only one data point per drug, one scheduling regime and one drug concentration. Therefore, some potential hit compounds may be missed. Alternatively, we could have carried out the screen using two different drug concentrations as all compounds have different potencies and therefore the use of two different concentrations may have helped us to further select hits and identify new ones. Experiment scheduling is important; for example, a compound might modulate 5-FU resistance in a combination treatment but not if treated sequentially (that would be the case for example if a compound was inhibiting the cellular internalization of 5-FU); conversely, a compound might modulate 5-FU resistance when used sequentially and not in a combination treatment (that would be the case, for example, for compounds with a mechanism of cytotoxicity dependant on pathways activated or inhibited upon 5-FU treatment). We decided to carry out both repeats in the same conditions by treating first the cells with 5-FU followed by 10 µM of the library of compounds as we believed, similar biological replicates would help selecting stronger hits.

2 Clotrimazole as a modulator of 5-FU resistance in DLD1 cells

We identified Clotrimazole as a modulator of 5-FU resistance in DLD1 cells only. We did not measure the Clotrimazole effect upon 5-FU treatment in U251 and U251.TR3 cell lines. Therefore, we cannot conclude if Clotrimazole is a modulator of MSH6-mediated 5-FU resistance or if this modulation is specific to DLD1 cells. It is possible that Clotrimazole is not only MSH6 specific but also depends on other mutations present in DLD1 and DLD1+chr2 cell lines. In a previous study, Liu *et al.* demonstrate that Clotrimazole can induce an arrest in the late G1-phase of the cell

cycle and sensitize glioblastoma cells to irradiation [431]. This study suggests a potential role for Clotrimazole in the DDR. However, the mechanism of enhanced sensitivity to irradiation by Clotrimazole treatment has not been intensely investigated. In order to understand the mechanism of this 5-FU modulation, we would need to investigate the effect of Clotrimazole alone or in addition to 5-FU in DLD1 and DLD1+chr2 upon cell cycle progression. Further investigation is necessary to identify if Clotrimazole modulates 5-FU response through a G1-phase cell cycle arrest and if this modulation is DLD1 cell line specific or specific to MSH6 deficiency.

3 Triamterene as a novel therapeutic strategy for the treatment of MMR deficient tumours

3.1 Triamterene is synthetically lethal in MMR deficient cell lines *in vivo*

We validated *in vitro* the synthetic lethal relationship between Triamterene treatment and MMR deficiency. We also measured this Triamterene-induced synthetic lethality in the DLD1 and DLD1+chr2 xenografted mice in order to validate Triamterene synthetic lethality in MMR deficiency *in vivo*, which is a necessary step, before initiating a clinical trial, to observe an overall effect of the treatment within the tumour microenvironment and eventual toxicity. We observed a significant decrease in tumour growth in the DLD1 xenografted mice treated with Triamterene in comparison with the vehicle treatment. We had issues to optimize the *in vivo* experiment in order to obtain the same rate of tumour growth in the DLD1 and DLD1+chr2 xenografted mice treated with vehicle treatment, which could be explained by the different proliferation rate of these cell lines *in vitro*. U251.TR3 cells have a slower proliferation rate compared to the MSH6 proficient U251 cells; which is the opposite of what was observed in DLD1 and DLD1+chr2 cell lines. The U251.TR3 cell line has been generated by continuous exposure to TMZ in U251 cells leading to an acquired MSH6 mutation. Therefore, the U251 and U251.TR3 cell lines do not only differ by their MMR status but also with regards to their secondary mutations; therefore, suggesting that these matched paired cell lines are closer to a MMR deficient tumour phenotype. Consequently it would be relevant to

carry out *in vivo* experiments with this matched paired cell lines. We decided to carry out a pilot experiment on the U251 and U251.TR3 cell lines in order to confirm whether the reduction in tumour growth in the DLD1 cells upon Triamterene treatment is independent of the difference in the proliferation rate of the cells. In this pilot experiment we did not observe tumour growth 4 weeks after cell injection (1 or 2.5 million cells in 1X PBS or 1 million cells in matrigel (1:1)) using the U251 and U251.TR3 cells. Tumours generally take 1-2 weeks to be visible and measurable after xenografting. According to previous reports, IP injection of 1 million U251 cells in matrigel (1:1) or 1.5 million in 1X PBS should lead to tumour formation in nude mice [432, 433]. We observed a small tumour after one week in the mouse injected with 2 million U251 cells, but the tumours had reduced and disappeared a week later. We carried out this pilot experiment in NOD-SCID mice rather than nude mice (as used for the published report using U251 cells) as they have been shown to be a better model to study anticancer treatment response *in vivo* [361]. However, it is arguably possible that U251 and U251.TR3 cells grow in nude mice and not in NOD-SCID mice. Therefore it would be necessary to repeat this pilot experiment in nude mice.

We did not observe toxic effect of Triamterene treatment on the mice. In total, four mice (for a total of 80 mice) showed signs of sickness. Two of which did not receive Triamterene but vehicle treatment, and one was underweight compared to the other ones prior to the experiment (Figure 16). Therefore we validated that Triamterene was synthetically lethal in MMR deficient tumours at a dose not toxic for the animal. This validates the potential use in the clinic for Triamterene treatment in patients with MMR deficient tumours.

3.2 Triamterene cytotoxicity in MMR deficient cells, is not due to its role as a sodium channel antagonist

The first step to understand the mechanism of Triamterene synthetic lethality in MMR deficient cell lines was to investigate the major known mechanism of action of the compound, which is the inhibition of the ENaC [383-385]. To this end, we used another compound, Amiloride, known to share the same mechanism of inhibition of the ENaC, and siRNA transfection to silence the different subunits of the ENaC [378]. We only validated siENaC transfection efficiency with internal siRNA

controls (siCtrl and siPLK1). We did not validate the silencing of ENaC subunits by western blot, which may suggest that the silencing of the ENaC was not synthetically lethal in MMR deficient cells due to low depletion efficiency of the ENaC siRNAs. However, the inhibition of the ENaC with Amiloride treatment did not trigger cell cytotoxicity; therefore suggesting that Triamterene is not synthetically lethal with MMR deficiency through the inhibition of the ENaC siRNAs. Another approach to identify the role for the ENaC in Triamterene cytotoxicity would be to investigate if reactivation of the ENaC would be able to rescue the cells from Triamterene cytotoxicity. There is no ENaC activator or ENaC inhibitor antagonist available. The addition of Na^+ in the media would potentially lead to an increase in ENaC activity and could enable us to further understand whether the ENaC subunits have any role in the Triamterene-induced cytotoxicity in MMR deficient cells.

3.3 Triamterene and the folate transporters

The pteridine structure of Triamterene implies it has an antifolate activity (Figure 33) [390-392]. It has been shown that Triamterene is incorporated into the cells by the same transporters as the folates [382, 434]. The fact that Triamterene cytotoxicity could be rescued with a range of folates could suggest a competition between Triamterene and these folates at the folate transporters and therefore, the addition of folate may inhibit the import of Triamterene into the cells. In that case, Triamterene would not be synthetically lethal in MMR deficiency through its antifolate activity. To investigate this further it would be interesting to know if the folate transporters are similarly expressed in MMR deficient and MMR proficient cells as to date there is no report on a differential activity of the folate transporters in MMR deficient cells.

If Triamterene was competing with folates at the folate transporter, we could speculate that Triamterene induces folate deficiency. However, it has been reported that Triamterene treatment does not trigger folate deficiency [435]. Moreover, MMR deficiency has been associated with resistance to folate deficiency through the decrease in TS activity [436, 437]. Taken together, these reports suggest that Triamterene is not cytotoxic through folate-depletion in cells.

3.4 Triamterene and DHFR activity

Triamterene was primarily described as a DHFR inhibitor, sharing the same mechanism of action as Methotrexate. There is a discrepancy with regards to the Triamterene effect on DHFR activity [390-392]. For example, Schalhorn *et al.* published in 1981 the effect of 1, 10 and 80 µM Triamterene treatment on cell viability, DHFR activity and dUMP/dTMP ratio [397]. They concluded that Triamterene inhibited DHFR activity which triggered a decrease in dTMP pool and cell death. However, these observations were true with 80 µM Triamterene and not with 1 and 10 µM Triamterene where they observed an increase in DHFR activity with no consequences on cell viability and dTMP pool. In our study, we observed that 10 µM Triamterene induces an increase in DHFR activity in DLD1 and DLD1+chr2 cells, and synthetic lethality in MMR deficient cell lines. Therefore, Schalhorn *et al.* report supports our results showing a Triamterene dependent up-regulation of DHFR activity at a concentration synthetically lethal for MMR deficient cells. Martin *et al.* showed that Methotrexate, a DHFR inhibitor, was synthetically lethal in MSH2 deficient tumours but not in MSH6 and MLH1 deficient tumours [317]. This further suggests that Triamterene is not synthetically lethal in MMR deficiency through the same mechanism of action as Methotrexate, the inhibition of DHFR. Methotrexate inhibits DHFR which triggers nuclear oxidative DNA damage that are cytotoxic in MSH2 deficient cells. We showed here that Triamterene was not a DHFR inhibitor and therefore is synthetically lethal in MMR deficient tumours through a different mechanism than Methotrexate.

In this PhD project, we showed that silencing DHFR leads to a higher Triamterene cytotoxicity; suggesting the observed up-regulation of DHFR upon Triamterene may act as a protective mechanism of action in Triamterene cytotoxicity. An up-regulation of DHFR activity would potentially increase the cellular folate pool and therefore protect the cells from Triamterene cytotoxicity by increasing the competition between folates and Triamterene at the folate transporters and therefore decreasing Triamterene incorporation into the cells. Our data on the Triamterene dependent up-regulation of DHFR do not allow us to conclude whether Triamterene is synthetically lethal through the folate pathway or whether Triamterene shares the same transporters as folates. Moreover, exogenous over-expression of DHFR was not cytoprotective for the Triamterene effect. DHFR activity may depend on the

folate present in the cells and therefore, DHFR over-expression alone might not be correlated with an up-regulation of DHFR activity. Therefore, suggesting a potential role for the folate transporters to increase the folate pool present in the cells. Taken together, we could not conclude if Triamterene was cytotoxic through a modulation of the folate pathway or was only dependent on the folate transporter.

We validated the requirement of TS expression and activity in Triamterene cytotoxicity through three different mechanisms: siRNA targeting TS and two TS inhibitors, 5-FU and Raltitrexed. These results convincingly validate the requirement for TS in Triamterene cytotoxicity. Inhibition of TS is not known to modulate folate transport but only the folate pathway and the production of dTMP in the cells. Therefore the requirement of TS expression suggests that Triamterene is synthetically lethal in MMR deficiency through the modulation of the folate pathway and does not only depend on the folate transporters.

3.5 Triamterene requires thymidylate synthase expression

Our data suggest that DHFR is not required for the synthetic lethality upon Triamterene treatment in MMR deficient cells. As previously mentioned, Schalhorn *et al.* report no cytotoxicity and a DHFR up-regulation upon 1 and 10 µM Triamterene, and also suggests that Triamterene does not modulate dTMP production and therefore does not modulate TS activity [397]. This has been confirmed by Chang *et al.* who reported no variation in dTMP incorporation into DNA upon Triamterene treatment *in vitro* and *in vivo* [438]. Taken together, these reports suggest that Triamterene does not modulate TS activity. As previously mentioned, MMR deficient cell lines are resistant to TS inhibition induced by 5-FU treatment or folate depletion [134, 436, 437]. However, we observed a requirement of TS expression for Triamterene cytotoxicity in MMR deficient cells. This suggests that the Triamterene synthetic lethality in MMR deficient cell lines is not due to a Triamterene dependent inhibition of TS activity.

Interestingly, we did not observe modulation of Triamterene synthetic lethality in TS over-expressed cells. However, THF is the rate limiting factor of TS activity, therefore, TS over-expression might not be associated with an increase in TS activity and therefore, TS over-expression would not necessarily modulate cell viability. We did not include a control such as 5-FU to validate a potential correlation between TS

over-expression and TS activity. The addition of THF, the rate-limiting factor of TS, rescued the cells from Triamterene synthetic lethality in MMR deficient cell lines which could be due to a THF mediated increase in TS activity.

3.6 Triamterene and MTHFR

Our results suggest that DHFR over-expression was a mechanism of protection upon Triamterene treatment and we validated the requirement for TS in the Triamterene-induced cytotoxicity. An increase in DHFR activity combined with an inhibition of TS activity would theoretically lead to an increase in the THF pool and potentially to an increase in MTHFR activity, as THF is a substrate for TS but also for MTHFR (Figure 11). Therefore, we could hypothesize that TS silencing can rescue the cells from Triamterene cytotoxicity through an increase in MTHFR activity and therefore, Triamterene would potentially act as an MTHFR inhibitor. MTHFR is the rate limiting enzyme responsible for the methyl cycle of the folate pathway and is often mutated in cancer [439]. Polymorphisms in MTHFR have a protective effect on the CRC onset in LS [343, 344]. Two studies have found a correlation between MTHFR 677TT mutation and MSI [345, 346]. However, Eaton *et al*. showed an inverse correlation between MTHFR 677TT and MSI in patients with adequate folate intake and no correlation in patients with low folate intake [347]. Therefore, the correlation between MTHFR and MSI associated CRC is not clear. To date, there is no antifolate known to target MTHFR. A study suggests MTHFR inhibition as a potential cancer therapeutic strategy [440]. They showed a 30 % decrease in cell viability in gastric cancer cells transfected with a siRNA targeting MTHFR. Inhibition of MTHFR would inhibit homocysteine conversion into methionine and therefore lead to hyperhomocysteine, which has been associated with oxidative stress (Figure 11) [441-444]. However, the mechanism of hyperhomocysteine-induced oxidative stress is not clear. Homocysteine can be converted into cysteine which is the rate-limiting factor in glutathione biosynthesis, which is the first non-enzymatic cellular antioxidant [445]. Taken together, it would be interesting, in our study, to investigate if MMR proteins and/or Triamterene treatment could modulate MTHFR expression and activity. In the case of a MMR and/or Triamterene dependent modulation of MTHFR, it would be interesting to understand how it could correlate

with the reports showing a protective effect of MTHFR mutation on the onset of CRC in LS and how this MTHFR modulation could regulate oxidative stress.

3.7 Triamterene treatment induces oxidative stress

Triamterene is synthetically lethal in MMR deficient cell lines through its TS dependent antifolate activity, which leads to an increase in ROS levels specifically in the MMR deficient cells. Previous reports have identified a synthetic lethal relationship between oxidative stress and MMR deficiency [315-319]. These reports showed an induced increase in oxidative DNA damage in MMR proficient and deficient cells and an MMR dependent repair leading to cell death in MMR deficient cell lines. Strikingly, our results showed a Triamterene dose-dependent and time-dependent increase in ROS levels in MMR deficient cell lines specifically. We were expecting an increase in ROS levels in both MMR deficient and proficient cell lines and an ability, specifically for the MMR proficient cell lines, to repair the ROS-induced DNA damage as it was previously shown [317, 319]. This suggests that the Triamterene-induced synthetic lethality in MMR deficient cells is not specifically due to the ability of MMR proficient cells to repair ROS-induced DNA damage but rather due to the ability of Triamterene to differentially induce ROS either through its antifolate activity or through a differential antioxidant response in the MMR deficient cells compared to the MMR proficient cells.

3.8 MMR deficiency and antifolates

The differential in ROS levels in MMR deficient and proficient cells upon Triamterene treatment questions on whether there is a potential difference in the folate pathway in MMR deficient and proficient cell lines. To date, no study has shown a significant MMR dependent regulation in the folate pathway. Two antifolates targeting DHFR, Methotrexate and Pemetrexed, are cytotoxic in MSH2 deficient cell lines [317, 355]. Methotrexate has been shown in this study to induce oxidative stress regardless of the MMR status through DHFR inhibition. Other antifolates, such as Raltitrexed, are not known for a differential outcome in MMR deficient compared to MMR proficient tumours. However, Raltitrexed is a TS inhibitor and therefore, MMR deficient tumours should be more resistant to Raltitrexed treatment compared to MMR proficient tumours, based on the 5-FU

response in MMR deficient cells. To better understand the role of MMR deficiency in the folate pathway, it would be interesting to screen a range of antifolates, or compounds with a pteridine structure in our panel of MMR deficient and MMR proficient cell lines. This might allow us to identify other antifolates sharing the same mechanism of action as Triamterene. Therefore enabling us to gain a better understanding of the Triamterene and MMR deficiency synthetic lethal relationship and maybe to identify an antifolate with a better potency than Triamterene.

3.9 Antioxidant response induced by Triamterene treatment

Oxidative stress can be triggered by a greater induction of ROS, a decreased cellular antioxidant response or by a combination of both. The differential induction in ROS levels upon Triamterene treatment in MMR deficient and proficient cells questions whether there is a differential antioxidant response. We measured NRF2 mRNA and the antioxidant response upon Triamterene treatment in MMR proficient and deficient cell lines upon TS silencing. As summarized in Figure 55, we observed, in MMR deficient cells treated with Triamterene, an increase in ROS, NRF2 expression and the antioxidant response. In TS silenced MMR deficient cells, we observed no difference in ROS and in the antioxidant response but an increase in NRF2 expression. In addition, TS silenced MMR deficient cells treated with Triamterene showed a partial rescuing effect of the Triamterene-mediated increase in ROS levels and in the antioxidant response.

First of all, Triamterene treatment did not induce ROS, NRF2 and antioxidant responses in MMR proficient cells which suggest these observations were dependent on MMR deficiency. The basal antioxidant response in U251.TR3 cells was significantly higher than in the U251 cells. There is no previous report of a differential antioxidant in MMR deficient and proficient cell lines. We observed a down-regulation of NRF1 and an up-regulation of SOD2 mRNA levels in DLD1 compared to DLD1+chr2 cell lines which was not confirmed in the U251 and U251.TR3 cell lines where we observed an up-regulation of SOD1 and a down-regulation of SOD2 mRNA levels. These results further suggest a differential expression in antioxidant related genes in MMR deficient and proficient cell lines. However, it would be necessary to measure the ARE antioxidant response in our panel of cell lines to be able to conclude if the differential antioxidant response is

due to MMR status. Also, if MMR deficient cells lines have a higher antioxidant response that MMR proficient cells, it is not clear how this could be correlated with a Triamterene dependent increase in ROS levels in the MMR deficient cell lines specifically. We could speculate that the MMR deficient cells use the total capacity of their antioxidant response in the basal condition in order to prevent lethal oxidative DNA damage and therefore, MMR deficient cells would be unable to adapt to exogenous oxidative stress. However, we showed that Triamterene treatment leads to an increase in the antioxidant response in MMR deficient cells specifically. The differential role for the antioxidant response in MMR deficient and proficient cells remain however intriguing and unclear.

3.10 Role of NRF2 in antioxidant response

We have described in the section 1.1.1.2 of the introduction, the key role for NRF2 in the antioxidant response and in the section 1.4 of the introduction, its important role in cancer and therefore the potential interest to develop therapeutic strategies targeting NRF2 activity [25, 101, 102]. In our study, we have observed a Triamterene dependent regulation of NRF2 in MMR deficient cell lines and we also observed an increase in NRF2 mRNA levels induced by TS silencing which suggest a role for NRF2 in Triamterene synthetic lethality in MMR deficient cell lines.

It has been published previously a role for the antioxidant response upon 5-FU treatment [446-449]. Two reports compared 5-FU resistant and 5-FU sensitive matched paired cell lines [448, 450]. The first study reported no difference in NRF2 expression in both cell lines but an increase in NRF2 levels after 5-FU treatment and higher 5-FU sensitivity in NRF2-silenced 5-FU resistant cells [448]. The other study observed higher NRF2 expression in the 5-FU resistant cells and confirmed the increase in 5-FU sensitivity in NRF2-silenced cells [450]. They did not describe the mechanism of acquired resistance to 5-FU, which might explain the different results on basal NRF2 expression. Other studies confirmed the increased sensitivity to 5-FU treatment in NRF2 silenced cells [446, 447]. One study identified an increase in NRF2 activity and ARE dependent antioxidant response upon 5-FU treatment [449]. This last study does not correlate with our results as we observed an increase in NRF2 mRNA levels in TS silenced cells but no difference in antioxidant response. In their study however, the 5-FU dependent increase in antioxidant response was not

directly associated with TS silencing therefore, it might be due to another mechanism of action of 5-FU. Also, they measured 5-FU dependent regulation of NRF2 and antioxidants in the colorectal HT-29 and SNUC5 cell lines, therefore, the correlation between NRF2 and antioxidant response upon 5-FU treatment might depend on the cell lines. Furthermore, we measured the antioxidant response 24 hrs after treatment and NRF2 expression 48 hrs after treatment. Therefore, TS-dependent antioxidant response might be a later event and therefore we did not observe it after 24 hrs treatment. It is also possible to hypothesise that in U251 and U251.TR3 cell lines, the up-regulation of NRF2 is not correlated with an increased antioxidant response due to the regulation of NRF2 activity by Keap1, and the regulation of ARE dependent antioxidants by NRF2 and NRF1. Therefore, it would be interesting to measure the expression of NRF2, but also NRF1 and Keap1, and the antioxidant response in a time-course experiment upon Triamterene treatment in TS-silenced cells.

In addition, we observed that Triamterene, in TS-silenced MMR deficient cells, does not induce ROS levels but induces an increase in NRF2 levels and a lower antioxidant response (compared to the TS expressing MMR deficient cells). These results suggest that the silencing of TS, which can rescue the cells from Triamterene cytotoxicity, can partially rescue both Triamterene-induced ROS and Triamterene-induced antioxidant response. We could speculate that TS silencing can abrogate the increase in ROS levels and therefore the ROS-induced protective antioxidant response is decreased. Further investigations are necessary to understand the potential direct role of TS in NRF2 and the antioxidant response by for example silencing NRF2 and TS in our cells lines to see if NRF2 would inhibit the TS dependant effect on Triamterene treatment.

Moreover, if the Triamterene dependent induction in the antioxidant response is a mechanism of cytoprotection, the combination of Triamterene treatment with an inhibitor of NRF2 might increase the MMR deficient tumour sensitivity to Triamterene treatment. However, further investigations are necessary to measure if the inhibition of NRF2 would be cytotoxic in MMR proficient cells.

3.11 Triamterene-induced accumulation of ROS levels triggers DNA double strand breaks

Oxidative stress induces oxidative DNA damage that, if not repaired, can lead to lethal DSBs. It has been shown that MMR deficient cell lines are unable to repair oxidative DNA damage leading ultimately to lethal DSBs. To see if the Triamterene dependent increase in ROS levels was cytotoxic through an accumulation of oxidative DNA damage and ultimately DSBs, we measured DSBs by measuring the formation of γH2AX foci. It has been shown previously that the formation of γH2AX foci, which is the phosphorylation at Ser 139 of H2A.X at the DBS, was a good marker for measuring DSBs [400, 401]. The comet assay, a single cell gel electrophoresis, is another method for identifying DSBs [451]. The pattern of DNA migration will resemble a comet with a ratio tail/body proportional to DNA strand breaks. γH2AX foci can be measured by confocal microscopy by counting the number of cells with more than 5 foci in the nucleus. In dying cells, DNA becomes degraded and therefore γH2AX is recruited. These cells will have a pan-genomic staining of γH2AX rather than γH2AX foci. Therefore, pan-genomic γH2AX staining is a marker for apoptotic cells and therefore is not counted as positive of γH2AX [400, 401]. Using γH2AX foci as a marker for DSBs is more accurate than the comet assay as the comet assay does not permit to differentiate SSBs and exclude apoptotic cells. We observed after 48 hrs treatment with Triamterene a significant increase in γH2AX foci formation and a low pan-genomic γH2AX staining. Therefore, we considered that the analysis of DBSs after 48 hrs treatment was relevant. In the U251 and U251.TR3 cells, we observed a higher number of cells with pan-genomic phosphorylation of H2A.X. Therefore, we decided to measure γH2AX foci in U251 and U251.TR3 cell lines after 24 hrs treatment with Triamterene. DSBs could be caused by an accumulation of DNA damage other than oxidative DNA damage; however, the addition of NAC, a ROS scavenger, could rescue the accumulation of DSBs therefore suggesting that the observed DSBs were caused by an increase in ROS levels. Avidin has been shown to bind 8-oxodG and an Avidin antibody has been successfully used in a recent study to show an increase in 8-oxodG into DNA by confocal microscopy analysis [452]. In this study, further experiments would be necessary to measure the level of 8-oxodG in MMR deficient and proficient cell lines upon Triamterene treatment by confocal microscopy using

an Avidin antibody. Taken together, we did not directly validate the correlation between the increase in ROS levels and the accumulation of DSBs by measuring 8-oxodG; however, we indirectly validated this correlation by observing a rescuing of the accumulation of DSBs upon Triamterene treatment and the addition of NAC.

3.12 Triamterene as a novel synthetic lethal compound in MMR deficient tumours

The high-throughput compound screen carried out in DLD1 and DLD1+chr2 cell lines upon 5-FU treatment allowed us to identify Triamterene, a potassium-sparing diuretic drug, as synthetically lethal *in vitro* and *in vivo* MMR deficiency through its antifolate activity. Triamterene was previously described as a weak antifolate [382]. Here we described Triamterene novel role for the treatment of MMR deficient tumours through its antifolate activity. We showed that Triamterene can induce an increase in ROS levels, leading to an accumulation of DSBs, in the MMR deficient cell lines specifically. The specific role for MMR pathway in the Triamterene-mediated increase in ROS levels is still not clear; however, this result is highly relevant for the clinic as a moderate increase in ROS level has been associated with cancer development [22, 23] and therefore, the ROS induction in MMR deficient tumours specifically would prevent an adverse effect of an increase in ROS levels in MMR proficient cells. We also identified the role for TS in Triamterene synthetic lethality through the regulation of ROS levels. TS over-expression has been described as a mechanism of resistance of 5-FU treatment [453]. It would be interesting to see if tumours with an acquired resistance to 5-FU treatment associated with an up-regulation of TS would be more sensitive to Triamterene treatment and if this would be dependent on MMR status. We also investigated the role of NRF2 and the antioxidant response but the Triamterene and TS-dependent regulation of NRF2 and ARE requires further investigation to further understand if it has a cytoprotective or cytotoxic role in response to Triamterene treatment. Taken together, we showed Triamterene as synthetically lethal in MMR deficiency through a TS-dependent increase in ROS levels, leading to an accumulation of DSBs (Figure 60).

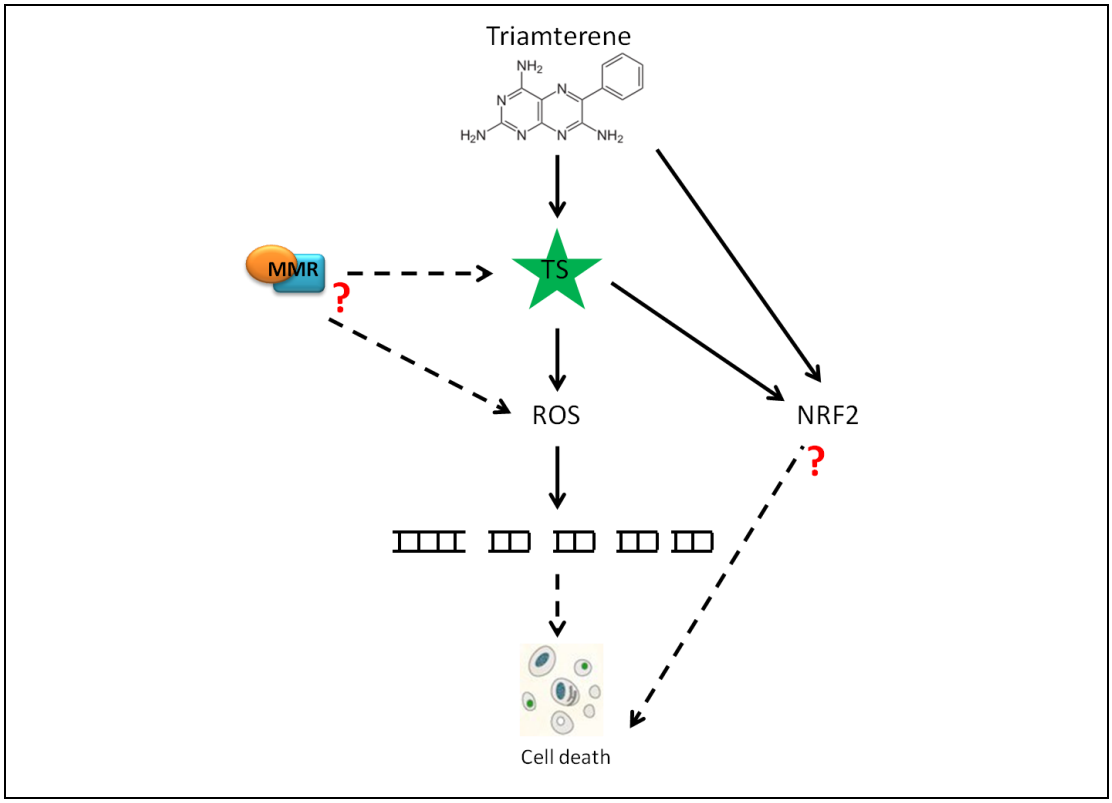

Figure 60: Triamterene is synthetically lethal with MMR deficient cell lines
Triamterene is synthetically lethal in MMR deficient cell lines through its antifolate activity and requires TS expression. It induces an increase in ROS levels specifically in the MMR deficient cell lines which ultimately leads to DSBs that are potentially lethal for the cells. The role for MMR pathway is not clear but is potentially upstream the increase in ROS levels. Further investigations to understand the role for the antioxidant response and more precisely NRF2 are necessary.

3.13 Limitations in Triamterene treatment for the treatment of MMR deficient tumours

The first limitation for Triamterene treatment in MMR deficiency would be long-term acquired resistance to the treatment. One of the mechanisms of Methotrexate resistance is through the up-regulation of the folate transporter [348]. Therefore, we could speculate that a long-term Triamterene treatment might lead to the same mechanism of resistance as they share the same folate transporters [434].

Another limitation for the treatment with Triamterene is a tumour dependent expression of different proteins in the folate pathway. For example, MTHFR is mutated in a number of tumours so we would need to investigate the role for these mutations in Triamterene treatment [454].

4 High-throughput siRNA screen to identify synthetic lethal interactions with MSH6 deficiency

4.1 High-throughput siRNA screen validation

To carry out the high-throughput siRNA screen, we used a siKinome library composed of SMARTpool siRNAs. The main advantage of using a library composed of SMARTpool siRNAs is to minimize the off-target effects by decreasing the concentration of each individual siRNA and by maximizing the on-target effect by using 4 siRNAs targeting the same gene [455]. To carry out this screen, we used one single concentration of siRNA (50 nM) which might represent a limitation for high-throughput screen because at a defined concentration, a number of siRNAs might be unable to efficiently silence their targeted genes or might efficiently silence their target as well as off-target genes. Two previous studies have successfully used the same kinome library at 50 nM. This concentration was also successfully used during the siRNA optimization experiments (with low toxicity of the siCtrl and high transfection efficiency measured with siPLK1). Therefore, we carried out the high-throughput screen at the concentration of 50 nM [318, 403].

4.2 AURKA inhibition in MMR deficiency

Based on our screen analysis, we selected 5 genes that are potentially synthetically lethal in MMR deficiency and validated AURKA as synthetically lethal in MSH6 deficiency. Further experiments are necessary to completely validate the synthetic lethal relationship between AURKA and MMR genes. Firstly, we would need to measure cell viability in a short and long-term experiment upon AURKA inhibitor treatment in our panel of MMR proficient and deficient cell lines. It would be interesting to know if AURKA inhibitor is only synthetically lethal with MSH6 or with MSH6 and MSH2 or with all MMR genes. We know that loss of MSH2 leads to MSH6 instability and therefore loss of MSH6 expression, and we also know that nuclear MSH2 is decreased in MSH6 deficient cells [140, 163]; therefore we could expect AURKA to be synthetically lethal with MSH6 and MSH2 deficiency. Our preliminary results showed no synthetic lethality in MLH1 deficiency; however repeats are necessary to be able to conclude.

4.3 AURKA inhibitors in clinic

The Aurora kinase family plays a critical role in regulating mitosis. AURKA is involved in regulating many of the early mitotic events. AURKA is located at the centrosome in interphase and at the spindle poles in mitotic cells. One target of AURKA is CDC25B, which plays a role in regulating entry into mitosis. AURKA also moderates the recruitment of proteins essential for centrosome maturation and separation. In addition, it regulates the microtubule network that forms mitotic spindles [456]. AURKA has been referred to as an oncogene and is significantly up-regulated in solid tumours including CRC, breast, ovarian neuroblastoma and cervical cancer [419, 420]. Due to the role of AURKA in mitosis, tumours with up-regulated AURKA manifest chromosome instability [457, 458]. The mechanism of AURKA in tumour progression is by facilitating checkpoint recovery allowing aberrant progression through mitosis [459].

Alisertib (MLN8237) is an AURKA inhibitor. It induces a G2/M phase cell arrest, chromosome misalignment and spindle defects [422]. A number of clinical trials are investigating its response in tumours alone (NCT00962091, NCT01045421); in combination with Irinotecan and TMZ in neuroblastoma (NCT01601535); in combination with erlotinib for the treatment of non small cell lung cancer (NCT01471964); or in combination with paclitaxel in ovarian and breast cancer (NCT01091428). So far, the clinical results have shown modest effect probably due to patient heterogeneity [456]. Alisertib has not yet been investigated in MSI cancers, therefore, we could speculate that the modest response observed in clinic might be representative of MSI tumours.

4.4 AURKA as a potential DNA repair modulator

AURKA has been described as a potential DNA repair modulator [418]. AURKA has a role in cell cycle progression by repressing G1 and G2 checkpoint arrests [460, 461]. AURKA has been shown to interact with p53 and over-expression of AURKA increases p53 expression [462]. However, in cancer tissues AURKA and p53 expression are inversely correlated [463]. Reports suggest that AURKA may play a role in DNA damage response through p53 inhibition [418]. Silencing AURKA facilitates p53 phosphorylation at ser15, which enhances the NHEJ pathway [464]. AURKA has also been shown to inhibit HR by inhibiting BRCA1/2 and RAD51

[456]. A combination treatment with IR and AURKA inhibitor increases IR-induced HR repair in p53 deficient cells [465]. Taken together, these data on AURKA role in DNA repair could help us to understand its synthetic lethal relationship with MMR deficiency. Primarily, as AURKA plays an important role in cell cycle progression, it could be hypothesized that AURKA inhibition mediated cytotoxicity was correlated with a higher proliferation rate. The MSH6 deficient DLD1 cells have a higher proliferation rate compared to their paired DLD1+chr2 cells and the MSH6 deficient U251.TR3 cells have a lower proliferation rate compared to their paired U251 cells; suggesting that AURKA synthetic lethality in MSH6 deficiency is independent of the cell proliferation. Therefore, it would be interesting to measure cell cycle progression in MSH6 deficient and proficient cell lines upon Alisertib treatment to investigate the role for MSH6 in AURKA regulation of the cell cycle.

As AURKA has been associated with HR and NHEJ, it would be relevant to measure γH2AX foci upon Alisertib treatment in our cell lines to measure if AURKA inhibition triggers unrepaired DSBs leading to apoptosis. As described in section 2.3.3 of the introduction MSH6 interacts with Ku70 and that MSH6 deficiency results in an impaired NHEJ repair [177]. Therefore, it would be interesting to investigate the NHEJ pathway upon treatment with Alisertib in our MSH6 proficient and deficient cell lines.

There is discrepancy with regards to the role of AURKA in the onset of CRC in LS [333, 335] and the mechanism behind this potential association has not been investigated (see the introduction section 3.2.3.4). Therefore, this synthetic lethal relationship is novel and promising and it would be relevant to test *in vivo* the role for AURKA inhibition in MMR deficient tumour development and growth.

Taken together, we identified a novel synthetic lethal relationship between AURKA and MSH6 using a high-throughput siRNA screen. Our results are very promising as AURKA is up-regulated in a number of solid tumours and associated with an early development of CRC in LS. AURKA inhibitors are already used in clinic and therefore, this synthetic lethal relationship could rapidly be translated into clinic. Therefore, there is a clinical need to investigate and understand the synthetic lethal relationship between MSH6 and AURKA gene. Further investigations are necessary

to better understand this synthetically lethal relationship but our preliminary results are promising.

My PhD project was to identify, via high-throughput compound and siRNA screens, modulators of 5-FU resistance and/or novel synthetic lethal relationships as new potential therapeutic targets in MMR deficient tumours. We identified a synthetic lethal relationship between Triamterene and MMR deficiency using a high-throughput compound screen and between AURKA and MSH6 using a high-throughput siRNA screen. We also identified the folate pathway as a novel therapeutic target for the treatment of different forms of MMR deficient tumours.

References

1. Stewart BW, Wild C, International Agency for Research on Cancer, World Health Organization: **World cancer report 2014**.
2. Sieber O, Heinimann K, Tomlinson I: **Genomic stability and tumorigenesis**. *Seminars in cancer biology* 2005, **15**(1):61-66.
3. Lengauer C, Kinzler KW, Vogelstein B: **Genetic instabilities in human cancers**. *Nature* 1998, **396**(6712):643-649.
4. Negrini S, Gorgoulis VG, Halazonetis TD: **Genomic instability--an evolving hallmark of cancer**. *Nature reviews Molecular cell biology* 2010, **11**(3):220-228.
5. Kim TM, Laird PW, Park PJ: **The landscape of microsatellite instability in colorectal and endometrial cancer genomes**. *Cell* 2013, **155**(4):858-868.
6. Loeb LA, Springgate CF, Battula N: **Errors in DNA replication as a basis of malignant changes**. *Cancer Res* 1974, **34**(9):2311-2321.
7. Toyota M, Ahuja N, Ohe-Toyota M, Herman JG, Baylin SB, Issa JP: **CpG island methylator phenotype in colorectal cancer**. *Proceedings of the National Academy of Sciences of the United States of America* 1999, **96**(15):8681-8686.
8. Suzuki H, Yamamoto E, Maruyama R, Niinuma T, Kai M: **Biological significance of the CpG island methylator phenotype**. *Biochemical and biophysical research communications* 2014, **455**(1-2):35-42.
9. Issa JP: **CpG island methylator phenotype in cancer**. *Nature reviews Cancer* 2004, **4**(12):988-993.
10. Geigl JB, Obenauf AC, Schwarzbraun T, Speicher MR: **Defining 'chromosomal instability'**. *Trends in genetics : TIG* 2008, **24**(2):64-69.
11. Lengauer C, Kinzler KW, Vogelstein B: **Genetic instability in colorectal cancers**. *Nature* 1997, **386**(6625):623-627.
12. Curtin NJ: **DNA repair dysregulation from cancer driver to therapeutic target**. *Nature reviews Cancer* 2012, **12**(12):801-817.
13. Broustas CG, Lieberman HB: **DNA damage response genes and the development of cancer metastasis**. *Radiation research* 2014, **181**(2):111-130.
14. Vindigni A, Gonzalo S: **The two faces of DNA repair: disease and therapy**. *Missouri medicine* 2013, **110**(4):314-319.
15. Hosoya N, Miyagawa K: **Targeting DNA damage response in cancer therapy**. *Cancer science* 2014, **105**(4):370-388.
16. Martin SA, Lord CJ, Ashworth A: **DNA repair deficiency as a therapeutic target in cancer**. *Current opinion in genetics & development* 2008, **18**(1):80-86.
17. Bouwman P, Jonkers J: **The effects of deregulated DNA damage signalling on cancer chemotherapy response and resistance**. *Nature reviews Cancer* 2012, **12**(9):587-598.
18. Lodish HF: **Molecular cell biology**, 4th edn. New York: W.H. Freeman; 2000.
19. Swenberg JA, Lu K, Moeller BC, Gao L, Upton PB, Nakamura J, Starr TB: **Endogenous versus exogenous DNA adducts: their role in carcinogenesis, epidemiology, and risk assessment**. *Toxicological sciences : an official journal of the Society of Toxicology* 2011, **120 Suppl 1**:S130-145.
20. Neeley WL, Essigmann JM: **Mechanisms of formation, genotoxicity, and mutation of guanine oxidation products**. *Chemical research in toxicology* 2006, **19**(4):491-505.

21. Gorrini C, Harris IS, Mak TW: **Modulation of oxidative stress as an anticancer strategy**. *Nature reviews Drug discovery* 2013, **12**(12):931-947.
22. Cairns RA, Harris IS, Mak TW: **Regulation of cancer cell metabolism**. *Nature reviews Cancer* 2011, **11**(2):85-95.
23. Liou GY, Storz P: **Reactive oxygen species in cancer**. *Free radical research* 2010, **44**(5):479-496.
24. Carocho M, Ferreira IC: **A review on antioxidants, prooxidants and related controversy: natural and synthetic compounds, screening and analysis methodologies and future perspectives**. *Food and chemical toxicology : an international journal published for the British Industrial Biological Research Association* 2013, **51**:15-25.
25. Sporn MB, Liby KT: **NRF2 and cancer: the good, the bad and the importance of context**. *Nature reviews Cancer* 2012, **12**(8):564-571.
26. Eggler AL, Liu G, Pezzuto JM, van Breemen RB, Mesecar AD: **Modifying specific cysteines of the electrophile-sensing human Keap1 protein is insufficient to disrupt binding to the Nrf2 domain Neh2**. *Proceedings of the National Academy of Sciences of the United States of America* 2005, **102**(29):10070-10075.
27. Huang HC, Nguyen T, Pickett CB: **Phosphorylation of Nrf2 at Ser-40 by protein kinase C regulates antioxidant response element-mediated transcription**. *The Journal of biological chemistry* 2002, **277**(45):42769-42774.
28. Gopalakrishna R, Jaken S: **Protein kinase C signaling and oxidative stress**. *Free radical biology & medicine* 2000, **28**(9):1349-1361.
29. Taguchi K, Motohashi H, Yamamoto M: **Molecular mechanisms of the Keap1-Nrf2 pathway in stress response and cancer evolution**. *Genes to cells : devoted to molecular & cellular mechanisms* 2011, **16**(2):123-140.
30. Niture SK, Khatri R, Jaiswal AK: **Regulation of Nrf2-an update**. *Free radical biology & medicine* 2014, **66**:36-44.
31. Itoh K, Chiba T, Takahashi S, Ishii T, Igarashi K, Katoh Y, Oyake T, Hayashi N, Satoh K, Hatayama I *et al*: **An Nrf2/small Maf heterodimer mediates the induction of phase II detoxifying enzyme genes through antioxidant response elements**. *Biochemical and biophysical research communications* 1997, **236**(2):313-322.
32. Rushmore TH, Pickett CB: **Transcriptional regulation of the rat glutathione S-transferase Ya subunit gene. Characterization of a xenobiotic-responsive element controlling inducible expression by phenolic antioxidants**. *The Journal of biological chemistry* 1990, **265**(24):14648-14653.
33. Nioi P, McMahon M, Itoh K, Yamamoto M, Hayes JD: **Identification of a novel Nrf2-regulated antioxidant response element (ARE) in the mouse NAD(P)H:quinone oxidoreductase 1 gene: reassessment of the ARE consensus sequence**. *The Biochemical journal* 2003, **374**(Pt 2):337-348.
34. Kwak MK, Itoh K, Yamamoto M, Kensler TW: **Enhanced expression of the transcription factor Nrf2 by cancer chemopreventive agents: role of antioxidant response element-like sequences in the nrf2 promoter**. *Molecular and cellular biology* 2002, **22**(9):2883-2892.
35. Zhu H, Itoh K, Yamamoto M, Zweier JL, Li Y: **Role of Nrf2 signaling in regulation of antioxidants and phase 2 enzymes in cardiac fibroblasts:**

protection against reactive oxygen and nitrogen species-induced cell injury. *FEBS letters* 2005, **579**(14):3029-3036.
36. Thimmulappa RK, Mai KH, Srisuma S, Kensler TW, Yamamoto M, Biswal S: **Identification of Nrf2-regulated genes induced by the chemopreventive agent sulforaphane by oligonucleotide microarray**. *Cancer Res* 2002, **62**(18):5196-5203.
37. Xiang M, Namani A, Wu S, Wang X: **Nrf2: bane or blessing in cancer?** *Journal of cancer research and clinical oncology* 2014, **140**(8):1251-1259.
38. Hayes JD, Dinkova-Kostova AT: **The Nrf2 regulatory network provides an interface between redox and intermediary metabolism**. *Trends in biochemical sciences* 2014, **39**(4):199-218.
39. Biswas M, Chan JY: **Role of Nrf1 in antioxidant response element-mediated gene expression and beyond**. *Toxicology and applied pharmacology* 2010, **244**(1):16-20.
40. Leung L, Kwong M, Hou S, Lee C, Chan JY: **Deficiency of the Nrf1 and Nrf2 transcription factors results in early embryonic lethality and severe oxidative stress**. *The Journal of biological chemistry* 2003, **278**(48):48021-48029.
41. Wang W, Kwok AM, Chan JY: **The p65 isoform of Nrf1 is a dominant negative inhibitor of ARE-mediated transcription**. *The Journal of biological chemistry* 2007, **282**(34):24670-24678.
42. Ohtsuji M, Katsuoka F, Kobayashi A, Aburatani H, Hayes JD, Yamamoto M: **Nrf1 and Nrf2 play distinct roles in activation of antioxidant response element-dependent genes**. *The Journal of biological chemistry* 2008, **283**(48):33554-33562.
43. Jena NR: **DNA damage by reactive species: Mechanisms, mutation and repair**. *Journal of biosciences* 2012, **37**(3):503-517.
44. Cooke MS, Evans MD, Dizdaroglu M, Lunec J: **Oxidative DNA damage: mechanisms, mutation, and disease**. *FASEB journal : official publication of the Federation of American Societies for Experimental Biology* 2003, **17**(10):1195-1214.
45. Xu-Welliver M, Pegg AE: **Degradation of the alkylated form of the DNA repair protein, O(6)-alkylguanine-DNA alkyltransferase**. *Carcinogenesis* 2002, **23**(5):823-830.
46. Fu D, Calvo JA, Samson LD: **Balancing repair and tolerance of DNA damage caused by alkylating agents**. *Nature reviews Cancer* 2012, **12**(2):104-120.
47. De Bont R, van Larebeke N: **Endogenous DNA damage in humans: a review of quantitative data**. *Mutagenesis* 2004, **19**(3):169-185.
48. Daniels DS, Woo TT, Luu KX, Noll DM, Clarke ND, Pegg AE, Tainer JA: **DNA binding and nucleotide flipping by the human DNA repair protein AGT**. *Nature structural & molecular biology* 2004, **11**(8):714-720.
49. Hsieh P, Yamane K: **DNA mismatch repair: molecular mechanism, cancer, and ageing**. *Mechanisms of ageing and development* 2008, **129**(7-8):391-407.
50. Jacobs AL, Schar P: **DNA glycosylases: in DNA repair and beyond**. *Chromosoma* 2012, **121**(1):1-20.
51. Krokan HE, Bjoras M: **Base excision repair**. *Cold Spring Harbor perspectives in biology* 2013, **5**(4):a012583.

52. Radicella JP, Dherin C, Desmaze C, Fox MS, Boiteux S: **Cloning and characterization of hOGG1, a human homolog of the OGG1 gene of Saccharomyces cerevisiae**. *Proceedings of the National Academy of Sciences of the United States of America* 1997, **94**(15):8010-8015.
53. Slupska MM, Baikalov C, Luther WM, Chiang JH, Wei YF, Miller JH: **Cloning and sequencing a human homolog (hMYH) of the Escherichia coli mutY gene whose function is required for the repair of oxidative DNA damage**. *Journal of bacteriology* 1996, **178**(13):3885-3892.
54. Lindahl T: **An N-glycosidase from Escherichia coli that releases free uracil from DNA containing deaminated cytosine residues**. *Proceedings of the National Academy of Sciences of the United States of America* 1974, **71**(9):3649-3653.
55. Neddermann P, Gallinari P, Lettieri T, Schmid D, Truong O, Hsuan JJ, Wiebauer K, Jiricny J: **Cloning and expression of human G/T mismatch-specific thymine-DNA glycosylase**. *The Journal of biological chemistry* 1996, **271**(22):12767-12774.
56. Haushalter KA, Todd Stukenberg MW, Kirschner MW, Verdine GL: **Identification of a new uracil-DNA glycosylase family by expression cloning using synthetic inhibitors**. *Current biology : CB* 1999, **9**(4):174-185.
57. Hendrich B, Hardeland U, Ng HH, Jiricny J, Bird A: **The thymine glycosylase MBD4 can bind to the product of deamination at methylated CpG sites**. *Nature* 1999, **401**(6750):301-304.
58. Nilsen H, Krokan HE: **Base excision repair in a network of defence and tolerance**. *Carcinogenesis* 2001, **22**(7):987-998.
59. Klungland A, Rosewell I, Hollenbach S, Larsen E, Daly G, Epe B, Seeberg E, Lindahl T, Barnes DE: **Accumulation of premutagenic DNA lesions in mice defective in removal of oxidative base damage**. *Proceedings of the National Academy of Sciences of the United States of America* 1999, **96**(23):13300-13305.
60. Engelward BP, Weeda G, Wyatt MD, Broekhof JL, de Wit J, Donker I, Allan JM, Gold B, Hoeijmakers JH, Samson LD: **Base excision repair deficient mice lacking the Aag alkyladenine DNA glycosylase**. *Proceedings of the National Academy of Sciences of the United States of America* 1997, **94**(24):13087-13092.
61. Nilsen H, Rosewell I, Robins P, Skjelbred CF, Andersen S, Slupphaug G, Daly G, Krokan HE, Lindahl T, Barnes DE: **Uracil-DNA glycosylase (UNG)-deficient mice reveal a primary role of the enzyme during DNA replication**. *Molecular cell* 2000, **5**(6):1059-1065.
62. Xie Y, Yang H, Cunanan C, Okamoto K, Shibata D, Pan J, Barnes DE, Lindahl T, McIlhatton M, Fishel R *et al*: **Deficiencies in mouse Myh and Ogg1 result in tumor predisposition and G to T mutations in codon 12 of the K-ras oncogene in lung tumors**. *Cancer Res* 2004, **64**(9):3096-3102.
63. Mol CD, Izumi T, Mitra S, Tainer JA: **DNA-bound structures and mutants reveal abasic DNA binding by APE1 and DNA repair coordination [corrected]**. *Nature* 2000, **403**(6768):451-456.
64. Fortini P, Dogliotti E: **Base damage and single-strand break repair: mechanisms and functional significance of short- and long-patch repair subpathways**. *DNA repair* 2007, **6**(4):398-409.

65. Fortini P, Pascucci B, Parlanti E, Sobol RW, Wilson SH, Dogliotti E: **Different DNA polymerases are involved in the short- and long-patch base excision repair in mammalian cells**. *Biochemistry* 1998, **37**(11):3575-3580.
66. Robertson AB, Klungland A, Rognes T, Leiros I: **DNA repair in mammalian cells: Base excision repair: the long and short of it**. *Cellular and molecular life sciences : CMLS* 2009, **66**(6):981-993.
67. Rice PA: **Holding damaged DNA together**. *Nature structural biology* 1999, **6**(9):805-806.
68. Kleppa L, Mari PO, Larsen E, Lien GF, Godon C, Theil AF, Nesse GJ, Wiksen H, Vermeulen W, Giglia-Mari G *et al*: **Kinetics of endogenous mouse FEN1 in base excision repair**. *Nucleic acids research* 2012, **40**(18):9044-9059.
69. Dianov GL, Hubscher U: **Mammalian base excision repair: the forgotten archangel**. *Nucleic acids research* 2013, **41**(6):3483-3490.
70. Marteijn JA, Lans H, Vermeulen W, Hoeijmakers JH: **Understanding nucleotide excision repair and its roles in cancer and ageing**. *Nature reviews Molecular cell biology* 2014, **15**(7):465-481.
71. Sugasawa K, Ng JM, Masutani C, Iwai S, van der Spek PJ, Eker AP, Hanaoka F, Bootsma D, Hoeijmakers JH: **Xeroderma pigmentosum group C protein complex is the initiator of global genome nucleotide excision repair**. *Molecular cell* 1998, **2**(2):223-232.
72. Hanawalt PC, Spivak G: **Transcription-coupled DNA repair: two decades of progress and surprises**. *Nature reviews Molecular cell biology* 2008, **9**(12):958-970.
73. Kamileri I, Karakasilioti I, Garinis GA: **Nucleotide excision repair: new tricks with old bricks**. *Trends in genetics : TIG* 2012, **28**(11):566-573.
74. Kathe SD, Shen GP, Wallace SS: **Single-stranded breaks in DNA but not oxidative DNA base damages block transcriptional elongation by RNA polymerase II in HeLa cell nuclear extracts**. *The Journal of biological chemistry* 2004, **279**(18):18511-18520.
75. Moldovan GL, D'Andrea AD: **How the fanconi anemia pathway guards the genome**. *Annual review of genetics* 2009, **43**:223-249.
76. Walden H, Deans AJ: **The Fanconi anemia DNA repair pathway: structural and functional insights into a complex disorder**. *Annual review of biophysics* 2014, **43**:257-278.
77. Kim H, D'Andrea AD: **Regulation of DNA cross-link repair by the Fanconi anemia/BRCA pathway**. *Genes & development* 2012, **26**(13):1393-1408.
78. Branzei D, Foiani M: **Regulation of DNA repair throughout the cell cycle**. *Nature reviews Molecular cell biology* 2008, **9**(4):297-308.
79. Hartlerode AJ, Scully R: **Mechanisms of double-strand break repair in somatic mammalian cells**. *The Biochemical journal* 2009, **423**(2):157-168.
80. Vilenchik MM, Knudson AG: **Endogenous DNA double-strand breaks: production, fidelity of repair, and induction of cancer**. *Proceedings of the National Academy of Sciences of the United States of America* 2003, **100**(22):12871-12876.
81. Aparicio T, Baer R, Gautier J: **DNA double-strand break repair pathway choice and cancer**. *DNA repair* 2014, **19**:169-175.

82. Collis SJ, DeWeese TL, Jeggo PA, Parker AR: **The life and death of DNA-PK**. *Oncogene* 2005, **24**(6):949-961.
83. Malu S, Malshetty V, Francis D, Cortes P: **Role of non-homologous end joining in V(D)J recombination**. *Immunologic research* 2012, **54**(1-3):233-246.
84. Garcia V, Phelps SE, Gray S, Neale MJ: **Bidirectional resection of DNA double-strand breaks by Mre11 and Exo1**. *Nature* 2011, **479**(7372):241-244.
85. Ristic D, Modesti M, van der Heijden T, van Noort J, Dekker C, Kanaar R, Wyman C: **Human Rad51 filaments on double- and single-stranded DNA: correlating regular and irregular forms with recombination function**. *Nucleic acids research* 2005, **33**(10):3292-3302.
86. Morrical SW: **DNA-Pairing and Annealing Processes in Homologous Recombination and Homology-Directed Repair**. *Cold Spring Harbor perspectives in biology* 2015, **7**(2).
87. Lange SS, Takata K, Wood RD: **DNA polymerases and cancer**. *Nature reviews Cancer* 2011, **11**(2):96-110.
88. Stallons LJ, McGregor WG: **Translesion synthesis polymerases in the prevention and promotion of carcinogenesis**. *Journal of nucleic acids* 2010, **2010**.
89. Sutton MD: **Coordinating DNA polymerase traffic during high and low fidelity synthesis**. *Biochimica et biophysica acta* 2010, **1804**(5):1167-1179.
90. Guo C, Kosarek-Stancel JN, Tang TS, Friedberg EC: **Y-family DNA polymerases in mammalian cells**. *Cellular and molecular life sciences : CMLS* 2009, **66**(14):2363-2381.
91. Humphrey T, Brooks G: **The mammalian cell cycle**. In: *Cell Cycle Control Mechanisms and Protocols.* Edited by Humphrey T, Brooks G, vol. 296; 2004: 113-115.
92. Morgan DO: **The cell cycle**. In: *The cell cycle : principles of control.* E. Lawrence, editor. New Science Press Ltd; 2007: xxvii, 297 p.
93. Cooper GM: **The Eukaryotic Cell Cycle**. In: *The cell: a molecular approach.* 2nd edn: Sunderland (MA): Sinauer Associates; 2000.
94. Menon V, Povirk L: **Involvement of p53 in the repair of DNA double strand breaks: multifaceted Roles of p53 in homologous recombination repair (HRR) and non-homologous end joining (NHEJ)**. *Sub-cellular biochemistry* 2014, **85**:321-336.
95. Lord CJ, Garrett MD, Ashworth A: **Targeting the double-strand DNA break repair pathway as a therapeutic strategy**. *Clin Cancer Res* 2006, **12**(15):4463-4468.
96. Kim JS, Krasieva TB, Kurumizaka H, Chen DJ, Taylor AM, Yokomori K: **Independent and sequential recruitment of NHEJ and HR factors to DNA damage sites in mammalian cells**. *The Journal of cell biology* 2005, **170**(3):341-347.
97. Bonner WM, Redon CE, Dickey JS, Nakamura AJ, Sedelnikova OA, Solier S, Pommier Y: **GammaH2AX and cancer**. *Nature reviews Cancer* 2008, **8**(12):957-967.
98. Flynn RL, Zou L: **ATR: a master conductor of cellular responses to DNA replication stress**. *Trends in biochemical sciences* 2011, **36**(3):133-140.
99. Weber AM, Ryan AJ: **ATM and ATR as therapeutic targets in cancer**. *Pharmacology & therapeutics* 2014.

100. Felty Q, Singh KP, Roy D: **Estrogen-induced G1/S transition of G0-arrested estrogen-dependent breast cancer cells is regulated by mitochondrial oxidant signaling**. *Oncogene* 2005, **24**(31):4883-4893.
101. Kansanen E, Kuosmanen SM, Leinonen H, Levonen AL: **The Keap1-Nrf2 pathway: Mechanisms of activation and dysregulation in cancer**. *Redox biology* 2013, **1**(1):45-49.
102. Ishikawa T: **Genetic polymorphism in the NRF2 gene as a prognosis marker for cancer chemotherapy**. *Frontiers in genetics* 2014, **5**:383.
103. Griffith OW: **Mechanism of action, metabolism, and toxicity of buthionine sulfoximine and its higher homologs, potent inhibitors of glutathione synthesis**. *The Journal of biological chemistry* 1982, **257**(22):13704-13712.
104. Trachootham D, Zhou Y, Zhang H, Demizu Y, Chen Z, Pelicano H, Chiao PJ, Achanta G, Arlinghaus RB, Liu J *et al*: **Selective killing of oncogenically transformed cells through a ROS-mediated mechanism by beta-phenylethyl isothiocyanate**. *Cancer Cell* 2006, **10**(3):241-252.
105. Seo SK, Lee HC, Woo SH, Jin HO, Yoo DH, Lee SJ, An S, Choe TB, Park MJ, Hong SI *et al*: **Sulindac-derived reactive oxygen species induce apoptosis of human multiple myeloma cells via p38 mitogen activated protein kinase-induced mitochondrial dysfunction**. *Apoptosis : an international journal on programmed cell death* 2007, **12**(1):195-209.
106. Lee S, Lim MJ, Kim MH, Yu CH, Yun YS, Ahn J, Song JY: **An effective strategy for increasing the radiosensitivity of Human lung Cancer cells by blocking Nrf2-dependent antioxidant responses**. *Free radical biology & medicine* 2012, **53**(4):807-816.
107. Hegi ME, Diserens AC, Gorlia T, Hamou MF, de Tribolet N, Weller M, Kros JM, Hainfellner JA, Mason W, Mariani L *et al*: **MGMT gene silencing and benefit from temozolomide in glioblastoma**. *N Engl J Med* 2005, **352**(10):997-1003.
108. Kaina B, Margison GP, Christmann M: **Targeting O(6)-methylguanine-DNA methyltransferase with specific inhibitors as a strategy in cancer therapy**. *Cellular and molecular life sciences : CMLS* 2010, **67**(21):3663-3681.
109. Kaina B, Muhlhausen U, Piee-Staffa A, Christmann M, Garcia Boy R, Rosch F, Schirrmacher R: **Inhibition of O6-methylguanine-DNA methyltransferase by glucose-conjugated inhibitors: comparison with nonconjugated inhibitors and effect on fotemustine and temozolomide-induced cell death**. *J Pharmacol Exp Ther* 2004, **311**(2):585-593.
110. Starcevic D, Dalal S, Sweasy JB: **Is there a link between DNA polymerase beta and cancer?** *Cell Cycle* 2004, **3**(8):998-1001.
111. Sweasy JB, Lang T, DiMaio D: **Is base excision repair a tumor suppressor mechanism?** *Cell Cycle* 2006, **5**(3):250-259.
112. Abbotts R, Madhusudan S: **Human AP endonuclease 1 (APE1): from mechanistic insights to druggable target in cancer**. *Cancer treatment reviews* 2010, **36**(5):425-435.
113. Hirai K, Ueda K, Hayaishi O: **Aberration of poly(adenosine diphosphate-ribose) metabolism in human colon adenomatous polyps and cancers**. *Cancer Res* 1983, **43**(7):3441-3446.

114. Zaremba T, Ketzer P, Cole M, Coulthard S, Plummer ER, Curtin NJ: **Poly(ADP-ribose) polymerase-1 polymorphisms, expression and activity in selected human tumour cell lines**. *Br J Cancer* 2009, **101**(2):256-262.
115. Rouleau M, Patel A, Hendzel MJ, Kaufmann SH, Poirier GG: **PARP inhibition: PARP1 and beyond**. *Nature reviews Cancer* 2010, **10**(4):293-301.
116. Andressoo JO, Hoeijmakers JH, de Waard H: **Nucleotide excision repair and its connection with cancer and ageing**. *Advances in experimental medicine and biology* 2005, **570**:45-83.
117. Koberle B, Grimaldi KA, Sunters A, Hartley JA, Kelland LR, Masters JR: **DNA repair capacity and cisplatin sensitivity of human testis tumour cells**. *Int J Cancer* 1997, **70**(5):551-555.
118. Prewett M, Deevi DS, Bassi R, Fan F, Ellis LM, Hicklin DJ, Tonra JR: **Tumors established with cell lines selected for oxaliplatin resistance respond to oxaliplatin if combined with cetuximab**. *Clin Cancer Res* 2007, **13**(24):7432-7440.
119. Auerbach AD, Weiner MA, Warburton D, Yeboa K, Lu L, Broxmeyer HE: **Acute myeloid leukemia as the first hematologic manifestation of Fanconi anemia**. *American journal of hematology* 1982, **12**(3):289-300.
120. Willems P, Claes K, Baeyens A, Vandersickel V, Werbrouck J, De Ruyck K, Poppe B, Van den Broecke R, Makar A, Marras E *et al*: **Polymorphisms in nonhomologous end-joining genes associated with breast cancer risk and chromosomal radiosensitivity**. *Genes, chromosomes & cancer* 2008, **47**(2):137-148.
121. Liu Y, Zhou K, Zhang H, Shugart YY, Chen L, Xu Z, Zhong Y, Liu H, Jin L, Wei Q *et al*: **Polymorphisms of LIG4 and XRCC4 involved in the NHEJ pathway interact to modify risk of glioma**. *Human mutation* 2008, **29**(3):381-389.
122. Woodbine L, Gennery AR, Jeggo PA: **The clinical impact of deficiency in DNA non-homologous end-joining**. *DNA repair* 2014, **16**:84-96.
123. Zhao Y, Thomas HD, Batey MA, Cowell IG, Richardson CJ, Griffin RJ, Calvert AH, Newell DR, Smith GC, Curtin NJ: **Preclinical evaluation of a potent novel DNA-dependent protein kinase inhibitor NU7441**. *Cancer Res* 2006, **66**(10):5354-5362.
124. Powell SN, Kachnic LA: **Roles of BRCA1 and BRCA2 in homologous recombination, DNA replication fidelity and the cellular response to ionizing radiation**. *Oncogene* 2003, **22**(37):5784-5791.
125. Garrett MD, Collins I: **Anticancer therapy with checkpoint inhibitors: what, where and when?** *Trends in pharmacological sciences* 2011, **32**(5):308-316.
126. Niida H, Murata K, Shimada M, Ogawa K, Ohta K, Suzuki K, Fujigaki H, Khaw AK, Banerjee B, Hande MP *et al*: **Cooperative functions of Chk1 and Chk2 reduce tumour susceptibility in vivo**. *The EMBO journal* 2010, **29**(20):3558-3570.
127. Lainchbury M, Matthews TP, McHardy T, Boxall KJ, Walton MI, Eve PD, Hayes A, Valenti MR, de Haven Brandon AK, Box G *et al*: **Discovery of 3-alkoxyamino-5-(pyridin-2-ylamino)pyrazine-2-carbonitriles as selective, orally bioavailable CHK1 inhibitors**. *Journal of medicinal chemistry* 2012, **55**(22):10229-10240.

128. Soussi T, Dehouche K, Beroud C: **p53 website and analysis of p53 gene mutations in human cancer: forging a link between epidemiology and carcinogenesis**. *Human mutation* 2000, **15**(1):105-113.
129. Wang Z, Sun Y: **Targeting p53 for Novel Anticancer Therapy**. *Translational oncology* 2010, **3**(1):1-12.
130. Bykov VJ, Wiman KG: **Mutant p53 reactivation by small molecules makes its way to the clinic**. *FEBS letters* 2014, **588**(16):2622-2627.
131. Lynch HT, Snyder CL, Shaw TG, Heinen CD, Hitchins MP: **Milestones of Lynch syndrome: 1895-2015**. *Nature reviews Cancer* 2015.
132. Fink D, Aebi S, Howell SB: **The role of DNA mismatch repair in drug resistance**. *Clin Cancer Res* 1998, **4**(1):1-6.
133. Stojic L, Brun R, Jiricny J: **Mismatch repair and DNA damage signalling**. *DNA repair* 2004, **3**(8-9):1091-1101.
134. Hewish M, Lord CJ, Martin SA, Cunningham D, Ashworth A: **Mismatch repair deficient colorectal cancer in the era of personalized treatment**. *Nature reviews Clinical oncology* 2010, **7**(4):197-208.
135. Martin SA, Lord CJ, Ashworth A: **Therapeutic targeting of the DNA mismatch repair pathway**. *Clin Cancer Res* 2010, **16**(21):5107-5113.
136. Guillotin D, Martin SA: **Exploiting DNA mismatch repair deficiency as a therapeutic strategy**. *Exp Cell Res* 2014, **329**(1):110-115.
137. Khan OA, Ranson M, Michael M, Olver I, Levitt NC, Mortimer P, Watson AJ, Margison GP, Midgley R, Middleton MR: **A phase II trial of lomeguatrib and temozolomide in metastatic colorectal cancer**. *Br J Cancer* 2008, **98**(10):1614-1618.
138. Iyer RR, Pluciennik A, Burdett V, Modrich PL: **DNA mismatch repair: functions and mechanisms**. *Chemical reviews* 2006, **106**(2):302-323.
139. Obmolova G, Ban C, Hsieh P, Yang W: **Crystal structures of mismatch repair protein MutS and its complex with a substrate DNA**. *Nature* 2000, **407**(6805):703-710.
140. de Wind N, Dekker M, Claij N, Jansen L, van Klink Y, Radman M, Riggins G, van der Valk M, van't Wout K, te Riele H: **HNPCC-like cancer predisposition in mice through simultaneous loss of Msh3 and Msh6 mismatch-repair protein functions**. *Nature genetics* 1999, **23**(3):359-362.
141. Constantin N, Dzantiev L, Kadyrov FA, Modrich P: **Human mismatch repair: reconstitution of a nick-directed bidirectional reaction**. *The Journal of biological chemistry* 2005, **280**(48):39752-39761.
142. Jiricny J: **The multifaceted mismatch-repair system**. *Nature reviews Molecular cell biology* 2006, **7**(5):335-346.
143. Cannavo E, Marra G, Sabates-Bellver J, Menigatti M, Lipkin SM, Fischer F, Cejka P, Jiricny J: **Expression of the MutL homologue hMLH3 in human cells and its role in DNA mismatch repair**. *Cancer Res* 2005, **65**(23):10759-10766.
144. Ranjha L, Anand R, Cejka P: **The Saccharomyces cerevisiae Mlh1-Mlh3 heterodimer is an endonuclease that preferentially binds to Holliday junctions**. *The Journal of biological chemistry* 2014, **289**(9):5674-5686.
145. Kadyrov FA, Dzantiev L, Constantin N, Modrich P: **Endonucleolytic function of MutLalpha in human mismatch repair**. *Cell* 2006, **126**(2):297-308.

146. Langle-Rouault F, Maenhaut-Michel G, Radman M: **GATC sequences, DNA nicks and the MutH function in Escherichia coli mismatch repair**. *The EMBO journal* 1987, **6**(4):1121-1127.
147. Ghodgaonkar MM, Lazzaro F, Olivera-Pimentel M, Artola-Boran M, Cejka P, Reijns MA, Jackson AP, Plevani P, Muzi-Falconi M, Jiricny J: **Ribonucleotides misincorporated into DNA act as strand-discrimination signals in eukaryotic mismatch repair**. *Molecular cell* 2013, **50**(3):323-332.
148. Nick McElhinny SA, Watts BE, Kumar D, Watt DL, Lundstrom EB, Burgers PM, Johansson E, Chabes A, Kunkel TA: **Abundant ribonucleotide incorporation into DNA by yeast replicative polymerases**. *Proceedings of the National Academy of Sciences of the United States of America* 2010, **107**(11):4949-4954.
149. Nick McElhinny SA, Kumar D, Clark AB, Watt DL, Watts BE, Lundstrom EB, Johansson E, Chabes A, Kunkel TA: **Genome instability due to ribonucleotide incorporation into DNA**. *Nature chemical biology* 2010, **6**(10):774-781.
150. Zhang Y, Yuan F, Presnell SR, Tian K, Gao Y, Tomkinson AE, Gu L, Li GM: **Reconstitution of 5'-directed human mismatch repair in a purified system**. *Cell* 2005, **122**(5):693-705.
151. Ramilo C, Gu L, Guo S, Zhang X, Patrick SM, Turchi JJ, Li GM: **Partial reconstitution of human DNA mismatch repair in vitro: characterization of the role of human replication protein A**. *Molecular and cellular biology* 2002, **22**(7):2037-2046.
152. Lau PJ, Kolodner RD: **Transfer of the MSH2.MSH6 complex from proliferating cell nuclear antigen to mispaired bases in DNA**. *The Journal of biological chemistry* 2003, **278**(1):14-17.
153. Pluciennik A, Dzantiev L, Iyer RR, Constantin N, Kadyrov FA, Modrich P: **PCNA function in the activation and strand direction of MutLalpha endonuclease in mismatch repair**. *Proceedings of the National Academy of Sciences of the United States of America* 2010, **107**(37):16066-16071.
154. Li LS, Morales JC, Veigl M, Sedwick D, Greer S, Meyers M, Wagner M, Fishel R, Boothman DA: **DNA mismatch repair (MMR)-dependent 5-fluorouracil cytotoxicity and the potential for new therapeutic targets**. *British journal of pharmacology* 2009, **158**(3):679-692.
155. Li GM: **Mechanisms and functions of DNA mismatch repair**. *Cell research* 2008, **18**(1):85-98.
156. Liu A, Yoshioka K, Salerno V, Hsieh P: **The mismatch repair-mediated cell cycle checkpoint response to fluorodeoxyuridine**. *Journal of cellular biochemistry* 2008, **105**(1):245-254.
157. Meyers M, Hwang A, Wagner MW, Bruening AJ, Veigl ML, Sedwick WD, Boothman DA: **A role for DNA mismatch repair in sensing and responding to fluoropyrimidine damage**. *Oncogene* 2003, **22**(47):7376-7388.
158. Pabla N, Ma Z, McIlhatton MA, Fishel R, Dong Z: **hMSH2 recruits ATR to DNA damage sites for activation during DNA damage-induced apoptosis**. *The Journal of biological chemistry* 2011, **286**(12):10411-10418.
159. Liu Y, Fang Y, Shao H, Lindsey-Boltz L, Sancar A, Modrich P: **Interactions of human mismatch repair proteins MutSalpha and MutLalpha with**

proteins of the ATR-Chk1 pathway. *The Journal of biological chemistry* 2010, **285**(8):5974-5982.
160. Palombo F, Gallinari P, Iaccarino I, Lettieri T, Hughes M, D'Arrigo A, Truong O, Hsuan JJ, Jiricny J: **GTBP, a 160-kilodalton protein essential for mismatch-binding activity in human cells**. *Science* 1995, **268**(5219):1912-1914.
161. Warren JJ, Pohlhaus TJ, Changela A, Iyer RR, Modrich PL, Beese LS: **Structure of the human MutSalpha DNA lesion recognition complex**. *Molecular cell* 2007, **26**(4):579-592.
162. Edelbrock MA, Kaliyaperumal S, Williams KJ: **Structural, molecular and cellular functions of MSH2 and MSH6 during DNA mismatch repair, damage signaling and other noncanonical activities**. *Mutation research* 2013, **743-744**:53-66.
163. Christmann M, Kaina B: **Nuclear translocation of mismatch repair proteins MSH2 and MSH6 as a response of cells to alkylating agents**. *The Journal of biological chemistry* 2000, **275**(46):36256-36262.
164. Umar A, Buermeyer AB, Simon JA, Thomas DC, Clark AB, Liskay RM, Kunkel TA: **Requirement for PCNA in DNA mismatch repair at a step preceding DNA resynthesis**. *Cell* 1996, **87**(1):65-73.
165. Kleczkowska HE, Marra G, Lettieri T, Jiricny J: **hMSH3 and hMSH6 interact with PCNA and colocalize with it to replication foci**. *Genes & development* 2001, **15**(6):724-736.
166. Bak ST, Sakellariou D, Pena-Diaz J: **The dual nature of mismatch repair as antimutator and mutator: for better or for worse**. *Frontiers in genetics* 2014, **5**:287.
167. Colussi C, Parlanti E, Degan P, Aquilina G, Barnes D, Macpherson P, Karran P, Crescenzi M, Dogliotti E, Bignami M: **The mammalian mismatch repair pathway removes DNA 8-oxodGMP incorporated from the oxidized dNTP pool**. *Current biology : CB* 2002, **12**(11):912-918.
168. DeWeese TL, Shipman JM, Larrier NA, Buckley NM, Kidd LR, Groopman JD, Cutler RG, te Riele H, Nelson WG: **Mouse embryonic stem cells carrying one or two defective Msh2 alleles respond abnormally to oxidative stress inflicted by low-level radiation**. *Proceedings of the National Academy of Sciences of the United States of America* 1998, **95**(20):11915-11920.
169. Mazurek A, Berardini M, Fishel R: **Activation of human MutS homologs by 8-oxo-guanine DNA damage**. *The Journal of biological chemistry* 2002, **277**(10):8260-8266.
170. Ni TT, Marsischky GT, Kolodner RD: **MSH2 and MSH6 are required for removal of adenine misincorporated opposite 8-oxo-guanine in S. cerevisiae**. *Molecular cell* 1999, **4**(3):439-444.
171. Earley MC, Crouse GF: **The role of mismatch repair in the prevention of base pair mutations in Saccharomyces cerevisiae**. *Proceedings of the National Academy of Sciences of the United States of America* 1998, **95**(26):15487-15491.
172. Gu Y, Parker A, Wilson TM, Bai H, Chang DY, Lu AL: **Human MutY homolog, a DNA glycosylase involved in base excision repair, physically and functionally interacts with mismatch repair proteins human MutS homolog 2/human MutS homolog 6**. *The Journal of biological chemistry* 2002, **277**(13):11135-11142.

173. Russo MT, De Luca G, Casorelli I, Degan P, Molatore S, Barone F, Mazzei F, Pannellini T, Musiani P, Bignami M: **Role of MUTYH and MSH2 in the control of oxidative DNA damage, genetic instability, and tumorigenesis**. *Cancer Res* 2009, **69**(10):4372-4379.
174. Zlatanou A, Despras E, Braz-Petta T, Boubakour-Azzouz I, Pouvelle C, Stewart GS, Nakajima S, Yasui A, Ishchenko AA, Kannouche PL: **The hMsh2-hMsh6 complex acts in concert with monoubiquitinated PCNA and Pol eta in response to oxidative DNA damage in human cells**. *Molecular cell* 2011, **43**(4):649-662.
175. Mojas N, Lopes M, Jiricny J: **Mismatch repair-dependent processing of methylation damage gives rise to persistent single-stranded gaps in newly replicated DNA**. *Genes & development* 2007, **21**(24):3342-3355.
176. Karran P, Hampson R: **Genomic instability and tolerance to alkylating agents**. *Cancer surveys* 1996, **28**:69-85.
177. Shahi A, Lee JH, Kang Y, Lee SH, Hyun JW, Chang IY, Jun JY, You HJ: **Mismatch-repair protein MSH6 is associated with Ku70 and regulates DNA double-strand break repair**. *Nucleic acids research* 2011, **39**(6):2130-2143.
178. Villemure JF, Abaji C, Cousineau I, Belmaaza A: **MSH2-deficient human cells exhibit a defect in the accurate termination of homology-directed repair of DNA double-strand breaks**. *Cancer Res* 2003, **63**(12):3334-3339.
179. Smith JA, Bannister LA, Bhattacharjee V, Wang Y, Waldman BC, Waldman AS: **Accurate homologous recombination is a prominent double-strand break repair pathway in mammalian chromosomes and is modulated by mismatch repair protein Msh2**. *Molecular and cellular biology* 2007, **27**(22):7816-7827.
180. Chen W, Jinks-Robertson S: **The role of the mismatch repair machinery in regulating mitotic and meiotic recombination between diverged sequences in yeast**. *Genetics* 1999, **151**(4):1299-1313.
181. Spell RM, Jinks-Robertson S: **Role of mismatch repair in the fidelity of RAD51- and RAD59-dependent recombination in Saccharomyces cerevisiae**. *Genetics* 2003, **165**(4):1733-1744.
182. Colombino M, Avallone A, Izzo F, Tatangelo F, Budroni M, Cossu A, Galimi F, Comella P, Botti G, Sini MC *et al*: **Molecular analysis of Fanconi anemia and mismatch repair genes in patients with colorectal carcinoma**. *Oncology reports* 2011, **25**(4):899-904.
183. van de Vrugt HJ, Eaton L, Hanlon Newell A, Al-Dhalimy M, Liskay RM, Olson SB, Grompe M: **Embryonic lethality after combined inactivation of Fancd2 and Mlh1 in mice**. *Cancer Res* 2009, **69**(24):9431-9438.
184. Williams SA, Wilson JB, Clark AP, Mitson-Salazar A, Tomashevski A, Ananth S, Glazer PM, Semmes OJ, Bale AE, Jones NJ *et al*: **Functional and physical interaction between the mismatch repair and FA-BRCA pathways**. *Human molecular genetics* 2011, **20**(22):4395-4410.
185. Peng M, Xie J, Ucher A, Stavnezer J, Cantor SB: **Crosstalk between BRCA-Fanconi anemia and mismatch repair pathways prevents MSH2-dependent aberrant DNA damage responses**. *The EMBO journal* 2014, **33**(15):1698-1712.
186. Chahwan R, Edelmann W, Scharff MD, Roa S: **Mismatch-mediated error prone repair at the immunoglobulin genes**. *Biomed Pharmacother* 2011, **65**(8):529-536.

187. Kadyrova LY, Blanko ER, Kadyrov FA: **CAF-I-dependent control of degradation of the discontinuous strands during mismatch repair**. *Proceedings of the National Academy of Sciences of the United States of America* 2011, **108**(7):2753-2758.
188. Schopf B, Bregenhorn S, Quivy JP, Kadyrov FA, Almouzni G, Jiricny J: **Interplay between mismatch repair and chromatin assembly**. *Proceedings of the National Academy of Sciences of the United States of America* 2012, **109**(6):1895-1900.
189. Kadyrova LY, Mertz TM, Zhang Y, Northam MR, Sheng Z, Lobachev KS, Shcherbakova PV, Kadyrov FA: **A reversible histone H3 acetylation cooperates with mismatch repair and replicative polymerases in maintaining genome stability**. *PLoS genetics* 2013, **9**(10):e1003899.
190. Li F, Mao G, Tong D, Huang J, Gu L, Yang W, Li GM: **The histone mark H3K36me3 regulates human DNA mismatch repair through its interaction with MutSalpha**. *Cell* 2013, **153**(3):590-600.
191. Kanu N, Gronroos E, Martinez P, Burrell RA, Yi Goh X, Bartkova J, Maya-Mendoza A, Mistrik M, Rowan AJ, Patel H *et al*: **SETD2 loss-of-function promotes renal cancer branched evolution through replication stress and impaired DNA repair**. *Oncogene* 2015.
192. Kaliyaperumal S, Patrick SM, Williams KJ: **Phosphorylated hMSH6: DNA mismatch versus DNA damage recognition**. *Mutation research* 2011, **706**(1-2):36-45.
193. Shen T, Huang S: **The role of Cdc25A in the regulation of cell proliferation and apoptosis**. *Anticancer Agents Med Chem* 2012, **12**(6):631-639.
194. Marumoto T, Honda S, Hara T, Nitta M, Hirota T, Kohmura E, Saya H: **Aurora-A kinase maintains the fidelity of early and late mitotic events in HeLa cells**. *The Journal of biological chemistry* 2003, **278**(51):51786-51795.
195. Aarnio M, Mecklin JP, Aaltonen LA, Nystrom-Lahti M, Jarvinen HJ: **Life-time risk of different cancers in hereditary non-polyposis colorectal cancer (HNPCC) syndrome**. *Int J Cancer* 1995, **64**(6):430-433.
196. Amjad AI, Singhi AD, Balaban EP, Dudley B, Brand RE, Bahary N: **First reported case of a squamous cell carcinoma arising in the duodenum in a patient with Lynch syndrome**. *International journal of clinical and experimental pathology* 2014, **7**(12):8988-8995.
197. Therkildsen C, Ladelund S, Rambech E, Persson A, Petersen A, Nilbert M: **Glioblastomas, astrocytomas and oligodendrogliomas linked to Lynch syndrome**. *European journal of neurology : the official journal of the European Federation of Neurological Societies* 2015.
198. Watson P, Vasen HF, Mecklin JP, Bernstein I, Aarnio M, Jarvinen HJ, Myrhoj T, Sunde L, Wijnen JT, Lynch HT: **The risk of extra-colonic, extra-endometrial cancer in the Lynch syndrome**. *Int J Cancer* 2008, **123**(2):444-449.
199. Lynch HT, Lynch PM, Pester J, Fusaro RM: **The cancer family syndrome. Rare cutaneous phenotypic linkage of Torre's syndrome**. *Archives of internal medicine* 1981, **141**(5):607-611.
200. Kastrinos F, Mukherjee B, Tayob N, Wang F, Sparr J, Raymond VM, Bandipalliam P, Stoffel EM, Gruber SB, Syngal S: **Risk of pancreatic cancer in families with Lynch syndrome**. *Jama* 2009, **302**(16):1790-1795.

201. Win AK, Young JP, Lindor NM, Tucker KM, Ahnen DJ, Young GP, Buchanan DD, Clendenning M, Giles GG, Winship I *et al*: **Colorectal and other cancer risks for carriers and noncarriers from families with a DNA mismatch repair gene mutation: a prospective cohort study**. *Journal of clinical oncology : official journal of the American Society of Clinical Oncology* 2012, **30**(9):958-964.
202. Bauer CM, Ray AM, Halstead-Nussloch BA, Dekker RG, Raymond VM, Gruber SB, Cooney KA: **Hereditary prostate cancer as a feature of Lynch syndrome**. *Familial cancer* 2011, **10**(1):37-42.
203. Raymond VM, Everett JN, Furtado LV, Gustafson SL, Jungbluth CR, Gruber SB, Hammer GD, Stoffel EM, Greenson JK, Giordano TJ *et al*: **Adrenocortical carcinoma is a lynch syndrome-associated cancer**. *Journal of clinical oncology : official journal of the American Society of Clinical Oncology* 2013, **31**(24):3012-3018.
204. Wimmer K, Kratz CP: **Constitutional mismatch repair-deficiency syndrome**. *Haematologica* 2010, **95**(5):699-701.
205. Plazzer JP, Sijmons RH, Woods MO, Peltomaki P, Thompson B, Den Dunnen JT, Macrae F: **The InSiGHT database: utilizing 100 years of insights into Lynch syndrome**. *Familial cancer* 2013, **12**(2):175-180.
206. Hitchins MP: **The role of epigenetics in Lynch syndrome**. *Familial cancer* 2013, **12**(2):189-205.
207. Verma L, Kane MF, Brassett C, Schmeits J, Evans DG, Kolodner RD, Maher ER: **Mononucleotide microsatellite instability and germline MSH6 mutation analysis in early onset colorectal cancer**. *Journal of medical genetics* 1999, **36**(9):678-682.
208. Beggs AD, Domingo E, Abulafi M, Hodgson SV, Tomlinson IP: **A study of genomic instability in early preneoplastic colonic lesions**. *Oncogene* 2013, **32**(46):5333-5337.
209. Nagasaka T, Rhees J, Kloor M, Gebert J, Naomoto Y, Boland CR, Goel A: **Somatic hypermethylation of MSH2 is a frequent event in Lynch Syndrome colorectal cancers**. *Cancer Res* 2010, **70**(8):3098-3108.
210. Moura Lima E, Ferreira Leal M, Cardoso Smith Mde A, Rodriguez Burbano R, Pimentel de Assumpcao P, Bello MJ, Rey JA, Ferreira de Lima F, Casartelli C: **DNA mismatch repair gene methylation in gastric cancer in individuals from northern Brazil**. *Biocell : official journal of the Sociedades Latinoamericanas de Microscopia Electronica et al* 2008, **32**(3):237-243.
211. Popat S, Hubner R, Houlston RS: **Systematic review of microsatellite instability and colorectal cancer prognosis**. *Journal of clinical oncology : official journal of the American Society of Clinical Oncology* 2005, **23**(3):609-618.
212. Drescher KM, Sharma P, Lynch HT: **Current hypotheses on how microsatellite instability leads to enhanced survival of Lynch Syndrome patients**. *Clinical & developmental immunology* 2010, **2010**:170432.
213. Boissiere-Michot F, Lazennec G, Frugier H, Jarlier M, Roca L, Duffour J, Du Paty E, Laune D, Blanchard F, Le Pessot F *et al*: **Characterization of an adaptive immune response in microsatellite-instable colorectal cancer**. *Oncoimmunology* 2014, **3**:e29256.

214. Xiao Y, Freeman GJ: **The microsatellite instable subset of colorectal cancer is a particularly good candidate for checkpoint blockade immunotherapy**. *Cancer discovery* 2015, **5**(1):16-18.
215. Llosa NJ, Cruise M, Tam A, Wicks EC, Hechenbleikner EM, Taube JM, Blosser RL, Fan H, Wang H, Luber BS *et al*: **The vigorous immune microenvironment of microsatellite instable colon cancer is balanced by multiple counter-inhibitory checkpoints**. *Cancer discovery* 2015, **5**(1):43-51.
216. Edelmann W, Yang K, Umar A, Heyer J, Lau K, Fan K, Liedtke W, Cohen PE, Kane MF, Lipford JR *et al*: **Mutation in the mismatch repair gene Msh6 causes cancer susceptibility**. *Cell* 1997, **91**(4):467-477.
217. Wei K, Kucherlapati R, Edelmann W: **Mouse models for human DNA mismatch-repair gene defects**. *Trends in molecular medicine* 2002, **8**(7):346-353.
218. de Wind N, Dekker M, Berns A, Radman M, te Riele H: **Inactivation of the mouse Msh2 gene results in mismatch repair deficiency, methylation tolerance, hyperrecombination, and predisposition to cancer**. *Cell* 1995, **82**(2):321-330.
219. Umar A, Boland CR, Terdiman JP, Syngal S, de la Chapelle A, Ruschoff J, Fishel R, Lindor NM, Burgart LJ, Hamelin R *et al*: **Revised Bethesda Guidelines for hereditary nonpolyposis colorectal cancer (Lynch syndrome) and microsatellite instability**. *Journal of the National Cancer Institute* 2004, **96**(4):261-268.
220. Imai K, Yamamoto H: **Carcinogenesis and microsatellite instability: the interrelationship between genetics and epigenetics**. *Carcinogenesis* 2008, **29**(4):673-680.
221. Zhang L: **Immunohistochemistry versus microsatellite instability testing for screening colorectal cancer patients at risk for hereditary nonpolyposis colorectal cancer syndrome. Part II. The utility of microsatellite instability testing**. *The Journal of molecular diagnostics : JMD* 2008, **10**(4):301-307.
222. Boland CR, Thibodeau SN, Hamilton SR, Sidransky D, Eshleman JR, Burt RW, Meltzer SJ, Rodriguez-Bigas MA, Fodde R, Ranzani GN *et al*: **A National Cancer Institute Workshop on Microsatellite Instability for cancer detection and familial predisposition: development of international criteria for the determination of microsatellite instability in colorectal cancer**. *Cancer Res* 1998, **58**(22):5248-5257.
223. Perucho M: **Correspondence re: C.R. Boland et al., A National Cancer Institute workshop on microsatellite instability for cancer detection and familial predisposition: development of international criteria for the determination of microsatellite instability in colorectal cancer. Cancer Res., 58: 5248-5257, 1998**. *Cancer Res* 1999, **59**(1):249-256.
224. Ogino S, Goel A: **Molecular classification and correlates in colorectal cancer**. *The Journal of molecular diagnostics : JMD* 2008, **10**(1):13-27.
225. Pritchard CC, Smith C, Salipante SJ, Lee MK, Thornton AM, Nord AS, Gulden C, Kupfer SS, Swisher EM, Bennett RL *et al*: **ColoSeq provides comprehensive lynch and polyposis syndrome mutational analysis using massively parallel sequencing**. *The Journal of molecular diagnostics : JMD* 2012, **14**(4):357-366.

226. Jarvinen HJ, Renkonen-Sinisalo L, Aktan-Collan K, Peltomaki P, Aaltonen LA, Mecklin JP: **Ten years after mutation testing for Lynch syndrome: cancer incidence and outcome in mutation-positive and mutation-negative family members**. *Journal of clinical oncology : official journal of the American Society of Clinical Oncology* 2009, **27**(28):4793-4797.
227. Cragun D, Radford C, Dolinsky JS, Caldwell M, Chao E, Pal T: **Panel-based testing for inherited colorectal cancer: a descriptive study of clinical testing performed by a US laboratory**. *Clinical genetics* 2014, **86**(6):510-520.
228. Shia J: **Immunohistochemistry versus microsatellite instability testing for screening colorectal cancer patients at risk for hereditary nonpolyposis colorectal cancer syndrome. Part I. The utility of immunohistochemistry**. *The Journal of molecular diagnostics : JMD* 2008, **10**(4):293-300.
229. (TCGA) TCGA: **Comprehensive molecular characterization of human colon and rectal cancer**. *Nature* 2012, **487**(7407):330-337.
230. Markowitz SD, Roberts AB: **Tumor suppressor activity of the TGF-beta pathway in human cancers**. *Cytokine & growth factor reviews* 1996, **7**(1):93-102.
231. Huang J, Papadopoulos N, McKinley AJ, Farrington SM, Curtis LJ, Wyllie AH, Zheng S, Willson JK, Markowitz SD, Morin P *et al*: **APC mutations in colorectal tumors with mismatch repair deficiency**. *Proceedings of the National Academy of Sciences of the United States of America* 1996, **93**(17):9049-9054.
232. Souza RF, Appel R, Yin J, Wang S, Smolinski KN, Abraham JM, Zou TT, Shi YQ, Lei J, Cottrell J *et al*: **Microsatellite instability in the insulin-like growth factor II receptor gene in gastrointestinal tumours**. *Nature genetics* 1996, **14**(3):255-257.
233. Rampino N, Yamamoto H, Ionov Y, Li Y, Sawai H, Reed JC, Perucho M: **Somatic frameshift mutations in the BAX gene in colon cancers of the microsatellite mutator phenotype**. *Science* 1997, **275**(5302):967-969.
234. Duval A, Hamelin R: **Mutations at coding repeat sequences in mismatch repair-deficient human cancers: toward a new concept of target genes for instability**. *Cancer Res* 2002, **62**(9):2447-2454.
235. Yip S, Miao J, Cahill DP, Iafrate AJ, Aldape K, Nutt CL, Louis DN: **MSH6 mutations arise in glioblastomas during temozolomide therapy and mediate temozolomide resistance**. *Clin Cancer Res* 2009, **15**(14):4622-4629.
236. Zhang J, Stevens MF, Laughton CA, Madhusudan S, Bradshaw TD: **Acquired resistance to temozolomide in glioma cell lines: molecular mechanisms and potential translational applications**. *Oncology* 2010, **78**(2):103-114.
237. Kat A, Thilly WG, Fang WH, Longley MJ, Li GM, Modrich P: **An alkylation-tolerant, mutator human cell line is deficient in strand-specific mismatch repair**. *Proceedings of the National Academy of Sciences of the United States of America* 1993, **90**(14):6424-6428.
238. Fink D, Nebel S, Norris PS, Aebi S, Kim HK, Haas M, Howell SB: **The effect of different chemotherapeutic agents on the enrichment of DNA mismatch repair-deficient tumour cells**. *Br J Cancer* 1998, **77**(5):703-708.
239. Koi M, Umar A, Chauhan DP, Cherian SP, Carethers JM, Kunkel TA, Boland CR: **Human chromosome 3 corrects mismatch repair deficiency**

and microsatellite instability and reduces N-methyl-N'-nitro-N-nitrosoguanidine tolerance in colon tumor cells with homozygous hMLH1 mutation. *Cancer Res* 1994, **54**(16):4308-4312.

240. Sherman SE, Lippard SJ: **Structural aspects of platinum anticancer drug interactions with DNA**. *Chemical reviews* 1987, **87**(5):1153-1181.
241. Aebi S, Kurdi-Haidar B, Gordon R, Cenni B, Zheng H, Fink D, Christen RD, Boland CR, Koi M, Fishel R *et al*: **Loss of DNA mismatch repair in acquired resistance to cisplatin**. *Cancer Res* 1996, **56**(13):3087-3090.
242. Strathdee G, MacKean MJ, Illand M, Brown R: **A role for methylation of the hMLH1 promoter in loss of hMLH1 expression and drug resistance in ovarian cancer**. *Oncogene* 1999, **18**(14):2335-2341.
243. Watanabe Y, Koi M, Hemmi H, Hoshai H, Noda K: **A change in microsatellite instability caused by cisplatin-based chemotherapy of ovarian cancer**. *Br J Cancer* 2001, **85**(7):1064-1069.
244. Fink D, Nebel S, Norris PS, Baergen RN, Wilczynski SP, Costa MJ, Haas M, Cannistra SA, Howell SB: **Enrichment for DNA mismatch repair-deficient cells during treatment with cisplatin**. *Int J Cancer* 1998, **77**(5):741-746.
245. Ercoli A, Ferrandina G, Raspaglio G, Marone M, Maggiano N, Del Mastro P, Benedetti Panici P, Mancuso S, Scambia G: **hMSH2 and GTBP expression in advanced stage epithelial ovarian cancer**. *Br J Cancer* 1999, **80**(10):1665-1671.
246. Samimi G, Fink D, Varki NM, Husain A, Hoskins WJ, Alberts DS, Howell SB: **Analysis of MLH1 and MSH2 expression in ovarian cancer before and after platinum drug-based chemotherapy**. *Clin Cancer Res* 2000, **6**(4):1415-1421.
247. Martin LM, Marples B, Coffey M, Lawler M, Lynch TH, Hollywood D, Marignol L: **DNA mismatch repair and the DNA damage response to ionizing radiation: making sense of apparently conflicting data**. *Cancer treatment reviews* 2010, **36**(7):518-527.
248. Franchitto A, Pichierri P, Piergentili R, Crescenzi M, Bignami M, Palitti F: **The mammalian mismatch repair protein MSH2 is required for correct MRE11 and RAD51 relocalization and for efficient cell cycle arrest induced by ionizing radiation in G2 phase**. *Oncogene* 2003, **22**(14):2110-2120.
249. Barwell J, Pangon L, Hodgson S, Georgiou A, Kesterton I, Slade T, Taylor M, Payne SJ, Brinkman H, Smythe J *et al*: **Biallelic mutation of MSH2 in primary human cells is associated with sensitivity to irradiation and altered RAD51 foci kinetics**. *Journal of medical genetics* 2007, **44**(8):516-520.
250. Colis LC, Raychaudhury P, Basu AK: **Mutational specificity of gamma-radiation-induced guanine-thymine and thymine-guanine intrastrand cross-links in mammalian cells and translesion synthesis past the guanine-thymine lesion by human DNA polymerase eta**. *Biochemistry* 2008, **47**(31):8070-8079.
251. Froelich-Ammon SJ, Osheroff N: **Topoisomerase poisons: harnessing the dark side of enzyme mechanism**. *The Journal of biological chemistry* 1995, **270**(37):21429-21432.
252. Simon JA, Szankasi P, Nguyen DK, Ludlow C, Dunstan HM, Roberts CJ, Jensen EL, Hartwell LH, Friend SH: **Differential toxicities of anticancer**

agents among DNA repair and checkpoint mutants of Saccharomyces cerevisiae. *Cancer Res* 2000, **60**(2):328-333.
253. Vilar E, Scaltriti M, Balmana J, Saura C, Guzman M, Arribas J, Baselga J, Tabernero J: **Microsatellite instability due to hMLH1 deficiency is associated with increased cytotoxicity to irinotecan in human colorectal cancer cell lines**. *Br J Cancer* 2008, **99**(10):1607-1612.
254. Jacob S, Aguado M, Fallik D, Praz F: **The role of the DNA mismatch repair system in the cytotoxicity of the topoisomerase inhibitors camptothecin and etoposide to human colorectal cancer cells**. *Cancer Res* 2001, **61**(17):6555-6562.
255. Fedier A, Schwarz VA, Walt H, Carpini RD, Haller U, Fink D: **Resistance to topoisomerase poisons due to loss of DNA mismatch repair**. *Int J Cancer* 2001, **93**(4):571-576.
256. Longley DB, Harkin DP, Johnston PG: **5-fluorouracil: mechanisms of action and clinical strategies**. *Nature reviews Cancer* 2003, **3**(5):330-338.
257. Heidelberger C, Chaudhuri NK, Danneberg P, Mooren D, Griesbach L, Duschinsky R, Schnitzer RJ, Pleven E, Scheiner J: **Fluorinated pyrimidines, a new class of tumour-inhibitory compounds**. *Nature* 1957, **179**(4561):663-666.
258. Diasio RB, Harris BE: **Clinical pharmacology of 5-fluorouracil**. *Clinical pharmacokinetics* 1989, **16**(4):215-237.
259. Hemminki A, Mecklin JP, Jarvinen H, Aaltonen LA, Joensuu H: **Microsatellite instability is a favorable prognostic indicator in patients with colorectal cancer receiving chemotherapy**. *Gastroenterology* 2000, **119**(4):921-928.
260. Jover R, Zapater P, Castells A, Llor X, Andreu M, Cubiella J, Balaguer F, Sempere L, Xicola RM, Bujanda L *et al*: **The efficacy of adjuvant chemotherapy with 5-fluorouracil in colorectal cancer depends on the mismatch repair status**. *Eur J Cancer* 2009, **45**(3):365-373.
261. Bracht K, Nicholls AM, Liu Y, Bodmer WF: **5-Fluorouracil response in a large panel of colorectal cancer cell lines is associated with mismatch repair deficiency**. *Br J Cancer* 2010, **103**(3):340-346.
262. Meyers M, Wagner MW, Hwang HS, Kinsella TJ, Boothman DA: **Role of the hMLH1 DNA mismatch repair protein in fluoropyrimidine-mediated cell death and cell cycle responses**. *Cancer Res* 2001, **61**(13):5193-5201.
263. Tajima A, Hess MT, Cabrera BL, Kolodner RD, Carethers JM: **The mismatch repair complex hMutS alpha recognizes 5-fluorouracil-modified DNA: implications for chemosensitivity and resistance**. *Gastroenterology* 2004, **127**(6):1678-1684.
264. Tajima A, Iwaizumi M, Tseng-Rogenski S, Cabrera BL, Carethers JM: **Both hMutSalpha and hMutSss DNA mismatch repair complexes participate in 5-fluorouracil cytotoxicity**. *PloS one* 2011, **6**(12):e28117.
265. Meyers M, Wagner MW, Mazurek A, Schmutte C, Fishel R, Boothman DA: **DNA mismatch repair-dependent response to fluoropyrimidine-generated damage**. *The Journal of biological chemistry* 2005, **280**(7):5516-5526.
266. O'Connell JB, Maggard MA, Ko CY: **Colon cancer survival rates with the new American Joint Committee on Cancer sixth edition staging**. *Journal of the National Cancer Institute* 2004, **96**(19):1420-1425.

267. Gustavsson B, Carlsson G, Machover D, Petrelli N, Roth A, Schmoll HJ, Tveit KM, Gibson F: **A Review of the Evolution of Systemic Chemotherapy in the Management of Colorectal Cancer**. *Clinical colorectal cancer* 2015, **14**(1):1-10.
268. Poon MA, O'Connell MJ, Moertel CG, Wieand HS, Cullinan SA, Everson LK, Krook JE, Mailliard JA, Laurie JA, Tschetter LK *et al*: **Biochemical modulation of fluorouracil: evidence of significant improvement of survival and quality of life in patients with advanced colorectal carcinoma**. *Journal of clinical oncology : official journal of the American Society of Clinical Oncology* 1989, **7**(10):1407-1418.
269. Petrelli N, Herrera L, Rustum Y, Burke P, Creaven P, Stulc J, Emrich LJ, Mittelman A: **A prospective randomized trial of 5-fluorouracil versus 5-fluorouracil and high-dose leucovorin versus 5-fluorouracil and methotrexate in previously untreated patients with advanced colorectal carcinoma**. *Journal of clinical oncology : official journal of the American Society of Clinical Oncology* 1987, **5**(10):1559-1565.
270. Thirion P, Michiels S, Pignon JP, Buyse M, Braud AC, Carlson RW, O'Connell M, Sargent P, Piedbois P: **Modulation of fluorouracil by leucovorin in patients with advanced colorectal cancer: an updated meta-analysis**. *Journal of clinical oncology : official journal of the American Society of Clinical Oncology* 2004, **22**(18):3766-3775.
271. Saltz LB, Cox JV, Blanke C, Rosen LS, Fehrenbacher L, Moore MJ, Maroun JA, Ackland SP, Locker PK, Pirotta N *et al*: **Irinotecan plus fluorouracil and leucovorin for metastatic colorectal cancer. Irinotecan Study Group**. *N Engl J Med* 2000, **343**(13):905-914.
272. Goldberg RM, Sargent DJ, Morton RF, Fuchs CS, Ramanathan RK, Williamson SK, Findlay BP, Pitot HC, Alberts SR: **A randomized controlled trial of fluorouracil plus leucovorin, irinotecan, and oxaliplatin combinations in patients with previously untreated metastatic colorectal cancer**. *Journal of clinical oncology : official journal of the American Society of Clinical Oncology* 2004, **22**(1):23-30.
273. Colucci G, Gebbia V, Paoletti G, Giuliani F, Caruso M, Gebbia N, Carteni G, Agostara B, Pezzella G, Manzione L *et al*: **Phase III randomized trial of FOLFIRI versus FOLFOX4 in the treatment of advanced colorectal cancer: a multicenter study of the Gruppo Oncologico Dell'Italia Meridionale**. *Journal of clinical oncology : official journal of the American Society of Clinical Oncology* 2005, **23**(22):4866-4875.
274. Tournigand C, Andre T, Achille E, Lledo G, Flesh M, Mery-Mignard D, Quinaux E, Couteau C, Buyse M, Ganem G *et al*: **FOLFIRI followed by FOLFOX6 or the reverse sequence in advanced colorectal cancer: a randomized GERCOR study**. *Journal of clinical oncology : official journal of the American Society of Clinical Oncology* 2004, **22**(2):229-237.
275. Hurwitz H, Fehrenbacher L, Novotny W, Cartwright T, Hainsworth J, Heim W, Berlin J, Baron A, Griffing S, Holmgren E *et al*: **Bevacizumab plus irinotecan, fluorouracil, and leucovorin for metastatic colorectal cancer**. *N Engl J Med* 2004, **350**(23):2335-2342.
276. Giantonio BJ, Catalano PJ, Meropol NJ, O'Dwyer PJ, Mitchell EP, Alberts SR, Schwartz MA, Benson AB, 3rd: **Bevacizumab in combination with oxaliplatin, fluorouracil, and leucovorin (FOLFOX4) for previously treated metastatic colorectal cancer: results from the Eastern**

Cooperative Oncology Group Study E3200. *Journal of clinical oncology : official journal of the American Society of Clinical Oncology* 2007, **25**(12):1539-1544.
277. Stintzing S: **Management of colorectal cancer**. *F1000prime reports* 2014, **6**:108.
278. Kaelin WG, Jr.: **The concept of synthetic lethality in the context of anticancer therapy**. *Nature reviews Cancer* 2005, **5**(9):689-698.
279. Hartwell LH, Szankasi P, Roberts CJ, Murray AW, Friend SH: **Integrating genetic approaches into the discovery of anticancer drugs**. *Science* 1997, **278**(5340):1064-1068.
280. Li YY, Jones SJ: **Drug repositioning for personalized medicine**. *Genome medicine* 2012, **4**(3):27.
281. Tutt A, Ashworth A: **The relationship between the roles of BRCA genes in DNA repair and cancer predisposition**. *Trends in molecular medicine* 2002, **8**(12):571-576.
282. Wooster R, Weber BL: **Breast and ovarian cancer**. *N Engl J Med* 2003, **348**(23):2339-2347.
283. Roy R, Chun J, Powell SN: **BRCA1 and BRCA2: different roles in a common pathway of genome protection**. *Nature reviews Cancer* 2012, **12**(1):68-78.
284. Hoeijmakers JH: **Genome maintenance mechanisms for preventing cancer**. *Nature* 2001, **411**(6835):366-374.
285. Farmer H, McCabe N, Lord CJ, Tutt AN, Johnson DA, Richardson TB, Santarosa M, Dillon KJ, Hickson I, Knights C *et al*: **Targeting the DNA repair defect in BRCA mutant cells as a therapeutic strategy**. *Nature* 2005, **434**(7035):917-921.
286. Gelmon KA, Tischkowitz M, Mackay H, Swenerton K, Robidoux A, Tonkin K, Hirte H, Huntsman D, Clemons M, Gilks B *et al*: **Olaparib in patients with recurrent high-grade serous or poorly differentiated ovarian carcinoma or triple-negative breast cancer: a phase 2, multicentre, open-label, non-randomised study**. *The Lancet Oncology* 2011, **12**(9):852-861.
287. Salmena L, Carracedo A, Pandolfi PP: **Tenets of PTEN tumor suppression**. *Cell* 2008, **133**(3):403-414.
288. Shen WH, Balajee AS, Wang J, Wu H, Eng C, Pandolfi PP, Yin Y: **Essential role for nuclear PTEN in maintaining chromosomal integrity**. *Cell* 2007, **128**(1):157-170.
289. Mendes-Pereira AM, Martin SA, Brough R, McCarthy A, Taylor JR, Kim JS, Waldman T, Lord CJ, Ashworth A: **Synthetic lethal targeting of PTEN mutant cells with PARP inhibitors**. *EMBO Mol Med* 2009, **1**(6-7):315-322.
290. Sultana R, McNeill DR, Abbotts R, Mohammed MZ, Zdzienicka MZ, Qutob H, Seedhouse C, Laughton CA, Fischer PM, Patel PM *et al*: **Synthetic lethal targeting of DNA double-strand break repair deficient cells by human apurinic/apyrimidinic endonuclease inhibitors**. *Int J Cancer* 2012, **131**(10):2433-2444.
291. Fong PC, Boss DS, Yap TA, Tutt A, Wu P, Mergui-Roelvink M, Mortimer P, Swaisland H, Lau A, O'Connor MJ *et al*: **Inhibition of poly(ADP-ribose) polymerase in tumors from BRCA mutation carriers**. *N Engl J Med* 2009, **361**(2):123-134.
292. Fong PC, Yap TA, Boss DS, Carden CP, Mergui-Roelvink M, Gourley C, De Greve J, Lubinski J, Shanley S, Messiou C *et al*: **Poly(ADP)-ribose**

polymerase inhibition: frequent durable responses in BRCA carrier ovarian cancer correlating with platinum-free interval. *Journal of clinical oncology : official journal of the American Society of Clinical Oncology* 2010, **28**(15):2512-2519.

293. Tutt A, Robson M, Garber JE, Domchek SM, Audeh MW, Weitzel JN, Friedlander M, Arun B, Loman N, Schmutzler RK *et al*: **Oral poly(ADP-ribose) polymerase inhibitor olaparib in patients with BRCA1 or BRCA2 mutations and advanced breast cancer: a proof-of-concept trial**. *Lancet* 2010, **376**(9737):235-244.
294. Aly A, Ganesan S: **BRCA1, PARP, and 53BP1: conditional synthetic lethality and synthetic viability**. *Journal of molecular cell biology* 2011, **3**(1):66-74.
295. Lord CJ, Tutt AN, Ashworth A: **Synthetic Lethality and Cancer Therapy: Lessons Learned from the Development of PARP Inhibitors**. *Annual review of medicine* 2015, **66**:455-470.
296. Lord CJ, Ashworth A: **Mechanisms of resistance to therapies targeting BRCA-mutant cancers**. *Nature medicine* 2013, **19**(11):1381-1388.
297. Ashworth A: **Drug resistance caused by reversion mutation**. *Cancer Res* 2008, **68**(24):10021-10023.
298. Sakai W, Swisher EM, Karlan BY, Agarwal MK, Higgins J, Friedman C, Villegas E, Jacquemont C, Farrugia DJ, Couch FJ *et al*: **Secondary mutations as a mechanism of cisplatin resistance in BRCA2-mutated cancers**. *Nature* 2008, **451**(7182):1116-1120.
299. Swisher EM, Sakai W, Karlan BY, Wurz K, Urban N, Taniguchi T: **Secondary BRCA1 mutations in BRCA1-mutated ovarian carcinomas with platinum resistance**. *Cancer Res* 2008, **68**(8):2581-2586.
300. Wang W, Figg WD: **Secondary BRCA1 and BRCA2 alterations and acquired chemoresistance**. *Cancer Biol Ther* 2008, **7**(7):1004-1005.
301. Cao L, Xu X, Bunting SF, Liu J, Wang RH, Cao LL, Wu JJ, Peng TN, Chen J, Nussenzweig A *et al*: **A selective requirement for 53BP1 in the biological response to genomic instability induced by Brca1 deficiency**. *Molecular cell* 2009, **35**(4):534-541.
302. Bouwman P, Aly A, Escandell JM, Pieterse M, Bartkova J, van der Gulden H, Hiddingh S, Thanasoula M, Kulkarni A, Yang Q *et al*: **53BP1 loss rescues BRCA1 deficiency and is associated with triple-negative and BRCA-mutated breast cancers**. *Nature structural & molecular biology* 2010, **17**(6):688-695.
303. Bunting SF, Callen E, Wong N, Chen HT, Polato F, Gunn A, Bothmer A, Feldhahn N, Fernandez-Capetillo O, Cao L *et al*: **53BP1 inhibits homologous recombination in Brca1-deficient cells by blocking resection of DNA breaks**. *Cell* 2010, **141**(2):243-254.
304. Jaspers JE, Kersbergen A, Boon U, Sol W, van Deemter L, Zander SA, Drost R, Wientjens E, Ji J, Aly A *et al*: **Loss of 53BP1 causes PARP inhibitor resistance in Brca1-mutated mouse mammary tumors**. *Cancer discovery* 2013, **3**(1):68-81.
305. Feng Z, Scott SP, Bussen W, Sharma GG, Guo G, Pandita TK, Powell SN: **Rad52 inactivation is synthetically lethal with BRCA2 deficiency**. *Proceedings of the National Academy of Sciences of the United States of America* 2011, **108**(2):686-691.

306. Lok BH, Carley AC, Tchang B, Powell SN: **RAD52 inactivation is synthetically lethal with deficiencies in BRCA1 and PALB2 in addition to BRCA2 through RAD51-mediated homologous recombination**. *Oncogene* 2013, **32**(30):3552-3558.
307. Ho GP, Margossian S, Taniguchi T, D'Andrea AD: **Phosphorylation of FANCD2 on two novel sites is required for mitomycin C resistance**. *Molecular and cellular biology* 2006, **26**(18):7005-7015.
308. Taniguchi T, Garcia-Higuera I, Xu B, Andreassen PR, Gregory RC, Kim ST, Lane WS, Kastan MB, D'Andrea AD: **Convergence of the fanconi anemia and ataxia telangiectasia signaling pathways**. *Cell* 2002, **109**(4):459-472.
309. Zhi G, Wilson JB, Chen X, Krause DS, Xiao Y, Jones NJ, Kupfer GM: **Fanconi anemia complementation group FANCD2 protein serine 331 phosphorylation is important for fanconi anemia pathway function and BRCA2 interaction**. *Cancer Res* 2009, **69**(22):8775-8783.
310. Kennedy RD, Chen CC, Stuckert P, Archila EM, De la Vega MA, Moreau LA, Shimamura A, D'Andrea AD: **Fanconi anemia pathway-deficient tumor cells are hypersensitive to inhibition of ataxia telangiectasia mutated**. *The Journal of clinical investigation* 2007, **117**(5):1440-1449.
311. Chen CC, Kennedy RD, Sidi S, Look AT, D'Andrea A: **CHK1 inhibition as a strategy for targeting Fanconi Anemia (FA) DNA repair pathway deficient tumors**. *Molecular cancer* 2009, **8**:24.
312. Xie L, Gazin C, Park SM, Zhu LJ, Debily MA, Kittler EL, Zapp ML, Lapointe D, Gobeil S, Virbasius CM *et al*: **A synthetic interaction screen identifies factors selectively required for proliferation and TERT transcription in p53-deficient human cancer cells**. *PLoS genetics* 2012, **8**(12):e1003151.
313. Belgiovine C, Chiodi I, Mondello C: **Telomerase: cellular immortalization and neoplastic transformation. Multiple functions of a multifaceted complex**. *Cytogenetic and genome research* 2008, **122**(3-4):255-262.
314. Essmann F, Schulze-Osthoff K: **Translational approaches targeting the p53 pathway for anti-cancer therapy**. *British journal of pharmacology* 2012, **165**(2):328-344.
315. Martin SA, McCabe N, Mullarkey M, Cummins R, Burgess DJ, Nakabeppu Y, Oka S, Kay E, Lord CJ, Ashworth A: **DNA polymerases as potential therapeutic targets for cancers deficient in the DNA mismatch repair proteins MSH2 or MLH1**. *Cancer Cell* 2010, **17**(3):235-248.
316. Mishra M, Kowluru RA: **Retinal mitochondrial DNA mismatch repair in the development of diabetic retinopathy, and its continued progression after termination of hyperglycemia**. *Investigative ophthalmology & visual science* 2014, **55**(10):6960-6967.
317. Martin SA, McCarthy A, Barber LJ, Burgess DJ, Parry S, Lord CJ, Ashworth A: **Methotrexate induces oxidative DNA damage and is selectively lethal to tumour cells with defects in the DNA mismatch repair gene MSH2**. *EMBO Mol Med* 2009, **1**(6-7):323-337.
318. Martin SA, Hewish M, Sims D, Lord CJ, Ashworth A: **Parallel high-throughput RNA interference screens identify PINK1 as a potential therapeutic target for the treatment of DNA mismatch repair-deficient cancers**. *Cancer Res* 2011, **71**(5):1836-1848.
319. Hewish M, Martin SA, Elliott R, Cunningham D, Lord CJ, Ashworth A: **Cytosine-based nucleoside analogs are selectively lethal to DNA**

mismatch repair-deficient tumour cells by enhancing levels of intracellular oxidative stress. *Br J Cancer* 2013, **108**(4):983-992.
320. McCabe N, Turner NC, Lord CJ, Kluzek K, Bialkowska A, Swift S, Giavara S, O'Connor MJ, Tutt AN, Zdzienicka MZ *et al*: **Deficiency in the repair of DNA damage by homologous recombination and sensitivity to poly(ADP-ribose) polymerase inhibition**. *Cancer Res* 2006, **66**(16):8109-8115.
321. Martin-Liberal J, Larkin J: **Vemurafenib for the treatment of BRAF mutant metastatic melanoma**. *Future Oncol* 2015, **11**(4):579-589.
322. Prahallad A, Sun C, Huang S, Di Nicolantonio F, Salazar R, Zecchin D, Beijersbergen RL, Bardelli A, Bernards R: **Unresponsiveness of colon cancer to BRAF(V600E) inhibition through feedback activation of EGFR**. *Nature* 2012, **483**(7387):100-103.
323. Liccardi G, Hartley JA, Hochhauser D: **EGFR nuclear translocation modulates DNA repair following cisplatin and ionizing radiation treatment**. *Cancer Res* 2011, **71**(3):1103-1114.
324. Plumb JA, Strathdee G, Sludden J, Kaye SB, Brown R: **Reversal of drug resistance in human tumor xenografts by 2'-deoxy-5-azacytidine-induced demethylation of the hMLH1 gene promoter**. *Cancer Res* 2000, **60**(21):6039-6044.
325. McIlhatton MA, Tyler J, Kerepesi LA, Bocker-Edmonston T, Kucherlapati MH, Edelmann W, Kucherlapati R, Kopelovich L, Fishel R: **Aspirin and low-dose nitric oxide-donating aspirin increase life span in a Lynch syndrome mouse model**. *Cancer Prev Res (Phila)* 2011, **4**(5):684-693.
326. Beck SL: **Effects of aspirin on colorectal cancer related to lynch syndrome**. *Journal of the advanced practitioner in oncology* 2012, **3**(6):395-398.
327. Burn J, Gerdes AM, Macrae F, Mecklin JP, Moeslein G, Olschwang S, Eccles D, Evans DG, Maher ER, Bertario L *et al*: **Long-term effect of aspirin on cancer risk in carriers of hereditary colorectal cancer: an analysis from the CAPP2 randomised controlled trial**. *Lancet* 2011, **378**(9809):2081-2087.
328. Edwards RA, Witherspoon M, Wang K, Afrasiabi K, Pham T, Birnbaumer L, Lipkin SM: **Epigenetic repression of DNA mismatch repair by inflammation and hypoxia in inflammatory bowel disease-associated colorectal cancer**. *Cancer Res* 2009, **69**(16):6423-6429.
329. Shi X, Ding M, Dong Z, Chen F, Ye J, Wang S, Leonard SS, Castranova V, Vallyathan V: **Antioxidant properties of aspirin: characterization of the ability of aspirin to inhibit silica-induced lipid peroxidation, DNA damage, NF-kappaB activation, and TNF-alpha production**. *Molecular and cellular biochemistry* 1999, **199**(1-2):93-102.
330. Durak I, Karaayvaz M, Cimen MY, Avci A, Cimen OB, Buyukkocak S, Ozturk HS, Ozbek H, Kacmaz M: **Aspirin impairs antioxidant system and causes peroxidation in human erythrocytes and guinea pig myocardial tissue**. *Human & experimental toxicology* 2001, **20**(1):34-37.
331. Wolin MS: **Novel antioxidant action of aspirin may contribute to its beneficial cardiovascular actions**. *Circulation research* 1998, **82**(9):1021-1022.
332. von Knebel Doeberitz M, Kloor M: **Towards a vaccine to prevent cancer in Lynch syndrome patients**. *Familial cancer* 2013, **12**(2):307-312.

333. Chen J, Etzel CJ, Amos CI, Zhang Q, Viscofsky N, Lindor NM, Lynch PM, Frazier ML: **Genetic variants in the cell cycle control pathways contribute to early onset colorectal cancer in Lynch syndrome**. *Cancer causes & control : CCC* 2009, **20**(9):1769-1777.
334. Kong S, Amos CI, Luthra R, Lynch PM, Levin B, Frazier ML: **Effects of cyclin D1 polymorphism on age of onset of hereditary nonpolyposis colorectal cancer**. *Cancer Res* 2000, **60**(2):249-252.
335. Talseth BA, Ashton KA, Meldrum C, Suchy J, Kurzawski G, Lubinski J, Scott RJ: **Aurora-A and Cyclin D1 polymorphisms and the age of onset of colorectal cancer in hereditary nonpolyposis colorectal cancer**. *Int J Cancer* 2008, **122**(6):1273-1277.
336. Bala S, Peltomaki P: **CYCLIN D1 as a genetic modifier in hereditary nonpolyposis colorectal cancer**. *Cancer Res* 2001, **61**(16):6042-6045.
337. Kruger S, Engel C, Bier A, Mangold E, Pagenstecher C, Doeberitz M, Holinski-Feder E, Moeslein G, Keller G, Kunstmann E *et al*: **Absence of association between cyclin D1 (CCND1) G870A polymorphism and age of onset in hereditary nonpolyposis colorectal cancer**. *Cancer letters* 2006, **236**(2):191-197.
338. Chen J, Sen S, Amos CI, Wei C, Jones JS, Lynch P, Frazier ML: **Association between Aurora-A kinase polymorphisms and age of onset of hereditary nonpolyposis colorectal cancer in a Caucasian population**. *Molecular carcinogenesis* 2007, **46**(4):249-256.
339. Yin G, Kono S, Toyomura K, Hagiwara T, Nagano J, Mizoue T, Mibu R, Tanaka M, Kakeji Y, Maehara Y *et al*: **Methylenetetrahydrofolate reductase C677T and A1298C polymorphisms and colorectal cancer: the Fukuoka Colorectal Cancer Study**. *Cancer science* 2004, **95**(11):908-913.
340. Weisberg I, Tran P, Christensen B, Sibani S, Rozen R: **A second genetic polymorphism in methylenetetrahydrofolate reductase (MTHFR) associated with decreased enzyme activity**. *Mol Genet Metab* 1998, **64**(3):169-172.
341. Guimaraes JL, Ayrizono Mde L, Coy CS, Lima CS: **Gene polymorphisms involved in folate and methionine metabolism and increased risk of sporadic colorectal adenocarcinoma**. *Tumour biology : the journal of the International Society for Oncodevelopmental Biology and Medicine* 2011, **32**(5):853-861.
342. Levine AJ, Figueiredo JC, Lee W, Conti DV, Kennedy K, Duggan DJ, Poynter JN, Campbell PT, Newcomb P, Martinez ME *et al*: **A candidate gene study of folate-associated one carbon metabolism genes and colorectal cancer risk**. *Cancer epidemiology, biomarkers & prevention : a publication of the American Association for Cancer Research, cosponsored by the American Society of Preventive Oncology* 2010, **19**(7):1812-1821.
343. Pande M, Chen J, Amos CI, Lynch PM, Broaddus R, Frazier ML: **Influence of methylenetetrahydrofolate reductase gene polymorphisms C677T and A1298C on age-associated risk for colorectal cancer in a caucasian lynch syndrome population**. *Cancer epidemiology, biomarkers & prevention : a publication of the American Association for Cancer Research, cosponsored by the American Society of Preventive Oncology* 2007, **16**(9):1753-1759.
344. Reeves SG, Meldrum C, Groombridge C, Spigelman AD, Suchy J, Kurzawski G, Lubinski J, McElduff P, Scott RJ: **MTHFR 677 C>T and 1298 A>C polymorphisms and the age of onset of colorectal cancer in**

hereditary nonpolyposis colorectal cancer. *European journal of human genetics : EJHG* 2009, **17**(5):629-635.
345. Chang SC, Lin PC, Lin JK, Yang SH, Wang HS, Li AF: **Role of MTHFR polymorphisms and folate levels in different phenotypes of sporadic colorectal cancers**. *International journal of colorectal disease* 2007, **22**(5):483-489.
346. Hubner RA, Lubbe S, Chandler I, Houlston RS: **MTHFR C677T has differential influence on risk of MSI and MSS colorectal cancer**. *Human molecular genetics* 2007, **16**(9):1072-1077.
347. Eaton AM, Sandler R, Carethers JM, Millikan RC, Galanko J, Keku TO: **5,10-methylenetetrahydrofolate reductase 677 and 1298 polymorphisms, folate intake, and microsatellite instability in colon cancer**. *Cancer epidemiology, biomarkers & prevention : a publication of the American Association for Cancer Research, cosponsored by the American Society of Preventive Oncology* 2005, **14**(8):2023-2029.
348. Gonen N, Assaraf YG: **Antifolates in cancer therapy: structure, activity and mechanisms of drug resistance**. *Drug resistance updates : reviews and commentaries in antimicrobial and anticancer chemotherapy* 2012, **15**(4):183-210.
349. Stanger O, Wonisch W: **Enzymatic and non-enzymatic antioxidative effects of folic acid and its reduced derivates**. *Sub-cellular biochemistry* 2012, **56**:131-161.
350. Lamberti M, Porto S, Marra M, Zappavigna S, Grimaldi A, Feola D, Pesce D, Naviglio S, Spina A, Sannolo N *et al*: **5-Fluorouracil induces apoptosis in rat cardiocytes through intracellular oxidative stress**. *Journal of experimental & clinical cancer research : CR* 2012, **31**:60.
351. Surmont VF, van Meerbeeck JP: **Raltitrexed in mesothelioma**. *Expert review of anticancer therapy* 2011, **11**(10):1481-1490.
352. Assaraf YG: **Molecular basis of antifolate resistance**. *Cancer metastasis reviews* 2007, **26**(1):153-181.
353. Cohen MH, Cortazar P, Justice R, Pazdur R: **Approval summary: pemetrexed maintenance therapy of advanced/metastatic nonsquamous, non-small cell lung cancer (NSCLC)**. *The oncologist* 2010, **15**(12):1352-1358.
354. Hazarika M, White RM, Johnson JR, Pazdur R: **FDA drug approval summaries: pemetrexed (Alimta)**. *The oncologist* 2004, **9**(5):482-488.
355. Tung CL, Chiu HC, Jian YJ, Jian YT, Chen CY, Syu JJ, Wo TY, Huang YJ, Tseng SC, Lin YW: **Down-regulation of MSH2 expression by an Hsp90 inhibitor enhances pemetrexed-induced cytotoxicity in human non-small-cell lung cancer cells**. *Exp Cell Res* 2014, **322**(2):345-354.
356. Zhang JH, Chung TD, Oldenburg KR: **A Simple Statistical Parameter for Use in Evaluation and Validation of High Throughput Screening Assays**. *Journal of biomolecular screening* 1999, **4**(2):67-73.
357. Liu X, Erikson RL: **Polo-like kinase (Plk)1 depletion induces apoptosis in cancer cells**. *Proceedings of the National Academy of Sciences of the United States of America* 2003, **100**(10):5789-5794.
358. Eruslanov E, Kusmartsev S: **Identification of ROS using oxidized DCFDA and flow-cytometry**. *Methods Mol Biol* 2010, **594**:57-72.
359. Chen X, Zhong Z, Xu Z, Chen L, Wang Y: **2',7'-Dichlorodihydrofluorescein as a fluorescent probe for reactive oxygen**

species measurement: Forty years of application and controversy. *Free radical research* 2010, **44**(6):587-604.
360. Woolley JF, Stanicka J, Cotter TG: **Recent advances in reactive oxygen species measurement in biological systems**. *Trends in biochemical sciences* 2013, **38**(11):556-565.
361. Richmond A, Su Y: **Mouse xenograft models vs GEM models for human cancer therapeutics**. *Disease models & mechanisms* 2008, **1**(2-3):78-82.
362. Tomayko MM, Reynolds CP: **Determination of subcutaneous tumor size in athymic (nude) mice**. *Cancer chemotherapy and pharmacology* 1989, **24**(3):148-154.
363. Miller RG: **Simultaneous Statistical Inference**. In: *Springer Series in Statistics,*. Second Edition. edn. New York, NY: Springer New York,; 1981: pages 6-8.
364. Mojallal M, Zheng Y, Hultin S, Audebert S, van Harn T, Johnsson P, Lenander C, Fritz N, Mieth C, Corcoran M *et al*: **AmotL2 disrupts apical-basal cell polarity and promotes tumour invasion**. *Nature communications* 2014, **5**:4557.
365. Mitra-Kaushik S, Harding JC, Hess JL, Ratner L: **Effects of the proteasome inhibitor PS-341 on tumor growth in HTLV-1 Tax transgenic mice and Tax tumor transplants**. *Blood* 2004, **104**(3):802-809.
366. Li J, Li W, Liang S, Cai D, Kieny MP, Jacob L, Linnenbach A, Abramczuk JW, Bender H, Sproesser K *et al*: **Recombinant CD63/ME491/neuroglandular/NKI/C-3 antigen inhibits growth of established tumors in transgenic mice**. *J Immunol* 2003, **171**(6):2922-2929.
367. Hillerdal V, Ramachandran M, Leja J, Essand M: **Systemic treatment with CAR-engineered T cells against PSCA delays subcutaneous tumor growth and prolongs survival of mice**. *BMC cancer* 2014, **14**:30.
368. Yao X, Buermeyer AB, Narayanan L, Tran D, Baker SM, Prolla TA, Glazer PM, Liskay RM, Arnheim N: **Different mutator phenotypes in Mlh1-versus Pms2-deficient mice**. *Proceedings of the National Academy of Sciences of the United States of America* 1999, **96**(12):6850-6855.
369. Modrich P: **Mechanisms in eukaryotic mismatch repair**. *The Journal of biological chemistry* 2006, **281**(41):30305-30309.
370. Umar A, Koi M, Risinger JI, Glaab WE, Tindall KR, Kolodner RD, Boland CR, Barrett JC, Kunkel TA: **Correction of hypermutability, N-methyl-N'-nitro-N-nitrosoguanidine resistance, and defective DNA mismatch repair by introducing chromosome 2 into human tumor cells with mutations in MSH2 and MSH6**. *Cancer Res* 1997, **57**(18):3949-3955.
371. Gallant JN, Allen JE, Smith CD, Dicker DT, Wang W, Dolloff NG, Navaraj A, El-Deiry WS: **Quinacrine synergizes with 5-fluorouracil and other therapies in colorectal cancer**. *Cancer Biol Ther* 2011, **12**(3):239-251.
372. Preet R, Mohapatra P, Mohanty S, Sahu SK, Choudhuri T, Wyatt MD, Kundu CN: **Quinacrine has anticancer activity in breast cancer cells through inhibition of topoisomerase activity**. *Int J Cancer* 2012, **130**(7):1660-1670.
373. Wang W, McLeod HL, Cassidy J: **Disulfiram-mediated inhibition of NF-kappaB activity enhances cytotoxicity of 5-fluorouracil in human colorectal cancer cell lines**. *Int J Cancer* 2003, **104**(4):504-511.

374. Penso J, Beitner R: **Clotrimazole decreases glycolysis and the viability of lung carcinoma and colon adenocarcinoma cells**. *Eur J Pharmacol* 2002, **451**(3):227-235.
375. Coelho RG, Calaca Ide C, Celestrini Dde M, Correia AH, Costa MA, Sola-Penna M: **Clotrimazole disrupts glycolysis in human breast cancer without affecting non-tumoral tissues**. *Mol Genet Metab* 2011, **103**(4):394-398.
376. Garcia-Quiroz J, Camacho J: **Astemizole: an old anti-histamine as a new promising anti-cancer drug**. *Anticancer Agents Med Chem* 2011, **11**(3):307-314.
377. Garcia-Quiroz J, Garcia-Becerra R, Barrera D, Santos N, Avila E, Ordaz-Rosado D, Rivas-Suarez M, Halhali A, Rodriguez P, Gamboa-Dominguez A *et al*: **Astemizole synergizes calcitriol antiproliferative activity by inhibiting CYP24A1 and upregulating VDR: a novel approach for breast cancer therapy**. *PloS one* 2012, **7**(9):e45063.
378. Busch AE, Suessbrich H, Kunzelmann K, Hipper A, Greger R, Waldegger S, Mutschler E, Lindemann B, Lang F: **Blockade of epithelial Na+ channels by triamterenes - underlying mechanisms and molecular basis**. *Pflugers Arch* 1996, **432**(5):760-766.
379. Hernandez-Diaz S, Werler MM, Walker AM, Mitchell AA: **Folic acid antagonists during pregnancy and the risk of birth defects**. *N Engl J Med* 2000, **343**(22):1608-1614.
380. Zhang B, Xie S, Shi W, Yang Y: **Amiloride off-target effect inhibits podocyte urokinase receptor expression and reduces proteinuria**. *Nephrol Dial Transplant* 2012, **27**(5):1746-1755.
381. National Toxicology P: **NTP technical report on the toxicology and carcinogenesis studies of triamterene (CAS no. 396-01-0) in F344/N rats and B6C3F₁ mice (feed studies)**. Research Triangle Park, N.C.; [Springfield, Va.]: U.S. Dept. of Health and Human Services, Public Health Service, National Institutes of Health ; [Available from the National Technical Information Service]; 1993.
382. Zimmerman J, Selhub J, Rosenberg IH: **Competitive inhibition of folic acid absorption in rat jejunum by triamterene**. *The Journal of laboratory and clinical medicine* 1986, **108**(4):272-276.
383. Cattell WR, Havard CW: **Diuretic action of triamterene in man**. *British medical journal* 1962, **2**(5316):1362-1366.
384. Baba WI, Tudhope GR, Wilson GM: **Triamterene, a new diuretic drug. I. Studies in normal men and in adrenalectomized rats**. *British medical journal* 1962, **2**(5307):756-760.
385. Wiebelhaus VD, Weinstock J, Maass AB, Brennan FT, Sosnowski G, Larsen T: **The diuretic and natruretic activity of triamterene and several related pteridines in the rat**. *J Pharmacol Exp Ther* 1965, **149**(3):397-403.
386. Turner P, Sowry GS: **Triamterene in the Treatment of Ascites in Hepatic Cirrhosis**. *The British journal of clinical practice* 1964, **18**:13-17.
387. Simpson FO, Waal HJ: **Clinical Trial of Triamterene in Hypertensive Patients**. *The New Zealand medical journal* 1964, **63**:199-202.
388. Baba WI, Tudhope GR, Wilson GM: **Triamterene, a new diuretic drug. II. Clinical trial in oedematous patients**. *British medical journal* 1962, **2**(5307):760-764.

389. Joossens JV, Verwilgen R, Verberckmoes R: **Triamterene Combined with Other Diuretics in Congestive Heart Failure**. *Acta cardiologica* 1964, **19**:32-50.
390. Roberts D, Hall TC: **Triamterene-induced elevation of dihydrofolate reductase activity in human leukocytes**. *Biochemical pharmacology* 1968, **17**(3):481-484.
391. Corcino J, Waxman S, Herbert V: **Mechanism of triamterene-induced megaloblastosis**. *Annals of internal medicine* 1970, **73**(3):419-424.
392. Sidhom MB, Velez MR: **Monitoring the effect of triamterene and hydrochlorothiazide on dihydrofolate reductase activity using a new spectrophotometric method**. *Journal of pharmaceutical and biomedical analysis* 1989, **7**(12):1551-1557.
393. Baer JE, Jones CB, Spitzer SA, Russo HF: **The potassium-sparing and natriuretic activity of N-amidino-3,5-diamino-6-chloropyrazinecarboxamide hydrochloride dihydrate (amiloride hydrochloride)**. *J Pharmacol Exp Ther* 1967, **157**(2):472-485.
394. Kellenberger S, Gautschi I, Schild L: **Mutations in the epithelial Na+ channel ENaC outer pore disrupt amiloride block by increasing its dissociation rate**. *Molecular pharmacology* 2003, **64**(4):848-856.
395. Zawada ET, Jr.: **Antihypertensive therapy with triamterene-hydrochlorothiazide vs amiloride-hydrochlorothiazide. Comparison of effects on urinary prostaglandin E2 excretion**. *Archives of internal medicine* 1986, **146**(7):1312-1314.
396. Loffing J, Schild L: **Functional domains of the epithelial sodium channel**. *Journal of the American Society of Nephrology : JASN* 2005, **16**(11):3175-3181.
397. Schalhorn A, Siegert W, Sauer HJ: **Antifolate effect of triamterene on human leucocytes and on a human lymphoma cell line**. *European journal of clinical pharmacology* 1981, **20**(3):219-224.
398. Abali EE, Skacel NE, Celikkaya H, Hsieh YC: **Regulation of human dihydrofolate reductase activity and expression**. *Vitamins and hormones* 2008, **79**:267-292.
399. Carreras CW, Santi DV: **The catalytic mechanism and structure of thymidylate synthase**. *Annual review of biochemistry* 1995, **64**:721-762.
400. Kuo LJ, Yang LX: **Gamma-H2AX - a novel biomarker for DNA double-strand breaks**. *In Vivo* 2008, **22**(3):305-309.
401. Sharma A, Singh K, Almasan A: **Histone H2AX phosphorylation: a marker for DNA damage**. *Methods Mol Biol* 2012, **920**:613-626.
402. Rogakou EP, Nieves-Neira W, Boon C, Pommier Y, Bonner WM: **Initiation of DNA fragmentation during apoptosis induces phosphorylation of H2AX histone at serine 139**. *The Journal of biological chemistry* 2000, **275**(13):9390-9395.
403. Mendes-Pereira AM, Lord CJ, Ashworth A: **NLK is a novel therapeutic target for PTEN deficient tumour cells**. *PloS one* 2012, **7**(10):e47249.
404. Liu X, Erikson RL: **Polo-like kinase (Plk)1 depletion induces apoptosis in cancer cells**. *Proc Natl Acad Sci U S A* 2003, **100**(10):5789-5794.
405. Gritsina G, Xiao F, O'Brien SW, Gabbasov R, Maglaty MA, Xu RH, Thapa RJ, Zhou Y, Nicolas E, Litwin S *et al*: **Targeted blockade of JAK/STAT3 signaling inhibits ovarian carcinoma growth**. *Molecular cancer therapeutics* 2015.

406. Yan J, Wang Q, Zou K, Wang L, Schwartz EB, Fuchs JR, Zheng Z, Wu J: **Inhibition of the JAK2/STAT3 signaling pathway exerts a therapeutic effect on osteosarcoma**. *Molecular medicine reports* 2015.
407. Younes A, Romaguera J, Fanale M, McLaughlin P, Hagemeister F, Copeland A, Neelapu S, Kwak L, Shah J, de Castro Faria S *et al*: **Phase I study of a novel oral Janus kinase 2 inhibitor, SB1518, in patients with relapsed lymphoma: evidence of clinical and biologic activity in multiple lymphoma subtypes**. *Journal of clinical oncology : official journal of the American Society of Clinical Oncology* 2012, **30**(33):4161-4167.
408. Hsu L, Armstrong AW: **JAK inhibitors: treatment efficacy and safety profile in patients with psoriasis**. *Journal of immunology research* 2014, **2014**:283617.
409. Mesa RA, Yasothan U, Kirkpatrick P: **Ruxolitinib**. *Nature reviews Drug discovery* 2012, **11**(2):103-104.
410. Lin HC, Zhang FL, Geng Q, Yu T, Cui YQ, Liu XH, Li J, Yan MX, Liu L, He XH *et al*: **Quantitative proteomic analysis identifies CPNE3 as a novel metastasis-promoting gene in NSCLC**. *Journal of proteome research* 2013, **12**(7):3423-3433.
411. Heinrich C, Keller C, Boulay A, Vecchi M, Bianchi M, Sack R, Lienhard S, Duss S, Hofsteenge J, Hynes NE: **Copine-III interacts with ErbB2 and promotes tumor cell migration**. *Oncogene* 2010, **29**(11):1598-1610.
412. LaRonde-LeBlanc N, Wlodawer A: **A family portrait of the RIO kinases**. *The Journal of biological chemistry* 2005, **280**(45):37297-37300.
413. Liu T, Deng M, Li J, Tong X, Wei Q, Ye X: **Phosphorylation of right open reading frame 2 (Rio2) protein kinase by polo-like kinase 1 regulates mitotic progression**. *The Journal of biological chemistry* 2011, **286**(42):36352-36360.
414. Read RD, Fenton TR, Gomez GG, Wykosky J, Vandenberg SR, Babic I, Iwanami A, Yang H, Cavenee WK, Mischel PS *et al*: **A kinome-wide RNAi screen in Drosophila Glia reveals that the RIO kinases mediate cell proliferation and survival through TORC2-Akt signaling in glioblastoma**. *PLoS genetics* 2013, **9**(2):e1003253.
415. Ives EB, Nichols J, Wente SR, York JD: **Biochemical and functional characterization of inositol 1,3,4,5, 6-pentakisphosphate 2-kinases**. *The Journal of biological chemistry* 2000, **275**(47):36575-36583.
416. Byrum J, Jordan S, Safrany ST, Rodgers W: **Visualization of inositol phosphate-dependent mobility of Ku: depletion of the DNA-PK cofactor InsP6 inhibits Ku mobility**. *Nucleic acids research* 2004, **32**(9):2776-2784.
417. El-Sherbiny YM, Cox MC, Ismail ZA, Shamsuddin AM, Vucenik I: **G0/G1 arrest and S phase inhibition of human cancer cell lines by inositol hexaphosphate (IP6)**. *Anticancer research* 2001, **21**(4A):2393-2403.
418. Wang Y, Sun H, Wang Z, Liu M, Qi Z, Meng J, Sun J, Yang G: **Aurora-A: a potential DNA repair modulator**. *Tumour biology : the journal of the International Society for Oncodevelopmental Biology and Medicine* 2014, **35**(4):2831-2836.
419. Bischoff JR, Anderson L, Zhu Y, Mossie K, Ng L, Souza B, Schryver B, Flanagan P, Clairvoyant F, Ginther C *et al*: **A homologue of Drosophila aurora kinase is oncogenic and amplified in human colorectal cancers**. *The EMBO journal* 1998, **17**(11):3052-3065.

420. Zhou H, Kuang J, Zhong L, Kuo WL, Gray JW, Sahin A, Brinkley BR, Sen S: **Tumour amplified kinase STK15/BTAK induces centrosome amplification, aneuploidy and transformation**. *Nature genetics* 1998, **20**(2):189-193.
421. Hilton JF, Shapiro GI: **Aurora kinase inhibition as an anticancer strategy**. *Journal of clinical oncology : official journal of the American Society of Clinical Oncology* 2014, **32**(1):57-59.
422. Katayama H, Sen S: **Aurora kinase inhibitors as anticancer molecules**. *Biochimica et biophysica acta* 2010, **1799**(10-12):829-839.
423. Nagao T, Oshikawa G, Wu N, Kurosu T, Miura O: **DNA damage stress and inhibition of Jak2-V617F cause its degradation and synergistically induce apoptosis through activation of GSK3beta**. *PloS one* 2011, **6**(11):e27397.
424. Jiang Z, Jiang J, Yang H, Ge Z, Wang Q, Zhang L, Wu C, Wang J: **Silencing of Aurora kinase A by RNA interference inhibits tumor growth in human osteosarcoma cells by inducing apoptosis and G2/M cell cycle arrest**. *Oncology reports* 2014, **31**(3):1249-1254.
425. Do TV, Xiao F, Bickel LE, Klein-Szanto AJ, Pathak HB, Hua X, Howe C, O'Brien SW, Maglaty M, Ecsedy JA *et al*: **Aurora kinase A mediates epithelial ovarian cancer cell migration and adhesion**. *Oncogene* 2014, **33**(5):539-549.
426. Asteriti IA, Giubettini M, Lavia P, Guarguaglini G: **Aurora-A inactivation causes mitotic spindle pole fragmentation by unbalancing microtubule-generated forces**. *Molecular cancer* 2011, **10**:131.
427. Manfredi MG, Ecsedy JA, Chakravarty A, Silverman L, Zhang M, Hoar KM, Stroud SG, Chen W, Shinde V, Huck JJ *et al*: **Characterization of Alisertib (MLN8237), an investigational small-molecule inhibitor of aurora A kinase using novel in vivo pharmacodynamic assays**. *Clin Cancer Res* 2011, **17**(24):7614-7624.
428. Malumbres M, Perez de Castro I: **Aurora kinase A inhibitors: promising agents in antitumoral therapy**. *Expert opinion on therapeutic targets* 2014, **18**(12):1377-1393.
429. Vandecandelaere A, Martin SR, Engelborghs Y: **Response of microtubules to the addition of colchicine and tubulin-colchicine: evaluation of models for the interaction of drugs with microtubules**. *The Biochemical journal* 1997, **323 (Pt 1)**:189-196.
430. Hauf S, Cole RW, LaTerra S, Zimmer C, Schnapp G, Walter R, Heckel A, van Meel J, Rieder CL, Peters JM: **The small molecule Hesperadin reveals a role for Aurora B in correcting kinetochore-microtubule attachment and in maintaining the spindle assembly checkpoint**. *The Journal of cell biology* 2003, **161**(2):281-294.
431. Liu H, Li Y, Raisch KP: **Clotrimazole induces a late G1 cell cycle arrest and sensitizes glioblastoma cells to radiation in vitro**. *Anti-cancer drugs* 2010, **21**(9):841-849.
432. Zhou X, Ren Y, Moore L, Mei M, You Y, Xu P, Wang B, Wang G, Jia Z, Pu P *et al*: **Downregulation of miR-21 inhibits EGFR pathway and suppresses the growth of human glioblastoma cells independent of PTEN status**. *Laboratory investigation; a journal of technical methods and pathology* 2010, **90**(2):144-155.

433. Milanovic D, Braun F, Weber W, Grosu AL, Behe M, Niedermann G: **The influence of the combined treatment with Vadimezan (ASA404) and taxol on the growth of U251 glioblastoma xenografts**. *BMC cancer* 2012, **12**:242.
434. Montalar M, Nalda-Molina R, Rodriguez-Ibanez M, Garcia-Valcarcel I, Garrigues TM, Merino V, Bermejo M: **Kinetic modeling of triamterene intestinal absorption and its inhibition by folic acid and methotrexate**. *Journal of drug targeting* 2003, **11**(4):215-223.
435. Mason JB, Zimmerman J, Otradovec CL, Selhub J, Rosenberg IH: **Chronic diuretic therapy with moderate doses of triamterene is not associated with folate deficiency**. *The Journal of laboratory and clinical medicine* 1991, **117**(5):365-369.
436. Huang RF, Ho YH, Lin HL, Wei JS, Liu TZ: **Folate deficiency induces a cell cycle-specific apoptosis in HepG2 cells**. *J Nutr* 1999, **129**(1):25-31.
437. Gu L, Wu J, Qiu L, Jennings CD, Li GM: **Involvement of DNA mismatch repair in folate deficiency-induced apoptosis small star, filled**. *The Journal of nutritional biochemistry* 2002, **13**(6):355-363.
438. Chang JC, Hall TC: **Effect of triamterene on nucleic acid synthesis**. *Clinical pharmacology and therapeutics* 1972, **13**(3):372-376.
439. Hubner RA, Houlston RS: **MTHFR C677T and colorectal cancer risk: A meta-analysis of 25 populations**. *Int J Cancer* 2007, **120**(5):1027-1035.
440. Sun DF, Weng YR, Chen YX, Lu R, Wang X, Fang JY: **Knock-down of methylenetetrahydrofolate reductase reduces gastric cancer cell survival: an in vitro study**. *Cell biology international* 2008, **32**(8):879-887.
441. Chambers JC, McGregor A, Jean-Marie J, Obeid OA, Kooner JS: **Demonstration of rapid onset vascular endothelial dysfunction after hyperhomocysteinemia: an effect reversible with vitamin C therapy**. *Circulation* 1999, **99**(9):1156-1160.
442. Jacobsen DW: **Hyperhomocysteinemia and oxidative stress: time for a reality check?** *Arteriosclerosis, thrombosis, and vascular biology* 2000, **20**(5):1182-1184.
443. Kanani PM, Sinkey CA, Browning RL, Allaman M, Knapp HR, Haynes WG: **Role of oxidant stress in endothelial dysfunction produced by experimental hyperhomocyst(e)inemia in humans**. *Circulation* 1999, **100**(11):1161-1168.
444. Nappo F, De Rosa N, Marfella R, De Lucia D, Ingrosso D, Perna AF, Farzati B, Giugliano D: **Impairment of endothelial functions by acute hyperhomocysteinemia and reversal by antioxidant vitamins**. *Jama* 1999, **281**(22):2113-2118.
445. Aquilano K, Baldelli S, Ciriolo MR: **Glutathione: new roles in redox signaling for an old antioxidant**. *Frontiers in pharmacology* 2014, **5**:196.
446. Hu XF, Yao J, Gao SG, Wang XS, Peng XQ, Yang YT, Feng XS: **Nrf2 overexpression predicts prognosis and 5-FU resistance in gastric cancer**. *Asian Pacific journal of cancer prevention : APJCP* 2013, **14**(9):5231-5235.
447. Samatiwat P, Prawan A, Senggunprai L, Kukongviriyapan V: **Repression of Nrf2 enhances antitumor effect of 5-fluorouracil and gemcitabine on cholangiocarcinoma cells**. *Naunyn-Schmiedeberg's archives of pharmacology* 2015.
448. Zhou S, Ye W, Duan X, Zhang M, Wang J: **The noncytotoxic dose of sorafenib sensitizes Bel-7402/5-FU cells to 5-FU by down-regulating 5-**

FU-induced Nrf2 expression. *Digestive diseases and sciences* 2013, **58**(6):1615-1626.
449. Akhdar H, Loyer P, Rauch C, Corlu A, Guillouzo A, Morel F: **Involvement of Nrf2 activation in resistance to 5-fluorouracil in human colon cancer HT-29 cells**. *Eur J Cancer* 2009, **45**(12):2219-2227.
450. Kang KA, Piao MJ, Kim KC, Kang HK, Chang WY, Park IC, Keum YS, Surh YJ, Hyun JW: **Epigenetic modification of Nrf2 in 5-fluorouracil-resistant colon cancer cells: involvement of TET-dependent DNA demethylation**. *Cell death & disease* 2014, **5**:e1183.
451. Tice RR, Agurell E, Anderson D, Burlinson B, Hartmann A, Kobayashi H, Miyamae Y, Rojas E, Ryu JC, Sasaki YF: **Single cell gel/comet assay: guidelines for in vitro and in vivo genetic toxicology testing**. *Environmental and molecular mutagenesis* 2000, **35**(3):206-221.
452. Gad H, Koolmeister T, Jemth AS, Eshtad S, Jacques SA, Strom CE, Svensson LM, Schultz N, Lundback T, Einarsdottir BO *et al*: **MTH1 inhibition eradicates cancer by preventing sanitation of the dNTP pool**. *Nature* 2014, **508**(7495):215-221.
453. Johnston PG, Drake JC, Trepel J, Allegra CJ: **Immunological quantitation of thymidylate synthase using the monoclonal antibody TS 106 in 5-fluorouracil-sensitive and -resistant human cancer cell lines**. *Cancer Res* 1992, **52**(16):4306-4312.
454. Kim YI: **Role of the MTHFR polymorphisms in cancer risk modification and treatment**. *Future Oncol* 2009, **5**(4):523-542.
455. Dorsett Y, Tuschl T: **siRNAs: applications in functional genomics and potential as therapeutics**. *Nature reviews Drug discovery* 2004, **3**(4):318-329.
456. Nikonova AS, Astsaturov I, Serebriiskii IG, Dunbrack RL, Jr., Golemis EA: **Aurora A kinase (AURKA) in normal and pathological cell division**. *Cellular and molecular life sciences : CMLS* 2013, **70**(4):661-687.
457. Zhu J, Abbruzzese JL, Izzo J, Hittelman WN, Li D: **AURKA amplification, chromosome instability, and centrosome abnormality in human pancreatic carcinoma cells**. *Cancer genetics and cytogenetics* 2005, **159**(1):10-17.
458. Chou CH, Yang NK, Liu TY, Tai SK, Hsu DS, Chen YW, Chen YJ, Chang CC, Tzeng CH, Yang MH: **Chromosome instability modulated by BMI1-AURKA signaling drives progression in head and neck cancer**. *Cancer Res* 2013, **73**(2):953-966.
459. Seki A, Coppinger JA, Jang CY, Yates JR, Fang G: **Bora and the kinase Aurora a cooperatively activate the kinase Plk1 and control mitotic entry**. *Science* 2008, **320**(5883):1655-1658.
460. Yang G, Chang B, Yang F, Guo X, Cai KQ, Xiao XS, Wang H, Sen S, Hung MC, Mills GB *et al*: **Aurora kinase A promotes ovarian tumorigenesis through dysregulation of the cell cycle and suppression of BRCA2**. *Clin Cancer Res* 2010, **16**(12):3171-3181.
461. Marumoto T, Hirota T, Morisaki T, Kunitoku N, Zhang D, Ichikawa Y, Sasayama T, Kuninaka S, Mimori T, Tamaki N *et al*: **Roles of aurora-A kinase in mitotic entry and G2 checkpoint in mammalian cells**. *Genes to cells : devoted to molecular & cellular mechanisms* 2002, **7**(11):1173-1182.
462. Zhang D, Hirota T, Marumoto T, Shimizu M, Kunitoku N, Sasayama T, Arima Y, Feng L, Suzuki M, Takeya M *et al*: **Cre-loxP-controlled periodic**

Aurora-A overexpression induces mitotic abnormalities and hyperplasia in mammary glands of mouse models. *Oncogene* 2004, **23**(54):8720-8730.
463. Hu W, Kavanagh JJ, Deaver M, Johnston DA, Freedman RS, Verschraegen CF, Sen S: **Frequent overexpression of STK15/Aurora-A/BTAK and chromosomal instability in tumorigenic cell cultures derived from human ovarian cancer**. *Oncology research* 2005, **15**(1):49-57.
464. Madan E, Gogna R, Pati U: **p53 Ser15 phosphorylation disrupts the p53-RPA70 complex and induces RPA70-mediated DNA repair in hypoxia**. *The Biochemical journal* 2012, **443**(3):811-820.
465. Tao Y, Zhang P, Frascogna V, Lecluse Y, Auperin A, Bourhis J, Deutsch E: **Enhancement of radiation response by inhibition of Aurora-A kinase using siRNA or a selective Aurora kinase inhibitor PHA680632 in p53-deficient cancer cells**. *Br J Cancer* 2007, **97**(12):1664-1672.

Appendix

Appendix 1: Z-scores of the high-throughput compound screen

Appendix 2: **Δ**Z-scores of the high-throughput siRNA screen

Appendix 1: Z-scores of the compound screen

GeneSymbol	DLD1		DLD1 + 5-FU		DLD1+chr2		DLD1+chr2 + 5-FU	
	REP1	REP2	REP1	REP2	REP1	REP2	REP1	REP2
(-) -Levobunolol hydrochloride	0.6585	0.2511	0.2557	-0.2044	1.2558	-0.2042	-0.3925	-0.3183
(-)-Adenosine 3',5'-cyclic monophosphate	0.2556	0.4657	1.0684	-1.3065	2.1727	0.5965	-0.2942	-1.0620
(-)-Cinchonidine	0.9572	1.0686	0.3041	0.8750	0.3145	0.2363	1.0602	0.5761
(-)-Eseroline fumarate salt	-0.4556	-0.0497	-0.0139	-1.6025	-0.1399	-0.1815	-0.3769	-0.5017
(-)-Isoproterenol hydrochloride	0.5960	0.6064	-0.7886	-0.9084	0.5521	-0.2874	0.6921	-0.9197
(-)-MK 801 hydrogen maleate	0.2867	0.9344	0.1971	0.2076	0.3022	0.4308	0.1874	-1.5465
(-)-Quinpirole hydrochloride	0.2290	1.3965	0.4091	2.2819	0.8297	-0.0410	0.3186	0.5188
(+) -Levobunolol hydrochloride	0.8687	0.1141	0.7762	0.3437	0.5833	0.2986	-7.1229	0.2839
(+)-Isoproterenol (+)-bitartrate salt	-0.9624	-1.0817	0.1532	-1.5110	-2.3120	-1.0112	-0.2656	-0.7479
(+,-)-Octopamine hydrochloride	0.0407	0.2852	-0.1988	0.3054	0.8151	0.7650	-0.9122	0.2768
(+,-)-Synephrine	-0.6728	-0.6037	-0.6184	-0.6344	-0.5292	-0.0257	-0.6847	0.5469
(±)-Nipecotic acid	0.5977	0.7378	-1.1126	-0.1288	0.7101	0.9528	-0.0805	-0.3130
(1-[(4-Chlorophenyl-4-methylpiperazine)	0.3225	0.7428	-1.4405	0.1459	0.4068	-0.0708	0.3954	-0.4140
(cis-) Nanophine	0.3242	0.0340	0.6384	-0.3568	0.2615	-0.0012	0.0244	1.0106
(d,l)-Tetrahydroberberine	0.4344	-0.7638	0.0127	0.8104	-0.3987	-1.4582	-1.0087	-1.1189
(R) -Naproxen sodium salt	-1.5235	0.0657	1.1919	0.0279	-0.2231	-0.0619	0.7017	0.3620
(R)-(+)-Atenolol	-0.0166	-0.0916	1.0209	-0.1796	-0.5257	0.2342	0.4426	0.4643
(R)-Propranolol hydrochloride	1.8874	1.2946	0.7580	1.5084	0.6192	1.3880	1.6777	1.3942
(S)-(-)-Atenolol	0.8461	0.6789	1.0493	-0.2597	0.3073	0.2241	-0.4054	-0.5638
(S)-(-)-Cycloserine	-0.4949	-0.4962	-0.8114	-0.1882	-0.5752	-0.6235	-0.4909	0.0698
(S)-propranolol hydrochloride	-0.1216	-1.2513	-1.1748	-0.7439	-1.2147	-1.1033	-0.7398	-0.8023
2-Aminobenzenesulfonamide	-0.5443	-0.2388	0.2679	0.5207	0.5274	-0.7343	0.4201	0.4550
2-Chloropyrazine	0.5539	0.3078	-0.1180	-0.1771	-0.2099	0.4061	-0.5182	0.6865
3-Acetamidocoumarin	0.0209	0.8479	-0.2762	1.5284	-0.3478	1.5594	0.9973	0.3681
3-Acetylcoumarin	0.7753	-0.8362	-0.4865	-1.7978	-3.1114	-0.6387	-0.0981	0.0093

3-alpha-Hydroxy-5-beta-androstan-17-one	0.6632	-0.0863	-0.4269	-0.1708	0.0947	-0.4451	-0.3285	-0.6944
6-Furfurylaminopurine	0.4580	-0.5691	-1.3625	-0.1002	-0.7614	-0.0132	-0.1855	-0.5523
6-Hydroxytropinone	1.5949	0.8376	-1.3220	1.3425	-0.0481	1.8382	0.9729	-0.7939
Acacetin	0.4591	0.1533	0.5190	1.0067	0.4848	0.1316	0.5144	-0.3666
Acebutolol hydrochloride	-1.2854	0.1637	0.8843	0.4490	0.4156	0.4622	-0.4893	-0.8880
Aceclofenac	-0.2443	0.4431	0.2926	0.6910	0.5921	0.4009	0.3227	0.1711
Acemetacin	1.2675	-0.1768	0.4565	1.0670	0.5016	0.1412	0.2055	0.0923
Acenocoumarol	-0.2642	0.4830	-0.3706	0.6555	0.6228	0.4223	-0.5106	1.0092
Acetaminophen	0.1728	0.6088	0.4368	-0.0357	0.2844	-0.2517	0.0687	-0.3526
Acetazolamide	0.3019	0.8450	0.9391	1.0348	0.3416	0.4603	2.4577	0.7798
Acetohexamide	-0.4612	-0.0268	-0.4251	-0.7620	-0.0567	-0.1786	-0.6987	0.4670
Acetopromazine maleate salt	-1.0161	0.0527	0.9004	-0.0163	0.0251	-0.1502	-1.1509	-0.7471
Acetylsalicylsalicylic acid	-0.4698	0.0082	1.3164	-0.4906	1.1123	-0.0328	0.0922	1.4974
Aconitine	-0.0358	0.2848	0.0437	0.3837	-0.2956	0.5969	-0.3674	0.9946
Acyclovir	0.2206	-0.3110	0.5895	1.8363	2.2438	1.9617	-0.0473	2.3817
Adamantamine fumarate	0.5222	0.0102	0.9179	0.2275	1.2619	-0.3900	0.9144	0.5706
Adenosine 5'-monophosphate monohydrate	0.5443	1.5780	1.7975	0.0554	1.2130	0.9455	1.1784	0.5104
Adiphenine hydrochloride	1.6022	2.0033	0.9123	0.8941	1.0627	1.5979	0.8320	1.2000
Adrenosterone	0.0025	0.2394	-0.1668	0.0903	-0.9235	-0.0249	-1.0593	0.7492
Ajmalicine hydrochloride	0.1056	-0.2034	-0.0091	0.4725	-0.3697	-0.5286	1.2020	0.8790
Ajmaline	-0.1355	-0.9907	-0.3808	-0.2029	-0.4161	-0.3057	0.8713	-0.4580
Albendazole	-10.0363	-7.3534	-7.2350	-10.4863	-7.5805	-6.3195	1.2691	-4.7381
Alclometasone dipropionate	-1.2327	-0.3755	-0.6796	-1.0509	-1.0933	-1.1626	-0.2238	-0.9272
Alcuronium chloride	1.1098	0.7442	1.2529	1.0260	1.5052	0.6912	0.4303	-0.1813
Alexidine dihydrochloride	-8.3798	-4.5348	-6.3699	-7.4139	-7.6046	-8.6891	-0.7880	-8.7479
Alfadolone acetate	-0.0691	-0.9352	0.6592	-0.8729	-0.1693	-0.7951	-0.9518	-0.4352
Alfaxalone	0.9237	-0.8220	-0.2021	0.1871	-0.6940	-0.2904	-0.1013	0.9953

Alfuzosin hydrochloride	2.2875	-1.1738	-0.2710	2.0067	-0.7685	0.2056	-0.6065	1.4880
Allantoin	-0.0900	1.4190	0.1699	-0.2927	-0.0158	1.1858	2.6976	0.1102
alpha-Santonin	-0.3197	-0.1693	-0.3970	-0.0290	0.1352	-0.3453	-0.0564	-1.0674
Alprenolol hydrochloride	0.6890	0.2657	0.2841	0.6499	1.7270	1.5041	0.8843	1.3361
Alprostadil	-0.0209	-0.4047	-0.2015	-0.0250	0.1892	-0.3999	-0.8973	-2.1216
Althiazide	0.4988	-0.1957	-0.4348	0.2209	-0.6972	1.7593	2.7292	0.1163
Altretamine	-0.2158	0.5590	-0.1062	-0.1096	0.5712	0.1604	-0.9343	-0.6882
Alverine citrate salt	-0.7330	0.3883	-1.1141	0.4050	0.9957	0.1903	-1.1180	0.6156
Ambroxol hydrochloride	0.6853	1.6711	0.3476	0.7728	1.2478	1.4406	0.1732	-0.2487
Amethopterin (R,S)	-9.1469	-14.9028	-7.0399	-11.0071	-12.2200	-16.0272	-1.1625	-11.8547
Amidopyrine	0.2602	-0.4218	-0.0843	2.2386	1.6074	1.5438	-0.8717	2.3498
Amikacin hydrate	0.3347	0.9990	0.3684	0.6920	0.3434	1.7027	1.1512	0.7590
Amiloride hydrochloride dihydrate	0.7486	0.8734	1.1736	0.9634	-0.2074	-0.5354	-0.0391	0.7642
Aminocaproic acid	0.9329	1.6788	-1.1112	0.5115	0.5878	1.9729	0.1226	1.2017
Aminohippuric acid	0.2773	0.6796	0.0241	0.6262	-0.4235	1.0543	0.8822	0.2869
Aminophylline	-0.1799	-0.3413	0.5841	0.9053	-0.1910	0.0278	0.3362	0.2286
Aminopurine, 6-benzyl	0.6688	-0.7836	1.0137	-0.4988	0.4374	-0.8699	-0.4038	-0.3865
Amiodarone hydrochloride	0.2437	-1.0049	-1.2824	-0.5336	0.3718	-1.5219	1.2869	1.2312
Amiprilose hydrochloride	0.7890	1.9554	1.2144	0.9484	0.9038	1.0972	-0.0259	1.1673
Amitryptiline hydrochloride	0.0227	1.5599	0.6792	1.7455	0.9088	0.8103	0.1461	0.5430
Amodiaquin dihydrochloride dihydrate	-0.0095	0.2646	0.4142	-0.2511	-0.2237	0.3819	-0.5624	-0.4343
Amoxapine	1.3022	-0.9007	1.3333	0.2583	-0.1654	-2.3732	-1.4283	0.7485
Amoxicillin	-0.3996	0.8905	-0.3621	0.7025	0.9647	-0.1606	-0.7027	0.1739
Amphotericin B	0.7741	-1.0839	-0.2452	0.9360	1.8532	-1.5629	1.4207	0.9273
Ampicillin trihydrate	0.5422	-0.0810	1.8551	-0.3065	0.6386	-0.3082	0.6527	-0.0094
Amprolium hydrochloride	0.2487	0.9352	-0.2612	0.4226	0.3388	0.2475	1.3398	0.7318
Ampyrone	-0.5397	-0.6360	-0.5750	-0.1211	-1.7552	-0.3061	-1.4380	0.1419

Amrinone	0.7731	1.4025	0.6652	0.2963	0.9956	1.3528	-0.1080	0.4734
Amyleine hydrochloride	-0.4843	-0.7250	0.2796	0.1500	0.1196	-0.1664	0.1136	-0.2703
Anabasine	0.3092	0.1956	-0.6916	0.4793	0.2087	0.2420	-0.1528	-0.4527
Androsterone	1.7373	-1.4072	0.0575	0.7519	-2.6252	0.3698	-1.2932	1.1223
Anisomycin	-13.2894	-17.1099	-11.5947	-13.4594	-10.8019	-14.3161	-0.3474	-9.6832
Antazoline hydrochloride	-0.1985	-0.2927	-1.1813	0.5834	0.5960	0.4261	0.3519	-0.9370
Antimycin A	-1.2505	-22.6619	-0.9318	-4.3591	-2.9644	-14.9649	0.0223	-4.7220
Antipyrine	0.6914	0.2100	-0.1839	-0.3519	-0.0699	-0.7039	0.1298	-0.1593
Antipyrine, 4-hydroxy	0.5819	-0.2946	0.2704	-0.3721	0.2774	-0.8168	-0.1591	0.5193
Apigenin	-0.8991	-0.0856	-1.1600	-0.6162	-0.8458	-0.3258	-1.2697	-0.3136
Apramycin	1.3722	1.6147	1.1233	1.8006	1.4792	1.6203	2.0599	1.9626
Arbutin	0.4508	0.0581	0.2227	-0.5358	0.6018	0.2753	-2.4337	0.3041
Arcaine sulfate	-0.0087	0.4889	0.9354	1.5328	0.9560	0.9158	1.0194	1.5824
Arecoline hydrobromide	0.9479	-0.5128	-0.3866	0.5023	0.0086	2.1618	0.7450	0.9867
Artemisinin	-1.3869	-0.5771	-0.5233	-1.0659	-0.7551	-0.9598	-0.1210	-0.3276
Articaine hydrochloride	0.9480	-1.0590	0.2077	-0.0053	1.1204	0.3577	0.8798	0.3440
Ascorbic acid	1.5737	0.8650	0.4087	1.0602	1.4897	0.2639	-2.9136	2.0150
Asiaticoside	-1.6695	0.1545	-0.4914	0.0053	-0.2663	-0.9303	0.3649	1.0438
Aspartic acid, N-acetyl (R,S)	1.3957	-0.0102	-0.1015	0.8490	-0.2900	-0.0911	-0.2371	0.4784
Astemizole	-3.2985	-0.8630	-2.5111	-2.5395	-0.5907	-0.4544	0.6101	-2.1926
Atovaquone	0.9362	0.4510	0.1640	-0.2217	-0.0003	0.1210	-0.1231	-0.5013
Atractyloside potassium salt	1.4464	0.1795	0.0299	0.3842	0.0144	0.1255	-1.4580	1.1610
Atracurium besylate	-0.8065	1.3394	0.9374	0.7173	0.0882	0.0010	0.5983	0.4087
Atropine sulfate monohydrate	0.7653	-0.7247	1.3122	2.0760	-0.5601	-0.0896	0.7298	0.2079
Austricine	-0.9110	-1.0291	-0.2308	-1.5792	-1.9258	-0.2963	0.0579	-0.8505
Avermectin B1	-0.8027	-0.2262	-1.3961	-0.6461	-1.0272	-0.0072	-1.6203	0.3257
Azacyclonol	0.4629	-0.3790	0.5745	-0.8868	-0.4574	0.5187	-0.4344	1.9682

Azacytidine-5	-0.6458	0.3501	-0.7286	-0.1803	0.8533	0.0537	-0.2662	0.4908
Azaguanine-8	-1.1486	-0.3515	-2.1494	-1.6599	-2.2279	-1.6899	-0.9409	-1.4958
Azaperone	0.4195	1.1268	-1.6793	1.8678	0.6456	1.0902	0.4001	0.3503
Azapropazone	0.2845	-0.1846	0.5185	0.9083	0.6931	0.0069	-6.4949	0.1706
Azathioprine	-5.6200	-7.1008	-4.1993	-7.6597	-8.8199	-12.9128	-0.2385	-7.8120
Azathymine, 6	1.5752	-0.2705	0.9091	1.5375	0.3079	0.9845	-5.4889	1.9130
Azlocillin sodium salt	-0.6217	-2.3452	-0.5699	-1.6357	-2.8611	-2.1236	-1.6403	-1.1499
Aztreonam	0.9369	-0.2133	0.5585	0.2369	0.6573	-0.0029	0.4242	0.6510
Bacampicillin hydrochloride	0.8335	-1.2355	0.3978	0.9897	-1.1314	-1.2440	0.2934	-0.4197
Bacitracin	0.1757	-0.0002	-0.1465	-0.1369	0.7888	-0.4714	-0.6374	0.3252
Baclofen (R,S)	0.2243	0.5666	0.4407	2.5817	1.9189	2.0306	0.3805	1.8718
Bambuterol hydrochloride	0.0861	-0.2473	0.5244	-1.8689	-0.6035	-0.0289	-2.8669	0.9225
Beclomethasone dipropionate	0.2955	0.0613	-0.2648	-0.6800	0.6469	0.0313	-0.0395	-0.1739
Bemegride	0.0907	0.1543	1.1279	0.9289	-0.6076	0.1195	0.6198	1.1781
Bendroflumethiazide	-0.3143	0.4131	0.9413	0.1527	0.3874	0.0963	-0.9949	0.1749
Benfluorex hydrochloride	0.3485	0.3088	0.2341	1.1337	0.4736	0.4749	0.3163	-0.8406
Benfotiamine	-0.2945	-0.6296	0.8246	1.1744	0.5475	-0.6819	-0.3454	0.2606
Benoxinate hydrochloride	-0.0952	0.0583	0.2319	-0.0502	0.0694	0.2144	-0.1688	-0.0811
Benperidol	-0.0398	0.2135	-1.6791	1.8726	-0.3006	1.6033	0.0037	2.3105
Benserazide hydrochloride	-0.6249	-0.0343	0.0552	0.1567	0.2162	-0.0106	0.1897	-0.2740
Benzamil hydrochloride	-0.0102	-0.7286	-1.0334	-1.5847	-1.6663	-0.8873	-0.1768	-1.2435
Benzathine benzylpenicillin	0.8735	0.2796	-0.0819	-0.2482	0.3636	0.1854	-6.2133	-1.5218
Benzbromarone	0.0423	-0.0401	0.1029	-0.0056	0.7844	-0.7514	-0.4229	-0.4899
Benzethonium chloride	-1.1237	-0.5285	-0.6652	-0.3374	0.0389	-0.2711	0.5012	-0.3900
Benzocaine	-0.2264	1.4611	-0.5447	1.5328	0.2560	1.3047	0.3104	0.5293
Benzonatate	0.1709	0.9067	1.2863	0.8158	-0.2749	1.2651	-0.2105	1.2779
Benzthiazide	0.7324	-0.8176	0.1177	-0.3138	-0.8563	-0.4447	0.9207	-0.3202

Benzydamine hydrochloride	0.6524	0.6100	-0.1805	0.9339	-0.3873	0.7212	-0.1633	0.5871
Benzylpenicillin sodium	-0.1662	0.0926	-0.6031	-1.2501	-0.2034	-0.2130	-8.4500	-1.0999
Bephenium hydroxynaphthoate	-0.3223	0.1385	-1.2637	0.8694	-0.0663	0.1722	1.2748	0.0552
Bepridil hydrochloride	-5.9149	-3.7333	-6.2894	-6.4649	-2.5645	-3.8066	0.0115	-6.0762
Berberine chloride	-0.4378	-2.3711	-0.8624	-1.2676	-0.8941	-3.4468	-9.9241	-1.7170
Bergenin monohydrate	-1.3083	-3.3166	-1.2463	-2.1632	-2.0138	0.7378	-0.6366	-0.6164
beta- Belladonnine dichloroethylate	-1.0326	-0.7462	-0.1896	-0.8238	-1.9731	-0.9493	-0.3918	-0.6244
Beta-Escin	-0.0538	0.7761	0.5910	0.9930	0.8844	0.5865	0.9158	0.2467
Betahistine mesylate	0.8921	0.2727	0.3307	0.4992	0.2988	0.9475	0.6584	0.0367
Betamethasone	-0.8920	-0.6394	0.0416	0.8916	-0.9399	-0.1311	-1.4252	-0.2053
Beta-sistosterol	0.9423	-0.0704	0.3277	0.6467	0.6492	-0.0982	0.2751	0.0569
Betaxolol hydrochloride	0.5894	0.0615	0.8485	0.2294	-0.3954	0.0794	-7.0292	0.0013
Betazole hydrochloride	0.1065	-0.0463	0.7717	-0.1706	0.3146	-0.4358	-0.5889	-0.0213
Bethanechol chloride	0.0295	0.8079	0.3185	-0.0377	-0.1638	0.2455	0.5746	0.9210
Betonicine	1.1583	1.0957	0.5623	-0.0271	0.2836	0.9464	-0.5192	1.5200
Betulin	-1.1587	-0.1585	-0.0833	0.2740	-0.4290	-0.7525	-0.3632	0.2631
Betulinic acid	0.8687	0.1021	0.2712	-0.1659	0.5643	-0.8087	-0.4744	-0.6755
Bezafibrate	0.3064	-0.0162	-0.1119	0.0825	0.3544	0.0647	-1.1644	0.1732
Bicuculline (+)	-0.7310	-1.3397	0.7893	0.6730	-0.0366	-0.7425	0.0101	-0.3736
Biotin	-0.9038	-0.1810	-1.8438	0.5566	0.7590	-0.3142	0.1712	-1.1719
Biperiden hydrochloride	-0.4236	-0.1345	-0.3126	0.2872	-0.4437	0.3562	-1.0225	1.0546
Bisacodyl	-3.8232	-4.6765	-4.2456	-4.4547	-5.9507	-6.8975	-1.1107	-5.6136
Bisoprolol fumarate	1.4259	0.8061	0.9108	0.2198	1.6761	0.4949	0.7227	1.0377
Boldine	-0.4540	-1.0416	0.0371	-0.0278	0.1050	-0.1877	-0.3310	-0.0135
Bretylium tosylate	0.2199	-0.5404	0.0144	-0.2440	-1.0464	-0.3878	0.0087	-0.7484
Brinzolamide	0.3493	1.2556	-0.3233	0.4494	1.5196	1.5697	0.4123	1.0166
Bromocryptine mesylate	-0.0195	-0.3293	-0.1238	-2.4985	-0.8281	-1.0825	-0.3553	-1.6855

Bromopride	-0.9820	0.4338	-0.9086	-1.5065	-0.0813	-0.1789	-0.2385	-0.3788
Bromperidol	0.0454	-0.5208	0.7280	-0.4680	-0.2690	0.0681	-0.5912	-0.7737
Brompheniramine maleate	1.1527	1.8858	1.1538	1.1380	1.4235	1.1478	0.8296	0.9197
Bucladesine sodium salt	0.5005	-1.2511	-0.0266	0.0784	-0.7879	0.0703	-0.0341	0.1502
Budesonide	-0.4223	-0.3806	-1.3666	0.3436	-0.0334	-1.1683	-0.2088	-0.9641
Bufexamac	-0.8871	0.4876	1.9872	1.5787	1.5429	2.5917	-1.8089	1.5199
Buflomedil hydrochloride	1.1285	0.3769	0.2491	0.1888	0.6916	0.5823	0.7992	-0.0257
Bumetanide	1.4459	0.3321	0.8103	-0.1677	1.3952	1.1576	0.6672	0.8965
Bupivacaine hydrochloride	0.5900	0.2563	-1.3502	-0.3304	-0.4747	-0.0087	-2.2121	-0.2935
Bupropion hydrochloride	0.2843	0.7544	-0.0832	0.3885	1.6601	1.1381	0.6233	0.8895
Buspirone hydrochloride	0.6271	-0.1213	-0.4583	0.3937	0.9401	0.5751	0.1611	-0.1992
Butacaine	-2.4313	-0.9015	-0.0781	-1.1036	-2.1698	-1.4684	-1.1275	-0.5213
Butamben	-1.8033	-1.7877	-1.4975	-1.7396	-1.6178	-0.7321	-0.0060	-1.1855
Butirosin disulfate salt	0.7249	0.9490	0.6800	0.7546	0.0069	1.8952	0.3145	1.4317
Butoconazole nitrate	-1.0291	-0.6107	-1.6086	-0.0659	-1.4747	-0.2080	-0.3286	0.3092
Butylparaben	-0.0025	-0.1422	-1.0220	-0.5761	-0.9153	0.7330	1.6326	0.8388
Caffeic acid	-0.6708	-0.0282	0.4482	0.4742	0.1475	-0.5446	-0.8896	-0.0027
Calciferol	-0.3827	-1.2390	0.0709	0.8067	0.4125	-0.8638	-0.0709	0.1763
Calycanthine	0.6798	0.1691	1.3044	1.4556	0.7365	0.8356	0.1512	1.3857
Camptothecine (S,+)	-15.2384	-19.3831	-12.0842	-17.0756	-18.1104	-27.5889	0.0394	-19.0685
Canavanine sulfate monohydrate (L,+)	0.0507	-0.3234	-0.2253	-0.8793	0.3704	-0.7406	-0.5854	-0.2318
Canrenoic acid potassium salt	0.1288	0.3520	0.2342	0.5350	-0.4708	0.2412	0.1889	0.1463
Cantharidin	-9.3595	-6.2389	-9.4561	-10.8550	-8.6002	-10.6448	1.9976	-8.1100
Capsaicin	-0.9497	0.8043	0.4325	0.5777	1.0960	1.5204	0.0256	0.2358
Captopril	-0.5946	-0.3172	-0.3013	-0.7627	-0.7416	-0.8519	-1.2419	0.0813
Carbachol	-0.8647	1.3491	1.2794	2.2509	0.6873	1.4020	-0.2075	1.8374
Carbamazepine	-0.3432	0.8251	0.1209	0.3110	0.6975	0.2496	0.9734	-0.3494

Carbarsone	1.0842	-0.5923	-0.6675	1.2601	-1.1554	0.1033	-1.0702	0.6002
Carbenoxolone disodium salt	-0.2681	0.7449	-0.4641	-0.3004	1.0011	0.0142	0.5864	-0.4920
Carbetapentane citrate	0.2578	0.3215	0.3022	0.3741	-0.1346	0.6399	0.2596	-0.4569
Carbimazole	0.4110	-1.2299	-0.5443	-0.0452	0.0869	-0.0746	-0.0013	0.3902
Carbinoxamine maleate salt	0.0087	-1.1836	-0.4093	0.0312	-0.9494	1.0194	0.3831	0.4050
Carcinine	1.0635	0.4273	0.1357	1.0690	-1.2801	0.7433	-1.4672	1.0591
Carisoprodol	0.7117	0.0164	0.1389	1.3355	-0.5058	0.5604	0.0013	1.1913
Carteolol hydrochloride	0.3883	0.8166	0.0963	0.5418	0.6301	0.8675	1.3822	1.3904
Catechin-(+,-) hydrate	0.7981	-0.1984	0.8370	-0.0825	-0.6712	-0.5531	0.5706	0.5175
Cefaclor	-0.4381	-0.0687	1.1280	0.4556	0.0003	1.5440	-9.3367	2.2977
Cefadroxil	-0.4682	0.3115	0.1661	0.9859	-0.0920	0.1072	1.4786	-0.6516
Cefalonium	0.6145	0.6784	-0.7735	0.6739	0.8467	0.7615	1.3879	0.6427
Cefamandole sodium salt	1.2502	0.7815	0.1014	0.9028	0.3724	-0.1927	0.5637	0.7092
Cefazolin sodium salt	-0.0835	-0.5414	-0.0583	0.5010	0.6933	0.2777	0.4998	-0.0202
Cefepime hydrochloride	-0.3278	0.4328	-0.0483	0.5691	0.9875	-0.0033	0.7737	0.5522
Cefixime	0.7563	1.1247	0.4680	0.7672	0.6568	-0.1119	-0.5213	-0.0954
Cefmetazole sodium salt	0.0102	-0.4892	-0.4613	0.3289	0.3416	0.4523	-0.0446	0.1869
Cefoperazone dihydrate	-0.1613	1.6672	1.0112	0.9340	1.9014	-0.9946	0.7171	1.2101
Ceforanide	-0.1946	-0.5147	0.0475	-1.0687	0.2080	-0.2126	-0.1700	0.3328
Cefotaxime sodium salt	-0.0824	0.7323	-0.1372	-0.3033	0.3456	0.5490	0.1626	0.1319
Cefotetan	-1.2111	1.6217	0.6959	0.6566	0.4581	0.7156	-0.9915	-0.0638
Cefotiam hydrochloride	0.5500	0.6330	0.3742	1.9136	0.0658	1.5959	-0.9987	2.2930
Cefoxitin sodium salt	-0.3362	0.1171	0.4128	-0.8471	-0.5047	0.0058	1.1252	-1.3771
Cefsulodin sodium salt	0.4215	-1.1642	1.5890	0.9220	-0.0365	-0.2090	0.0392	-0.0206
Ceftazidime pentahydrate	-0.8554	-0.5202	0.1141	0.6584	0.6188	0.8562	0.0956	0.4087
Cefuroxime sodium salt	0.8638	1.6043	1.2871	0.8648	0.9089	2.5400	0.4372	1.0969
Cephaeline dihydrochloride heptahydrate	-13.0400	-13.8626	-11.4975	-13.7170	-12.9033	-16.3530	-5.5625	-12.5135

Cephalexin monohydrate	-0.0639	1.1120	0.1216	-0.0063	0.7402	0.4786	0.4784	-0.3371
Cephalosporanic acid, 7-amino	0.6014	0.9433	1.0720	1.0604	-0.5811	0.4633	0.9748	0.4568
Cephalothin sodium salt	0.7575	1.5601	1.3265	-0.6743	0.9083	1.7766	0.6216	1.1010
Cetirizine dihydrochloride	0.7247	-0.0921	0.7309	-0.3048	-0.4897	-0.4120	0.8494	1.0575
Chelidonine (+)	-11.8685	-8.1023	-8.4351	-8.3030	-8.9972	-10.0665	-19.4341	-6.9415
Chenodiol	2.2178	1.7541	1.2515	0.3191	1.6435	1.5095	0.6346	0.7382
Chicago sky blue 6B	0.7438	0.1935	0.7996	0.7989	1.0383	0.6069	-0.3217	0.0897
Chlorambucil	-0.5114	0.1603	-0.5913	-0.2381	-0.0898	0.0668	-0.9043	-0.2018
Chloramphenicol	0.7205	-0.9509	-0.2508	-0.8268	-0.9339	-1.3733	-0.4802	1.4032
Chlorhexidine	-0.0312	-0.1795	-0.3755	-0.5173	-0.3548	-1.0535	0.1050	-0.9780
Chlormezanone	0.0963	0.8863	1.7203	0.0555	0.6856	0.6141	0.1552	0.0094
Chlorogenic acid	-0.1276	-0.3687	-2.0388	-0.9482	0.0133	0.1947	0.3668	-0.6564
Chloropyramine hydrochloride	1.2471	1.1351	0.8392	1.0915	-0.4076	1.1848	0.3063	0.2570
Chloroquine diphosphate	-0.3948	0.3830	0.5804	-0.9431	0.3895	0.3636	-0.5390	-0.2983
Chlorothiazide	-0.3264	-0.4163	2.1104	1.0893	-1.3926	0.7106	-0.3373	-0.4088
Chlorotrianisene	-0.3884	-0.1800	0.4143	-0.3604	0.1148	-0.4922	1.0403	-0.6759
Chlorpheniramine maleate	0.5106	0.5547	1.0154	0.9572	0.7824	0.2904	0.4635	-0.1283
Chlorphensin carbamate	0.5109	2.6025	0.6161	0.3536	-0.3862	1.2174	-8.4812	1.0293
Chlorpromazine hydrochloride	-1.0367	-2.3760	-2.4674	-0.5641	-1.0664	-2.0580	-1.3946	-1.7968
Chlorpropamide	1.3090	-0.1821	-0.5031	1.6630	0.1102	0.3817	0.7369	1.2380
Chlorprothixene hydrochloride	-1.5951	-0.8664	-0.3184	-0.8851	0.0512	-1.4092	-6.1589	-0.6482
Chlortetracycline hydrochloride	-0.2118	0.3545	1.2185	-0.2422	-0.1028	0.0509	0.2788	-1.0010
Chlorthalidone	-1.0722	-0.4373	-0.2294	-0.5421	-1.0787	-0.7309	-2.1392	-0.2441
Chlorzoxazone	0.4736	0.9508	0.6168	0.9927	-0.1586	0.5148	1.1474	1.0367
Cholecalciferol	-0.1395	-0.7936	0.2173	0.6529	0.4560	-0.4356	0.7868	0.5580
Chrysene-1,4-quinone	-8.3785	0.2632	-2.1983	-0.2956	-0.5803	0.5051	0.3119	-0.3214
Chrysin	1.1483	0.9068	0.9393	-0.8981	0.8238	0.4424	0.7693	-0.7622

Ciclopirox ethanolamine	-5.4754	-8.5130	-5.7074	-12.0652	-5.9572	-7.6349	-1.3811	-11.6191
Cimetidine	0.7782	0.5527	-0.9897	-0.3007	0.4546	-0.3625	0.3762	0.5446
Cinchonine	-0.2440	0.1363	-0.3062	-0.3729	0.2987	-0.5587	0.1581	-0.6397
Cinnarizine	0.9763	0.0944	0.2811	-0.4874	1.2587	-0.3236	0.9496	-0.1300
Cinoxacin	-0.4291	0.3928	0.0642	-0.0069	-0.5306	-0.6187	-1.3673	-0.8075
Ciprofibrate	0.6871	0.9591	1.6949	0.2693	0.7998	0.9700	-5.4904	0.5084
Ciprofloxacin hydrochloride	0.7785	0.0409	2.1281	-0.7830	0.7149	-1.0182	0.0742	0.7464
Cisapride	-0.2291	-1.6675	0.2897	-0.0079	0.9481	-0.2974	-2.6738	-0.2503
Citalopram Hydrobromide	-0.1882	-0.2082	-0.0127	-0.1942	-1.1596	0.0683	0.0503	0.1889
Clebopride maleate	0.1742	0.2966	-1.0666	0.6544	0.9008	-0.1721	-0.6157	-0.1673
Clemastine fumarate	-1.1639	-0.6419	-0.7370	-0.7424	-0.3251	-0.6461	-0.4777	-0.7625
Clemizole hydrochloride	-0.4458	0.0777	-0.8957	-1.4816	-0.8223	-0.7494	0.5588	-0.3183
Clenbuterol hydrochloride	-0.2867	1.1335	0.8584	0.7184	1.1778	-0.0050	0.0381	0.1767
Clidinium bromide	-0.1525	-0.8326	0.8560	-0.2403	-1.2387	-0.1708	0.8313	0.0064
Clindamycin hydrochloride	0.9205	0.3051	-0.1903	-0.2219	0.3694	0.2017	0.5926	-0.2031
Clioquinol	-0.8413	0.7867	-1.0196	0.1468	-0.1581	-0.5254	0.3625	-0.0963
Clobetasol propionate	-1.4611	-1.0480	-1.6673	-1.4085	-1.3223	-1.1778	0.0030	-1.0594
Clocortolone pivalate	0.3158	0.1518	1.4747	1.0663	0.6743	1.0854	0.1459	0.1211
Clofazimine	-6.2548	-5.6064	-5.7027	-7.1204	-4.3411	-5.3049	-0.1609	-6.4398
Clofibric acid	-0.4820	0.6299	-1.5123	-0.2343	-0.5720	-0.0350	-0.8787	0.2037
Clofilium tosylate	0.4629	1.5540	-0.6700	0.3945	-0.3901	0.6389	0.0883	0.9309
Clomiphene citrate (Z,E)	-5.0003	-2.2767	-3.4909	-3.1480	-3.9490	-1.0626	1.5009	-1.0315
Clomipramine hydrochloride	-0.7395	-2.5012	-0.5532	-1.8752	-0.0589	-1.8900	0.0733	-1.7089
Clonidine hydrochloride	-0.9588	1.2428	0.2044	0.0984	1.3862	1.7109	0.7927	1.3596
Clopamide	-0.2718	0.8021	1.3317	0.2668	0.5507	0.4137	0.6367	0.2850
Cloperastine hydrochloride	-1.6345	-0.4724	-0.6874	0.2790	-0.9762	-0.3698	1.0973	0.4554
Clorgyline hydrochloride	0.3420	0.5629	0.0573	0.1373	1.1954	0.0855	0.3494	0.1161

Clorsulon	-0.4189	-0.5951	-0.8129	-1.7331	-0.0371	0.5513	0.5725	-0.8003
Clotrimazole	-1.8675	-1.9626	-3.0619	-3.2614	-0.3097	-1.5379	1.3807	-1.2697
Cloxacillin sodium salt	0.6521	0.3400	1.5880	-0.0538	0.4440	-0.8950	-1.0114	0.5746
Clozapine	-0.0472	-0.9668	-0.0017	-0.3813	0.9248	-0.5038	0.0942	-0.1976
Colchicine	-11.7908	-12.4254	-8.5046	-9.8702	-10.5441	-11.7848	-0.8539	-8.3685
Colistin sulfate	-0.2872	0.0772	-0.1029	0.9670	0.4842	0.5281	-1.1479	0.1886
Condelphine	-0.1259	0.0021	0.3676	0.4403	-0.4203	0.1189	-0.2602	-0.1987
Conessine	0.8559	1.3325	1.3945	2.0405	1.3557	1.7953	-0.3917	0.5487
Convolamine hydrochloride	-0.2068	0.3197	0.9500	0.1632	0.3273	0.1349	-0.5119	1.1202
Coralyne chloride hydrate	-0.7465	-1.0881	0.0641	-0.2087	-2.0933	-1.6730	-0.4779	0.0708
Corticosterone	-0.1027	0.1496	0.2107	0.4459	0.2533	0.4252	-0.9442	-0.0665
Cortisone	1.8144	0.0395	0.8398	0.0589	0.8509	0.1747	0.1854	0.6242
Corynanthine hydrochloride	0.6352	-0.3596	-1.5165	0.0915	-0.0004	-1.1446	-1.4288	-0.3392
Cotinine (-)	-0.3361	-1.1750	-0.4232	1.9637	-0.2118	1.8924	-1.2016	2.6624
Cromolyn disodium salt	-0.5604	-1.7810	0.3932	-0.1327	-0.9328	0.5456	0.7310	1.3258
Crotamiton	-2.2086	-1.2517	1.0822	0.0599	-1.2425	0.1105	0.0217	-0.7769
Cyanocobalamin	0.4334	0.0370	-0.0719	0.8092	1.2191	0.4651	0.5375	1.7761
Cyclacillin	1.2592	0.5110	1.0696	1.2126	1.3531	1.2017	-12.3375	-0.3275
Cyclizine hydrochloride	0.5498	-0.2037	-0.2984	-0.9730	0.2776	-0.3326	-0.2451	-0.7235
Cyclobenzaprine hydrochloride	1.8001	1.3480	0.6179	1.6937	1.3440	1.4247	1.5057	1.8099
Cycloheximide	-8.2885	-5.7627	-5.6171	-6.9842	-8.1054	-8.3972	-1.0541	-7.7022
Cyclopenthiazide	0.9055	0.4450	0.2744	0.9730	0.2862	0.4723	0.3815	0.9919
Cyclopentolate hydrochloride	0.2673	0.9980	1.4263	0.8190	0.8782	0.7722	0.1184	-0.5039
Cyclosporin A	0.9157	0.0946	0.2578	1.5842	1.8273	0.4779	0.5934	1.3543
Cyproheptadine hydrochloride	0.0803	-1.3557	-0.2413	0.2313	-0.2270	-0.7727	-0.5863	0.2767
Cyproterone acetate	1.1645	0.7978	1.2786	0.4219	0.3023	0.5555	0.5745	1.4712
Cytisine (-)	0.0386	-0.4045	1.1955	-0.0634	0.3811	0.2905	-0.3969	0.1934

Dacarbazine	-1.2696	-0.4423	-0.6010	-0.2297	-1.2120	-1.0067	1.0150	-2.7275
Danazol	0.6426	0.3417	0.4199	-0.7059	0.4002	-0.0856	0.5235	-0.5058
Dantrolene sodium salt	-0.4773	-1.8635	-0.1185	0.0636	-0.7665	-1.4133	-0.3421	-0.3226
Dapsone	1.9495	0.9242	0.2664	1.1747	0.0088	0.7802	1.0663	1.3246
Daunorubicin hydrochloride	-11.1394	-2.8526	-8.4682	-5.7646	-13.8311	-13.4280	-0.0045	-11.5996
D-cycloserine	0.7720	0.8812	0.9460	1.6595	0.3181	1.0379	0.5884	0.5333
Debrisoquin sulfate	-0.4760	0.4687	0.0789	-0.0611	-0.6803	-0.4776	-1.4307	0.4350
Decamethonium bromide	1.4597	0.7657	0.0220	0.4485	-0.4796	1.1251	0.8361	-0.0160
Deferoxamine mesylate	-3.5992	-0.9348	-2.0747	-1.6172	-3.2429	0.4040	1.7155	-1.1773
Dehydrocholic acid	1.1823	-0.0690	0.5045	-0.6777	0.2315	-0.9951	-0.5787	0.9185
Dehydroisoandosterone 3-acetate	-0.6430	0.4017	-0.5058	0.4734	0.9584	-0.4734	-0.2675	-0.1305
Delcorine	-0.4284	-0.3568	0.9296	-0.0158	-0.2212	0.2690	-0.0355	-0.0021
Delsoline	-0.3891	0.1541	0.0203	-0.2732	-0.0240	0.0335	-0.0553	-0.9266
Deltaline	0.7766	-0.0340	1.0066	0.5364	-0.1890	-0.4561	0.8247	-0.1655
Demecarium bromide	0.1405	0.3232	0.6060	-1.3303	0.0537	0.0380	0.9105	0.5560
Demeclocycline hydrochloride	0.4084	0.5873	-1.0071	-0.5968	-0.4672	0.3583	1.0387	-0.9235
Denatonium benzoate	-0.0780	-0.9870	0.3593	0.8547	-2.2032	0.7154	1.3746	0.1867
Deoxycorticosterone	-0.0478	1.1746	0.4507	1.3169	0.4314	1.4247	0.4173	-0.4761
Deptropine citrate	-0.0551	-0.4249	-0.8070	-0.7568	-0.2026	-0.2574	-11.1526	-1.2840
Dequalinium dichloride	-3.8695	-3.2822	-3.1960	-2.3696	-5.1401	-2.8623	0.8778	-2.9317
Desipramine hydrochloride	-0.8290	-0.4791	-0.5996	-0.1312	-0.6799	-1.3525	-1.0598	-0.0452
Dexamethasone acetate	-0.3425	-0.0104	0.2161	0.6431	0.4961	0.0754	0.3142	0.5901
Dextromethorphan monohydrate	-0.0494	0.7319	-0.3632	-0.2750	0.3134	-0.0477	-1.6206	0.2954
Diazoxide	1.3142	0.8941	0.6204	2.7133	1.7815	2.2921	-11.8092	1.8101
Dibucaine	0.5140	1.7917	-0.0056	2.0449	0.7256	1.6073	1.1685	1.1502
Dichlorphenamide	1.3526	0.3449	0.2292	0.1411	0.4391	0.4558	1.3380	1.0450
Diclofenac sodium	0.4795	0.0321	1.0870	1.2166	0.1357	-0.1454	1.5746	0.5113

Dicloxacillin sodium salt	-0.2615	-0.9785	-0.6323	-0.1048	0.4062	-0.4759	-0.0743	0.2245
Dicumarol	0.5254	-0.4562	-0.2856	0.5189	-0.0228	-0.9908	0.1202	-0.9918
Dicyclomine hydrochloride	0.2088	-0.1043	0.1935	0.2775	0.0670	-0.3536	-0.4488	-0.9550
Dienestrol	-0.2474	1.4736	0.9026	0.6851	1.1741	1.0764	0.5839	1.6350
Diethylcarbamazine citrate	2.1345	0.4576	0.9043	1.4358	0.8784	0.1470	0.9798	0.1001
Diethylstilbestrol	1.3112	1.0595	1.8206	-0.7553	1.3616	0.8427	0.2932	0.4343
Diflorasone Diacetate	0.0991	0.1917	-1.2396	-1.4320	0.8933	0.0349	-0.6285	-0.7805
Diflunisal	0.9596	0.1145	0.1572	-1.3110	-1.6782	-0.3841	0.5520	-0.2803
Digitoxigenin	-8.9621	-7.9132	-9.4008	-9.7768	-7.4044	-6.0036	1.1945	-4.7274
Digoxigenin	-10.6264	-11.0669	-9.5291	-11.6926	-7.1985	-9.4316	1.7106	-7.3923
Digoxin	-13.2141	-12.6405	-14.4103	-14.8958	-12.0641	-9.5917	-0.2993	-7.1805
Dihydroergocristine mesylate	-0.8168	-1.0837	0.6805	1.0336	-0.8820	0.2451	0.3505	0.2060
Dihydroergotamine tartrate	0.1570	1.1284	-0.9085	-0.0834	0.3424	0.8898	-1.4209	-0.0200
Dihydroergotoxine mesylate	0.2012	-2.3719	-0.3030	-0.4631	-0.0070	-0.5925	0.0510	0.0004
Dihydrostreptomycin sulfate	1.3314	1.8846	-1.0142	0.3624	0.5331	2.1367	-0.1877	2.4497
Dilazep dihydrochloride	1.0432	2.8829	0.8590	0.7500	-0.6289	1.5869	-0.0737	0.6588
Diloxanide furoate	0.5822	-0.9137	-0.1448	0.7488	0.2870	-0.3566	0.9309	-0.0473
Diltiazem hydrochloride	0.4589	-0.7614	0.5557	-0.5615	-0.2038	-0.8808	0.3027	-0.6495
Dimaprit dihydrochloride	0.9991	-0.2491	0.7164	0.4902	-0.0423	0.6904	-0.2361	1.0276
Dimenhydrinate	0.2581	0.0837	0.9368	0.7342	1.5408	0.9361	1.1779	-0.1636
Dimethadione	-0.1508	-0.5531	-0.8589	-0.1266	0.0814	0.1595	-0.2236	0.4097
Dimethisoquin hydrochloride	0.7223	-0.1146	0.3943	0.0191	0.0778	-0.4133	-0.3093	-0.1120
Dinoprost trometamol	0.2749	-0.0766	0.2506	-0.4088	-0.2602	-0.3202	0.2059	-0.4629
Dioxybenzone	1.1398	-0.4340	-0.1194	-0.4331	-0.9310	-0.3441	0.8862	-0.5598
Diperodon hydrochloride	-0.1230	-0.2987	-0.1697	-0.0589	-0.3804	-0.3648	-0.3258	0.0864
Diphemanil methylsulfate	0.5027	2.0561	-1.2927	2.2443	0.8508	1.7255	0.6637	-0.0748
Diphenhydramine hydrochloride	0.4539	0.1373	0.5872	0.9732	0.3604	0.0371	-0.3994	-0.7460

Diphenidol hydrochloride	-0.0970	0.5124	0.7800	-0.7285	-0.7754	1.5219	0.3939	0.4384
Diphenylpyraline hydrochloride	-0.3106	0.4842	-0.3310	-0.0058	0.5057	0.2883	0.4732	-0.8150
Dipivefrin hydrochloride	-0.1023	0.8810	0.1344	1.3945	1.3175	1.4054	0.2258	0.7784
Diprophylline	0.5225	0.5049	0.7827	-0.1059	0.3544	0.4870	1.1578	0.6310
Dipyridamole	0.2993	0.4189	-1.8603	0.1777	-0.7196	-0.8870	0.6447	-0.0598
Dipyrone	-1.7843	1.5165	-0.6365	1.1079	-0.0743	1.0126	0.2079	0.2941
Dirithromycin	0.3687	0.9724	0.6167	1.2572	1.0178	1.3921	0.6461	2.2213
Disopyramide	0.2825	0.5558	0.0064	0.2406	0.3810	0.9849	1.8441	0.7245
Disulfiram	-4.9934	0.8349	-4.1883	0.3402	0.9648	0.9967	0.4315	0.0941
Dizocilpine maleate	0.7511	0.4797	0.1992	0.1930	1.3711	0.2279	-0.2293	0.6493
DO 897/99	0.2402	2.4662	0.1234	1.1659	0.7969	1.7763	1.0740	0.8249
Dobutamine hydrochloride	-0.2737	0.9776	-0.1421	0.1667	-0.6119	0.1694	-1.7438	-0.0181
Domperidone maleate	-0.3280	0.8229	0.9425	0.1190	-0.8057	-0.4725	-0.4567	-0.0864
Dorzolamide hydrochloride	0.1667	-0.0441	1.1555	0.5084	0.8882	0.4770	0.5745	0.1291
Dosulepin hydrochloride	-0.4400	0.7771	-0.9361	0.2142	-0.1668	0.9720	-0.4306	-0.0919
Doxazosin mesylate	0.3446	0.0817	-0.6039	-0.4992	0.4723	-0.3515	-0.5133	-0.9225
Doxepin hydrochloride	2.0027	0.0152	0.5735	0.4292	0.0037	0.6584	0.4603	0.6831
Doxorubicin hydrochloride	-9.3018	-4.9217	-7.3497	-7.7180	-9.3085	-11.9234	-0.0696	-7.7097
Doxycycline hydrochloride	-2.5487	-1.0619	-1.4182	-0.0446	-1.1341	-1.3180	-0.1579	-1.8178
Doxylamine succinate	0.4200	-0.3238	-0.9971	0.8089	-0.2899	-0.8430	-0.0293	0.0479
Drofenine hydrochloride	-0.7636	0.2213	-1.2908	0.1900	-0.1823	-0.1494	-0.1795	-0.2263
Droperidol	-0.1050	0.6276	-0.2669	-0.1793	0.0913	0.1232	0.4806	0.2774
Dropropizine (R,S)	-1.6571	1.0873	0.3560	1.1189	2.4708	2.1590	0.5069	1.3730
Dubinidine	1.2927	1.6942	1.6546	1.5532	0.7648	1.8610	0.0963	1.0240
Dyclonine hydrochloride	0.4425	-0.1999	1.0285	1.7102	0.5352	0.7776	1.4527	0.6981
Dydrogesterone	-0.4767	-0.9061	-0.9389	-1.1240	-1.6494	-0.8638	-0.5005	-0.6581
Ebselen	-0.7264	-0.3198	0.1182	0.2499	-0.5046	-0.2032	-8.7838	0.9851

Eburnamonine (-)	0.4744	-0.2613	0.2246	-0.2074	0.5209	-0.1314	-0.8941	-0.0790
Econazole nitrate	-0.2524	-0.0309	-1.1188	-2.0878	-0.6829	-1.0413	-0.2039	-0.3825
Edrophonium chloride	0.8628	0.1138	0.1278	3.1846	1.0894	2.1914	0.1177	2.5258
Ellipticine	-17.9786	-24.4589	-17.8691	-17.3602	-17.6602	-25.0310	-0.5154	-19.4442
Emetine dihydrochloride	-11.4306	-12.4664	-10.6107	-11.9873	-10.2428	-14.5263	-0.0101	-11.4579
Enalapril maleate	0.5671	1.5632	0.8833	1.3173	0.2114	0.9428	0.2496	0.8436
Enilconazole	0.2751	-0.6794	0.1051	0.3983	-1.1096	0.9334	2.1307	0.6324
Enoxacin	0.8951	0.6312	0.0208	0.4506	0.4109	0.7358	-1.8275	0.8981
Epiandrosterone	0.9724	-1.3015	-0.2303	-0.3730	0.5496	-0.1137	-0.4509	0.7744
Epicatechin-(-)	0.5828	2.0171	0.5038	1.8925	0.7951	1.1131	1.0900	1.7075
Epirizole	-0.2260	0.7947	-0.0818	-0.3758	0.2331	0.2453	0.5391	1.1688
Epitiostanol	0.7500	0.2680	-0.0608	0.1868	1.1026	0.3434	0.5680	0.4847
Epivincamine	-0.6539	0.9256	1.1787	0.8712	0.8400	1.2561	-0.4511	0.8227
Equilin	-0.0322	-0.2088	-0.7359	0.2636	0.0948	-0.0058	-8.6450	-0.3855
Ergocryptine-alpha	-0.2276	-0.8312	-1.0124	-0.5436	0.9406	1.4804	0.6723	0.6380
Erythromycin	-0.2182	-0.1690	0.1430	-0.8905	0.9697	0.1407	0.0185	-0.7014
Esculetin	-0.3554	-0.1712	-0.0001	-0.0861	0.2929	-0.1141	0.0166	-0.6951
Esculin Hydrate	0.3191	0.4540	-0.1132	-0.7190	-1.9943	0.6035	-0.0640	0.1652
Eserine sulfate, physostigmine sulfate	0.1766	0.2073	0.5209	0.7847	-0.0042	0.5224	0.5860	0.8941
Estradiol-17 beta	0.7789	0.9505	0.5818	0.4705	-0.9999	-0.3941	-3.2942	0.6877
Estriol	0.0158	0.3415	0.2994	0.1608	2.2483	0.3935	-1.0818	-0.5313
Estrone	-0.1932	0.3431	0.6167	0.8636	0.8229	-0.5149	0.5272	-0.5401
Estropipate	0.5103	-0.3142	0.3357	0.4096	0.1281	-0.0974	0.1261	-0.7321
Etanidazole	0.6946	1.4893	-0.4604	1.1677	-0.0069	1.5389	0.0802	1.5136
Ethacrynic acid	0.1738	0.2552	1.4150	-0.2953	1.0520	0.3230	0.3483	-1.0389
Ethambutol dihydrochloride	0.7462	0.0190	0.2894	-0.1171	-0.1160	-0.8759	1.1323	-1.0729
Ethamivan	0.4683	-0.7205	-0.7804	0.8931	-0.3821	-0.6399	0.4352	0.3032

Ethamsylate	0.3291	0.5749	0.9663	0.7891	0.8959	0.1621	-0.6117	0.6400
Ethaverine hydrochloride	-1.7157	-3.0895	-2.5103	-2.8057	-2.6585	-4.1079	-0.5242	-4.3786
Ethionamide	0.9518	1.4157	0.9777	0.3240	0.6697	0.8545	0.5877	-0.2198
Ethisterone	-2.3816	-0.0938	-2.9129	-3.0377	-2.1311	-3.3645	1.6844	-3.2328
Ethopropazine hydrochloride	-0.5116	-0.7915	-1.3983	-1.0319	-0.2502	-0.5959	-14.3331	-1.2214
Ethosuximide	-0.4409	0.8394	1.7121	1.7104	1.6153	0.7633	0.5180	1.1119
Ethotoin	0.3837	0.2110	-0.4667	-0.6592	0.5050	-0.4580	-0.1259	0.4653
Ethoxyquin	0.2860	0.5618	0.8674	0.6292	1.5664	1.3824	0.6636	-0.0171
Ethynodiol diacetate	1.1070	0.0276	0.7431	-0.4788	-0.1311	0.0454	-0.4569	-0.2425
Ethynylestradiol 3-methyl ether	1.2265	0.9847	0.7214	0.4855	1.1943	-0.1241	1.1444	1.1371
Etidronic acid, disodium salt	-1.3903	-0.3521	-2.1738	0.2407	-0.0652	-0.6569	0.2711	-0.7138
Etifenin	0.4673	-0.1407	0.8761	1.0117	-0.0238	0.4477	-0.8697	1.3196
Etilefrine hydrochloride	0.6344	0.6499	1.5944	0.1774	1.0800	-0.1946	-0.1591	0.4013
Etodolac	-0.1852	1.8492	0.0673	-0.1090	-0.0977	1.0801	-0.0798	1.0106
Etofylline	0.3406	0.2258	0.0230	1.0793	0.5794	-0.1062	-2.3517	0.5300
Etomidate	-0.4304	0.2079	-0.7687	-0.3421	0.1059	-0.1559	1.9992	0.5943
Etoposide	-0.9310	1.2682	0.2089	0.4817	-1.8928	2.3549	1.6505	0.3489
Eucatropine hydrochloride	-0.7087	0.5188	0.9215	-0.3015	0.3043	1.0803	1.3289	1.1591
Evoxine	-0.7510	-0.8353	0.5668	0.5446	-0.8400	-0.1855	-0.0887	0.1674
Famotidine	0.9739	0.3714	0.1844	-1.5123	1.2369	0.1393	-0.7036	1.2865
Famprofazone	-1.3841	0.1012	-0.8418	-0.5758	-0.0820	-0.3848	-0.0244	0.2939
Felbinac	0.5705	-0.6709	-0.2958	-0.6538	-0.9273	0.4990	0.3932	-0.6053
Felodipine	-0.3289	1.2882	0.1439	1.4470	0.8833	2.0250	1.1462	0.4139
Fenbendazole	-10.1649	-9.2580	-8.3047	-9.8932	-8.5624	-10.5877	-0.0126	-9.8748
Fenbufen	-0.3520	0.1589	-0.4641	0.0983	-0.1556	-0.0835	0.2980	-0.3707
Fendiline hydrochloride	-1.2695	-1.2919	-0.9098	-2.3054	-0.0218	-0.9628	-0.3276	-1.7712
Fenofibrate	0.7903	1.1996	0.5469	1.1557	1.3486	1.5833	1.1070	1.0201

Fenoprofen calcium salt dihydrate	-0.0426	-0.0603	0.4814	-0.5906	0.3962	0.9828	0.6748	0.0292
Fenoterol hydrobromide	0.6759	-0.2554	0.5868	0.6875	-0.3234	-0.8462	-0.1602	-0.7029
Fenspiride hydrochloride	0.6528	0.3328	0.2322	-0.1516	0.6020	0.4669	-1.5765	-0.3849
Fillalbin	-0.6783	-0.7310	-0.3414	-1.1260	-1.1310	-0.1911	0.7234	-0.5733
Finasteride	0.0102	1.8220	-0.8529	1.1977	0.7688	1.9996	0.9345	0.1946
Fipexide hydrochloride	0.2545	0.0198	-0.8189	0.0888	0.4948	-0.0416	-0.4048	0.1752
Flavoxate hydrochloride	-2.6655	0.7982	0.4054	1.0037	0.7455	1.8574	-1.2485	1.8008
Flecainide acetate	0.4532	0.1911	-0.3547	0.6217	-0.1008	0.5677	1.6829	-0.2722
Florfenicol	-0.5855	-0.9302	0.4360	0.5849	-0.8409	-1.1621	-1.4812	-0.3283
Flucloxacillin sodium	-0.7708	-1.1550	-0.5433	0.2222	-0.0036	-0.7691	-1.1397	-0.8502
Flucytosine	-0.1170	0.0430	-0.2854	0.5224	0.3484	0.2910	0.0894	0.3036
Fludrocortisone acetate	0.7571	-1.0485	-0.0064	-0.2752	-0.5868	-0.9741	-1.1220	-0.2085
Flufenamic acid	1.0153	-0.1533	0.0904	-0.0021	0.6393	-0.5296	0.2948	-0.1307
Flumequine	1.3440	0.0150	-0.2190	1.1908	1.3060	0.5244	-0.2662	0.7617
Flumethasone	0.5558	-0.5531	-0.3153	-0.5203	-0.5297	-0.2384	-4.7241	-0.5335
Flunarizine dihydrochloride	-0.0013	0.2519	-1.1950	1.4477	0.2660	-1.4344	0.4376	0.1114
Flunisolide	1.0508	1.0660	0.1163	1.8363	0.2823	0.7572	-0.4844	2.3383
Flunixin meglumine	1.0174	-0.2970	0.6615	1.0929	0.2353	0.1417	0.4352	0.2569
Fluocinonide	0.8447	0.2805	0.6406	0.5575	0.7481	0.0028	0.5993	-0.2278
Fluorocurarine chloride	-0.6796	0.0900	0.8645	0.3028	-0.2004	0.4130	-7.1043	0.1106
Fluorometholone	-0.2077	1.5507	0.4506	0.4460	0.9199	1.7805	0.7575	0.3299
Fluoxetine hydrochloride	-0.9686	0.0020	-0.1801	0.3784	-0.5836	-0.3384	-1.7794	-0.0973
Flupentixol dihydrochloride cis-(Z)	0.1661	0.2227	-0.2510	0.2632	0.0221	0.4407	0.2007	0.2682
Fluphenazine dihydrochloride	-0.0017	1.0980	-1.6529	0.4260	-0.5472	1.1297	0.7836	1.9990
Flurandrenolide	0.9680	0.7814	-0.8566	-0.7106	0.5355	1.2214	-0.9216	1.3419
Flurbiprofen	-0.0141	0.3282	0.5464	-0.0735	0.3675	-0.0939	0.7287	0.3682
Fluspirilen	1.0073	0.3442	0.2276	-0.0668	0.8079	-0.7571	1.3875	0.0837

Flutamide	-0.3364	-1.5206	0.1571	0.3494	0.8828	-1.3960	-0.3319	-0.7486
Fluticasone propionate	0.6640	0.3300	-0.6114	-0.3714	0.6557	0.3603	0.0586	-1.0170
Fluvastatin sodium salt	-1.0961	-1.0680	-2.2768	-2.7809	-2.3104	-3.2042	-0.7648	-3.4384
Fluvoxamine maleate	1.0514	1.2990	0.1504	1.4353	0.9140	0.3409	-3.4899	1.7040
Folic acid	0.4328	-0.1957	0.2933	1.0861	0.6655	0.2693	-0.9488	0.9985
Folinic acid calcium salt	0.4960	-0.6966	-0.0769	-0.1280	-0.7008	0.1239	-0.1353	0.1101
Foliosidine	0.4683	-0.4065	-0.6812	-0.1588	0.3763	-0.2393	0.1282	-0.7543
Fosfosal	0.4136	-0.4177	1.0763	0.0366	-0.0284	-0.1692	1.6968	0.2559
Furaltadone hydrochloride	-1.1030	0.2472	0.8431	0.5508	0.6512	-0.0847	1.0854	-1.0586
Furazolidone	0.1866	0.6079	-0.3634	-0.2659	-0.6545	0.3184	0.5602	-0.7695
Furosemide	-0.2411	-1.2177	-1.2701	0.3745	-1.0706	0.3988	-2.4503	0.3301
Fursultiamine Hydrochloride	0.8756	0.2305	0.3515	0.1130	1.0429	0.0174	0.5405	-0.4087
Fusaric acid	0.0453	0.6029	-1.0446	-0.9029	-0.8761	0.2790	-0.6488	0.8557
Fusidic acid sodium salt	0.2250	0.5784	1.1105	-0.6206	-0.2027	0.0050	-7.3399	-0.4215
Gabapentin	-0.9162	-1.3002	-0.6946	-0.6170	-1.8656	-1.3846	-1.2658	-0.7999
Gabazine	0.6201	-0.0442	-0.3406	-0.0625	-0.0565	0.8833	1.1032	0.9334
Gabexate mesilate	0.3575	0.2429	-0.1940	-0.3224	1.1417	-0.0968	-4.6025	-0.3658
Galanthamine hydrobromide	-0.7251	-0.0254	0.4280	-0.3924	0.3096	-1.0498	-0.6082	-1.4557
Gallamine triethiodide	1.2904	1.2857	0.2580	0.3340	0.4549	2.0895	0.7713	1.2048
Ganciclovir	-0.2151	0.1434	0.0228	0.0700	0.2993	-0.4511	-0.3183	-0.9990
GBR 12909 dihydrochloride	-4.3819	-3.2422	-2.6530	-3.3739	-1.7892	-1.8078	-0.0781	-1.9064
Gelsemine	-0.2672	-1.0746	-0.5068	0.2464	-1.4092	-0.2536	-0.1859	-1.1326
Gemfibrozil	1.0424	-0.0344	0.6021	0.2522	0.5420	0.3184	-18.9290	0.0043
Gentamicine sulfate	1.1089	2.3823	0.3401	1.9553	0.8868	2.3095	-1.0010	1.6412
Gibberellic acid	0.8853	0.4087	-0.3611	0.7016	-0.3991	1.5312	1.9096	1.0206
Ginkgolide A	0.3157	1.4473	1.3980	1.7129	0.2543	0.9032	0.8249	-0.1770
Glafenine hydrochloride	0.6263	-0.4961	0.5750	0.8195	-0.1284	-0.2740	-0.6636	0.3367

Glibenclamide	1.1391	1.4242	1.2887	1.6487	-0.0791	1.0275	0.6741	0.8313
Gliclazide	0.2619	1.1225	0.8478	1.5785	0.7093	1.6136	0.6097	0.9798
Glimepiride	-0.9182	-0.9425	-0.9146	1.2630	-1.4182	-0.8239	-0.6557	-0.9590
Glipizide	0.4674	-0.2136	-0.1256	-1.4608	-1.5498	-0.5968	0.2191	-0.6986
Gliquidone	-0.5743	-0.9045	0.5259	-1.7486	-0.4425	-1.1368	-1.2241	-0.4355
Glutethimide, para-amino	0.3829	0.7217	1.7914	1.3240	1.8240	2.3009	-0.3670	2.0498
Glycocholic acid	0.5494	0.3997	0.7276	-0.7572	0.3388	0.0373	-0.9625	0.4735
Glycopyrrolate	0.1223	0.2053	0.4383	0.0016	0.5399	-0.3539	1.2084	0.0610
Gossypol	1.0328	-0.3267	0.5877	0.1564	0.4050	-0.0421	0.1329	0.1830
Gramine	0.3799	0.5472	-0.0760	-0.3053	0.9576	0.8915	-0.2717	0.1557
Graveoline	-0.5707	0.5007	0.8901	0.2588	-0.2502	-0.8041	0.4561	-0.4805
Griseofulvin	0.6063	0.6458	-0.2346	0.0216	0.0948	0.0177	-0.0095	0.3574
Guaifenesin	0.0665	0.3574	-0.1900	-0.0016	0.2232	-0.5326	-2.3899	-0.6337
Guanabenz acetate	-0.1170	-0.5962	1.4982	0.1934	0.2200	-0.8445	-0.0044	-0.2246
Guanadrel sulfate	0.7698	0.3384	0.5062	-0.8615	0.5131	-0.5564	-1.5875	-0.4613
Guanethidine sulfate	0.5823	1.9882	0.3346	1.4064	1.0905	0.8084	0.0844	1.6950
Guanfacine hydrochloride	0.1724	-2.3377	0.0881	-0.0171	0.1601	0.3094	0.4485	1.3343
Halcinonide	-0.3834	-1.1312	-0.6261	-0.4796	-0.6081	-0.3765	-0.0818	-1.3371
Halofantrine hydrochloride	-1.5569	-1.3849	-1.3106	-0.6347	0.0754	-2.0822	0.1072	-0.5874
Haloperidol	1.0998	1.6048	1.3560	0.2666	1.4684	1.2162	0.5417	1.1240
Harmaline hydrochloride dihydrate	-0.4384	-0.0264	-0.6618	-0.3931	-0.0004	0.1206	-0.7906	0.3256
Harmalol hydrochloride dihydrate	-0.2402	0.1211	-1.0290	-0.7892	-0.4316	0.7826	0.5592	0.0411
Harmane hydrochloride	-0.1110	0.5300	-0.8935	-0.4381	0.1949	0.1921	-0.5885	-0.0507
Harmine hydrochloride	-1.6100	0.3189	-0.9301	-0.6650	-1.3977	-0.2994	0.5847	-1.2008
Harmol hydrochloride monohydrate	-1.4997	-0.2304	0.0091	-0.8270	-0.5169	1.1973	0.5995	-1.2028
Harpagoside	0.1111	-0.6246	-0.1651	0.0273	0.0019	-0.4376	-1.4346	0.7690
Hecogenin	0.2543	-0.3482	-0.3960	0.8608	-1.0452	0.8827	0.9774	1.9626

Heliotrine	0.2644	-0.1720	2.2864	-0.1801	-0.4102	-0.1077	0.4499	0.6020
Helveticoside	-9.1939	-10.2313	-10.1399	-11.5354	-8.5015	-7.2062	0.9337	-5.1342
Hemicholinium bromide	1.7053	1.0658	0.3863	0.8923	0.6771	1.4309	-2.1530	0.8271
Heptaminol hydrochloride	0.5278	0.2250	-0.2374	1.6158	-0.2969	-0.1241	0.3354	0.5756
Hesperetin	0.5160	0.4879	1.6358	-0.2757	0.6585	0.4352	1.0735	0.1795
Hesperidin	0.6996	2.1924	-0.4622	0.9765	0.3305	2.7275	-0.3170	0.3222
Hexamethonium dibromide dihydrate	0.1060	-0.5122	0.6419	-0.1594	-0.5303	-0.3078	0.1406	0.0172
Hexestrol	0.0277	0.5149	0.6390	-0.5730	0.4236	-0.2071	0.0354	0.0324
Hexetidine	-1.3232	1.1743	0.2941	0.0141	0.3202	1.9383	0.3536	0.5112
Hexylcaine hydrochloride	0.3176	0.2500	-0.6307	1.0919	0.5032	-0.1945	0.8517	-0.6682
Hippeastrine hydrobromide	-0.2971	0.7769	0.4021	1.5410	0.4092	1.4191	1.2190	0.5334
Homatropine hydrobromide (R,S)	-1.4716	0.7465	0.0487	1.1251	0.5149	0.3444	-0.4227	-0.1206
Homochlorcyclizine dihydrochloride	2.0082	-0.2258	0.2039	-1.2749	0.7547	-0.2018	-0.2600	-0.1978
Homosalate	-0.1487	-1.1004	1.4087	0.0272	0.0970	-0.6308	-0.0493	0.2186
Hycanthone	-3.5097	-0.1741	-2.9759	-2.8543	-3.1799	-0.4336	0.8424	-3.1016
Hydralazine hydrochloride	-0.1231	0.1399	0.9174	0.1559	1.3617	0.7222	0.1302	0.4313
Hydrastine hydrochloride	-1.8897	-0.7034	-1.3045	0.3280	-1.6051	-0.5714	0.2882	-0.6076
Hydrastinine hydrochloride	2.1302	0.8957	1.2383	1.5771	1.3843	1.3771	1.7811	1.2245
Hydrochlorothiazide	0.2253	0.7820	0.0903	-1.5509	-0.0088	-0.6221	1.5573	0.7024
Hydrocortisone base	0.3979	0.4588	-0.3477	-0.1914	0.6294	0.6962	0.9181	0.2233
Hydrocotarnine hydrobromide	0.6336	0.8661	0.9237	1.7148	1.1427	0.8459	0.8294	1.1281
Hydroflumethiazide	0.2707	-0.7281	-0.4914	-0.3302	-0.2337	0.4604	0.9691	1.0792
Hydroquinine hydrobromide hydrate	0.0499	1.1909	0.8723	2.1811	1.0373	1.6905	0.2872	0.5431
Hydroxytacrine maleate (R,S)	0.0200	0.7204	-1.5671	0.2061	0.0443	0.0953	0.7303	-0.5100
Hydroxyzine dihydrochloride	1.2903	0.1149	-0.0931	0.5860	-0.0186	0.0538	0.5558	-0.9662
Hymecromone	-0.0880	-1.4623	-0.8330	-0.1352	-1.1510	-0.8494	0.0498	0.0777
Hyoscyamine (L)	0.7397	2.0966	0.2173	0.4967	-0.3470	1.6051	-0.3680	0.5766

Idazoxan hydrochloride	0.8259	0.7410	1.3759	1.2759	1.2782	0.6540	-1.9589	1.0781
Idoxuridine	-0.6158	-0.4369	-0.0513	-1.6893	-0.8512	-0.9879	-0.0787	0.4539
Ifenprodil tartrate	-0.2897	0.6344	-0.4183	1.4454	0.7875	0.7738	0.6801	1.1380
Ifosfamide	-0.0652	-0.2103	2.2404	-0.9119	-0.1080	-0.2798	1.0522	-1.0351
Imidurea	-0.6323	-2.1535	-0.3733	-0.1329	-0.6274	-2.0757	-0.9724	0.0428
Imipenem	-0.0791	0.7073	-0.9740	-0.5096	-0.0164	-0.4928	-0.3552	-1.1660
Imipramine hydrochloride	-0.6303	1.0996	0.0608	1.3435	0.4105	0.7053	0.6236	0.2016
Indapamide	-0.2234	0.8876	-0.5583	0.4141	-0.3032	0.1382	-0.1032	-0.1471
Indomethacin	0.6150	-0.9843	-1.2106	-1.0012	0.2561	-0.5441	-0.2432	-0.2565
Indoprofen	0.0446	1.7540	1.1642	0.4945	1.4069	0.2588	1.4784	0.0818
Iobenguane sulfate	0.0032	-0.4048	-0.9811	0.3862	-0.3543	-2.0105	0.6184	-0.0279
Iocetamic acid	-0.5570	0.4139	0.0602	-0.4891	-0.0017	-1.0480	0.9625	-0.4510
Iodipamide	-0.3269	0.0769	-0.6552	0.4157	0.4763	0.2244	-0.8763	0.2785
Iodixanol	0.6784	0.1914	0.2890	0.6069	0.4258	-0.8931	0.2394	-0.6056
Iohexol	0.5290	0.4881	0.5883	1.2709	-0.0019	0.7357	-0.3436	0.4317
Iopamidol	-0.5058	-0.1899	-0.0228	-0.3576	0.2165	0.4441	-0.1761	0.2059
Iopanoic acid	1.0047	0.0626	0.0194	0.4147	-0.7900	0.4836	-9.1306	0.0395
Iopromide	-0.7692	-0.1595	0.7409	1.2065	0.0017	1.1762	-0.0178	0.5899
Ioversol	0.2478	1.1798	0.2355	1.1709	0.8764	1.5911	0.0051	0.3345
Ioxaglic acid	0.2551	-0.5799	0.1246	-1.1399	-0.8946	-0.0080	0.3181	0.4370
Ipratropium bromide	0.0052	-0.3633	-0.2645	0.7243	-0.3039	-0.2192	-0.4016	-0.0773
Iproniazide phosphate	-0.1665	-0.2994	0.4287	0.8002	1.2329	0.2740	-0.5708	0.6832
Isocarboxazid	-0.0894	0.6595	0.0286	0.8657	0.8284	1.0857	-6.9879	0.5539
Isoconazole	-0.3274	0.2110	-0.8544	0.7572	-0.0836	-0.3053	0.0462	-0.7071
Isocorydine (+)	0.0944	0.3091	0.1957	-0.7380	0.4934	-0.8987	-1.5379	0.5974
Isoetharine mesylate salt	0.1301	0.2504	-0.4961	-0.0359	-0.0733	-0.2710	0.2363	-0.4655
Isoflupredone acetate	1.0612	0.6838	0.0327	1.3662	-0.0332	0.0069	-0.0455	1.3681

Isometheptene mucate	0.8441	0.0049	0.1869	-0.5162	0.6313	0.3581	0.0523	-0.3859
Isoniazid	-0.9696	0.9031	-1.0586	1.4911	-1.2235	0.5096	-0.2119	1.8393
Isopropamide iodide	0.2077	-0.6301	0.8114	-0.3366	-0.0048	-0.4620	-1.1891	1.1868
Isopyrin hydrochloride	0.0426	0.6309	0.1761	-0.0541	0.7228	2.6540	1.7962	1.2399
Isoquinoline	0.5380	0.8520	0.5316	-0.0814	0.0406	0.2425	-0.5090	0.6185
Isosorbide dinitrate	-0.6429	1.3005	0.3648	0.5270	0.3731	1.4895	0.3763	0.5741
Isotretinoin	-0.3280	0.3578	1.1562	-0.1927	1.0332	1.0470	-6.9612	0.1778
Isoxicam	0.4213	-0.4910	0.0157	1.1469	1.0010	0.1348	0.6803	-0.6529
Isoxsuprine hydrochloride	-0.3264	-0.0444	1.1476	1.0557	0.1940	0.3106	-0.0742	-0.8665
Isradipine	-0.6976	-0.6493	0.1918	-0.0088	-0.0241	-0.3019	-0.5251	-0.3474
Ivermectin	-0.1029	0.0847	1.2202	-0.5926	-0.1052	0.3865	-5.3198	0.6179
Josamycin	0.6851	0.7136	-0.2299	0.1573	-0.0455	1.4631	0.7206	-0.2300
Kaempferol	0.1980	-0.0021	1.2424	-0.2160	0.1403	0.2451	0.4627	-0.5460
Kanamycin A sulfate	-0.0423	1.2875	0.9112	0.1591	0.1620	1.6379	0.5683	0.1258
Karakoline	1.0638	0.3997	0.0293	0.2599	0.3305	0.1920	0.9684	0.2883
Kawain	0.5432	0.1509	0.4174	-0.6911	0.5253	0.4206	0.4700	-0.1635
Ketanserin tartrate hydrate	0.9791	1.3019	0.7876	0.3809	0.4312	2.2450	-0.3650	1.5809
Ketoconazole	0.4879	1.0101	0.1572	0.3577	0.3822	0.7815	-0.6191	-0.9477
Ketoprofen	-0.0432	0.3443	0.3512	-0.1482	0.0745	0.1078	-0.3097	-0.1618
Ketorolac tromethamine	0.2336	-0.1348	-0.1020	-0.0274	0.4079	-0.4470	0.1220	0.3502
Ketotifen fumarate	-0.4406	-0.3654	-0.8863	-0.3854	-0.1834	0.1664	-1.4372	0.1135
Khellin	-0.4915	-1.0304	0.2573	0.1307	-1.9193	-0.4693	-1.0623	0.8150
Kynurenine, 3-hydroxy (R,S)	-0.5215	0.8849	-0.7413	-0.3653	-0.8870	0.3792	-1.0910	-0.1637
L(-)-vesamicol hydrochloride	-0.6595	0.0002	-0.6835	0.7154	-0.2982	0.2899	-0.1039	0.6978
Labetalol hydrochloride	0.6565	0.0386	0.4417	-0.3098	1.0402	0.0172	-0.0147	0.2406
Lactobionic acid	-0.5736	1.4910	0.0269	0.5723	-0.9901	0.3072	-1.2392	0.3683
Lanatoside C	-15.0569	-15.0227	-14.1654	-14.6998	-13.0280	-11.2218	-0.4002	-6.7280

Lansoprazole	-0.8724	-0.2697	-0.2763	-0.0132	-0.8603	-0.8361	0.6056	-0.4177
Lasalocid sodium salt	-3.2676	-3.4683	-3.6186	-3.9492	-4.5715	-6.8756	-0.0051	-6.2887
Laudanosine (R,S)	-0.5331	-0.9398	-0.7049	0.4938	-1.4144	-1.1739	0.0756	-0.3660
Leflunomide	-0.4416	0.1595	-0.3972	-0.3908	-0.4680	0.9318	-0.2701	-0.1700
Letrozole	-0.6227	0.4348	0.6747	-0.2682	0.7222	0.3026	-11.6073	-1.7143
Leucomisine	0.5847	0.3256	1.1301	0.8886	0.2795	0.4914	0.4842	1.0532
Levamisole hydrochloride	0.3209	-0.1939	-0.8416	-0.4706	-0.8835	-1.1438	-0.9599	0.0708
Levocabastine hydrochloride	-0.1436	1.1606	-0.0515	-0.3425	1.2274	1.0462	0.2620	-0.4413
Levodopa	-0.1872	-0.1543	0.2556	-0.5663	-1.0207	-0.8248	-1.5449	-0.1038
Levonordefrin	-0.2072	0.0002	-0.2016	0.2913	-0.5881	-0.2083	-0.0030	0.3621
Levopropoxyphene napsylate	-0.0099	0.0761	0.7454	-1.3549	-0.3243	0.1126	-0.6127	-0.2744
Lidocaïne hydrochloride	0.5586	-0.2420	1.2152	-1.1874	0.4687	-0.3696	-0.6899	-0.6330
Lidoflazine	0.7763	-1.0728	0.5017	-0.6284	-0.0182	-0.5416	-1.3689	-0.6874
Lincomycin hydrochloride	0.4912	0.5647	0.2440	-1.1635	-0.3903	-1.1112	-0.4913	-0.5135
Liothyronine	-1.3308	0.3667	-0.4669	-0.2101	0.0834	-0.2735	0.0710	0.2591
Lisinopril	0.1763	-0.5925	-0.6761	0.2386	-0.7307	-0.3356	-1.4275	0.9945
Lisuride (S)(-)	1.5138	0.1079	0.8278	0.4671	1.4433	-0.2292	0.3236	1.0140
Lithocholic acid	-0.5597	1.1158	0.4992	0.7508	1.0520	1.1381	0.2833	0.5822
Lobelanidine hydrochloride	0.6848	-0.1150	-0.8743	0.6595	-0.7618	0.3640	-0.1274	1.0113
Lobeline alpha (-) hydrochoride	0.1306	-0.4713	0.2463	-0.5652	-0.1282	0.0213	0.5498	-1.0143
Lomefloxacin hydrochloride	0.6570	2.8066	0.9548	0.7658	0.0389	1.3162	0.9501	0.7699
Loperamide hydrochloride	-1.1117	-1.0535	0.2982	-0.8222	-0.8438	-1.3318	1.2328	-0.5602
Loracarbef	-0.5855	-0.5261	0.1527	0.1870	-0.5769	-1.1422	-0.1291	-0.6860
Lorglumide sodium salt	1.5929	1.9210	2.1375	1.4392	1.5572	1.2400	1.6227	1.6433
Lovastatin	-0.4378	0.8740	-0.0118	-0.9276	-1.0320	-0.3414	0.2659	-1.3863
Loxapine succinate	-0.3688	-0.9461	-0.9065	-0.0743	-0.9114	-3.4089	-0.0097	-0.6242
Lumicolchicine gamma	0.9134	1.2175	-0.5174	0.0451	0.0056	0.7931	0.1947	0.0906

Luteolin	-0.3330	0.3510	-0.8801	0.7746	-0.6797	0.4980	-0.4520	0.2381
Lycorine hydrochloride	-7.4552	-5.5147	-6.8653	-6.9344	-7.5920	-9.7467	0.1524	-6.8765
Lymecycline	-1.3922	-0.1027	-0.2936	0.1395	0.2125	-0.2941	-0.1035	-0.3284
Lynestrenol	-6.9863	0.8549	0.7649	-1.0524	1.1653	0.4630	0.6707	0.6188
Lysergol	0.8354	1.2746	0.4982	0.0079	0.2280	1.4187	-0.4371	-0.0812
Mafenide hydrochloride	0.2501	1.2220	2.8080	0.4579	1.0064	1.1365	0.8843	0.8201
Maprotiline hydrochloride	0.2672	-0.0765	0.0704	-0.6478	0.0569	-1.1131	0.0962	-1.2250
Mebendazole	-9.7106	-8.3089	-7.3245	-9.8774	-9.0624	-6.6234	0.3406	-8.0074
Mebeverine hydrochloride	-0.7971	0.0635	-0.5913	-0.3960	-0.4333	0.6252	-4.2543	0.5909
Mebhydroline 1,5-naphtalenedisulfonate	-0.8449	0.6739	0.0043	0.7726	-0.4605	0.3858	0.6467	0.5988
Mecamylamine hydrochloride	-0.5390	-0.3632	0.8565	0.7483	1.1068	0.0033	-5.7943	-0.6838
Meclocycline sulfosalicylate	-0.8385	0.8941	-0.2519	-1.1020	-1.3420	-0.4487	0.6521	-1.6452
Meclofenamic acid sodium salt monohydrate	1.1795	0.8651	0.7154	0.9604	1.3387	0.6555	0.2100	-0.1444
Meclofenoxate hydrochloride	-0.5068	-0.6858	-1.3070	-0.3708	0.4585	-0.0475	0.0374	-0.9872
Meclozine dihydrochloride	0.6069	1.3682	-1.0000	0.0848	1.2247	1.0546	0.3487	0.8307
Medrysone	-0.9830	-0.7411	0.1779	0.5478	-0.4472	-0.0028	-0.4482	-0.9675
Mefenamic acid	0.5114	0.1957	0.2824	-0.0279	0.6196	-0.6765	-0.4121	-1.0654
Mefexamide hydrochloride	0.4844	0.7999	-0.3445	-0.0765	0.2137	0.5641	-8.1821	-0.1735
Mefloquine hydrochloride	-2.0969	-0.5229	0.4608	0.1389	0.3338	-0.3519	1.1848	0.2738
Megestrol acetate	0.2859	-0.1684	-2.0818	0.9871	0.4819	1.7374	0.8690	0.2708
Meglumine	1.0818	0.9015	0.2583	-0.7157	0.1988	0.6308	2.4209	0.8605
Melatonin	0.2257	-0.3605	0.4454	0.1087	0.3048	0.2638	-0.9571	0.3002
Memantine Hydrochloride	0.5936	-0.4092	0.8043	-1.1590	-0.3784	-1.4786	0.7780	-0.5822
Menadione	-0.0200	0.1118	-0.1839	-1.2069	-0.0056	-0.2203	-2.5882	-1.2145
Mepenzolate bromide	0.0617	0.0682	-0.1516	0.1703	-1.1224	0.1877	-0.2181	0.0952
Mephenesin	-0.5713	-0.0030	-0.6595	0.2590	0.2742	-0.0834	-0.0161	-0.1868
Mephentermine hemisulfate	0.7430	-0.4681	-0.6826	-0.3104	0.6539	1.3971	1.7625	0.4087

Mephenytoin	-0.0072	-0.5736	0.4159	0.0132	-0.0494	-0.7351	0.3929	-0.3531
Meprylcaine hydrochloride	0.8602	0.0793	1.1409	0.0203	0.0965	0.4602	-0.0348	0.1076
Meptazinol hydrochloride	-0.2504	0.7343	-0.6707	0.7046	1.0138	1.1432	-0.4310	0.7421
Merbromin	-0.5582	0.5871	0.1530	0.1767	0.5487	0.3322	-0.1225	0.0171
Meropenem	-0.0047	-0.0977	1.0882	1.1753	0.1124	-0.3831	0.4798	0.1192
Mesalamine	-0.2709	0.1000	-0.3434	-0.3748	-0.1836	0.3327	-0.0491	0.1761
Mesoridazine besylate	-0.3654	0.1393	-0.5138	-1.5518	0.1713	0.3375	-0.1748	-0.5047
Metampicillin sodium salt	0.4840	2.5042	0.8258	0.4784	0.4936	1.6242	-0.1173	0.6902
Metanephrine hydrochloride DL	0.0248	-0.1391	0.0164	-0.1629	-0.2096	-0.4668	-0.0683	-0.3609
Metaproterenol sulfate, orciprenaline sulfate	0.3401	-0.1151	0.3734	-0.0357	0.1853	0.1227	0.5871	0.8175
Metaraminol bitartrate	0.0550	-0.4405	0.3368	0.4550	0.4054	0.1482	0.3028	-0.6231
Metergoline	-3.0480	0.2989	-1.0826	-1.7366	-1.1583	0.1020	0.0419	-0.0283
Metformin hydrochloride	0.0293	1.5409	-0.9669	0.5244	0.2027	1.0662	1.6611	0.5067
Methacholine chloride	0.0557	0.5818	0.6091	-0.5241	-0.0743	-0.6345	-0.7834	0.1422
Methacycline hydrochloride	1.0439	0.9298	0.1513	0.7710	-0.9628	0.7987	0.8679	0.2829
Methantheline bromide	0.6115	-0.1173	0.9667	0.5258	0.1328	-0.0766	0.0026	0.4729
Methapyrilene hydrochloride	0.0463	0.7098	0.6659	1.0536	0.1399	0.2121	-1.0362	0.2978
Methazolamide	1.1146	0.3507	0.6786	1.7545	0.0139	0.1839	1.4522	0.6291
Methiazole	-9.8207	-8.9253	-7.5109	-9.5101	-8.6962	-8.3529	0.4860	-8.8924
Methimazole	0.4417	0.2190	-0.2670	0.5680	1.0059	-0.5186	-0.3526	0.2720
Methionine sulfoximine (L)	0.5106	0.9025	1.0915	0.4937	0.1761	-0.0153	1.1668	0.9049
Methiothepin maleate	-0.6257	-1.4113	-0.1350	0.3524	-0.1819	-0.5710	-0.1082	-0.7043
Methocarbamol	1.1040	-0.1937	1.1222	-0.0671	0.9911	-0.0466	0.4717	0.6433
Methotrexate	-8.3646	-15.0067	-7.3348	-13.6595	-11.1177	-16.6247	1.3970	-13.8662
Methotrimeprazine maleat salt	0.1789	-0.4471	0.8668	-1.1834	0.3956	0.5323	0.4898	0.4057
Methoxamine hydrochloride	1.3244	-0.1281	0.3691	-0.2085	0.4394	-0.1119	-0.9489	0.2896
Methoxy-6-harmalan	-1.5039	0.0254	0.7895	-1.6706	0.0004	-0.0967	-0.3998	-0.0571

Methoxy-8-psoralen	0.3880	0.7274	-0.2790	0.3786	1.0857	1.8489	0.4349	-0.0103
Methyl benzethonium chloride	-1.7309	0.3236	-2.4002	-1.2067	-1.1349	-0.4572	-0.9029	-1.3748
Methylatropine nitrate	0.2359	-0.2714	0.6258	-0.6079	-0.6809	0.0549	-0.7719	-0.1058
Methyldopa (L,-)	1.6038	1.4946	0.0878	1.4359	0.7240	-0.2345	1.4046	0.9890
Methyldopate hydrochloride	1.0621	0.7559	0.2779	-1.2811	0.9809	0.8008	0.8811	0.5064
Methylergometrine maleate	0.7372	-1.4519	0.5025	0.0559	0.0182	0.1843	0.5260	-0.0964
Methylhydantoin-5-(D)	-1.7475	0.5279	-0.5082	-0.5124	-0.1254	-0.1580	0.2184	-0.8880
Methylhydantoin-5-(L)	-0.1583	-0.1637	-0.1173	-0.5342	0.2253	0.3613	-0.8036	-0.0024
Methylprednisolone, 6-alpha	0.1245	-0.5803	-0.4193	0.2780	0.7180	-0.5714	-0.5582	0.0011
Meticrane	0.9862	-0.4851	-0.1795	-0.2124	-0.7763	0.7931	-0.7661	1.3258
Metixene hydrochloride	-1.3171	0.3935	0.1092	0.1034	-1.0573	-0.9880	-1.4595	0.8962
Metoclopramide monohydrochloride	-0.4823	-0.2965	-0.9204	-0.9065	0.3474	-0.1467	0.0726	-0.4124
Metolazone	0.8989	-0.2767	0.2105	-0.0606	-0.0422	-2.8736	0.0044	-0.0574
Metoprolol-(+,-) (+)-tartrate salt	0.2673	-1.1689	-1.1991	-0.2371	-0.3189	-0.1730	1.8795	0.0330
Metrizamide	-1.0979	0.4256	-0.0806	-0.6524	-0.4007	0.3923	-0.2177	0.2217
Metronidazole	0.2103	0.1488	0.1061	2.3377	-0.2377	1.9399	-0.0528	1.4975
Metyrapone	0.1864	0.2029	0.3640	0.3295	0.1695	-0.1910	1.2600	0.7460
Mevalonic-D, L acid lactone	0.8594	-0.1346	-0.2697	0.5091	-0.0690	-0.2954	-0.5845	-0.4862
Mexiletine hydrochloride	-0.1322	0.3536	0.7470	1.4544	-0.1390	1.6185	-2.3010	1.8325
Mianserine hydrochloride	-0.2087	-0.7707	-1.2617	0.3280	0.0186	0.0057	0.1443	-0.2739
Miconazole	-1.4426	-0.2312	-0.8195	0.0342	-0.3373	-0.5990	-0.7149	-2.1975
Midecamycin	-0.3626	0.6918	0.2265	0.0038	0.8854	1.1832	0.0786	0.3148
Midodrine hydrochloride	0.4524	-0.6477	-0.4762	-0.4845	-2.2661	-0.7871	-1.1532	-0.2736
Mifepristone	0.6366	0.1297	-0.0381	-0.5406	0.4204	-0.1462	0.0147	-0.0042
Milrinone	2.1896	-0.1033	0.2228	0.2188	0.2737	0.6731	-0.4396	0.0897
Mimosine	-0.2764	-1.1471	-0.8552	0.8801	0.6283	0.1248	-0.1626	0.4034
Minaprine dihydrochloride	-0.7793	0.4086	0.1757	0.9859	0.2447	0.3857	0.6306	-0.4071

Minocycline hydrochloride	-0.3197	1.0833	0.0647	-0.3761	-1.7310	-1.0311	0.8494	-2.6759
Minoxidil	0.8786	-0.4393	0.5891	-1.9502	-0.6245	-1.1598	0.7129	0.1431
Mitoxantrone dihydrochloride	-11.1268	-11.6850	-9.8560	-11.1455	-14.6502	-17.4142	0.5832	-11.3322
Molindone hydrochloride	1.5672	0.7234	1.1183	-0.8198	1.3894	1.1337	1.1817	0.2861
Molsidomine	0.2539	0.4295	-0.4036	0.1322	0.5154	0.1674	0.2068	-0.4340
Mometasone furoate	-2.9484	-0.6504	-3.0873	-0.4813	-2.2514	-0.3761	0.9050	-1.3229
Monensin sodium salt	-7.9082	-3.8261	-7.4964	-6.9538	-6.1435	-4.7245	0.8166	-7.1686
Monobenzone	-0.9716	-0.4100	-0.3879	0.0020	0.2652	-1.1891	0.1943	-0.8904
Monocrotaline	0.3253	-1.2377	0.7273	0.7988	-0.0582	-0.9308	1.3136	0.2067
Morantel tartrate	-0.5597	-0.0517	0.8526	0.5492	-0.0779	0.2600	0.4085	-0.7796
Moricizine hydrochloride	0.0891	-1.4393	-0.4654	-2.0013	-0.4568	-0.9304	-1.6520	-0.6832
Moroxidine hydrochloride	0.3936	1.1571	-0.4292	2.4051	2.0721	2.0705	0.8293	1.6588
Moxalactam disodium salt	0.6048	-0.5124	-0.1989	-0.2096	-0.4490	0.0346	-0.6480	0.2976
Moxisylyte hydrochoride	-0.5739	-0.7392	-0.0893	0.0128	0.3883	-0.1833	0.7447	-0.2773
Moxonidine	-0.7610	-0.0778	0.3628	1.2676	0.3740	0.0501	-4.8925	0.0160
Muramic acid, N-acetyl	0.5810	1.6523	-1.4007	0.3464	0.1768	0.8352	-0.2383	-0.6288
Mycophenolic acid	-6.7716	-6.0946	-5.7244	-6.6943	-5.1556	-6.7793	1.3848	-6.7712
Myosmine	0.6772	0.7193	-0.0799	-0.1110	0.5253	1.1537	-1.4123	1.0922
Myricetin	1.1692	0.4507	0.1988	0.4967	0.5689	0.2297	-0.3330	0.2712
N6-methyladenosine	0.2540	0.7049	0.0269	-0.4993	0.8792	-0.0206	0.7821	0.7385
Nabumetone	0.3917	-0.4122	0.4866	-0.6198	-0.1287	-0.2497	-0.5528	-0.5101
N-Acetyl-DL-homocysteine Thiolactone	1.7063	1.1295	0.1555	1.5773	0.4081	1.2347	0.5853	1.2087
N-Acetyl-L-leucine	0.8206	-0.3491	-0.3890	-0.4736	0.0064	-0.2469	1.4855	0.1793
Nadide	-1.7140	-0.4941	-0.0130	-0.1591	-2.2371	-1.8582	-0.1531	-0.8948
Nadolol	1.0487	-0.5489	0.4337	0.3577	-0.4833	-0.4947	0.3272	-0.3328
Nafcillin sodium salt monohydrate	-0.3347	0.5564	1.3394	-1.1072	0.6907	-0.7042	0.4281	-0.5455
Nafronyl oxalate	-0.6653	-0.9843	-1.2082	0.6712	-0.6747	-0.0582	-7.3228	-0.5183

Naftifine hydrochloride	0.3292	-0.1649	0.9368	0.1174	-0.1131	-0.0045	0.1270	0.0453
Naftopidil dihydrochloride	0.4565	-0.2538	-0.9628	-1.5046	-0.8078	-0.2756	-0.0190	0.2690
Nalbuphine hydrochloride	-0.0077	0.3381	0.4480	0.0574	0.6097	-0.2746	0.1304	-0.4064
Nalidixic acid sodium salt hydrate	-0.0443	-0.4144	1.1540	0.6736	0.6088	-0.3431	-6.5058	0.4342
Naloxone hydrochloride	0.0594	-1.5155	-0.4726	-0.9147	-0.3093	-2.1908	-0.8405	0.0945
Naltrexone hydrochloride dihydrate	1.1854	0.4298	1.6403	0.3735	1.3274	-0.0244	-1.2511	0.7411
Napelline	0.5016	-0.5113	0.2928	-0.6518	0.3297	0.5286	-0.8337	0.1602
Naphazoline hydrochloride	-0.6526	0.1280	0.2239	0.5074	0.5681	0.2010	0.0293	0.6575
Naproxen	1.5910	0.9120	-0.3920	1.5775	0.8518	0.7072	0.4672	-0.1982
Naringenine	0.9317	0.6814	0.5056	-0.4059	1.1110	0.1841	-0.7295	-0.0069
Naringin hydrate	0.8510	0.9025	-0.9826	-0.3785	1.5409	0.5516	0.3943	0.2032
Natamycin	0.5950	0.2429	0.4266	0.2498	0.1118	-0.1992	0.6114	-0.1076
Nefopam hydrochloride	0.0405	0.5828	-0.6538	0.0173	-0.7784	0.1925	0.3271	0.0768
Neomycin sulfate	1.3819	1.0819	0.9457	-0.0038	0.4756	1.3770	0.3301	1.1824
Neostigmine bromide	-0.6087	0.0119	0.0319	0.1958	0.6943	-0.0122	0.2811	-1.0993
Netilmicin sulfate	-0.7563	-0.8458	-1.0165	-0.0253	-1.4825	-1.6477	-0.3742	-1.8692
Niacin	-0.0712	-0.1375	1.2198	-1.9189	-0.9579	-0.7274	-0.4916	0.1967
Nialamide	0.0264	0.1062	0.3454	-0.6565	-0.3770	-0.4181	-1.2390	-1.3419
Nicardipine hydrochloride	-0.2949	0.0162	0.3294	-2.8609	-0.2968	-0.0897	-0.2818	-1.2575
Nicergoline	0.2176	0.2695	0.7583	0.6076	-0.1490	0.4763	0.8353	0.6943
Niclosamide	-0.7753	-0.6633	-1.2227	-2.6331	-0.1784	-1.9065	-0.7658	-0.3595
Nifedipine	0.2365	-0.4830	-0.0688	0.6409	-0.0243	0.1249	-0.6900	-0.9389
Nifenazone	0.9233	1.1288	-0.2978	-0.2046	0.3751	0.1621	0.0724	1.1717
Niflumic acid	0.4026	0.2703	1.5577	1.5435	0.4392	1.1100	1.4606	0.8419
Nifuroxazide	0.3980	1.0142	-0.1202	0.6627	0.1484	1.6818	0.7691	0.5383
Nifurtimox	-0.6884	0.2455	-0.8869	-0.8625	0.3244	-0.1610	0.9915	-1.0793
Nilutamide	0.9141	-0.0811	-0.7567	0.4910	0.8708	0.0106	0.1011	0.4632

Nimesulide	1.1117	-0.7773	2.4016	0.2729	0.1921	-0.4506	0.7355	-0.6250
Nimodipine	-0.2208	-0.3916	-1.0209	-0.5924	-0.6066	-0.5938	0.3834	0.1025
Niridazole	0.4467	1.0812	-0.0043	-0.6955	0.9698	-0.4463	-0.2304	-0.0200
Nisoxetine hydrochloride	0.2021	-1.0021	0.0627	0.9989	-0.4032	-0.5408	-0.5507	-0.0614
Nitrarine dihydrochloride	0.8660	0.2362	0.7719	1.5136	0.8298	1.0052	0.9053	1.5844
Nitrendipine	0.7758	0.1751	0.6513	0.3959	1.1642	0.1429	0.1980	1.1618
Nitrocaramiphen hydrochloride	-0.3285	-2.1483	0.5311	-0.2771	-1.2473	-1.1937	-1.4028	-0.6150
Nitrofural	-0.6787	0.4519	0.4574	1.0967	-1.5489	0.8758	0.6695	1.4416
Nitrofurantoin	-0.9931	1.2621	1.3157	0.2416	1.7642	1.2955	0.8273	0.7999
Nizatidine	0.2714	-0.9354	0.0649	-0.2080	-0.4229	-0.4129	0.2150	0.0827
Nocodazole	-11.6404	-8.5557	-9.2541	-8.5399	-8.8561	-10.8045	-0.1020	-6.1323
Nomegestrol acetate	0.4113	0.4191	0.8673	-0.2961	1.2235	0.9441	1.7658	-0.3415
Nomifensine maleate	0.6769	0.2742	1.2121	0.1970	0.4491	-0.3297	-0.5024	0.0542
Norcyclobenzaprine	0.2981	-0.4372	0.4691	1.2720	-0.1702	-0.2144	1.4046	-0.2540
Norethindrone	1.5406	-0.0152	1.1804	0.2503	0.6113	1.1481	0.4516	-0.7115
Norethynodrel	0.1644	0.4937	0.2830	0.4988	0.6595	0.0565	0.9657	1.1791
Norfloxacin	-0.0338	0.3918	0.0082	-0.5415	-0.5104	-0.4491	-0.2588	0.2397
Norgestrel-(-)-D	0.5757	-0.7009	-0.0609	0.1619	-0.1874	0.0128	0.4915	-0.6947
Nortriptyline hydrochloride	0.6617	-1.4624	-0.1308	-0.3596	-0.5579	-0.1661	1.0274	-0.6252
Noscapine	-1.7930	0.5270	-0.3393	1.6454	0.2418	-0.0113	0.8525	-1.3531
Novobiocin sodium salt	-0.2748	-0.1315	1.6063	-0.9925	-0.0888	-0.5823	2.2142	-0.4377
Nystatine	0.5457	-0.0448	-0.1414	0.7926	0.2857	-0.4809	0.5361	-0.6735
Ofloxacin	0.0759	2.5260	-0.6067	1.0770	-0.0401	2.1307	0.7464	1.9768
Oleandomycin phosphate	-0.0046	0.1036	-0.2286	0.1100	0.4074	-1.1724	0.5381	-0.6384
Omeprazole	0.2941	-0.1280	0.8849	2.0561	-1.3191	0.2105	2.2044	1.4960
Ondansetron Hydrochloride	-1.1035	-0.2060	-1.7195	-1.3471	-0.7605	-0.6484	0.1851	-0.9138
Ornidazole	1.1974	1.0778	2.0852	1.4626	0.4661	0.9442	1.2401	1.4804

Orphenadrine hydrochloride	1.1867	2.0841	-1.4360	0.3636	-0.6151	1.4700	1.1773	1.7149
Oxalamine citrate salt	1.0182	-0.0588	0.9287	-0.9547	-0.3900	-0.6407	1.0053	-0.1451
Oxantel pamoate	0.9534	2.4860	0.4543	0.2134	0.0227	2.7025	0.7656	-0.0038
Oxaprozin	-0.8144	-0.7955	-0.7186	-1.6169	-0.2071	-0.9226	0.3255	-0.1196
Oxethazaine	-0.9945	-0.7226	0.8391	-0.6845	-0.0614	-0.7286	-0.3576	-0.3126
Oxolinic acid	1.0151	0.0030	0.8059	1.0448	0.5903	0.4599	0.4614	0.7177
Oxprenolol hydrochloride	-1.4387	-0.2518	-1.4231	-2.2548	-0.8714	-0.2203	1.0873	-0.0060
Oxybenzone	1.7338	2.4910	-0.7119	0.2211	0.9122	-0.9994	-6.8724	0.6553
Oxybutynin chloride	0.7117	0.4549	0.6944	0.5682	0.6806	0.0931	1.0612	0.3930
Oxymetazoline hydrochloride	0.9886	1.2408	1.0027	0.2240	0.0417	0.0561	-0.3611	-0.0981
Oxyphenbutazone	-0.6124	0.3620	-0.5799	0.0851	-0.0852	1.0115	0.1848	0.4921
Oxytetracycline dihydrate	1.3839	0.7736	0.0183	0.9655	0.0442	-0.0387	-0.3202	-0.1060
Ozagrel hydrochloride	-0.8501	-0.2034	-0.3706	0.7953	-0.9352	-0.8673	0.5063	0.3568
Paclitaxel	-9.0994	-6.9804	-6.9408	-8.3411	-9.3243	-11.3532	0.1258	-7.1257
Palmatine chloride	0.8223	-1.8346	-1.4605	-0.2267	-0.4714	-0.9354	0.1053	-0.3519
Pancuronium bromide	0.6941	0.4919	0.2476	-0.1791	1.0293	0.5386	2.3770	-0.2058
Panthenol (D)	0.0253	1.0560	0.6408	0.0757	1.0415	0.5458	1.0373	1.1194
Pantothenic acid calcium salt monohydrate	0.8527	2.1697	0.4455	0.4864	0.1824	1.6838	0.6343	0.0069
Papaverine hydrochloride	-0.3970	-3.5132	-0.1929	-0.1855	-1.6182	-3.3095	0.9607	-1.2744
Parbendazole	-9.9899	-9.2412	-3.8848	-6.4864	-9.3868	-8.5899	-0.0026	-7.5440
Pargyline hydrochloride	0.7235	-0.0105	0.0933	-0.6140	0.1428	-0.3653	-1.0539	0.6109
Paromomycin sulfate	0.2611	-0.0249	-0.7081	0.5174	0.1504	0.2295	-2.1813	-0.1235
Paroxetine Hydrochloride	-1.7756	-2.0617	-1.8087	-1.7746	-1.6971	-1.1334	-0.9170	-1.4458
Parthenolide	-2.2838	-0.6259	-4.1964	-2.7264	-0.0516	-0.3649	0.5386	-1.3405
Pempidine tartrate	-0.7493	0.1769	0.2532	-0.2644	-0.2168	-0.7267	0.1435	-0.0622
Penbutolol sulfate	0.5351	1.1647	0.2431	0.0434	-0.6961	0.4774	1.8679	-0.1006
Pentamidine isethionate	-0.7434	-1.5498	-0.1190	0.1400	-0.1130	-0.8358	0.8977	-2.0184

Pentetic acid	-0.6847	-1.0536	0.0154	-0.3429	-2.0333	-0.7220	0.0197	-0.3448
Pentolinium bitartrate	-0.4609	-0.6727	1.1838	0.2053	0.1859	-0.3166	0.2951	0.4368
Pentoxifylline	3.4068	-0.1277	0.6644	0.5615	1.1190	0.1964	1.3371	-0.5758
Pentylenetetrazole	-2.6569	0.5671	-0.3139	0.6487	-0.0389	1.0766	0.4846	0.3051
Pepstatin A	2.0572	-0.2902	0.7092	1.0670	0.7029	-0.0020	0.3940	1.8880
Pergolide mesylate	1.7026	0.6512	-0.2600	0.2366	0.2092	0.3804	-0.1725	0.5372
Perhexiline maleate	-3.5171	-0.9921	-4.5170	-3.0514	-1.2025	-1.4678	-6.3774	-1.2786
Perphenazine	0.3631	0.3631	-0.5430	0.2188	0.8518	0.2855	1.7631	0.2785
Phenacetin	1.2376	0.1141	2.2653	0.4124	0.3830	-0.2339	-0.5758	0.3160
Phenazopyridine hydrochloride	-1.4882	0.7434	0.1891	-1.3349	-0.8193	0.6383	0.1999	-1.3270
Phenelzine sulfate	0.7233	0.8441	1.9800	-0.1096	1.4228	0.7453	-9.4634	0.2784
Phenethicillin potassium salt	0.6675	-0.0540	-0.0747	1.3756	1.3451	1.9997	2.4752	0.9317
Phenformin hydrochloride	-0.0248	-1.4010	-0.1780	-0.4061	-0.2763	-4.0785	-0.0133	-1.3193
Phenindione	-0.4906	-0.0034	-0.9210	-0.6447	0.3185	-0.4752	0.4145	-1.0640
Pheniramine maleate	-0.8607	-0.0014	0.0721	-1.3464	0.4503	0.0976	0.3029	-1.1384
Phenoxybenzamine hydrochloride	-0.3334	-0.3564	-1.0849	-0.0020	-0.3932	0.0883	-0.8514	-0.7256
Phensuximide	-0.5657	-1.2436	-0.9023	-2.2599	-0.5758	-1.3677	-1.5148	0.5997
Phentolamine hydrochloride	0.0767	1.6058	-0.7639	-0.0439	-0.4157	0.4065	-0.1811	-0.0043
Phenylpropanolamine hydrochloride	0.9778	0.8473	0.4853	0.9837	1.3165	0.5051	0.9893	1.0979
Phthalylsulfathiazole	-1.2618	-0.1662	-1.0272	0.0435	0.4428	0.4313	-0.7142	0.0176
Picotamide monohydrate	-0.2237	0.3867	0.1103	1.0467	1.1352	0.1719	0.1184	-0.6236
Picrotoxinin	-0.6805	-0.0997	0.4790	1.4657	-0.3825	0.2937	-0.0782	1.3015
Pilocarpine nitrate	-0.6162	-1.4217	0.0974	-0.6178	0.3529	0.8666	-0.1583	-0.6192
Pimethixene maleate	0.4113	-0.8470	0.9358	0.2451	0.0265	-0.6377	-0.0614	-0.0654
Pimozide	-0.0986	-1.3301	-1.7821	-0.1545	0.1315	-1.8801	-0.9237	-0.2377
Pinacidil	-1.2312	0.3644	-0.1654	0.2214	1.4501	1.1067	-5.7705	0.7079
Pindolol	0.4953	-0.4685	-0.9488	1.3864	1.6026	1.4897	-1.5755	2.2406

Pipemidic acid	1.0557	0.4454	-0.0989	-0.1461	-0.8000	0.2804	0.3450	0.2442
Pipenzolate bromide	-0.2082	-0.1402	1.0493	0.5826	0.0048	-0.4885	-0.6648	-0.2345
Piperacetazine	-0.4228	1.0833	-1.2844	0.2898	0.1379	0.8396	0.3683	0.5534
Piperacillin sodium salt	1.1864	1.6839	0.6477	1.4472	0.0790	1.6741	1.3805	0.8740
Piperidolate hydrochloride	1.3584	0.5859	-0.7239	-0.8935	-0.1121	0.6876	1.8407	0.8368
Piperine	0.5079	1.8473	0.0204	0.4590	0.3298	1.5620	0.7643	-0.5027
Piperlongumine	-0.2110	0.0749	-1.8741	-0.9144	0.0059	0.4092	1.1882	0.0866
Piracetam	-0.1728	-0.0020	0.0703	0.0920	0.3355	-0.0103	0.8121	-0.6332
Pirenperone	0.7776	0.6802	0.8114	-0.6298	0.0605	0.6594	-0.9309	0.7992
Pirenzepine dihydrochloride	0.9337	0.1654	0.8790	0.0707	0.0696	0.3976	-0.6641	1.1839
Piretanide	0.3213	0.5932	-1.9393	0.7156	0.2169	1.4454	1.5643	-0.0563
Piribedil hydrochloride	-1.1713	-0.4025	-0.0416	-0.5569	-0.6617	-0.0069	0.4207	1.0493
Pirlindole mesylate	0.3201	-0.5343	1.2173	-0.0666	-0.7399	-0.1275	0.2638	0.3534
Piromidic acid	1.2145	1.3024	-0.4681	0.3933	-0.0822	1.6247	1.6048	1.1891
Piroxicam	-0.4684	-0.4374	-1.2917	-0.1713	-1.3911	-0.1114	-2.4790	-0.1796
Pivampicillin	-1.4542	0.1589	-0.2640	-0.3371	0.7446	-0.2531	0.1570	-0.5073
Pivmecillinam hydrochloride	-0.0985	0.0698	-1.2297	0.2177	0.2018	0.2758	0.6865	-0.2292
Pizotifen malate	-0.7785	-1.3813	-0.8345	0.3873	-0.2471	-0.9377	-0.4500	0.7711
Podophyllotoxin	-12.2032	-13.1279	-11.5430	-10.5838	-8.9742	-11.4319	0.1939	-7.0560
Practolol	1.4082	-0.4395	1.0098	-0.2298	0.2587	0.7211	-1.1104	0.9962
Pralidoxime chloride	-0.6247	0.1732	0.8494	-0.2157	-0.7059	0.1432	-0.2131	-0.8867
Pramoxine hydrochloride	0.0764	1.8686	1.2157	0.7514	0.9648	1.8724	1.3019	0.2424
Praziquantel	0.0023	-0.4600	-1.3064	-0.2794	1.3707	-0.0099	0.4974	-1.0466
Prazosin hydrochloride	-0.6366	0.5646	-0.4573	-0.4523	0.1498	0.3776	-0.0820	-0.0032
Prednicarbate	1.3798	0.9380	0.1043	2.1845	0.5090	0.9424	2.3940	0.9928
Prednisolone	1.7739	0.1636	0.0730	-1.1320	1.4866	0.3377	1.1986	0.0941
Prednisone	0.7596	1.6511	0.0227	1.0134	1.0320	1.7055	-0.0746	0.6129

Pregnenolone	1.0789	0.5622	1.0379	-0.1526	0.4763	0.5192	0.3279	0.3237
Prenylamine lactate	-0.0032	-0.3625	-0.3994	0.2709	0.0070	0.7304	0.6681	-0.3046
Pridinol methanesulfonate salt	-0.5659	0.5272	0.3240	-0.1977	0.8205	1.2939	1.0808	0.3700
Prilocaine hydrochloride	0.3752	-0.5799	-0.8526	-0.5926	0.0871	-1.1069	0.1926	-1.9598
Primaquine diphosphate	-0.7610	2.3343	-0.2358	0.6553	1.2056	1.7434	0.8736	0.4176
Primidone	-0.4000	-0.1343	-0.5215	0.2323	-0.6866	0.0146	-0.3710	-0.2731
Proadifen hydrochloride	-0.0614	0.0254	-2.2474	-0.3254	-0.5551	-0.6731	-19.1546	-2.1051
Probenecid	0.3061	1.1012	0.2356	-0.7117	0.7096	1.7098	-0.3332	0.6565
Probucol	0.8887	-0.1459	0.6541	-0.7625	-0.1874	-0.4220	0.7028	-0.6452
Procainamide hydrochloride	0.1034	1.0108	0.0017	-0.9261	1.1658	0.6752	-0.2069	0.3236
Procaine hydrochloride	-0.0459	-0.8255	-0.4939	-0.6154	0.0330	-0.3953	0.3102	0.5290
Procarbazine hydrochloride	0.2501	0.8560	1.4517	1.3460	0.4696	0.6925	0.4991	-0.7021
Prochlorperazine dimaleate	1.0063	1.6718	-0.2389	-0.0197	-0.1854	2.2455	-0.1852	-0.8300
Procyclidine hydrochloride	0.3410	0.9567	1.6745	0.3434	0.1200	-0.6416	0.2816	0.1754
Progesterone	0.7858	1.3890	-1.2194	0.8725	0.9980	0.9369	0.8654	0.7996
Proglumide	0.5339	2.8239	-1.0052	0.3411	-0.0794	1.7938	0.0295	0.9134
Proguanil hydrochloride	-1.4418	-0.0049	-1.1743	-1.2708	-0.0286	-0.6443	-0.6038	-0.1954
Promazine hydrochloride	-0.5926	-0.7689	-0.6484	-0.2523	-1.1119	-1.2375	-0.0259	0.0347
Promethazine hydrochloride	1.6061	0.2101	-0.0528	-0.7585	1.0362	-0.7886	-0.3482	1.1433
Pronethalol hydrochloride	0.6730	0.2121	0.0639	0.5306	0.1641	0.1194	0.5819	-0.2054
Propafenone hydrochloride	-0.8838	-0.7534	-0.3792	-0.1452	-0.2198	-1.0768	-0.0863	-1.1993
Propantheline bromide	0.1693	-0.2866	0.8194	-0.4908	0.0981	-0.7122	0.4064	-0.7084
Proparacaine hydrochloride	-0.1950	1.3482	-0.1130	0.9881	0.5862	1.5661	-0.3336	0.1476
Propidium iodide	-0.5333	0.0952	0.0130	0.5808	-0.4193	0.3904	1.4290	0.0470
Propofol	-1.3228	-0.9651	0.4750	-1.6360	-1.8734	-0.9954	0.1093	-1.3136
Propoxycaine hydrochloride	-0.1195	-0.0454	-2.6525	-1.3409	-0.6447	-0.9895	-5.9277	-0.2263
Propranolol hydrochloride	-1.1533	-1.0358	-0.1876	0.3502	-0.8517	0.2093	-1.0757	-0.7774

Propylthiouracil	0.0892	0.8039	-0.4685	1.3163	-0.2137	-0.3302	0.8282	0.4351
Proscillaridin A	-13.4107	-13.9577	-12.6317	-15.6228	-12.2211	-12.7556	-0.7601	-11.0272
Protoveratrine A	0.3827	1.6653	2.3266	1.5506	1.2427	1.9769	0.4501	1.1892
Protriptyline hydrochloride	0.3350	-0.9864	0.8237	-0.4343	-0.0562	-0.5835	0.3961	-0.6947
Proxyphylline	1.2705	0.9676	1.5807	-0.4892	-0.0305	0.7370	0.5029	1.1481
Pseudopelletierine hydrochloride	0.8633	0.2586	0.6743	0.0648	0.5018	0.1636	-0.3789	0.3512
Puromycin dihydrochloride	-6.4675	-1.8855	-6.7723	-6.9249	-11.5332	-17.3642	1.3559	-13.4882
Pyrantel tartrate	-0.5618	-0.7580	-0.0082	-0.9528	0.1272	-0.2234	-1.9572	0.0296
Pyrazinamide	1.1516	0.9170	-0.2787	0.7303	0.5093	0.2290	1.0529	0.3302
Pyridoxine hydrochloride	-0.0052	-0.0837	-0.1317	-0.3236	0.7242	0.0109	1.0796	0.2900
Pyrilamine maleate	1.8302	-0.3615	0.4144	-0.0709	1.0129	0.2310	-0.5580	0.3498
Pyrimethamine	-7.6459	-10.4182	-7.0888	-12.4550	-6.0241	-5.9983	-5.4734	-5.1452
Pyrithyldione	0.3322	0.7212	-0.0804	2.1651	0.0833	1.4492	2.1385	0.3382
Pyrvinium pamoate	-3.6629	-0.4540	-4.0134	-1.8962	-6.1464	-2.6682	0.7849	-2.2738
Quercetine dihydrate	-0.5880	-0.1773	0.4865	-0.1774	0.4960	-0.9541	-0.1601	-1.0580
Quinacrine dihydrochloride dihydrate	-2.4038	1.2208	-5.2810	-0.2155	-1.2288	0.0814	0.5427	-0.5143
Quinethazone	0.4586	0.4628	-0.4455	-1.7220	0.7496	0.4916	1.2333	0.4820
Quinic acid	0.0047	-0.0181	1.0488	0.3573	-0.7071	-0.3106	-0.1095	-0.6930
Quinidine hydrochloride monohydrate	-1.4082	-1.3894	0.5417	-0.3337	0.3705	-0.5221	0.1337	-0.0011
Quipazine dimaleate salt	0.1592	0.6752	0.1428	-0.2348	0.5211	-0.1826	-1.3699	0.1328
R(-) Apomorphine hydrochloride hemihydrate	0.3147	-0.5267	0.0216	-1.4659	-2.1106	-0.0057	-1.0750	-0.3021
Racecadotril	0.7074	0.1394	0.5597	0.3922	0.3296	0.6339	0.5221	-0.0004
Raloxifene hydrochloride	-2.0792	-0.2817	-1.5947	-0.1467	-1.4558	-1.4111	-1.8864	0.1669
Ramipril	0.3809	-0.0915	-1.4644	-0.0618	-0.0270	-0.5756	0.4864	-0.0898
Ranitidine hydrochloride	-0.7147	-0.5804	0.1710	-0.0016	-0.8789	-0.2784	-7.5050	-0.1081
Rauwolscine hydrochloride	-1.1109	0.2342	0.3581	-0.5144	-0.4905	-1.1071	-0.9739	0.0651
Remoxipride Hydrochloride	-0.7013	-1.6379	0.6533	0.0586	-2.0419	-0.8946	0.1696	-1.8242

Repaglinide	0.7834	1.4085	0.7899	0.8134	0.0270	0.8897	0.9546	0.9391
Rescinnamin	0.3231	-0.2087	-0.2498	0.6018	-0.9354	-0.3560	-0.1585	0.1479
Reserpine	0.3956	0.8043	0.3122	0.7932	0.6477	1.0799	1.3737	1.3705
Reserpinic acid hydrochloride	0.6841	-0.0124	0.7709	-0.0600	0.2700	0.0931	0.0190	0.7682
Resveratrol	-0.2168	-0.4214	-0.6234	-0.0449	0.5356	-0.5071	-0.0037	-0.7549
Retinoic acid	-1.2533	0.5042	-0.2758	0.0604	1.4481	1.2958	0.1546	-1.7609
Retrorsine	0.8961	1.7623	1.8023	1.2173	1.3563	1.7804	-0.1281	1.3570
Ribavirin	0.6760	1.4137	0.7149	0.5283	-0.4097	0.5037	-0.4638	0.6938
Riboflavine	-11.3832	0.1874	-9.7572	-1.3652	-6.9816	-2.5846	0.4692	-4.0668
Ribostamycin sulfate salt	0.7531	0.1995	0.7646	-0.0728	0.0647	-0.6275	-0.3262	-0.1757
Ricinine	0.4914	-0.5570	-0.2883	0.2017	0.5429	0.1329	0.3075	-0.1680
Rifabutin	-0.9159	-0.5305	0.3862	1.5600	-0.5142	-0.7476	0.0328	-0.7806
Rifampicin	1.9502	1.4105	0.5882	1.4167	0.8774	1.3292	-1.0306	2.0455
Rilmenidine hemifumarate	0.3229	-0.4903	0.4342	0.8605	-0.7487	-0.7762	-1.1896	1.1210
Riluzole hydrochloride	-0.6056	0.3153	1.5433	-0.8045	1.6751	1.0208	0.4878	0.7626
Rimexolone	-0.8418	0.0178	-0.6863	-0.5806	0.2678	-0.3674	-0.0423	-0.0324
Risperidone	-1.5067	0.0413	-0.4133	0.1237	0.5355	-0.1428	0.1913	-0.4401
Ritodrine hydrochloride	0.2221	-0.8785	-0.5271	0.2928	0.4153	-0.0462	-0.0115	-0.1562
Rolipram	0.2582	0.1131	1.8827	0.3576	0.8894	0.6070	1.4760	0.9266
Rolitetracycline	0.3898	0.0382	0.5982	0.7902	0.2738	-0.0266	-0.0150	-0.2621
Ronidazole	0.3571	0.4931	-2.8545	1.4685	0.1403	1.3940	0.8720	0.3377
Roxarsone	-0.1623	1.1799	-0.0976	1.0720	-0.9164	2.2581	1.1011	0.9532
Roxithromycin	0.7288	0.2925	-0.6199	0.3971	0.8086	0.0293	0.5468	-0.0437
S(-)Eticlopride hydrochloride	-1.1591	-0.0667	0.5148	-0.2508	-1.3583	-0.4254	-0.3798	-0.1175
S(-)-terguride hydrogen maleate	-0.0437	-0.4375	0.5487	1.0300	0.9448	-0.2041	0.4305	0.8182
S-(+)-ibuprofen	0.7642	0.5860	0.9542	0.7998	-0.0090	-0.4222	0.2941	0.4745
Salbutamol	1.6360	-0.6042	-1.2785	-0.6621	0.0518	-0.2902	0.0856	-1.6649

Salmeterol	0.0467	0.4145	-0.4584	-0.2832	0.4600	-0.3816	-0.5825	-0.5982
Salsolinol hydrobromide	0.8702	0.2221	-0.7573	0.0163	0.9982	0.2710	-0.2625	-0.0146
Sanguinarine	-17.1693	-20.7820	-18.1952	-26.4478	-18.7017	-29.1133	-12.2206	-22.1436
Saquinavir mesylate	0.4650	0.3894	0.1134	0.8846	0.4010	1.1947	0.0488	0.4954
Scopolamine hydrochloride	0.3345	0.3766	0.1188	1.3481	0.9876	0.6925	0.2966	0.3263
Scopolamin-N-oxide hydrobromide	0.6503	1.2768	-0.4736	0.7187	0.4636	1.2022	-0.1907	0.3646
Scopoletin	-0.3971	0.5815	-0.2336	1.1973	-1.2248	1.6481	0.8509	0.5574
Scoulerine	-8.5310	-4.3963	-7.7195	-6.7401	-7.2100	-4.9172	-0.0295	-4.5043
Securinine	-2.9039	-1.2267	-1.6029	-2.8870	-3.7101	-2.8614	-1.2285	-2.7645
Selegiline hydrochloride	-0.0574	1.6080	0.5810	0.7030	0.6905	3.0719	0.0305	1.9881
Seneciphylline	0.5244	-0.6988	-0.6066	-0.2473	0.2775	-0.2774	-1.0673	0.1017
Serotonin hydrochloride	0.5772	-0.0700	1.6034	1.9992	-0.4058	1.1642	-1.8198	1.8228
Sertaconazole nitrate	-0.9100	0.8908	-1.7507	-0.7790	-0.5397	1.8431	1.8348	0.1706
Sertraline	-0.3546	-0.9099	-0.0128	0.1307	0.3980	-0.1615	0.0300	-2.0425
Simvastatin	-1.3291	-0.0219	-0.2206	-0.5368	-0.0025	-0.3352	-0.1795	-0.3243
Sisomicin sulfate	1.1805	0.6008	1.7651	-0.3058	0.0293	0.7093	0.4940	0.0279
Skimmianine	1.0317	-0.5505	0.3190	-0.0839	-0.2990	0.1816	-0.3921	0.0468
Solanine alpha	0.0234	1.4391	-2.8816	0.7027	1.6222	2.1981	-11.1202	1.1253
Solasodine	0.0855	-0.3421	-0.5999	0.0625	-1.4520	-0.0964	0.0799	0.5135
Sotalol hydrochloride	-0.2114	-0.3086	-1.1568	0.7626	-0.7742	0.2619	0.6087	0.3336
Spaglumic acid	-0.3944	-0.0806	0.7557	-0.1063	1.1089	-1.7832	-0.3895	-0.3791
Sparteine (-)	0.1861	0.7997	0.5187	-0.1732	1.1361	0.5306	-0.9928	-0.5364
Spectinomycin dihydrochloride	1.5616	0.6416	1.7723	1.5944	0.2256	2.2786	1.8322	0.2570
Spiperone	1.0805	-0.7390	-0.3931	-0.4240	0.5281	-0.7543	-0.1366	-0.4735
Spiramycin	1.2717	-0.0837	-0.2769	0.2136	0.1454	0.5448	-0.3472	1.2422
Spironolactone	0.0346	-0.0082	-0.3609	0.1547	0.5109	0.3414	-0.6688	0.0334
SR-95639A	1.7607	-1.0916	1.1829	-0.0109	1.6511	-0.3226	1.2259	1.6603

Stachydrine hydrochloride	-0.5613	0.3821	0.1215	-0.3553	0.6686	0.9181	0.4046	0.3607
Streptomycin sulfate	0.9467	-1.3141	0.3920	1.4578	-0.5628	0.8941	-1.2598	1.7239
Streptozotocin	0.0773	0.2337	-1.7499	1.1736	-0.0603	1.1201	0.9435	0.4278
Strophanthidin	-12.4280	-11.3972	-9.0961	-11.1715	-7.7558	-6.8591	-7.0114	-3.8935
Strophantine octahydrate	-11.7411	-14.8386	-10.1322	-18.6534	-8.5376	-18.5993	-0.2959	-12.2891
Succinylsulfathiazole	-0.5929	0.6557	0.0240	0.6505	-0.6130	-0.3607	-0.2046	-0.4260
Sulconazole nitrate	0.5724	0.7626	-0.2774	0.2217	-0.2920	0.3858	0.6215	0.0823
Sulfabenzamide	-0.1440	0.7851	0.2422	0.4890	0.0750	0.3960	1.0832	-0.0769
Sulfacetamide sodic hydrate	0.1090	0.6936	0.6335	0.0897	0.1841	0.4967	1.4458	0.3244
Sulfachloropyridazine	0.7574	1.0271	0.8666	1.4779	0.9255	1.4456	0.7856	1.3331
Sulfadiazine	0.6118	0.6606	-0.4312	-0.9387	0.2066	0.1997	0.5514	0.4986
Sulfadimethoxine	0.7189	-0.6489	0.3014	-0.1626	0.5067	1.3131	1.8582	0.2983
Sulfadoxine	0.5937	0.7413	1.6325	0.1932	0.3148	0.7047	0.1890	-0.9607
Sulfaguanidine	0.5471	-0.4855	0.9719	0.0481	-0.0318	-0.8363	0.4236	0.7509
Sulfamerazine	0.3453	-0.2796	1.0638	0.0058	0.4415	0.1875	0.8885	0.0021
Sulfameter	0.3410	-0.4661	0.4742	-0.2255	0.1695	-0.5898	2.4651	-0.7456
Sulfamethazine sodium salt	0.3120	0.3326	0.0906	0.2282	0.6858	0.0730	-11.3929	0.3926
Sulfamethizole	-0.6824	0.0811	0.6730	0.7159	-0.4190	0.8899	-0.6993	0.2920
Sulfamethoxazole	-0.3403	-0.0919	-0.2512	1.0223	0.1808	-0.1234	0.3398	0.4206
Sulfamethoxypyridazine	1.1340	-0.1074	1.1637	-0.1036	0.3174	1.7993	2.1620	-0.1554
Sulfamonomethoxine	-0.9477	-0.6386	-0.3109	-0.0312	-0.2400	-0.3242	1.8174	0.4270
Sulfanilamide	0.0544	-1.0929	0.6246	0.3026	0.3894	1.1451	1.3351	1.3516
Sulfaphenazole	0.9341	0.1397	-0.0241	0.0105	-0.4270	0.0257	0.0722	0.7998
Sulfapyridine	-0.6270	-0.0002	-0.2957	-0.4271	-0.4211	0.3052	-1.1137	-0.9463
Sulfaquinoxaline sodium salt	-1.0309	-1.7155	-1.2995	-0.8011	-1.4615	-1.4427	-0.6905	-0.3784
Sulfasalazine	0.0179	-0.3602	0.0910	-0.0141	0.0332	-0.6177	-0.2391	-0.6780
Sulfathiazole	-0.4708	-0.7840	0.7580	0.5429	0.0954	-0.2353	0.9926	0.8388

Sulfinpyrazone	0.7136	-0.4013	0.4629	0.1889	0.3436	-0.3111	-0.0528	-0.0531
Sulfisoxazole	0.9461	0.3814	2.0034	-0.0429	0.5328	0.2394	0.7847	1.1534
Sulindac	0.3714	1.3246	0.7412	0.2161	1.1179	1.5571	0.5954	0.4287
Sulmazole	0.6146	0.6464	-0.3551	2.1286	-0.1228	1.2009	-0.2133	-0.7920
Suloctidil	-1.2654	-0.3474	-2.0348	-0.6603	-3.2326	-0.0521	-1.2518	-0.6631
Sulpiride	-0.0738	0.0014	0.2283	0.6850	0.5788	-0.2457	0.3560	-0.2936
Suprofen	0.7415	0.0219	0.3304	-0.1445	-0.4123	-0.7327	0.8835	0.0525
Suxibuzone	0.1184	-0.8298	0.1569	-0.2022	-0.0825	-0.0983	-0.5856	-0.1713
Syrosingopine	0.7580	-0.5299	0.0352	1.7255	-0.2009	0.4867	-0.8841	1.1228
Tacrine hydrochloride hydrate	0.4999	1.6498	0.4566	0.9445	1.3010	0.2518	1.1156	0.4036
Talampicillin hydrochloride	-0.8588	-0.3620	0.2511	-0.3331	-0.2191	-0.4841	0.5596	0.1465
Tamoxifen citrate	-0.8818	0.3063	0.8483	0.3799	0.4792	0.2433	0.6430	0.4434
Telenzepine dihydrochloride	0.4719	0.1763	-0.8476	0.3222	0.2833	0.1012	-1.7220	0.2809
Tenoxicam	0.5526	0.3084	-0.7618	0.2042	0.7666	0.0103	0.1869	-0.3383
Terazosin hydrochloride	-1.7417	-0.9638	-0.3046	-1.7022	-1.8045	-1.0278	0.5553	-0.4151
Terbutaline hemisulfate	0.3718	0.8838	0.0491	0.0056	0.3487	1.2909	0.4441	1.3077
Terconazole	-16.9738	0.3985	-0.5956	-0.2297	-0.9568	-0.2733	-0.4366	0.9215
Terfenadine	-17.6016	-26.3361	-0.2788	-0.2652	-18.0506	-0.4052	0.0044	-1.7246
Testosterone propionate	1.8308	-0.7893	0.9243	0.5775	-0.1696	1.5478	0.2195	1.2094
Tetracaïne hydrochloride	-1.2090	-0.4422	-0.4950	0.6383	-0.6140	0.3621	0.5186	-0.7952
Tetracycline hydrochloride	-1.7017	0.7252	-0.7032	-1.1481	0.0985	0.2857	-0.7816	-0.8560
Tetrahydroxy-1,4-quinone monohydrate	1.5076	1.3456	1.8907	1.6310	1.6409	1.0950	2.4892	0.0024
Tetrahydrozoline hydrochloride	0.1053	-0.2976	0.2938	-0.2263	0.1364	-0.2074	-0.2789	-0.1547
Tetramisole hydrochloride	0.5997	0.1326	0.0551	-0.2305	0.2331	0.7684	0.0928	-0.7613
Tetrandrine	-0.9115	-0.3953	-1.0439	-0.3751	-0.9255	0.3014	-0.3793	-0.8942
Thalidomide	0.5749	-0.1783	1.7681	-0.8489	-0.7103	-0.5879	-1.0533	-1.0167
Theobromine	0.2320	0.0448	0.6554	0.8635	0.7866	1.2075	0.5095	0.1298

Theophylline monohydrate	-0.3861	-0.6889	-0.4686	0.1623	0.3753	0.9861	0.7413	1.0131
Thiamine hydrochloride	-0.3363	1.0274	-0.2634	1.6305	0.8485	1.2004	-0.5082	0.1610
Thiamphenicol	-0.0591	-1.3133	-0.9107	-0.4195	-0.7970	-2.8457	-0.8483	0.6082
Thiethylperazine malate	-0.4097	-0.2803	-1.8488	-0.4290	-0.1725	-0.4795	-12.0424	0.0317
Thiocolchicoside	0.1921	0.7346	0.0118	-1.0695	0.3012	-1.1963	-0.0252	-0.8968
Thioguanosine	-10.8458	-12.8421	-9.9201	-11.4013	-12.0507	-16.7969	0.6170	-12.1044
Thioperamide maleate	-0.3443	-1.4120	1.2012	-0.3111	-0.7395	-0.8679	-0.2716	-0.8689
Thioproperazine dimesylate	-0.2811	0.7283	-1.1875	0.0830	-0.6140	1.0206	0.2822	-0.5942
Thioridazine hydrochloride	-2.1241	0.7988	-2.4411	-0.2420	-0.0878	0.2757	-2.0486	-2.0946
Thiorphan	-0.1190	1.2623	0.2442	1.3612	1.0121	1.2709	0.7253	1.0880
Thiostrepton	0.2664	-1.6651	-0.4710	-1.6505	-0.6861	-2.1367	-0.3998	-0.3996
THIP Hydrochloride	0.1410	-0.3082	0.8151	0.2587	-0.0330	-0.5105	1.1087	0.4610
Thonzonium bromide	-1.0254	1.0874	0.4859	0.2293	-0.3038	0.4937	0.9960	-2.2013
Thyroxine (L)	0.6768	-0.2071	1.3389	-0.5154	1.0426	0.4428	-0.0930	-0.3668
Tiabendazole	1.2236	0.7722	0.1994	0.0561	0.3734	1.4119	0.3623	0.8746
Tiapride hydrochloride	1.4400	0.5803	0.0953	0.3267	0.6951	-0.1367	-0.0514	-0.2782
Tiaprofenic acid	0.1458	0.1532	0.1945	1.2398	-0.8093	-0.5512	0.2755	-0.1471
Ticarcillin sodium	-0.9112	-0.1304	-0.7800	-0.8865	-0.2164	-0.0901	-0.8982	0.0060
Ticlopidine hydrochloride	-0.2680	0.1814	-0.9157	0.2614	0.2550	-0.2774	0.6419	-0.2575
Tiletamine hydrochloride	-0.1993	0.5486	0.0128	-0.7926	-0.1689	0.2777	0.5837	-0.9751
Timolol maleate salt	-0.6169	0.0841	-0.5514	-0.2854	0.5931	0.2462	0.1661	-0.2625
Tinidazole	0.0961	0.2796	0.8478	0.4802	1.0173	0.4864	0.0524	-0.0852
Tiratricol, 3,3',5-triiodothyroacetic acid	0.9548	-0.0324	-0.1429	-0.1999	-0.2051	-0.7094	-0.5827	-0.1428
Tobramycin	0.8506	1.0158	1.6022	1.2300	0.1274	-0.1470	-0.3121	-0.7191
Tocainide hydrochloride	-0.2712	0.3780	0.2696	-0.4939	0.4388	0.4501	0.3000	-1.3189
Tocopherol (R,S)	1.7959	-0.2437	0.6653	0.5785	0.9385	-0.3661	1.6223	1.1452
Todralazine hydrochloride	-0.1832	1.2779	-0.6295	1.1183	0.8370	1.4166	1.0071	0.4719

Tolazamide	0.2641	1.6176	0.4797	1.3883	0.3530	2.0740	0.0936	0.9488
Tolazoline hydrochloride	-0.4917	-0.4462	0.0056	0.0277	0.3786	-0.3742	-0.1254	-0.2922
Tolbutamide	-0.1046	-0.7396	0.4916	-0.4671	0.2748	0.0173	0.0095	-0.7913
Tolfenamic acid	1.1151	1.0980	0.2670	1.1942	1.6020	1.8213	0.6938	0.2925
Tolmetin sodium salt dihydrate	0.9965	0.2629	-0.2481	0.2702	0.8924	-0.3222	0.1959	0.7466
Tolnaftate	0.4794	0.1044	0.2421	0.5826	0.0620	0.1075	-0.1568	-0.1534
Tomatidine	0.2225	0.5688	-1.2502	1.5420	-0.4386	0.6001	0.0773	-0.0277
Tomatine	0.7795	0.7121	-0.0865	0.1146	0.6931	0.6464	0.6266	0.8819
Torsemide	-0.2864	0.6361	-0.0915	-0.5709	0.6312	-0.0492	-0.1800	-0.1012
Tracazolate hydrochloride	-0.1171	-0.5932	-0.5675	-0.3427	-0.6108	-1.3836	0.4698	-1.4073
Tranexamic acid	-0.5535	-0.6361	-0.8578	0.5563	-1.5764	-0.1117	-0.9875	0.0419
Tranylcypromine hydrochloride	-0.4099	-0.1746	0.2894	1.2676	-0.3193	0.1097	-0.7928	0.1709
Trapidil	0.0727	-0.1945	-0.4311	-1.9922	-0.0019	-0.0138	0.2593	-1.9730
Trazodone hydrochloride	-1.0717	-0.8576	-0.8748	0.3979	-0.2385	-0.6738	-0.0918	-0.3504
Tremorine dihydrochloride	1.2251	-0.8161	-0.4263	0.3422	-0.1259	-0.5218	-3.5654	0.6355
Triamcinolone	-0.3170	0.3627	0.5143	0.9153	0.7909	0.6613	-0.2627	0.6477
Triamterene	-2.0784	-0.6789	-3.2047	-2.4284	-0.4760	-0.6824	-0.1118	-0.0526
Tribenoside	-0.9470	-0.3645	-1.4918	-0.5356	-0.1223	-0.6020	-0.1462	-1.3879
Trichlorfon	-0.0381	-0.6973	-0.7970	-1.4862	0.1858	-0.0010	-0.7231	-0.1934
Trichlormethiazide	0.1391	0.1904	-0.3778	0.1843	0.1445	0.1429	0.5497	-0.0028
Tridihexethyl chloride	-0.3740	0.2748	-0.5586	1.5540	-0.1764	0.7537	1.7438	0.1719
Trifluoperazine dihydrochloride	-0.2019	1.0055	-1.0826	0.1327	-0.0037	0.3348	0.3975	0.7402
Triflupromazine hydrochloride	0.7531	-0.7800	-0.3002	-1.2806	-0.2345	-0.5846	-0.0741	0.0855
Trifluridine	-1.6467	-0.2333	-0.2534	-2.1292	-3.5519	-2.0545	1.1864	-1.0407
Triflusal	0.7201	0.3979	-1.5000	-0.0349	0.1666	-0.0860	-0.6983	-0.4414
Trigonelline	0.5282	0.3086	-0.4606	1.0698	-0.1491	-0.0109	2.0302	0.7373
Trihexyphenidyl-D,L Hydrochloride	-0.9801	-0.5830	-0.9163	-0.1386	-1.6186	-1.1582	-0.4538	-0.5392

Trimeprazine tartrate	-0.8056	-2.3082	0.0527	-0.1336	-1.2755	-1.4983	0.5772	-0.6493
Trimetazidine dihydrochloride	-0.2318	0.8455	0.1059	0.9340	0.1868	0.5259	-0.0496	-0.2055
Trimethadione	1.8530	0.8555	0.8133	1.8262	1.0412	0.9699	1.3517	0.5951
Trimethobenzamide hydrochloride	1.3375	1.7267	-0.4307	1.0718	0.8466	1.2632	0.7727	0.6922
Trimethoprim	0.2561	-0.1240	0.5776	-0.1457	0.3513	0.0029	0.1831	-1.4115
Trimethylcolchicinic acid	0.1868	-1.2007	-0.6990	-0.7804	-0.2514	-0.2567	-0.3187	-0.8012
Trimipramine maleate salt	1.3089	-0.7133	-1.4150	1.5501	-0.8336	0.6094	1.8672	-0.3191
Trioxsalen	-0.6406	0.1728	-1.0530	-0.8988	0.2407	0.0012	-0.5156	-0.8761
Triprolidine hydrochloride	0.0016	-0.8230	1.2143	-0.6683	-1.2186	-0.0323	-0.1105	0.7125
Troleandomycin	0.5945	0.6503	-1.3647	-0.0105	0.3201	0.4012	0.1197	0.8324
Trolox	0.0905	-0.5023	-0.6982	-0.7172	0.1622	-0.5111	0.5343	-0.7367
Tropicamide	0.3059	1.0242	0.5595	-0.7391	-0.2077	0.3591	0.3080	0.4041
Tropine	0.6660	0.2336	-0.4934	-1.4211	0.0615	-0.1151	-10.8733	0.0764
Tubocurarine chloride pentahydrate (+)	-0.1007	-0.2725	0.3902	0.8107	-0.4010	0.7802	1.1776	-0.4636
Tyloxapol	-0.1621	-0.0523	-0.1461	1.1474	0.0719	0.6552	0.4144	-0.6365
Ungerine nitrate	0.2308	-0.2381	0.4855	0.6949	0.3485	-0.0217	-0.6263	-0.1258
Urapidil hydrochloride	0.2705	-0.1849	0.1196	1.3325	0.5281	1.0370	0.9590	0.5367
Urosiol	-0.1217	1.3729	-0.2443	1.9158	0.5165	1.2303	-1.6394	0.7123
Ursolic acid	0.9147	-0.0524	0.6764	1.8959	1.6633	1.9550	0.7902	1.2654
Vancomycin hydrochloride	-0.7583	0.4725	0.1148	1.1794	-0.0613	-0.5859	0.4065	0.3677
Verapamyl hydrochloride	0.4758	-1.2027	-0.6917	-0.9622	-0.8602	-0.9969	-7.8718	-0.5775
Verteporfin	-3.1278	-1.0866	-3.3684	0.5164	-1.1916	-1.5628	0.0048	-2.0995
Vidarabine	0.3909	-0.7818	0.1114	0.4845	0.7599	-0.4845	-0.8779	-0.9955
Vigabatrin	0.4491	0.1017	-0.7194	-0.1086	-0.9292	-0.2886	-2.1008	0.9970
Vincamine	0.7873	-1.1802	-0.0583	-0.6890	-1.0957	-0.6978	-0.8374	-0.0625
Vinpocetine	0.0013	-0.8495	1.0972	-0.8161	0.0085	0.0087	-0.8876	0.3627
Viomycin sulfate	-0.0682	-0.1981	0.1706	0.6455	0.0891	0.4595	1.0119	-0.6924

vitamin D	-0.5412	-0.6735	-1.7898	-2.0806	-1.3024	-0.8576	-1.9099	0.2078
Vitamin K2	-0.6488	-0.9946	1.3710	-0.8133	1.4984	-1.2260	-0.3633	-1.3754
Vitexin	-1.1864	-2.2242	0.8919	-0.9144	-1.7712	-0.7146	0.1947	-0.8364
Xamoterol hemifumarate	0.1555	0.1018	1.1999	0.4369	-0.0064	-0.3637	-0.3382	-0.0701
Xylazine	-0.1855	-0.4368	-1.6201	-0.4689	0.2918	-0.9790	-0.4151	-0.5337
Xylometazoline hydrochloride	0.3263	0.4859	0.4883	1.0226	-0.0621	-0.0194	0.5862	0.7575
Yohimbine hydrochloride	-0.0567	0.2189	0.4184	0.2540	-0.3706	0.2483	1.0266	-0.2295
Yohimbinic acid monohydrate	0.6181	-0.0901	0.2256	0.3188	-0.1683	-0.4569	-0.5165	0.3426
Zalcitabine	-0.0911	0.8276	0.3016	-0.8427	1.4459	2.1229	-1.2991	1.3575
Zaprinast	1.1568	0.7800	-0.7232	0.6206	0.7514	0.2095	0.6448	0.4376
Zardaverine	-0.2700	-0.4554	0.0263	0.2573	-0.7549	-0.8062	0.6177	0.0872
Zidovudine, AZT	1.3724	0.0220	1.0604	-1.4963	0.5082	0.7904	-1.6130	0.7684
Zimelidine dihydrochloride monohydrate	0.0116	-0.7579	1.3186	0.6104	-0.3353	-0.9218	-0.4200	1.8692
Zomepirac sodium salt	0.3268	0.4525	-0.8400	0.2929	0.2890	-0.3991	-0.2973	0.9307
Zoxazolamine	1.2335	1.3646	0.8576	1.0316	1.4255	-0.5102	1.0251	-0.0576
Zuclopenthixol hydrochloride	0.0774	0.5377	-0.3373	-0.7556	0.1579	0.0229	0.3474	-0.8398

Appendix 2: ΔZ-scores of the siRNA screen

Gene Symbol	ΔZ-scores
AATK	-1.1362
ABL1	-0.5420
ACVR2B	-1.6242
ADRBK1	3.2001
AIP1	-0.7245
AK1	-0.0850
AK2	-0.0801
AK3L1	-0.1428
AK7	-0.7821
AKT1	-1.1905
ALS2CR7	6.5185
AMHR2	-0.7525
ANKK1	-0.2568
ANKRD3	3.4949
ARAF1	-0.4774
ARK5	-0.4630
ATR	-0.0824
AURKA	-1.9110
AURKC	0.7062
BAIAP1	0.4156
BCKDK	5.0849
BCR	0.0729
BLK	7.2034
BMP2K	0.8351
BMPR1A	-0.3566
BMPR1B	0.7043
BMPR2	0.3154
BMX	-0.4127
BRAF	0.0608
BRD2	-8.9891
BRD3	-0.6315
BRD4	-0.0577
BRDT	0.1785
BUB1	-0.3878
C10ORF89	0.0132
C14ORF20	-0.4357
C7ORF2	-0.8909
C9ORF12	-3.8041
C9ORF96	0.4248
CALM1	-0.0913
CALM2	-0.5202
CALM3	-1.2498
CAMK1	-0.7367
CAMK1D	-0.4001
CAMK2A	-0.0241
CAMK2B	-0.2675
CAMK2D	-0.6576
CAMK2G	1.7399
CAMK4	0.2418
CAMKK1	-0.0717
CAMKK1	0.1469
CAMKK2	-0.2467
CCRK	0.2017
CDADC1	-0.4568
CDC2L1	-0.0780
CDC2L2	0.1595
CDC42BPB	4.4886
CDK10	-5.5877
CDK2	0.4080
CDK3	-0.1334
CDK4	-1.1851
CDK5R1	0.5354
CDK8	-0.2060
CDK9	0.2497
CDKL1	-0.6807
CDKL2	-0.8871
CDKL3	-6.3042
CDKL5	3.3947
CDKN1C	1.6061
CDKN2B	0.3049
CDKN2C	-0.8528
CDKN2D	-0.0176
CHEK2	0.8371
CHKA	0.4742
CHKB	0.1611
CHUK	-0.2237
CKB	0.3892
CKM	-1.2317
CKS1B	-0.1804
CLK1	0.1934
CLK3	1.0648
CLK4	0.1026
COASY	-0.5724
COL4A3BP	0.1736
COMMD3	-0.4168
CPNE3	-6.9373
CRIM1	0.0422
CRK7	0.2804
CRKL	0.4620
CSK	0.3189
CSNK1A1	-0.0667
CSNK1A1L	0.1089
CSNK1G1	0.3685
CSNK2A1	-0.5132
CSNK2A2	-0.8995
DCAMKL1	-0.1707
DDR1	-0.3492
DDR2	-0.3236
DGKA	6.6224
DGKB	-0.4458
DGKD	-0.0344
DGKH	-0.2795
DGKK	-0.6130
DGKQ	-1.2252
DGUOK	3.4762
DKFZP434	0.1960
DLG1	0.6026
DLG2	-0.0987
DLG3	-0.4635
DLG4	-0.9935
DMPK	-0.4989
DUSP21	-0.4758
DYRK1A	-0.1204
DYRK1B	-0.5344
DYRK2	-1.2254
DYRK4	0.1431
EFNA3	0.5744
EFNA5	-0.3309
EFNB3	-0.1268
EIF2AK3	0.7770
EIF2AK4	-0.4881
EPHA1	0.1913
EPHA10	-1.1217
EPHA4	0.1804

EPHA5	0.0074
EPHA6	0.3782
EPHB1	-0.6153
EPHB2	-0.6546
EPHB3	0.0391
EPHB4	0.2671
EPHB6	-0.2316
ERBB3	0.6306
ERN1	-0.5697
ERN2	-0.4812
EXOSC10	-0.1026
FASTK	-1.2096
FER	0.3877
FES	-1.0333
FGFR1	-0.7329
FGFR2	-0.0178
FGFR3	-0.1518
FGFR4	-0.5210
FGFRL1	0.1892
FGR	-0.3792
FLJ10761	0.1916
FLJ13052	-0.6153
FLJ25006	-0.7474
FLJ34389	-0.2650
FLT1	0.4160
FN3K	-0.5458
FUK	-1.5844
FYN	-0.5284
GAK	-0.0314
GALK1	-0.0672
GALK2	0.8709
GCK	-1.1166
GK	0.3638
GK2	-0.2717
GNE	-0.3527
GOLGA5	-0.2858
GRK1	-0.5816
GRK6	-0.4676
GRK7	0.1070
GSG2	0.4070
GSK3A	0.3769
GSK3B	-0.6754
GTF2H1	0.6703
GUCY2C	0.2750
GUCY2D	-3.8166
GUCY2F	-0.3308
GUK1	0.8274
HAK	0.0681
HCK	0.2932
HIPK4	0.1566
HK1	-0.9225
HK2	-3.4199
HSPB8	3.4576
HUNK	0.5050
HUS1	0.4061
ICK	0.3455
IGF1R	-0.2413
IGF2R	0.8380
IHPK1	-0.3091
IHPK2	0.2694
IHPK3	0.2145
IKBKAP	-0.2090
IKBKB	0.1155
IKBKE	-0.5186
IKBKG	-0.1102
ILK	-0.9624
ILK-2	-0.1504
INSR	0.1090
INSRR	0.4356
IPMK	0.0956
IRAK3	-0.6053
IRAK4	0.7903
ITPK1	0.5232
ITPKA	0.2105
ITPKB	0.0513
JAK1	0.1616
JAK2	-9.6118
JIK	-0.0921
KALRN	6.1814
KCNH8	5.5232
KDR	0.6364
KHK	-0.0347
KIAA1639	-0.2607
KIAA1765	0.1261
KIAA2002	-0.6992
KIT	0.2394
KUB3	0.7405
LAK	4.6959
LATS1	0.8305
LCK	0.2238
LIMK2	-0.6073
LMTK2	4.9509
LMTK3	0.5394
LOC340156	0.2656
LOC390226	-0.2639
LYK5	0.0636
MAGI-3	0.3502
MAK	0.3483
MAP2K1	0.3729
MAP2K2	-0.7447
MAP2K5	-0.7782
MAP2K6	-0.1853
MAP2K7	5.7255
MAP3K1	-0.2376
MAP3K10	-0.7835
MAP3K11	-0.7090
MAP3K13	-0.0715
MAP3K14	-1.2408
MAP3K15	-1.0959
MAP3K4	-0.0748
MAP3K5	0.1827
MAP3K6	0.0784
MAP3K7	-1.0219
MAP3K8	-0.3918
MAP3K9	0.5961
MAP4K2	-0.6885
MAP4K3	-0.3878
MAP4K4	-0.7280
MAP4K5	0.2205
MAPK10	-0.4821
MAPK12	0.1224
MAPK14	-0.4760
MAPK4	-0.4755
MAPK6	-0.9201
MAPK7	-0.5321
MAPK9	-0.3647
MAPKAPK 5	0.0960
MARK4	0.9129
MAST3	0.1286
MAST4	0.0184
MATK	0.3930
MELK	0.1017
MERTK	-0.8349
MET	-0.1559
MGC16169	0.0465
MGC42105	0.2917
MGC45428	1.2126
MGC4796	-0.8883
MGC4796	-0.6204
MGC8407	0.0166
MIDORI	0.2422
MINK	-0.7897
MKNK1	-0.7710

MKNK2	0.4724
MLCK	-6.8983
MOS	-0.2126
MPP1	0.1755
MPP3	1.3329
MST1R	-0.2362
MYLK	-0.1835
MYLK2	-1.0275
MYO3B	0.7135
N4BP2	-0.1624
NEK1	0.0946
NEK11	-1.0479
NEK2	0.4267
NEK3	1.2799
NEK4	3.3101
NEK6	0.6969
NEK7	-1.0707
NEK9	0.3649
NME1	-0.2431
NME2	0.2806
NME3	-0.5411
NME4	-0.0991
NME6	-0.2484
NME7	-0.5958
NPR2	-0.0385
NRBP2	-2.2019
NRK	-0.0155
NTRK1	0.0645
NYD-SP25	-0.3774
OSR1	0.3282
P101-PI3K	-0.3580
PAK2	-0.6841
PAK3	0.3910
PAK6	-1.1951
PANK2	-0.5729
PANK3	-0.1607
PANK4	-0.0998
PASK	-1.4546
PCK2	0.7097
PCTK1	-0.1120
PCTK2	0.8055
PCTK3	-0.0565
PDGFRA	0.3637
PDIK1L	0.3283
PDK1	-0.0817
PDK4	0.3925
PFKFB1	0.9943
PFKFB2	-0.4939
PFKFB4	0.0975
PFKL	0.4071
PFKM	0.1509
PFKP	0.2878
PFTK1	-0.2891
PGK1	-0.0012
PGK2	-1.0533
PHKB	-0.3384
PI4K2B	-0.5890
PIK3C2A	0.0688
PIK3C2B	0.3994
PIK3C3	0.6241
PIK3CA	-3.2893
PIK3CB	0.1341
PIK3CD	0.6283
PIK3CG	-0.5412
PIK3R4	0.5625
PIK4CA	-1.6802
PIM1	-0.3634
PIM3	-0.0019
PIP5K1A	0.2617
PIP5K1C	2.7507
PIP5K2B	0.4752
PIP5K2C	-0.0989
PIP5K3	-0.1976
PKIA	0.3301
PKIB	0.9084
PKLR	-0.5593
PKM2	0.9850
PKN3	-0.6977
PLK3	0.2125
PMVK	-1.4498
PNCK	0.2634
PRKAA1	-0.0162
PRKAA2	-0.4687
PRKAB1	-0.6487
PRKAB2	-0.4403
PRKACG	0.4874
PRKAG1	-0.3479
PRKAG2	-1.3497
PRKAG3	3.7424
PRKAR2B	0.8502
PRKCA	-0.6439
PRKCB1	0.4312
PRKCD	0.0540
PRKCE	0.1515
PRKCH	0.5920
PRKCI	-0.6407
PRKCL1	0.1616
PRKCL2	3.2261
PRKCN	-0.2768
PRKCQ	-0.3348
PRKCSH	-0.1614
PRKCZ	2.8588
PRKDC	0.3030
PRKG1	0.4342
PRKG2	-0.1300
PRKR	-0.0472
PRKWNK1	0.4638
PRKWNK2	-0.6047
PRKWNK3	0.3138
PRKY	-0.9873
PRPF4B	-1.0101
PRPS1L1	-0.7832
PRPS2	-2.4037
PSKH1	0.3973
PSKH2	0.6727
PTK2	-0.4360
PTK2B	0.5726
PTK6	0.0416
PTK9	-0.2958
PTK9L	-0.2344
PXK	-0.2000
RAF1	-0.0353
RAGE	0.1641
RET	-0.0654
RFK	0.6618
RIOK2	-6.3990
RIOK3	0.1780
RIPK1	-1.4787
RIPK3	-0.4787
RNASEL	-0.6602
ROCK1	0.5041
ROCK2	1.4203
ROR1	-0.0897
ROR2	-0.0227
ROS1	-0.0291
RP6-213H19.1	-0.3798
RPS6KA1	-0.0223
RPS6KA2	0.8358
RPS6KA4	-0.1918
RPS6KA5	0.0542
RPS6KA6	-0.4310
RPS6KC1	-0.9462
RYK	0.1601

SAST	-0.0525
SCAP1	-0.0447
SCYL1	0.2226
SGK	0.3527
SGK2	0.4021
SGKL	-0.6869
SIK2	0.3606
SLK	2.5186
SMG1	0.6726
SNARK	0.2385
SNF1LK	0.3735
SNRK	-0.6685
SPHK1	-0.8344
SPHK2	-0.0833
SRMS	-0.7131
SRP72	-1.4150
SRPK2	0.0089
SSTK	-0.1434
SSTK	3.9546
STK10	-0.7597
STK11	0.0805
STK16	0.4717
STK17A	-0.0556
STK17B	-0.5788
STK19	-0.1012
STK24	-0.7200
STK25	-7.3425
STK29	4.2860
STK32A	0.0727
STK32C	0.8206
STK33	0.3361
STK36	0.1526
STK38	-0.0609
STK38L	-1.6414
STK39	0.4515
STK4	0.4084
SYK	-0.5127
TAF1	0.3739
TAO1	-1.2308
TBK1	-0.9884
TEC	-0.1571
TESK1	-0.0661
TEX14	-0.2656
TGFBR3	-0.0417
THNSL1	-0.1508
TJP2	0.1743
TK2	-0.1022
TLK1	0.7019
TLK2	-0.4134
TNIK	8.9723
TNK2	0.2602
TOPK	-0.3789
TPK1	-0.6430
TRIB1	-0.3995
TRIB3	0.0972
TRPM6	0.1106
TRPM7	0.0273
TSKS	0.0012
TYK2	0.1000
TYRO3	3.9665
UCK1	0.0026
ULK1	0.1436
ULK2	0.6388
ULK4	1.5188
VRK1	0.4347
VRK2	0.3988
VRK3	0.0246
WEE1	0.2839
WNK4	0.7495
XYLB	0.3765
YES1	4.0901
ZAK	0.0519
ZAP70	0.1186